



REFERENCE ONLY

UNIVERSITY OF LONDON THESIS

Degree phd Year 2005 Name of Author CANDY, T.A.

COPYRIGHT

This is a thesis accepted for a Higher Degree of the University of London. It is an unpublished typescript and the copyright is held by the author. All persons consulting the thesis must read and abide by the Copyright Declaration below.

COPYRIGHT DECLARATION

I recognise that the copyright of the above-described thesis rests with the author and that no quotation from it or information derived from it may be published without the prior written consent of the author.

LOANS

Theses may not be lent to individuals, but the Senate House Library may lend a copy to approved libraries within the United Kingdom, for consultation solely on the premises of those libraries. Application should be made to: Inter-Library Loans, Senate House Library, Senate House, Malet Street, London WC1E 7HU.

REPRODUCTION

University of London theses may not be reproduced without explicit written permission from the Senate House Library. Enquiries should be addressed to the Theses Section of the Library. Regulations concerning reproduction vary according to the date of acceptance of the thesis and are listed below as guidelines.

- A. Before 1962. Permission granted only upon the prior written consent of the author. (The Senate House Library will provide addresses where possible).
- B. 1962 - 1974. In many cases the author has agreed to permit copying upon completion of a Copyright Declaration.
- C. 1975 - 1988. Most theses may be copied upon completion of a Copyright Declaration.
- D. 1989 onwards. Most theses may be copied.

This thesis comes within category D.



This copy has been deposited in the Library of UCL



This copy has been deposited in the Senate House Library, Senate House, Malet Street, London WC1E 7HU.

**ASPECTS OF PRION PROTEIN DYNAMICS
IN CELL CULTURE MODELS**

TIMOTHY ADAM LANDY

**UNIVERSITY COLLEGE LONDON
Ph.D.**

UMI Number: U592229

All rights reserved

INFORMATION TO ALL USERS

The quality of this reproduction is dependent upon the quality of the copy submitted.

In the unlikely event that the author did not send a complete manuscript and there are missing pages, these will be noted. Also, if material had to be removed, a note will indicate the deletion.



UMI U592229

Published by ProQuest LLC 2013. Copyright in the Dissertation held by the Author.
Microform Edition © ProQuest LLC.

All rights reserved. This work is protected against
unauthorized copying under Title 17, United States Code.



ProQuest LLC
789 East Eisenhower Parkway
P.O. Box 1346
Ann Arbor, MI 48106-1346

Acknowledgements

I would like to thank my supervisor and all those in the laboratory for their help with the work that contributed to this thesis. I would also like to thank all those who have supported me throughout the period of this Ph.D.

Abstract

The cell biology of Prion formation and transfer is not well understood. In order to further elucidate the dynamics of PrP^c and PrP^{sc} in a cellular context, fusions between Green Fluorescent Protein (GFP) and PrP were constructed and infected/uninfected cell line pairs expressing these constructs were created. Biochemical analysis indicated that the C-terminal PrP^c portion of the fusion protein successfully converted to PrP^{sc}. However, further studies demonstrated that proteolysis occurs between GFP and PrP and therefore the fusion protein cannot be employed as a direct reporter for PrP^{sc}.

A Time-Lapse microscopy system was set up and studies were undertaken with infected and uninfected cell lines expressing the fusion construct or cytoplasmic markers to observe events that may be related to transfer of infectivity. Although no exchange of fusion protein is observed, cytoplasmic material is released from both infected and uninfected cell lines.

Fluorescence recovery after photobleaching (FRAP) was carried out to establish a system for further investigation of PrP dynamics in the plane of the membrane. Early experiments indicate the possibility of a difference in the diffusion of PrP between infected and uninfected contexts.

It is not currently known how Prion glycoform profile is transmitted and maintained following a new infection. The glycoform profile of PrP^{sc} was perturbed in order to investigate the causal role of PrP^{sc} glycotypes in transmission and maintenance of Prion glycoform profile. The results indicate that perturbation of PrP^{sc} glycoform profile in an infectious source does not lead to a correlated perturbation of glycoform profile in the newly established infection. Therefore the glycosylation of PrP^{sc} in an infectious source is not a required source of information for establishing the glycoform profile of a Prion infection.

Table of Contents

Abstract.....	3
Table of Figures	8
List of Tables.....	9
Supporting Data	10
Abbreviations.....	10
Chapter 1 Introduction	14
1.1. Introduction overview	15
1.2. Animal TSE's.....	15
1.3. Human Prion Disease	17
1.3.1. Sporadic Prion disease	18
1.3.2. Acquired human Prion disease	18
1.3.3. Genetic Prion Disease	21
1.4. The Prion concept.....	23
1.4.1. Mechanisms of Prion replication	26
1.4.2. Yeast and Other Prions.....	28
1.5. PrP gene structure and expression	31
1.6. Prion protein Structure	32
1.7. PrP biogenesis and trafficking.....	34
1.7.1. Endocytic trafficking of PrP ^c	35
1.7.2. Lipid rafts and internalisation	37
1.7.3. PrP ^{sc} localisation and site of conversion	38
1.7.4. Topological variants of PrP	40
1.7.5. Proteasomal processing and ERAD (Endoplasmic Reticulum Associated Degradation)	41
1.8. Function of PrP	43
1.8.1. Copper binding and SOD activity	43
1.8.2. PrP and Cell signalling.....	44
1.8.3. PrP and cell survival	45
1.8.4. PrP binding molecules	45
1.9. Animal models of Prion disease	47
1.9.1. PrP knockout mice	47
1.9.2. Transgenic models of human Prion diseases	48

1.9.3.	Transgenic studies of the species barrier	49
1.9.4.	Transgenic models of Prion strains.....	50
1.10.	In vitro models of Prion disease	52
1.11.	Cell Culture Models.....	55
1.11.1.	Cell culture models supporting Prion replication	56
1.11.2.	Mutant PrP molecules in cell culture	59
1.11.3.	Insights into Prion transfer from culture models	60
1.12.	Progression of Prion disease and Pathogenesis.....	61
1.12.1.	Peripheral entry site for Prion.....	61
1.12.2.	Prions and Lymphocytes.....	62
1.12.3.	Prion entry into the nervous system.....	63
1.12.4.	Spread of Prion within the CNS	64
1.13.	Neuropathology.....	64
1.14.	Prion therapeutics	65
1.15.	Rationale for experiments of this thesis	67
Chapter 2	Materials and Methods.....	68
2.1.	Molecular Biology.....	69
2.1.1.	Standard protocols employed for molecular biology	69
2.1.1.1.	PCR (polymerase chain reaction)	69
2.1.1.2.	Restriction digestion and ligation of DNA.....	69
2.1.1.3.	Preparation of DNA.....	69
2.1.2.	Generation of constructs: GFP in fusion with PrP, DsRedII in fusion with PrP and 3F4 mutant fusion.....	70
2.1.3.	Site-directed mutagenesis to generate the 3F4 epitope.....	71
2.1.4.	Other vectors employed.....	71
2.2.	Cell culture	72
2.2.1.	Cell transfection	72
2.2.2.	Cell lines and cell media	72
2.2.3.	Cell lines expressing fusion protein.....	73
2.2.4.	Preparation of culture materials by lysis	74
2.2.5.	Preparation and infection with dead cell freeze-thaw lysates...	74
2.2.6.	Treatment with Tunicamycin	75
2.2.7.	Biotinylation protocol (Walmsley, Zeng et al. 2001)	75
2.2.8.	PIPLC treatment to cleave GPI anchored fusion protein.....	75

2.2.9.	Preparation of cells for Microscopy	76
2.2.9.1.	Time-lapse	76
2.2.9.2.	Preparation of cells for Immunocytochemistry	76
2.2.9.3.	Preparation of cells for Confocal microscopy	76
2.3.	Microscopy	78
2.3.1.	Time-lapse microsocopy	78
2.3.2.	Microscopy for immunocytochemical studies	80
2.3.3.	Use of confocal for FRAP (fluorescence recovery after photobleaching) measurements	80
2.3.3.1.	Experimental set 1	80
2.3.3.2.	Experimental set 2	81
2.3.3.3.	Data analysis of FRAP experiments	81
2.4.	Biochemistry	82
2.4.1.	Processing for analysis of PrP ^{sc} and PrP ^c	82
2.4.2.	BCA assay for total protein quantification	82
2.4.3.	Preparation of samples with N-glycanase	83
2.4.4.	Western blotting	83
2.4.4.1.	Quantification of western blots	84
2.4.5.	Immunoprecipitation	84
2.4.6.	Immunoflourescence studies	85
2.4.6.1.	Fixation protocols	85
2.5.	Reagents	86
2.5.1.	Antibodies	86
2.5.1.1.	For western blotting	86
2.5.1.2.	For immunocytochemistry	86
2.5.2.	Solutions and Buffers	86
2.5.2.1.	General purpose	86
2.5.2.2.	Cell culture	87
2.5.2.3.	Preparation for and generation of Western blot	87
2.5.2.4.	Western blotting procedure	88
2.5.2.5.	Immunoprecipitation	88
Chapter 3	The Role of Glycoform in Infection	89
3.1.	Introduction	90
3.2.	SMB and PS: Assay for infectivity	92

3.3.	PrP localisation	94
3.4.	Glycosylation of PrP ^{sc} and PrP ^c	97
3.5.	Relative contribution of glycoform species to <i>in vivo</i> conversion.....	99
3.5.1.	Glycosylation as a determinant of Prion infection	102
3.6.	Discussion.....	107
Chapter 4	Cell lines expressing PrP fluorescent fusion proteins	111
4.1.	Introduction	112
4.2.	Construction of fluorescent fusion proteins	113
4.3.	Transient expression of constructs.....	115
4.4.	Biochemistry of transiently expressed fluorescent fusion proteins	117
4.5.	Creation of Stable Transfectants.....	120
4.6.	Conversion of PrP ^c in fusion to PrP ^{sc}	126
4.6.1.	Immunoprecipitation experiments	132
4.7.	Discussion.....	136
Chapter 5	Applications of fluorescent fusion proteins in the study of system dynamics.....	139
5.1.	Introduction	140
5.2.	The time-lapse approach and Proteasomal inhibition	142
5.3.	Investigations of Prion protein transfer between cells by time-lapse microscopy.....	149
5.4.	Diffusion of Prion protein in the plasma membrane: An analysis by FRAP (Fluorescence Recovery After Photobleaching)	157
5.5.	Discussion.....	164
Chapter 6	Summary, discussion, and future directions.....	168
7.	References	178
8.	Appendix Matlab script	197

Table of Figures

Figure 1.1.	Diagram of mutations in Prnp known to cause pathogenesis...	21
Figure 1.2.	Diagram of PrP before and after cleavage with Proteinase K..	25
Figure 1.3.	Schema for conversion of PrP ^c to PrP ^{sc}	28
Figure 1.4.	NMR structure of human PrP	33
Figure 1.5.	Diagram of PrP modifications in the ER following synthesis of the polypeptide... ..	35
Figure 1.6.	Diagram illustrating the two potential routes of PrP endocytosis	36
Figure 1.7.	Topological variants of PrP	40
Figure 1.8.	Assay for PrP ^c and PrP ^{sc}	57
Figure 2.1.	Time-lapse apparatus.	78
Figure 3.1.	Analysis of TSE strain glycoform profiles passaged in mice	91
Figure 3.2.	Processing of SMB and PS cells for detection of Prion and normal isoforms.....	93
Figure 3.3.	Immunocytochemistry of PS and SMB cells.....	95
Figure 3.4.	Surface biotinylation of SMB cells.....	96
Figure 3.5.	Manipulation of PrP ^{sc} and PrP ^c glycoform species in SMB cells	98
Figure 3.6.	SMB cells treated with tunicamycin.....	100
Figure 3.7.	Quantification of total PrP ^c (A) and total PrP ^{sc} (B) following tunicamycin treatment and quantification of normal glycoform profile of PrP ^c (C) and PrP ^{sc} (D) in SMB cells.	101
Figure 3.8.	Washout of tunicamycin from SMB cells.....	103
Figure 3.9.	Schema of process of infection with manipulated Prion glycoforms....	105
Figure 3.10.	Inoculums used for infection	106
Figure 3.11.	Analysis of PS cells after infection with cell derived inoculums	106
Figure 3.12.	Schema of two hypotheses for glycoform maintenance.....	109
Figure 4.1.	Construction of GFP-PrP fluorescent fusion proteins.....	114
Figure 4.2.	Transient expression of constructs in PS and SMB cells	116
Figure 4.3.	Transient expression of GFP-PrP fusion protein.....	119
Figure 4.4.	Transient expression of F4-GFP-PrP fusion protein	119
Figure 4.5.	Micrographs of stable transfectants	122
Figure 4.6.	PIPLC treatment of cell pairs expressing F4-GFP-PrP	123
Figure 4.7.	Micrographs of fixed F4-GFP-PrPst uninfected cells	124

Figure 4.8. Micrographs of fixed F4-GFP-PrPstInf, infected cells stained with antibodies to PrP or GFP.....	125
Figure 4.9. Transient expression of F4-GFP-PrP in SMB cells	129
Figure 4.10. Conversion to Prion isoform of PrP ^c in fusion protein expressed in stable transfectants	130
Figure 4.11. Cleavage of the fusion protein	131
Figure 4.12. Schema for Immuno precipitation of fusion protein from infected cells.....	134
Figure 4.13. Immunoprecipitation of fusion protein from infected stable transfectants.....	135
Figure 5.1. Effects of proteasomal inhibition on F4-GFP-PrPst cells	146
Figure 5.2. Effects of proteasomal inhibition on F4-GFP-PrPst cells in detail.....	147
Figure 5.3. Effect of Proteasomal inhibition on PS cells.....	148
Figure 5.4. Release of cytoplasmic material from uninfected cells expressing DsRed.....	153
Figure 5.5. Release of cytoplasmic DsRed from Infected PS cells expressing DsRed.....	154
Figure 5.6. Expression of a fusion construct between DsRedII and PrP in PS cells.....	155
Figure 5.7. Time-lapse of cells expressing cytoplasmic fluorescent proteins.....	156
Figure 5.8. Illustrative diagramme of technique for fluorescence recovery after photo bleaching	160
Figure 5.9. Experimental result from FRAP using a Zeiss LSM 510	161
Figure 5.10. Results of FRAP experiments on uninfected (panels in A) and infected F4-GFP-PrP cells (panels in B).....	162

List of Tables

Table1.1	Summary of Animal TSE's	15
Table1.2	Human prion diseases summary.....	17
Table1.3	Summary of cell types utilised for the study of prion infection..	56
Table5.1.	Diffusion coefficients associated with experimental results depicted in Figure 5.10	163

Supporting Data

In addition to the printed thesis, a CD-ROM is included containing supplementary time-lapse movie data which is not essential to the presentation of material in this thesis but is intended to complement it. The contents of the CD-ROM is listed below. Please refer to the indicated figures within the thesis for further descriptions. The disk and its movies have been tested to run on PC and Macintosh computers (OS X).

Movie name : corresponding to figure legend and chapter	Description
5.1	Investigation of proteasomal inhibition
5.1A	F4-GFP-PrPst cells 40x resolution Time-lapse 15 hours
5.1B	F4-GFP-PrPst cells treated with Mg132 (50 μ M) 40x resolution Time-lapse 15 hours
5.1C	Zsreen expressing cells with Mg132 (to 50 μ M) 40x resolution Time-lapse 15 hours
5.4 and 5.5	Investigation of fusion protein transfer
5.4	F4-GFP-PrP-stInf cells with uninfected cells expressing DSRed 40x resolution Time = 5 hours
5.5	F4-GFP-PrPst cells with infected cells expressing DSRed 40x resolution Time = 6 hours
5.7	Investigation of transfer of cytoplasmic material
5.7A	Uninfected GFP vs Uninfected DSRed expressing cells 20x resolution Time 24 hours
5.7B	Area of interest from 5.7A over 3 hours, illustrating an event following contact between two cells (includes frames from figure 5.7B which span a 45 minute period).

Abbreviations

Ala – alanine (A)
Arg – arginine (R)
Asn – asparagine (N)
Asp – aspartic acid (D)
BCA - Bicinchoninic acid protein assay
BrdU - 5-bromo-2'-deoxy-uridine
BSA – bovine serum albumin
BSE – bovine spongiform encephalopathy
cDNA – copy DNA
C terminal – Carboxy terminal
CFP – cyan fluorescent protein
CJD – Creutzfeldt-Jakob Disease
CHO – Chinese hamster ovary
CLD – caveolae-like domain
CNS – central nervous system
CPE - cytoplasmic polyadenylation element
CPEB – cytoplasmic polyadenylation element binding protein
CWD – Chronic Wasting Disease
Cys – cysteine (C)
DMEM – Dulbecco's modified Eagle's medium
Dpl - Doppel
DNA – deoxyribonucleic acid
DsRed – Discosoma red protein
EDTA - ethylenediaminetetraacetic acid
EM – electron microscopy
EndoH – endoglycosidase H
ER – endoplasmic reticulum
ERAD – endoplasmic reticulum-associated degradation
E.Coli – Escherichia Coli
fCJD – familial CJD
FCS – foetal calf serum
FDC – follicular dendritic cell

FFI – Fatal Familial Insomnia
FITC - fluorescein isothiocyanate
FRAP – fluorescence recovery after photobleaching
FVB – Friend leukaemia virus B
GABA - gamma-aminobutyric acid
GFP – green fluorescent protein
Gln – glutamine (Q)
Glu - glutamic acid (E)
Gly – glycine (G)
GPI – glycol-phosphatidyl-inositol
GSS - Gertsmann-Straussler-Scheinker syndrome
His – Histidine (H)
HSP – heat shock protein
IAH – Institute of Animal Health
Ile – isoleucine (I)
IG – immunoglobulin
Leu – leucine (L)
LR – laminin receptor
LRP – laminin receptor precursor protein
LT - lymphotoxin
LTP – long-term potentiation
Lys – lysine (K)
Met – methionine (M)
MoPrP –mouse Prp
mRNA – messenger ribonucleic acid
N linked – Asparagine-linked
N terminal – amino terminal
NMR – nuclear magnetic resonance
NP40 – Nonidet P40
PAGE – polyacrylamide gel electrophoresis
PCR – polymerase chain reaction
PFA - paraformaldehyde
Phe – phenylalanine (F)
PIPLC – phosphatidylinositol-specific phospholipase C

PK – Proteinase K
PMCA – protein misfolding cyclic amplification
PMSF - phenyl methyl sulfonyl fluoride
PNS – peripheral nervous system
Prnp – Prion Protein gene
Prnd – Doppel gene
Pro – proline (P)
PrP-res – protease-resistant PrP
PrP^{SC} – Scrapie Prion Protein
PrP^C – Cellular Prion Protein
PS – pentosan sulphate
Rb – retinoblastoma
RML – Rocky Mountain Laboratory
RNA – ribonucleic acid
RNase – ribonuclease
SDS – sodium dodecyl sulphate
Ser – serine (S)
sFFI – sporadic familial fatal insomnia
SMB – scrapie mouse brain
SOD – superoxide dismutase
TBS – Tris-buffered saline
Thr – threonine (T)
TME – Transmissible Mink Encephalopathie
TRITC - tetramethyl rhodamine isothiocyanate
Trp – tryptophan (W)
Tyr – tyrosine (Y)
TSE - Transmissible Spongiform Encephalopathie
UTR – untranslated region
UV – ultra violet
Val – valine (V)
vCJD – variant Creutzfeldt-Jakob Disease
YFP – yellow fluorescent protein

Chapter 1 Introduction

1.1. Introduction overview

The Transmissible Spongiform Encephalopathies (TSE's) are a group of neurodegenerative diseases now thought to be associated with a novel form of infectious agent called a prion. An aberrant conformer, PrP^{sc}, of a normal cellular protein, PrP^c is thought to propagate by co-opting normal protein into its conformation by an as yet undiscovered mechanism. The introduction below reviews the group of diseases associated with the Prion phenomenon and then discusses the Prion hypothesis in more detail. In the context of models of the diseases, some of the key issues of the field are highlighted and discussed including the basis for strain variation, the transfer of a Prion infection, and the cell biology of the normal and abnormal forms of the Prion protein (PrP^c and PrP^{sc} respectively). Finally, potential therapeutics are considered for a group of diseases which have so far proved untreatable.

1.2. Animal TSE's

Table 1.1 Summary of Animal TSE's
adapted from (Aguzzi and Sigurdson 2004)

Disease	Natural host species	Transmission route	Other Susceptible species
Scrapie	Sheep and Goats	Horizontal/Vertical	Primates, hamsters, wild-type mice, ovine PRNP-transgenic mice
Chronic wasting disease	Mule deer, white-tailed deer and Rocky mountain elk	Horizontal/Vertical	Ferrets
Bovine spongiform encephalopathy	Cattle	Ingestion of BSE-contaminated feed	Primates, wild-type mice, bovine/human Prnp-transgenic mice
Spongiform encephalopathy of zoo animals	Zoological bovids and primates	Ingestion of BSE-contaminated feed	Wild-type mice
Feline spongiform encephalopathy	Zoological and domestic felids	Ingestion of BSE-contaminated feed	Wild-type mice
Transmissible mink encephalopathy	Mink	Ingestion, origin of epidemic unclear	Wild-type mice

Scrapie is a naturally occurring disease of sheep and goats which is endemic in Europe, and was first identified over 200 years ago. Surprisingly, little is known

about the key mode of transmission of Scrapie although it is thought to be both horizontal, (Pattison, Hoare et al. 1972) and vertical (Elsen, Amigues et al. 1999). There is no epidemiological evidence for a connection between Scrapie and Creutzfeldt-Jakob disease (CJD), a human prion-associated disease (Brown, Cathala et al. 1987). A wide variety of Scrapie strains exist as defined by vacuolation profile in the CNS (central nervous system), incubation time in animal models, and these strains are associated with a wide range of PrP^{sc} glycosylation profiles (Somerville, Chong et al. 1997). A number of studies have indicated that the natural incidence of Scrapie in a flock is dependent on the genetic background and the allelic variation amongst sheep. Three polymorphisms in the PrP gene are particularly linked with the occurrence of Scrapie: A136V, R154H, Q171R/H. The alleles ARQ, ARH, VRQ are commonly associated with susceptibility to disease in contrast to ARR and AHQ which are associated with resistance (Spraker, Miller et al. 1997; Baylis and Goldmann 2004). This finding has led to a European wide initiative to select ARR/ARR sheep in favour of other allelic variants in order to breed out Scrapie. It is noteworthy however, in the light of the BSE (Bovine spongiform encephalopathy) epidemic, that ARR/ARR sheep are susceptible to BSE (Kao, Gravenor et al. 2002; Kao, Houston et al. 2003).

Other animal TSEs (summarised in Table 1.1) include Transmissible Mink Encephalopathy (TME) (Bessen and Marsh 1992; Marsh and Hadlow 1992) and Chronic wasting disease (CWD) of mule deer and elk, a common condition in wild deer and elk in Colorado (Spraker, Miller et al. 1997; Miller and Williams 2004). Of particular interest to Prion theory is the existence of two distinct TME strains which were identified after passage to hamster and named *hyper* and *drowsy* for their distinct clinical presentations (Bessen and Marsh 1992; Bessen and Marsh 1992). These strains, after passage through hamsters, demonstrate different vacuolation profiles, incubation periods and different sensitivity to Proteinase K digestion. The latter property has been taken as one possible indication of conformational differences which might underlie the difference in strain properties.

In 1986 a new Prion disease BSE was identified at the start of what was to become an epidemic which led to an estimated total number of 1 million infected animals in the U.K. (Wilesmith, Ryan et al. 1991; Anderson, Donnelly et al. 1996). Epidemics of smaller size were also reported in a number of other European countries (Collinge 2001). Hypotheses for the cause of the disease initially included transmission of Scrapie to cattle but it is more likely that rare sporadic cases of cattle disease entered into the food chain. The change in the 1970s in the rendering process of the protein supplement , meat and bone meal that is fed to the animals may have led to an increased Prion content and a resultant increase in exposure (Collinge 2001).

Many other species of Bovidae and Felidae, probably fed with the same rendered meat and bone meal, have since been identified as having contracted the disease (Bruce, Chree et al. 1994; Collinge, Sidle et al. 1996). The range of species is particularly noteworthy when comparing BSE with natural Scrapie because these reports of BSE crossing the species barrier have highlighted the difference in host range of the new disease.

1.3. Human Prion Disease

Table 1.2 Human prion diseases summary

adapted from (Aguzzi and Sigurdson 2004)

Disease	Natural host species	Transmission route	Other Susceptible species
Creutzfeldt-Jakob disease	Humans	Familial (PRNP germ line mutation), sporadic, or iatrogenic	Primates, hamsters, wild-type mice, Human PRNP-transgenic mice
Variant Creutzfeldt-Jakob disease	Humans	Ingestion of BSE-contaminated food	Wild-type mice, Human PRNP-transgenic mice
Kuru	Humans	Ingestion or ritualistic cannibalism	Primates
Fatal familial Insomnia	Humans	Familial (PRNP germ line mutation)	Wild-type mice
Gertsmann-Straussler-Scheinker syndrome (GSS)	Humans	Familial (PRNP germ line mutation)	Primates and mutated PRNP-transgenic mice

The human TSE's (summarised in table 5.2) were originally identified through their symptomatic and then pathological profiles, with Creutzfeldt-Jakob disease

(CJD) the first to be described in 1926. They present as infectious (acquired), genetic and sporadic conditions (Ironside 1998). The extent of shared aetiology between these types of Prion disease remains to be determined.

1.3.1. Sporadic Prion disease

The annual incidence of CJD has been established at an average of 1 case per million of the population and sporadic CJD accounts for 85 % of all CJD cases (Brown, Preece et al. 1992; Will 1998). The disease is characterised by a stereotyped, rapidly progressive clinical course with median duration of 4 months and occurring in the 45-75 age range, with mean age 66 (Collinge 2001). There is no predictable geographic clustering (Will, Matthews et al. 1986) and no established common environmental risk factor (Wientjens, Davanipour et al. 1996). A genetic risk factor has been identified in relation to codon129 (M129V) polymorphism of the PrP gene (Palmer, Dryden et al. 1991). The brain pathology associated with CJD includes spongiform degeneration, exhibiting a wide variety of intensities and distributions from case to case, and reactive astrocytic gliosis (DeArmond 2004).

1.3.2. Acquired human Prion disease

Kuru was first recorded as an acquired human Prion disease, when an epidemic occurred in the Fore people of Papua New Guinea. The central clinical feature is progressive cerebellar ataxia. In sharp contrast to CJD dementia is often absent. It was transmitted through the cannibalistic rituals associated with consumption rites for deceased relatives and community members (Alpers 1987). The epidemic is thought to have originated following the consumption of a community member that had died from CJD of sporadic origin. Although the cannibalism ceased in the late 1950's, cases of Kuru still occur in the region suggesting incubation periods of up to 40 years. The incidence in children indicates that incubation period can be as short as 4 years (Alpers 1987).

Iatrogenic transmission has been suggested in numerous surgical interventions. In 1974 transmission of CJD was found in a patient who had received a corneal

implant from a donor that had died of CJD (Duffy, Wolf et al. 1974). It has also been suggested that transmission of CJD has occurred through the use of depth electrodes and cases have been reported of transmission through dura matter grafts (Thadani, Penar et al. 1988). Transmission of CJD through growth pituitary derived growth hormone and gonadotrophin have also been reported (Koch, Berg et al. 1985).

All of these transmissions have involved cross contamination with material from the brain, where the expected titre of infection is presumed to be high, and have involved parenteral inoculation through surgery or intramuscular injection. Interestingly, cases resulting from intracerebral or optic inoculation manifest as conditions similar to classical CJD, with a rapidly progressive dementia. In contrast, cases resulting from peripheral inoculation often present with progressive cerebellar ataxia, a presentation more reminiscent of Kuru (Collinge 2001).

It is still unclear if Prion transmission is possible through other infected tissues such as the blood. Laboratory studies have shown both the presence of infectivity and the development of disease in animal models (Diringer 1984; Casaccia, Ladogana et al. 1989). Case control studies have not identified increased risk in haemophiliacs of CJD (Wientjens, Davanipour et al. 1996) and claims of transfusion related patient cases of CJD have not been substantiated (Klein and Dumble 1993).

The evidence indicates that transmission of CJD via the blood route is unlikely. However, this does not necessarily apply to New Variant CJD (vCJD) transmission and the finding that BSE infection via blood, from sheep to sheep, is reasonably efficacious is of particular concern (Houston, Foster et al. 2000; Hunter, Foster et al. 2002). A recent case of a blood transfusion recipient who contracted vCJD has highlighted the possibility of its transmission via the blood (Aguzzi and Glatzel 2004).

Following the BSE epidemic, surveillance of CJD in the UK was instituted in 1990 to assess the possibility of transmission to humans. By 1995 a number of

cases of CJD with distinct clinical presentation and pathology had emerged. Presentation of illness was identified with a mean age of onset of 29 years in comparison to 66 years for sporadic CJD and with 14 months illness duration compared to 4.5 months. The clinical presentation was unusually uniform and the pathological profile distinct (Will, Ironside et al. 1996).

The case for a causal link between BSE and vCJD has been argued epidemiologically and through reference to pathology, biochemistry and findings using animal models. To date there have been less than 150 cases of vCJD identified world wide with the majority in the U.K. The geographical clustering and the relative timing of the majority of these vCJD and BSE cases in the U.K., has indicated BSE as a novel risk factor (Will and Kimberlin 1998). The neuropathological features of vCJD have been reproduced by macaque monkeys inoculated with BSE (Lasmez, Deslys et al. 1996) and the existence of similar Prion glycoform patterns has been argued as evidence of common strain (Collinge, Sidle et al. 1996). Of particular note, given the reproducibility of incubation time with strain type, BSE and vCJD inoculation into mouse models has demonstrated similar incubation period and vacuolation profile, features that would ordinarily indicate a common strain of Prion (Bruce, Will et al. 1997; Hill, Desbruslais et al. 1997).

One risk factor that has emerged consistently is the genetic background of the patients. In all cases of vCJD infection to date the patients are homozygous for methionine at Prnp codon 129 (Zeidler and Ironside 2000).

Epidemiologists have struggled with the paucity of data available to formulate consistent estimates for the final numbers of people that will suffer from vCJD as a result of the BSE epidemic, and predictions vary widely from a few hundred people to tens of thousands (Cousens, Vynnycky et al. 1997; Ghani, Ferguson et al. 2000; d'Aignaux, Cousens et al. 2001; Ghani 2002; Ghani, Ferguson et al. 2003).

1.3.3. Genetic Prion Disease

Inherited Prion disorders account for around 10 percent of human Prion diseases and are all autosomal dominant conditions (Cohen 1994). Currently 55 pathogenic mutations and 16 polymorphisms have been identified in the Prnp gene. These are described by either point mutations in the gene, which result in an amino acid substitution/stop codon, or insertions/deletions in the octapeptide repeat region (Fig 1.1)

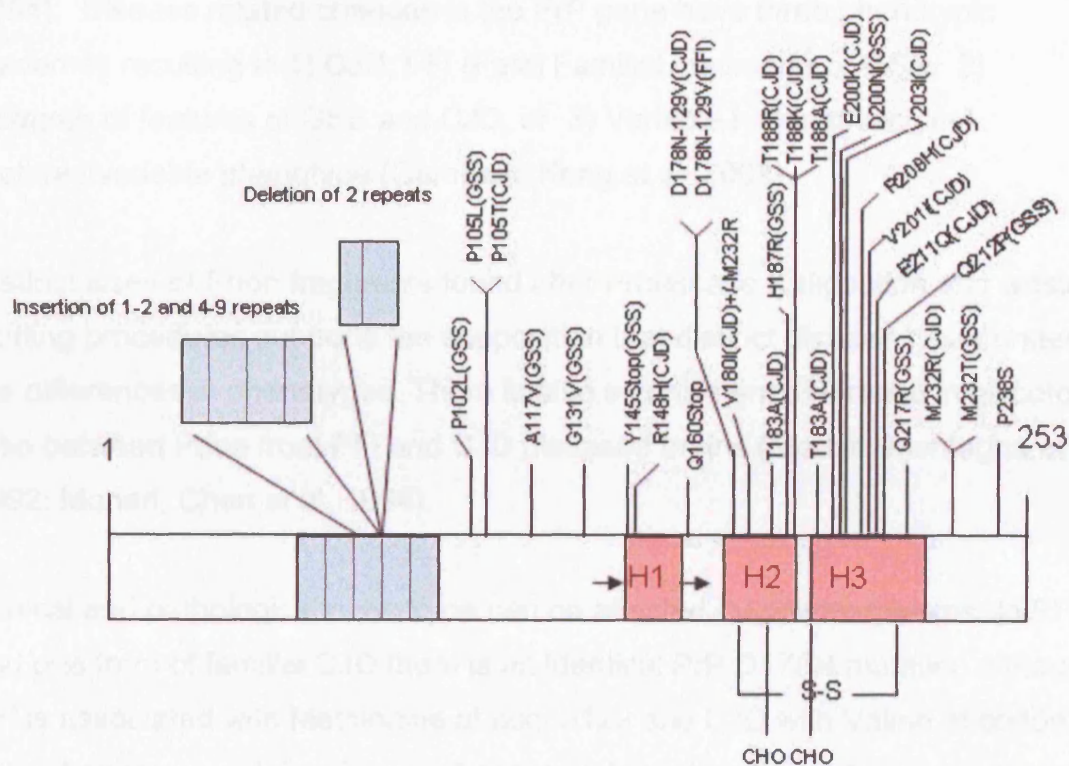


Figure 1.1. Diagram of mutations in Prnp known to cause pathogenesis.

β -sheet is indicated by arrows and alpha helix (H) in the light red shade.

'CHO' and 'S-S' indicates glycosylation and disulphide bond respectively.

Octapeptide repeat region is indicated in the blue shaded region. Disease association is stated (CJD, FFI, GSS), otherwise a variable phenotype is associated with the mutation, as with the octapeptide repeat insertions/deletions.

(Figure adapted from Kong et al 2004)

Models have suggested that mutations may favour spontaneous conversion to the Prion state by lowering the activation energy barrier for conversion from PrP^C to PrP^{Sc} (Cohen 1994). However, the aetiological background shared by exogenous infections and heritable Prion disease remains unclear (Mallucci and Collinge 2004). Familial Prion diseases have been demonstrated to be infectious as evidenced by transmission of CJD and GSS (Gertsmann-Straussler-Scheinker syndrome) to nonhuman primates (Prusiner 1998).

Classification of inherited Prion disease is often associated with phenotype rather than haplotype. (Medori, Montagna et al. 1992; Monari, Chen et al. 1994). Disease related changes in the PrP gene have three phenotypic outcomes resulting in 1) CJD, FFI (Fatal Familial Insomnia) or GSS, 2) mixtures of features of GSS and CJD, or 3) Variable histopathological features/variable phenotype (Gambetti, Kong et al. 2003).

Distinct sizes of Prion fragments found after Proteinase K digestion and western blotting procedures supports the supposition that distinct disease types underlie the differences in phenotypes. There is also a consistent difference in glycoform ratio between Prion from FFI and CJD diseased brains (Medori, Montagna et al. 1992; Monari, Chen et al. 1994).

Clinical and pathological phenotype can be affected by polymorphisms. In FFI and one form of familial CJD there is an identical PrP D178N mutation although FFI is associated with Methionine at codon 129 and CJD with Valine at codon 129. Phenotypic variation in age of onset and duration have also been shown to be affected by the E219K polymorphism. It is therefore important to describe the full haplotype when considering the inherited Prion diseases. (Ironside 1996; Ironside 1998).

GSS was first recognised as being linked with the P102L mutation (Hsiao, Baker et al. 1989) and is now recognised as being linked with many others including a Y145 stop mutation which results in truncated PrP protein (Ghetti, Dlouhy et al. 1995).

Variable phenotypes, have been associated with the insertion of 1-2 and 4-9 repeats in the octapeptide region of the gene and with deletions of 1 or 2 repeats in this region (Ironside 1998). Patients with five, six, seven, eight, and nine extra octapeptide repeats show an autosomal dominant pattern of inheritance and features of CJD, GSS, or atypical dementia, patients with one, two, or four extra repeats have typical CJD (Rossi, Giaccone et al. 2000).

1.4. The Prion concept

Following the recognition that Scrapie and Kuru showed similarities in pathology, the transmissibility of Kuru was established by intracerebral inoculation of chimpanzees (Gajdusek, Gibbs et al. 1966). CJD was later shown to be transmissible to animals and to result in a spongiform condition (Gibbs, Gajdusek et al. 1968). On this basis a group of transmissible diseases was identified which resulted in a spongiform encephalopathy prior to death, and included familial as well as classically infectious cases.

The Prion concept was initially postulated by Griffith in 1967 along with other concepts for replication in biological systems. Later it was taken up by Prusiner to explain a series of findings associated with the Scrapie agent. Prusiner defines a Prion as 'a proteinaceous infectious particle that lacks nucleic acid'. One might represent the implicit assumptions that comprise the modern Prion theory by the following statements:

- 1) A Prion is a protein that is able to replicate without the intervention of nucleic acid
- 2a) Replication refers to a property of the protein and not just a material copy
- 2b) In the case of the Scrapie Prion, the property that is replicated is responsible for the transmission of disease and or pathogenesis.
- 2c) the property is an alternate conformation of the protein.

Before the impact of transgenic mice on the field, theories concerning the nature of the agent abounded. It was argued by Stanley Prusiner that the agent could not be a carbohydrate, lipid, or nucleic acid based infectious agent and that the agent was a protein (Bolton, McKinley et al. 1982; Prusiner 1982;

Prusiner, Bolton et al. 1982). The Scrapie agent is unusually resistant to attempted inactivation by U.V. and ionising radiation in comparison to virus related material. (Alper, Haig et al. 1966; Alper, Cramp et al. 1967; Latarjet, Muel et al. 1970). The implication of these results is that a traditional nucleic acid is unlikely to be part of the active virus and in search for a Scrapie specific nucleic acid associated with a viral like particle, many experiments have been performed which demonstrate that it would have to be smaller than 50-100 bases (Prusiner 1998).

Radiation inactivation studies also indicated that the infectious agent itself would have to be limited to a minimum size of 55 kda (Alper, Haig et al. 1966; Prusiner, Hadlow et al. 1978; Bellinger-Kawahara, Kempner et al. 1988) which on a protein only model implies a PrP dimer as the minimum size of the infectious particle.

Viral related theories have responded to these results, which inveigh heavily against the involvement of nucleic acid, by postulating that the viral DNA might have coat proteins that were highly homologous to PrP or protected by PrP^{sc}, and/or that PrP^c functioned as a viral receptor. The explanatory strength of viral theories has been an implicit model for the infectious process and an imagined clearer view of strain variation. However adaptations of previous versions of viral agent hypotheses suffered the charge of poor explanatory benefit and ad hoc adjustments to fit other data.

Work in transgenic mice has reinforced the hypothesis that a protein might be responsible for infectious propagation. Numerous experiments have confirmed the findings that PrP^c is necessary for propagation of infectivity, because knockout mice do not support disease infection, and that the efficacy of disease has been shown to be correlated with levels of expression of the PrP gene (Prusiner 1998). Although these experiments indicate the necessity of PrP for infection, the data is still compatible with a theory that might include viral transmission. The final test of the theory will be provided by confirmation of the *in vitro* production of Prion (see below).

Originally, studies on the sedimentation properties of Scrapie using sucrose gradients demonstrated that infectivity was poly-dispersed, making standard purification procedures difficult (Prusiner, Hadlow et al. 1977; Prusiner, Hadlow et al. 1978). A critical limit to research progression had been the length of time and number of animals necessary to assay for infectivity, despite the passage of Scrapie material within mouse models which decreased incubation times. The development of an assay which reduced incubation time and increased Prion titres in Syrian Hamsters by a factor of 5, (Marsh and Kimberlin 1975) permitted quantitative assessment of fractions enriched for infectivity and led to the now characteristic biochemical assay for PrP^{Sc}: A procedure including detergent extraction, protease digestion, and differential centrifugation was employed to purify infectious material and in turn led to sequencing of the protease resistant core of PrP^{Sc} (Bolton, McKinley et al. 1984) and later the cloning of Prnp (Basler, Oesch et al. 1986).

The resistant core is now associated with a cleaved product of PrP named PrP27-30 and it is understood that only part of the molecule acquires this resistance on conversion (see Figure 1.2).

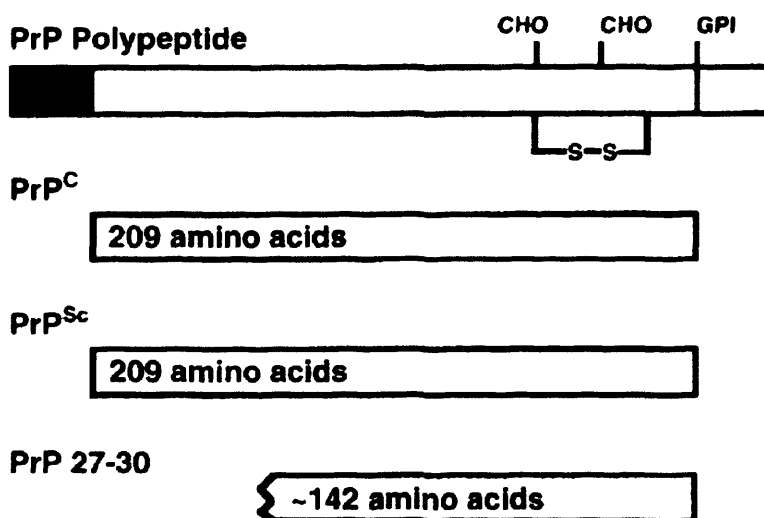


Figure 1.2. Diagram of PrP before and after cleavage with Proteinase K

Full length PrP polypeptide, PrP species following removal of N-terminal signal peptide, and the 142 amino acid protease resistant core of PrP^{Sc} following Proteinase K digestion (Adapted from Prusiner 1998)

The ratio of infectious units to PrP^{sc} molecules is 1:10⁵ and one interpretation of this is that only a small number of the PrP^{sc} related molecules in an infectious sample, as defined by protease resistance and detergent insolubility, are actually responsible for infection (Bolton, Rudelli et al. 1991). This has prompted theories that a particular species might be responsible for infection other than the traditionally defined PrP^{sc} (Weissmann 1991).

The most difficult aspect of the Prion hypothesis remains the explanation of the variety of TSE strains that exist. The simple solution has been to posit the existence of multiple, corresponding conformations. Although there is some evidence for association of strain with conformation (see 1.9.4) there is little evidence for the general scope of this hypothesis.

The idea that information is transferred by a Prion mechanism took a long time to be absorbed into the main stream because viral theories embodied the paradigm for envisaging how replication/transmission of information was thought to occur in disease. The discovery of DNA had set down a dogma in general for replication in biological systems. Now that the theory has been widely accepted there seem to be many additions to what was a straightforward protein only theory 20 years ago. Amongst these is the suggestion that accessory molecules are necessary for the conversion process and ironically, as reviewed elsewhere in this introduction, it has also been suggested that these accessory molecules may include nucleic acids.

1.4.1. Mechanisms of Prion replication

At present there is little evidence in favour of any particular model of conversion from PrP^c to PrP^{sc}. This is because there is no structural data from NMR or X-ray crystallography on PrP^{sc} and it has not been established which, if any, of the species produced from *in vitro* reactions are pertinent to actual physiological infection. Nevertheless, two basic models (see Figure 1.3) have been suggested for conversion of PrP^c to PrP^{sc}, a template-directed refolding model and a nucleation-dependent polymerisation model (Jarrett and Lansbury 1993; Lansbury and Caughey 1995; Weissmann 1996; Harrison, Chan et al. 1999).

The template assisted refolding model in its basic form posits a high activation energy barrier which under ordinary circumstances prevents the spontaneous conversion of PrP^c to PrP^{sc} . Templating of PrP^c with PrP^{sc} promotes conversion by lowering the barrier and shifting the equilibrium towards the PrP^{sc} form, a process which may include an unfolding step for PrP^c prior to a refolding step. The process then becomes self fuelling leading to an effective chain reaction in producing more PrP^{sc} to elicit more conversion of the cellular pool of PrP^c (Weissmann 1991; Weissmann 1996). On this model inherited Prion disease would be explained by alteration of the initial energy barrier due to an alteration in kinetics of protein folding caused by the mutation. However, this does not explain why the familial Prion diseases take many years before onset, despite expression of mutant genes. A more involved version of this model introduces a chaperone or protein X that is necessary for conversion (Telling, Scott et al. 1995). Here protein X binds to PrP^c and forms a complex that is able to convert when further templating with PrP^{sc} . The complex has been denoted $\text{PrP}^*/\text{protein X}$, to imply the difference in nature of the associated PrP species from the point of view of conversion potential.

The nucleation-dependent polymerisation process model, much along the lines suggested in work on yeast Prion, posits the slow formation of an infectious seed: a rate limiting step (Jarrett and Lansbury 1993). The seed then acts to promote further conversion, perhaps by stabilising PrP^{sc} , taking it out of a weak equilibrium with PrP^c . Predictions which distinguish this model from the template assisted refolding theory include the existence of a threshold concentration at which seed formation will occur, and the existence of a lag phase up to the point where seeding begins to take root. Evidence for this model has been found from *in vitro* studies (Kocisko, Come et al. 1994; Bessen, Kocisko et al. 1995; Kocisko, Priola et al. 1995; Kocisko, Lansbury et al. 1996). In the case of infectious disease, the model posits that exogenous seed like material is introduced to catalyse further conversion.

The two models are not necessarily mutually exclusive and it is possible that components of each may play a role in the production of infectious Prion. It is

also conceivable that protein X like phenomena could be explained in the context of a nucleation-dependent polymerisation.

1.4.2. Yeast and Other Prions

There is an open question as to how ubiquitous the Prion phenomenon is in the biological world which is of particular interest because Prion offers a distinct form of heritable information transfer.

Two non-Mendelian cytoplasmically inherited traits in *Sacharomyces cerevisiae* were explained by the [PSI⁺] and [URE3] associated Prion states (Wickner 1994; Wickner, Masison et al. 1995).

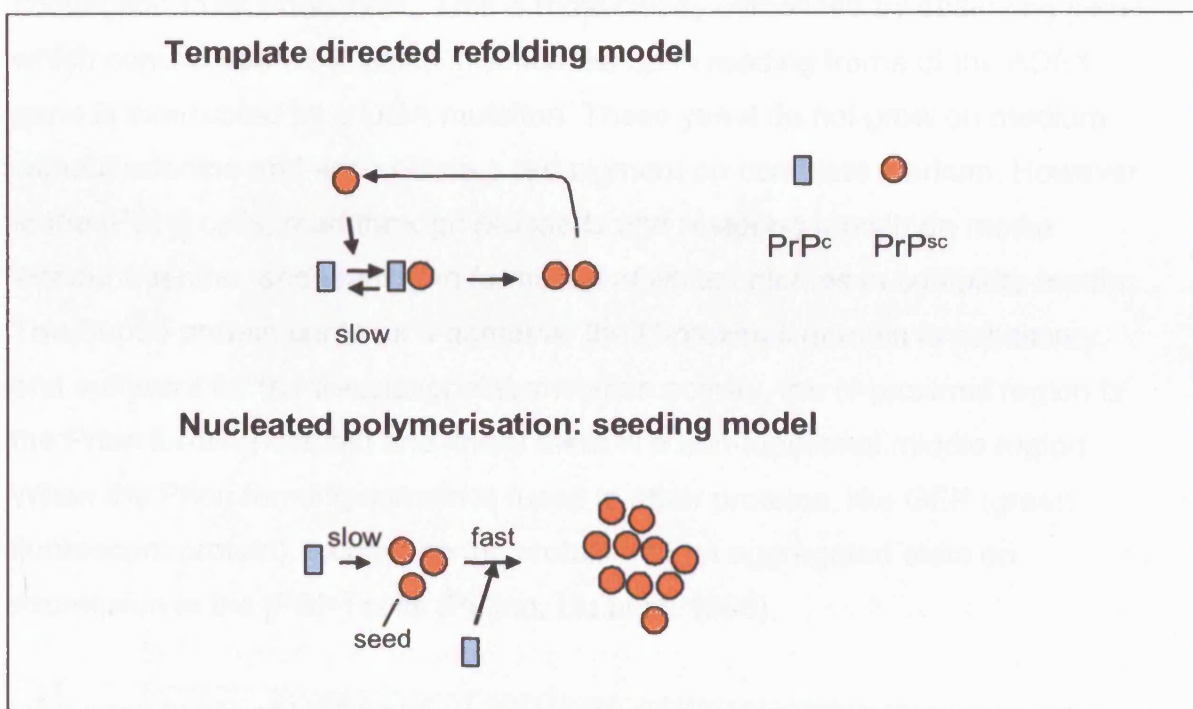


Figure 1.3. Schema for conversion of PrP^{C} to PrP^{Sc}

Template directed refolding model: Templating of PrP^{C} with PrP^{Sc} elicits conversion in an otherwise thermodynamically unstable reaction.

Seeding model: The conformational change occurs independently of a templating step but is stabilised by formation of a seed, the rate limiting step, and then further formation of larger aggregates. (Adapted from Weissmann 1996)

The existence of the Prions underlying these states explained a) that for propagation the expression of the SUP35 and URE2 genes were necessary, b) that growth on guanidine hydrochloride returns the yeast to their original states, and c) that overexpression of URE2 and Sup35p increased the frequency of the novel states. More Prion related states in yeast and other systems have since been discovered including [Het-S] [RNQ+], [NU+] (Osherovich and Weissman 2002; Uptain and Lindquist 2002). Of particular interest is the fact that these non-mammalian Prions are often associated with either gain or loss of function as a result of conversion to the Prion form.

Sup35, a normal yeast gene, has been implicated in the process of translational termination (Chernoff, Uptain et al. 2002). In [PSI+] cells, the Prion state, nonsense suppression occurs because the usual function of Sup35 is lost upon conversion to its Prion form. This is most clearly evidenced by observing yeast which contain ade1-14 alleles in which the open reading frame of the ADE1 gene is interrupted by a UGA mutation. These yeast do not grow on medium without adenine and accumulate a red pigment on complete medium. However in the [PSI+] cells, read through proceeds and restoring growth on media without adenine, and leading to formation of white colonies in complete media. The Sup35 protein contains 3 domains: the C-proximal domain is necessary and sufficient for the translational termination activity, the N-proximal region is the Prion forming domain and finally there is a non-functional middle region. When the Prion forming domain is fused to other proteins, like GFP (green fluorescent protein), it converts the protein into an aggregated state on expression in the [PSI+] cells (Patino, Liu et al. 1996).

Increased levels of HSP104 have been shown to affect PSI+ propagation in yeast (Chernoff, Lindquist et al. 1995). Overproduction of HSP104 in yeast cells leads to curing of [PSI+]. However, deletion of HSP-104 also results in the loss of the [PSI+] and reversion to [PSI-]. The apparent contradiction has been partially resolved by work which demonstrates a subtle disaggregating role for the chaperone in cooperation with other chaperone protein (Sanchez, Taulien et al. 1992; Glover and Lindquist 1998). Models suggest that the function of HSP-104 is to disaggregate, which leads to curing of the Prion state. However,

disaggregation of Prion by HSP-104, is also necessary for maintenance of seeds of the right size in order to continue the process of conversion. In favour of the latter part of the model, GFP-Sup35 fusion proteins rapidly accumulate and form large GFP-Sup35 aggregates on loss of HSP104 activity (Wegrzyn, Bapat et al. 2001). It is an interesting model that might have some relevance in the mammalian system, although this remains to be tested in the light of future advances in antibody technologies. Other chaperones, including Hsp70 and Hsp40, have also been implicated in yeast Prion propagation (Glover and Lindquist 1998; Allen, Wegrzyn et al. 2004).

In some ways the yeast system is the envy and goal of present studies in mammalian systems. For example, two aspects of Prion theory have been clearly demonstrated, enabling models for further research into the molecular basis of Prion phenomena in yeast. Firstly, *in vitro* forms of Prion can be prepared which demonstrate activity *in vivo*: Induction of [PSI⁺] could be achieved by the introduction of recombinant fragments of Sup35 into [PSI⁻] cells (Sparrer, Santoso et al. 2000). Secondly, distinct strain types can be produced *in vitro* which are associated with conformational differences, and are propagated faithfully *in vivo*. *In vitro* Prion was formed by protocols at different temperatures resulting in different conformations of the recombinant amino-terminal fragments. Different Prion strains were then generated and faithfully propagated following introduction of the *in vitro* formed conformers into [PSI⁻] cells (Tanaka, Chien et al. 2004).

It may also be the case that alternative Prions exist in mammals. A role for mRNA at the synapse has been postulated in the formation of long term potentiation and a leading candidate for regulation of mRNA translation in this regard has been cytoplasmic polyadenylation element binding protein (CPEB)(Richter 2001; Huang, Carson et al. 2003). CPEB activates translationally dormant mRNA in *Xenopus* oocytes by binding to polyadenylation binding elements (CPE) within the 3'UTR following synaptic stimulation (Richter 2001; Huang, Carson et al. 2003). In *Aplysia* ApCREB has an N-terminal motif with multiple Glutamine/Asparagine repeats, reminiscent of the yeast Prion domains. Following overexpression CPEB demonstrates the

ability to bind to CPE's and activate translation. It also demonstrates Proteinase K resistance and the ability, *in vitro*, to confer this property on newly formed protein. The system therefore indicates a potential switch for LTP (long term potentiation): overexpression of CPEB, caused by dendritic stimulation, and subsequent conversion to the Prion state, produces an effectively maintained 'ON' state, in which CPEB can bind and activate translation of mRNA (Si, Giustetto et al. 2003; Si, Lindquist et al. 2003).

1.5. PrP gene structure and expression

All known mammalian and avian PrP gene coding regions reside within a single exon (Prusiner and Scott 1997). One implication of this is that differences in protein structure associated with PrP^{sc}, or cellular properties of PrP, cannot be attributed to gene splicing. PrP protein is encoded by the gene locus *Prnp*, which is now thought to be proximal to a second locus, 19kb downstream, termed *Prnd*, which encodes the Doppel (*Dpl*) gene (Moore, Lee et al. 1999). The *Prnd* locus has 24% coding sequence identity with the *Prnp* locus.

Sequencing of PrP from multiple species has demonstrated that there is a high degree of conservation between the mammalian and avian PrP genes (Schatzl, Da Costa et al. 1995). The chicken sequence is more divergent from the human gene than the others (Gabriel, Oesch et al. 1992). There is a high degree of conservation of the P(H/Q)GGG(G)WGQ sequence found repeated in the octapeptide repeat region (Goldmann, Hunter et al. 1991; Prusiner, Fuzi et al. 1993) and a conserved Alanine-Glycine rich region found from A113 to Y128, the C-terminal end of the octapeptide repeat region (Hsiao, Cass et al. 1991).

Prnp haplotype diversity and coding allele frequencies suggest that strong balancing selection has occurred during the evolution of modern humans, and indicates possible selection for disease resistance. The implication is that Prion disease has had some influence on the gene's structure (Mead, Stumpf et al. 2003).

Studies have suggested that prp message is expressed in the adult brain of animals in neurons, and to varying extents in glia (Chesebro, Race et al. 1985; Oesch, Westaway et al. 1985; Ford, Burton et al. 2002) and that it is highly regulated during development (Mobley, Neve et al. 1988). Expression of PrP has also been detected in heart, lung, spleen, skeletal muscle and testis (Oesch, Westaway et al. 1985; Bendheim, Brown et al. 1992). By contrast, Dpl is expressed at low levels in the CNS and very high levels in testis (Moore, Lee et al. 1999).

1.6. Prion protein Structure

The key event underlying the Prion phenomenon is the molecular switch between PrP^c and its abnormal conformer PrP^{sc}. In terms of pure folding theory this should provide an unusual insight into how two stable forms of a protein can exist and effect a transition between conformational states. However, it has proven impossible to form crystals from PrP^{sc} because it is too insoluble, either as full length protein or PrP27-30. Electron micrographs of PrP27-30 have revealed fibrillar structures which appear as visible rod like entities which, after staining with congo red, demonstrate birefringence common to amyloids (Prusiner, McKinley et al. 1983). *In vivo*, Prion is found in the form of diffuse deposits, amyloid fibres, condensed and florid plaques (Prusiner 1998).

The difference in solubility of PrP^{sc} and PrP^c is likely to be a consequence of the secondary and tertiary structures of the molecules. Large differences in secondary structure are apparent from studies using circular dichroism and infra red spectroscopy which demonstrate that PrP^{sc} is a mix of roughly equal alpha helix and beta sheet in contrast to PrP^c which is almost entirely alpha helix in content and less than 5% beta sheet. (Caughey, Dong et al. 1991; Safar, Roller et al. 1993).

NMR studies of PrP^c have been undertaken on recombinant protein fragments (Riek, Hornemann et al. 1996; Donne, Viles et al. 1997; Zahn, Liu et al. 2000) and more recently x-ray crystal structures have been solved for sheep PrP (Haire, Whyte et al. 2004) and for a truncated mutant of human PrP (Knaus,

Morillas et al. 2001). PrP for mouse, human, and sheep (Zahn, Liu et al. 2000) share the structure of 3 alpha helices (amino acids 114-154, 175-193, 200-219) and a small antiparallel beta sheet (amino acids 128-131 and 161-164) and are structurally speaking homologous. NMR studies of the full length protein (23-231) demonstrated that the C-terminal portion (126-231) comprised the entire globular domain and reveals that the N-terminus was in fact largely unstructured (Riek, Hornemann et al. 1997). A disulphide bridge connects helix 2 and 3 between amino acids 166 and 171

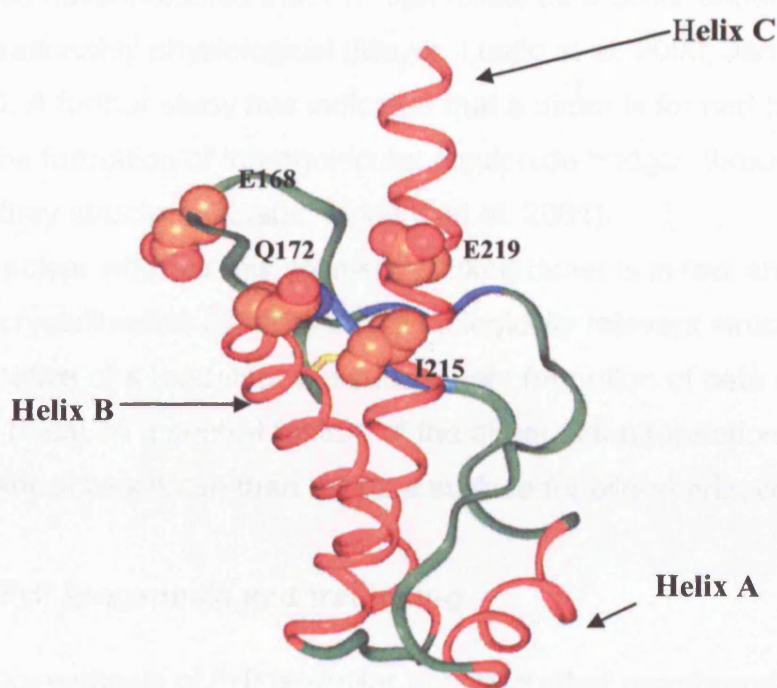


Figure 1.4. NMR structure of human PrP

Structure of Human PrP highlighting positions of those residues corresponding to the protein X binding site in mouse PrP. Adapted from (Zahn, Liu et al. 2000)

It is presumed that the carbohydrate residues, which were not present in these studies, do not affect the overall conformation of the backbone and it is unclear whether the addition of copper ions might bind and contribute to the structuring of the N-terminus. The contribution to structure as a whole of GPI anchorage to the membrane surface remains to be determined.

Local intra-species differences between the beta sheet and helix 2 (amino acids 166-171) and helix 3 are of particular interest. Differences in structure of mouse and hamster PrP as compared with bovine and human PrP are restricted to that part of the molecule (Lopez Garcia, Zahn et al. 2000; Zahn, Liu et al. 2000). This putative region has been argued to be the region for protein X binding which in turn has been argued is a determinant of the species barrier and an important part of Prion replication *in vivo* (see Fig 1.4).

Studies have indicated that PrP can exist as a dimer under conditions which are reasonably physiological (Meyer, Lustig et al. 2000; Jansen, Schafer et al. 2001). A further study has indicated that a dimer is formed by domain swapping and the formation of intermolecular disulphide bridges through a reorganisation of tertiary structure (Knaus, Morillas et al. 2001).

It is unclear whether this covalently linked dimer is in fact an artefact of long-term crystallisation conditions or a biologically relevant structure. However, it is suggestive of a model for the subsequent formation of beta sheet in transit to PrP^{Sc} because a central feature of the dimer is the formation of an inter-chain beta sheet which can then act as a surface for oligomerisation.

1.7. PrP biogenesis and trafficking

The biosynthesis of PrP is similar to that of other membrane and secreted proteins. A summary of modifications to PrP during biosynthesis is represented in Figure 1.5. During synthesis PrP^C is translocated into the Endoplasmic Reticulum (ER) where its N-terminal signal peptide is cleaved and, following cleavage of its c-terminal Glycosyl-phosphatidyl-inositol (GPI) signal, it is derivatised with a GPI anchor (Stahl, Borchelt et al. 1987). It also undergoes non-obligatory glycosylation at asparagines, N180 and N196 (Endo, Groth et al. 1989) and a disulphide bond is formed (Turk, Teplow et al. 1988). The N-linked oligosaccharides are of high mannose content and are sensitive to endoglycosidase H (endoH) digestion. When progressing to the Golgi PrP^C oligosaccharides are modified to complex type chains containing sialic acid and are no longer resistant to endoH.

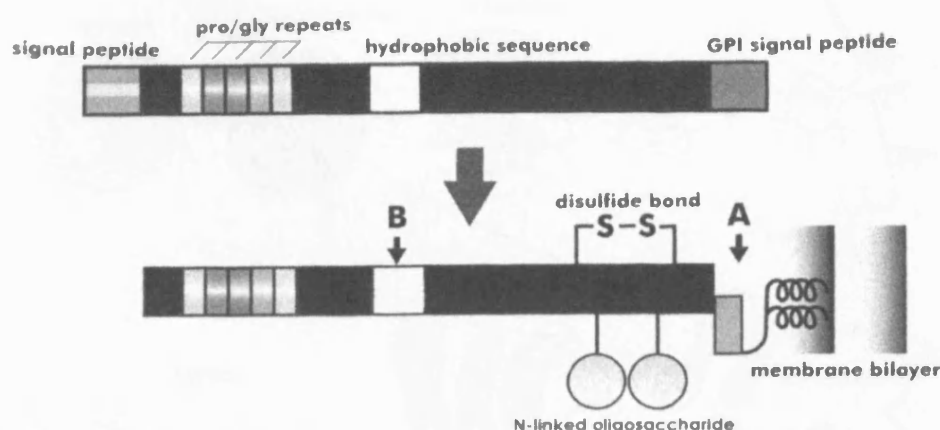


Figure 1.5. Diagram of PrP modifications in the ER following synthesis of the polypeptide

Following synthesis of the polypeptide, the signal peptide is cleaved N-terminally and a GPI anchor is added (A), tethering the protein to the membrane surface. The hydrophobic region implicated in the alternative transmembrane form of PrP is also indicated (B). A disulphide bond is formed and oligosaccharide chains are added to two potential sites.

1.7.1. Endocytic trafficking of PrP^C

Following transit down the secretory pathway and subsequent tethering to the plasma membrane by the GPI anchor, some PrP^C constitutively cycles between the membrane and an endocytic compartment (Shyng, Huber et al. 1993).

Figure 1.6 represents a summary of the trafficking of PrP^C. The cycle time of approximately 60 minutes has been demonstrated during kinetic studies which also indicate that 5% of the PrP molecules undergo proteolytic cleavage near residue 110 (Harris, Huber et al. 1993). A PrP-GFP fusion has also been shown to co-localise with Transferrin and FM4-64, indicating an endosomal recycling location (Borchelt, Taraboulos et al. 1992; Magalhaes, Silva et al. 2002).

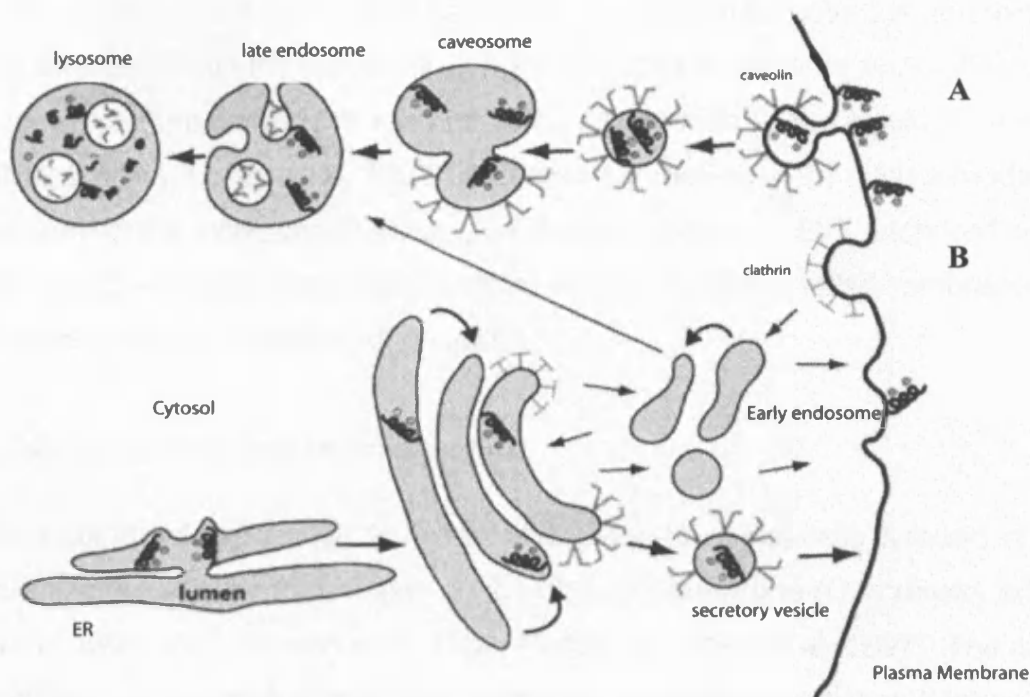


Figure 1.6. Diagram illustrating the two potential routes of PrP endocytosis

A) PrP is endocytosed directly by caveolae (indicated in the figure) or by caveolae like domains.

B) PrP finds its way to clathrin coated pits which are subsequently endocytosed

Experiments localising PrP^c through immunogold labelling and electron microscopy have indicated that clathrin coated pits appear to be associated with PrP uptake (Shyng, Heuser et al. 1994; Madore, Smith et al. 1999) and incubation with hypertonic sucrose, which disrupts clathrin lattices, abolishes internalisation of PrP (Shyng, Heuser et al. 1994). Expression of a dominant negative mutant of dynamin I prohibits invagination of clathrin coated pits from the membrane, and leads to accumulation of PrP^c containing structures beneath the membrane which co-localise with endocytic markers. (Shyng, Moulder et al. 1995; Magalhaes, Silva et al. 2002)

It is not clear how endocytosis of PrP is able to proceed via clathrin coated pits because PrP^c is in its majority not transmembrane and therefore does not present a c-terminal domain for cytoplasmic interaction with adaptor proteins and clathrin. It has been hypothesised that a PrP receptor, a transmembrane protein, must exist which has the necessary clathrin coated pit localisation signal and has a PrP binding site in its N-terminus (Harris, Gorodinsky et al.

1996). A number of candidates have been suggested as potential partners for this interaction but the existence of a PrP receptor to mediate endocytosis through clathrin coated pits remains to be established (Gauczynski, Peyrin et al. 2001; Zanata, Lopes et al. 2002). A precedent does exist for such a model in the form of the interaction between urokinase receptor (a GPI anchored protein) and the low-density lipoprotein receptor related protein, a transmembrane protein (Czekay, Kuemmel et al. 2001).

1.7.2. Lipid rafts and internalisation

The majority of PrP protein in neuronal and non-neuronal cells is found in detergent resistant raft domains on the plasma membrane (Gorodinsky and Harris 1995; Vey, Pilkuhn et al. 1996; Naslavsky, Stein et al. 1997). The raft domains are composed of sphingolipids and cholesterol and represent an ordered lipid environment (Simons and Ikonen 1997). This environment is enriched with other GPI anchored proteins and protein tyrosine kinases but excludes most transmembrane proteins. Rafts have been suggested as potentially important sites for signalling (Anderson 1998) and in the case of PrP resident in raft domains, signal transduction via fyn kinase has been suggested (Mouillet-Richard, Ermonval et al. 2000). The rafts are defined biochemically but also ultrastructurally and PrP containing invaginations are apparent on the surface of culture cells which are reminiscent of caveolae – rafts containing caveolin family proteins. Many cultured cell lines, including N2a cells, lack caveolin and therefore these domains have been nominated caveolae-like domains. PrP-containing rafts are a distinct subset from rafts containing other GPI anchored proteins; a significant proportion of PrP is fully soluble in non-ionic detergents, indicating an additional presence in non raft domains (Madore, Smith et al. 1999). An N-terminal motif of basic residues may be a necessary feature for the internalisation of PrP and is sufficient for the re-localisation of Thy-1 to distinctive PrP containing rafts (Sunyach, Jen et al. 2003). Internalisation of PrP may also occur via non clathrin coated pit mechanisms. Perturbation of PrP trafficking following various changes in cholesterol metabolism, along with the raft localisation of PrP are suggestive of

internalisation by clathrin independent means such as caveolae (Kaneko, Vey et al. 1997; Marella, Lehmann et al. 2002).

In summary, PrP^c is found to be abundant in raft domains but also to exist outside of raft domains on the cell surface. It is unclear whether its internalisation occurs principally through clathrin-mediated means or through the raft domain itself. It is difficult at present to see how a clear conclusion can be drawn on the issue of non-clathrin mediated endocytosis because perturbation of cholesterol, the main tool for assessment of raft mediated trafficking, has ramifications for cell trafficking in general.

1.7.3. PrP^{sc} localisation and site of conversion

Work in the area of Prion cell biology has been hampered by the lack of a reagent which enables specific detection of the Scrapie form of PrP in a cyto-chemical context. Nevertheless techniques have been employed as surrogates for the absence of such a marker which usually rely on the differential biochemical properties of PrP^{sc} from its normal cellular counterpart: for example the use of Proteinase K followed by centrifugation in non-ionic detergents. Immunofluorescence studies in Scrapie infected N2a cells have shown mixed distribution of PrP^{sc} residing intracellularly and co-localising with the Golgi markers in some cases (Taraboulos, Serban et al. 1990). Further studies in N2a cells and also brain sections have shown localisation of PrP^{sc} with late endosomal and lysosomal markers (McKinley, Taraboulos et al. 1991; Arnold, Tipler et al. 1995). The cell surface has also been consistently implicated as a site of PrP^{sc} accumulation through electron microscopy and the use of membrane-impermeable labelling reagents (Jeffrey, Goodsir et al. 1992; Shyng, Moulder et al. 1995; Vey, Pilkuhn et al. 1996).

It is perhaps even more difficult to establish the subcellular location of Prion conversion which is a crucial locus in understanding the cell biology of Prion disease. Evidence points to a site along the endocytic pathway, after passage down the secretory pathway to the plasma membrane.

Treatment of cells with Brefeldin A, effectively dissolving the Golgi and blocking secretion, prevents the formation of PrP^{sc}, implying a post Golgi conversion process (Taraboulos, Raeber et al. 1992). Chasing PrP conversion by use of surface iodination of infected cells demonstrates incorporation of radiolabel into PrP^{sc} (Caughey and Raymond 1991). Furthermore, treatment of infected cells with phosphatidylinositol-specific phospholipase C (PIPLC), inhibits the production of PrP^{sc} and implies the necessity of a PrP precursor which would otherwise be available on the cell surface (Caughey and Raymond 1991; Borchelt, Taraboulos et al. 1992).

Further studies focussed on the issue of the presence of PrP^{sc} in lipid rafts have more narrowly defined the locus of conversion. Depletion of cellular cholesterol which disrupts rafts also appears to inhibit PrP^{sc} formation (Taraboulos, Scott et al. 1995). However, as discussed above, cholesterol depletion as a manipulation has wide ranging effects on cellular metabolism. Furthermore, addition of trans-membrane domains in place of the GPI-anchor causes relocation to clathrin coated pits, and leads to the disruption of the conversion process (Kaneko, Vey et al. 1997). These studies have been taken as evidence for caveolae like domains (CLDs) as the likely locus for conversion.

1.7.4. Topological variants of PrP

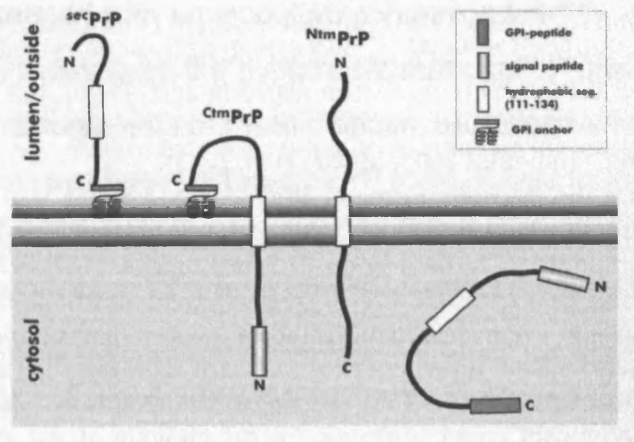


Figure 1.7. Topological variants of PrP

sec PrP indicates the most abundant form of PrP which is transported down the secretory pathway and tethered at the plasma membrane; ctm PrP is a transmembrane form where PrP is tethered to the surface of the ER by a GPI anchor; ntm PrP is another transmembrane form but the N terminal of the molecule is luminal and it is not GPI anchored; Cytosolic PrP is indicated as a species unassociated with membrane and possibly formed by ERAD (Endoplasmic Reticulum-associated degradation).

Distinct PrP topologies were originally observed as outputs of *in vitro* translation studies ((Hegde, Mastrianni et al. 1998; Hegde, Voigt et al. 1998)). These include PrP, as described previously, which is anchored by its GPI anchor, a cytosolic PrP species, and two other species termed ntmPRP and ctmPRP which span the membrane bilayer via a hydrophobic region from amino acids 111-134. These species constitute less than 10 percent of normal PrP biosynthesis (Harris 2003).

Mutation in or near to the transmembrane region can however effect the production in favour of the membrane forms. For example, the mutation A117V and P105L, associated with GSS, increases the proportion of ctmPRP that is formed by up to 30 percent (Hegde, Mastrianni et al. 1998; Kim, Rahbar et al. 2001). Competition at the translocon between the signal peptide, amino acids 1-22, and the hydrophobic residues 111-134, is responsible for either secPrP and NtmPrP on the one hand and ctmPrP on the other.

Animals expressing A117V mutants which favour production of ctmPrP (Hegde, Mastrianni et al. 1998) develop a Scrapie like neurological disease without any detectable PrP^{sc}. Interestingly the amount of ctmPrP increases when these animals are challenged with an inoculum containing PrP^{sc}.

In order to further investigate the hypothesis that ctmPrP may be a key molecule in the pathogenesis of Prion disease, mutations were identified that led to the exclusive synthesis of the ctmPrP form. It was found that L9R mutation in the signal peptide with a 3AV mutation in the transmembrane domain led to a production of a pure ctmPrP form. L9R/3AV PrP, was found to be absent from the cell surface although an intact GPI anchor indicated an interesting topology of a species which is transmembrane and yet anchored to the ER membrane in which it is retained, as assessed by endoH resistance. (Stewart, Drisaldi et al. 2001).

On the basis of ER retention it has been hypothesised that ctmPrP may be toxic in virtue of its ability to activate an ER-stress response pathway leading to cell death. Against the idea of ctmPrP as the primary toxic molecule in Prion disease is the finding that mutations associated with disease outside of the hydrophobic 111-134 segment do not lead to an increase in ctmPrP over normal levels and little ctmPrP has been identified in actual Prion disease (Stewart, Drisaldi et al. 2001; Stewart and Harris 2001)

In summary, the membrane form of PrP, ctmPrP has been shown to be an interesting potential molecule as a candidate for a toxic PrP species in culture studies. However, it remains to be clarified whether this has relevance to *in vivo* Prion disease and in particular a robust connection remains to be proven between infection and changes in the level of this membrane form of PrP.

1.7.5. Proteasomal processing and ERAD (Endoplasmic Reticulum Associated Degradation)

ER associated degradation describes the control process of the ER in degrading inappropriately folded or misprocessed proteins. Further export

down the secretory pathway of these proteins is blocked and they are retro-translocated into the cytoplasm where they are destined for degradation by the proteasome (Ellgaard, Molinari et al. 1999). It has been suggested that as part of normal PrP biosynthesis about 10 percent of the population undergoes ERAD, a small proportion of which are ubiquitinated (Yedidia, Horonchik et al. 2001). In the presence of proteasomal inhibitors PrP accumulates in the cytosol where it forms aggregates of 26kda and a corresponding 19-kD protease resistant core (Ma and Lindquist 2001; Yedidia, Horonchik et al. 2001; Ma and Lindquist 2002). This accumulation might provide evidence for the claim that PrP undergoes retrotranslocation from the ER. Interestingly, following transient proteasomal inhibition and subsequent recovery of the proteasome an increase in the quantity of aggregated PrP is found which indicates that the conversion to a protease resistant form is self perpetuating (Ma and Lindquist 2002). The role of the cytosolic PrP species in cytotoxicity has also been suggested in N2a cells where PrP accumulation is cytotoxic in contrast to Presenilin-1, and in animal models where N and C terminal PrP deletion mutants, which do not enter the ER, are found to cause cytotoxicity (Ma, Wollmann et al. 2002).

The model emerging from the work described above suggests a convergence of explanation for both initial Prion formation and subsequent cytotoxicity. At present it is unknown how sporadic CJD is initiated and this work may provide a key insight. However, it is notable that only an unglycosylated PrP is present in the cytosolic species which accumulates following proteasomal inhibition. This fact is consistent with work which has found that PrP accumulating in the presence of proteasomal inhibition has an intact signal peptide and c-terminal GPI-anchor sequence (Drisaldi, Stewart et al. 2003). This work suggests that ERAD does not occur following proteasomal inhibition and consequently that there is no evidence for ERAD of normal PrP. In the same experiments it was found that proteasomal inhibition led to a sustained increase in PrP transcription which might explain the apparent self-perpetuating nature of the species formed. It might also offer an alternative explanation for the phenomenon of proteasomal targeting, given that overexpression can lead to saturation of translocational machinery and consequent proteasomal degradation (Drasaldi,

Stewart et al. 2003). The role of cytoplasmic forms of PrP as causes of cytotoxicity in ordinary disease remains to be established.

1.8. Function of PrP

Although no clear phenotype has been found in knockout mice, some of the subtler findings like perturbed sleep (Tobler, Gaus et al. 1996) and loco-motor activity (Roesler, Walz et al. 1999) have been suggestive of minor neuronal deficits. More in depth electrophysiological studies have indicated that GABA-A receptor mediated fast inhibition and long term potentiation are both impaired in the knockout mice (Collinge, Whittington et al. 1994). This work has been contradicted by other studies which demonstrate intact synaptic transmission in both the hippocampus (Lledo, Tremblay et al. 1996) and the cerebellum (Herms, Kretschmar et al. 1995) of knockout mice. In conditional knockouts, CA1 cells demonstrate some reduction in after hyperpolarisation potentials (Mallucci, Ratte et al. 2002), and in comparison high levels of PrP^c mediate a more robust synaptic transmission in the hippocampus (Carleton, Tremblay et al. 2001). The search for deficits in knockout mice has brought up a number of interesting issues connected with Prion protein and its cellular function, however the overall picture is that there is no clear function which can be attributed to PrP^c at present. Some of the putative roles are described below.

1.8.1. Copper binding and SOD activity

PrP^c binds copper with micromolar affinity (Brown, Qin et al. 1997) and also binds zinc and magnesium, although with lower affinity (Pan, Stahl et al. 1992; Jackson, Murray et al. 2001). The N-terminus mediates binding at six conserved Histidine residues, four of which are situated within the octapeptide repeats (Jackson, Murray et al. 2001). Given the suggested role of the N-terminus in binding other ligands it is possible that copper binding has a role to play in PrP interactions. Knockout mice demonstrate reduction of 50% copper concentration in synaptosomal fractions, indicating a possible role in reuptake of copper (Kretschmar, Tings et al. 2000) and copper addition to N2a cells stimulates PrP endocytosis (Pauly and Harris 1998). It has therefore been

suggested that PrP^c may play a role in copper metabolism as a transport mechanism across the cell membrane.

PrP^c may also play a role as an antioxidant (Brown, Wong et al. 1999) and has some activity akin to that of a copper/zinc-dependent superoxide dismutase (SOD1). A decrease of SOD1 activity in the brains of knockout mice (Brown, Wong et al. 1999) and an increase in SOD1 activity and copper loading in transgenic mice over-expressing PrP (Brown and Besinger 1998) is consistent with this hypothesis. However, these findings remain contentious and others have found little difference in copper concentrations in subcellular brain fractions from knockout mice and little difference in SOD1 activity (Waggoner, Drisaldi et al. 2000).

1.8.2. PrP and Cell signalling

There is some evidence that PrP acts as a signalling molecule. Forcing dimerisation of PrP^c in cell-culture models can activate the non-receptor tyrosine kinases (Mouillet-Richard, Ermonval et al. 2000). However, it is unclear whether the signal is mediated directly via PrP^c. Mice suffer loss of hippocampal, cortical and cerebellar neurons following stereotactic injection of PrP specific monoclonal antibodies into the right hippocampus in contrast to knockout controls (Solfrosi, Criado et al. 2004). This result might be taken to argue for a direct signalling role of PrP as a cause of neuronal apoptosis although it remains unclear whether a neuro-protective signal is abrogated or a direct apoptotic signal is initiated. It might be argued that this result taken in combination with the inducible PrP mouse models which do not show apoptosis on removal of PrP indicates a direct apoptotic signal mediated by the cross-linked PrP species. It is difficult to assess signalling function by interventions like dimerisation because gross changes in membrane environment may themselves be responsible for the signalling changes.

1.8.3. PrP and cell survival

There have been conflicting reports of the contribution that PrP makes to cell survival. PrP^c can bind Bcl-2 (Kurschner and Morgan 1995) and has been shown to protect neuroblasts and retinal rat explants from anisomycin induced cell death (Chiarini, Freitas et al. 2002; Zanata, Lopes et al. 2002). Neurons taken from knockout mice have an increased sensitivity to serum deprivation and over-expression of Bcl-2 re-establishes normal levels of resistance (Kuwahara, Takeuchi et al. 1999). Bax mediated cell death in primary neurons was abrogated by PrP overexpression to the same levels as that of Bcl-2 overexpression (Bounhar, Zhang et al. 2001).

An alternative picture is delineated by the finding that over-expression of PrP can sensitise N2a cells to staurosporine induced apoptosis and lead to an increase in caspase 3 activity (Paitel, Alves da Costa et al. 2002).

Perhaps it is not surprising that a protein which is highly expressed in neuronal populations and connected with a disease that leads to neuronal death should be a focus of discussion as a candidate molecule with a role in cell survival. However, the evidence for the hypothesis that PrP^c clearly mediates cell survival in some form remains to be firmly established.

1.8.4. PrP binding molecules

Putative PrP-interacting molecules and receptors might shed some light on both the function of PrP and the necessary determinants for its normal cellular behaviour. Yeast two hybrid screens have been used to identify interacting proteins from cDNA libraries and have led to the suggestions that potential interactors might include Bcl-2 (Kurschner and Morgan 1995; Kurschner and Morgan 1996), the chaperones protein HSP60 (Edenhofer, Rieger et al. 1996), the laminin receptor precursor protein LRP or Laminin receptor LR (Rieger, Edenhofer et al. 1997) and Grb2 (Spielhaupter and Schatzl 2001) amongst others. Immuno precipitation experiments have shown mutual pull down of PrP with antibodies to grp94, protein disulphide isomerase, calnexin and calreticulin (Capellari, Zaidi et al. 1999).

The stress inducible protein 1 (ST1-1) , a cofactor for chaperones such as HSP70 and HSP90, has also been implicated as a binding partner and was identified through its complementary hydrophathy profile in comparison with a PrP¹¹³⁻¹²⁸ peptide (Zanata, Lopes et al. 2002). It is also a potential mediator of a PrP^c neuroprotective signal through interaction at the cell surface with PrP.

Heparin sulphates have consistently been implicated in the cellular behaviour of PrP and also in the process of infection. Heparin sulphates interact with a central binding domain in the N-terminal region of PrP^c (Gabizon, Meiner et al. 1993; Caughey, Brown et al. 1994; Brimacombe, Bennett et al. 1999). There is a possibility that binding occurs to the octapeptide repeat itself, which is important given the potential copper binding to this region of PrP (Brimacombe, Bennett et al. 1999; Warner, Hundt et al. 2002). PrP internalisation has also been shown to be affected by the presence of glycosaminoglycans (Shyng, Lehmann et al. 1995; Wong, Xiong et al. 2001), and sulphated glycans appear to stimulate cell-free conversion reactions (Snow, Wight et al. 1990; McBride, Wilson et al. 1998).

The laminin receptor precursor protein and the laminin receptor (LRP/LR) have been implicated in a number of studies as an important interacting protein. LRP/LR undergoes a complex maturation process involving acylation, and phosphorylation of the precursor of which several isoforms are present in the brain (Simoneau, Haik et al. 2003).

A role in the endocytic pathway of LR has been suggested given its demonstrated mediation in the binding and internalisation of PrP^c to cells in culture models. It is also possible that LRP/LR might act as the cellular receptor for PrP molecules to interact with other cells for the purposes of signalling necessary for survival (Rieger, Edenhofer et al. 1997; Gauczynski, Peyrin et al. 2001).

In culture models, knock down of LRP/LR using antisense and RNAi leads to a decrease in infectivity and hence LRP/LR may play an important role in the process of Prion conversion (Leucht, Simoneau et al. 2003).

In summary, a large number of putative PrP binding proteins have been suggested. Of particular interest is the Laminin Receptor which has also been implicated in the conversion of PrP to Prion. However, it remains to be confirmed whether any of these molecules has any clear role to play in either the normal cellular metabolism of PrP^c or in Prion infection.

1.9. Animal models of Prion disease

Animal models have been seminal in securing the link between PrP expression and infection, demonstrating the necessity of PrP expression, gene dosage effects on incubation, the existence of a species barrier and the existence of distinct reproducible strains of Prion.

1.9.1. PrP knockout mice

Two strategies have been employed for removal of PrP expression. The first involves disruption of the open reading frame of PrP (Bueler, Fischer et al. 1992; Manson, Clarke et al. 1994). Both the Zurich I mouse and the Edinburgh knockout demonstrate disruption of PrP expression by this method. The animals develop normally, no obvious pathology is evident and they are resistant to Prion infection. Milder phenotypes described include disruption of circadian rhythms (Tobler, Gaus et al. 1996), changes in superoxide dismutase activity (Brown, Schulz-Schaeffer et al. 1997) and defects in copper metabolism (Brown, Qin et al. 1997). It is also noteworthy that some studies have suggested GABA-A receptor mediated fast inhibition and LTP are impaired in hippocampal slices (Collinge, Whittington et al. 1994; Collinge, Sidle et al. 1996) although these studies have not been substantiated (Herms, Kretschmar et al. 1995; Lledo, Tremblay et al. 1996).

The second strategy for knockout of PrP involved deletion of both the reading frame and flanking regions (Sakaguchi, Katamine et al. 1996). In contrast to the first two knockout lines described these mice, Nagasaki and Zurich II, exhibit severe ataxia, and purkinje cell loss later in life (Sakaguchi, Katamine et al. 1996; Moore, Lee et al. 1999; Rossi, Cozzio et al. 2001). The disparity between

the models has since been clarified with the discovery of a downstream gene locus *Prpnd* and the associated *Doppel* (*Dpl*) gene. Ectopic brain expression of *doppel* in the *PrP* knockouts, as a result of the wider deletion strategy, leads to the toxic phenotypes (Moore, Lee et al. 1999).

Dpl is an N-glycosylated, GPI anchored protein expressed in many tissues but not in the brain. *Dpl* and *PrP* show about 25 percent homology (Moore, Lee et al. 1999; Silverman, Qin et al. 2000) and knockout leads to male sterility in mice (Behrens, Genoud et al. 2002).

1.9.2. Transgenic models of human Prion diseases

The single base mutation P102L is directly linked to GSS with 100 percent penetrance (Hsiao, Baker et al. 1989). Transgenic mice with the equivalent mutation at amino acid 101 in murine *PrP* have been produced. Mice with a high copy number of the *Prnp* P101L transgenes developed a neurodegenerative disorder, exhibiting spongiform change and *PrP* containing amyloid plaques in the brain, in the apparent absence of *PrP^{Sc}* (Hsiao, Groth et al. 1994). In low copy number mice, where transgene expression was only twice that of endogenous expression, signs of CNS disorder were not apparent until 600 days and then only in a few mice (Kaneko, Ball et al. 2000). Nevertheless the high copy number disease could be transmitted to low copy number animals efficiently, but not to wild type mice (Telling, Parchi et al. 1996). This has been argued to provide evidence for a protein only hypothesis.

A second model introduced the 101L mutation through targeted means, thereby avoiding complications associated with overexpression. The finding in this model contrasted starkly with the overexpressed transgene described above, and did not evidence a spontaneously generated disease (Moore, Redhead et al. 1995; Manson, Jamieson et al. 1999).

Other models of disease have included the creation of mice expressing *PrP* with nine octapeptide insertions, which demonstrate a slow progressive, neurological disorder (Chiesa, Piccardo et al. 1998). Mice homozygous for the

transgene acquire ataxia at roughly 65 days compared to the hemizygous mice and partially Proteinase K resistant PrP species were found to accumulate in spinal cord , skeletal muscle and heart.(Chiesa, Pestronk et al. 2001).

Not all Prion diseases find analogues in mouse models. Transgenic mice overexpressing a mutant PrP gene, E200K , demonstrate the equivalent mutation to the E200K mutation found in one form of familial CJD. These animals did not display any sort of neurological disorder (Telling, Haga et al. 1996).

1.9.3. Transgenic studies of the species barrier

Prions are not always transferred efficiently between species, which constitutes a species barrier. In mice, abrogation of this barrier can often be attained by serial passage of infected materials from those mice that do come down with disease, leading to a decreasing incubation time with passage until the barrier is overcome (Pattison 1965). The emerging model is that Prions which are synthesised in the new host species ultimately reflect the sequence of that species and not that of the PrP^{sc} molecules in the initial inoculum (Bockman, Prusiner et al. 1987).

Expression of transgenes allows for efficient transfer across the species barrier without passaging. One example of this is the introduction of a Syrian hamster PrP into mice rendering them susceptible to hamster Prion disease, and demonstrating gene dosage effects (Scott, Foster et al. 1989). When these transgenic mice were infected with mouse Prion they produced Prions pathogenic for normal mice, in contrast to inoculation with hamster Prion, which produced Prions that would only infect hamsters. The results of this work indicated the importance of the primary structure of the PrP gene in determining the nature, and possibly the conformation of the Prion produced following infection (Prusiner, Scott et al. 1990).

Introducing a parallel transgene into a mouse model does not always overcome the problem of the species barrier. For example, transgenic mice expressing a

Human PrP are not infected with CJD. In contrast, expression of the same transgene on a knockout background permits infection. The implication here is that endogenous mouse PrP interferes in some way with the process of infection directed through the transgene. When a chimera, MHu2M, of the human and mouse Prion is expressed on the normal background, infection is also able to proceed (Telling, Scott et al. 1995). The hypothesis from these experiments was that mouse and human PrP compete for a factor X which is necessary for conversion, and the mouse PrP has a significantly higher affinity for factor X. The chimera was converted because it was able to bind to this factor given the shared amino acid sequence at the N and C terminal portions PrP.

Scrapie infected N2a cells have been used to clarify the important binding residues to protein X. The side chains of residues 214 and 218 were delineated as part of a discontinuous epitope with residues 167 and 171 in an adjacent loop (Kaneko, Zulianello et al. 1997).

1.9.4. Transgenic models of Prion strains

Different TSE isolates have different characteristics which are maintained following infectious transfer to another organism. The different phenotypes resulting from TSE infection have been attributed to the existence of multiple strains. The most studied system has been mice through which Scrapie, BSE or CJD from a range of isolates have been passaged. From these studies a number of criteria have emerged for distinguishing strains which include the pathological brain profile of an animal, the incubation time, and the biochemical characteristics of the Scrapie agent formed following infection. The incubation period for a given strain is highly replicable in mice studies given the same dose and genetic background and different strains show reproducibly different incubation periods (Bruce, McConnell et al. 1991). Pathology in TSEs varies according to vacuolation severity and area profile. 'Lesion profile' represents a score of these variables and appears to be reasonably characteristic for strains (Bruce, McConnell et al. 1991). Glycosylation profile of brain PrP^{sc} has been

suggested as one possible marker of strain (Collinge, Sidle et al. 1996; Somerville, Chong et al. 1997). Conformational differences revealed by distinct Proteinase K digestion products (Telling, Parchi et al. 1996) and antibody binding propensities (Safar, Wille et al. 1998) have also been suggested as useful criteria.

The protein only hypothesis needs to account for the additional subtlety of information transfer that is associated with strain. Experiments indicating conformational variation as the molecular basis are therefore critical. Two strains of TME were found to produce distinct strain types as assayed by incubation period and clinical symptoms in hamsters. Critically the two strains demonstrated differences in their Proteinase K cleavage sites (Bessen and Marsh 1992).

This provides some evidence for conformational distinctness underlying the difference in the two strains. Further evidence for the conformational basis of strain has come from differences in Proteinase K cleavage site in Prion from sFFI (sporadic FFI) or fCJD (familial CJD) (E200K) patients (Telling, Parchi et al. 1996). The associated cleavage products of 19 and 21 kda for sFFI and fCJD respectively remain constant when the material is passaged through a transgenic mouse expressing a chimeric hamster-mouse transgene.

Studies comparing different sporadic and iatrogenic CJD cases with codon 129 genotypes have also been shown to be typed according to PrP^{sc} fragment sizes following Proteinase K digestion (Telling, Parchi et al. 1996).

Differential glycosylation has been taken as one indicator of strain and it remains to be established what the exact effects of PrP^c glycosylation or PrP^{sc} glycosylation are on the infectious process. This is discussed in the introduction and discussion of Chapter 3.

1.10. In vitro models of Prion disease

The first test for the protein only hypothesis came from the challenge to form PrP^{sc} *in vitro*. PrP^c was radiolabelled and incubated with unlabeled PrP^{sc} which produced a small amount of Protease resistant, radiolabelled PrP species (Kocisko, Come et al. 1994). The newly formed material is here nominated PrP-res because it is not proven to have the infectious properties of PrP^{sc} *in vivo*. Importantly, other amyloid related material, such as beta amyloid, could not act to convert PrP^c in this assay. Validation for *in vitro* models came from results indicating preservation of the species barrier (Kocisko, Priola et al. 1995; Raymond, Hope et al. 1997; Horiuchi, Priola et al. 2000), and of strain characteristics (Bessen and Marsh 1994). However a key problem has been the demonstration of the *in vivo* efficacy of the newly produced PrP-res in propagating Prion infection and attempts to test infectivity produced by cell free reactions have not proven positive (Hill, Antoniou et al. 1999). One key issue has been the production of sufficient quantities of PrP-res and this is indicative of the fact that the conversion reaction is highly inefficient - ratios of roughly 50:1 in initial PrP^{sc} to PrP^c are necessary to run this reaction successfully (Supattapone 2004).

The reaction has been used to assess mechanistic aspects of conversion. The species that is associated with the converting activity appears not to be a monomer and is more likely a multimer or aggregate (Caughey, Kocisko et al. 1995; Caughey, Raymond et al. 1997). Partial denaturation of PrP^c or addition of chaperones like GroEL or hsp1054, can lead to enhancement of the conversion, perhaps indicating something about the need for refolding steps in the conversion process (DeBurman, Raymond et al. 1997). A result consistent with a nucleated polymerisation model is the finding that PrP^c substrate binds and remains bound to PrP^{sc} during the process of the reaction (Bessen, Raymond et al. 1997; Horiuchi and Caughey 1999; Horiuchi and Caughey 1999; Horiuchi, Priola et al. 2000).

A conformational change occurs following binding of PrP^c to PrP^{sc} at the C-terminal end of the third helix and subsequently PrP^c is more slowly converted

to the high beta sheet containing state. It has been postulated that the breakage of the disulphide bond in PrP^C (Welker, Wedemeyer et al. 2001) and formation of intermolecular disulphide bonds or domain swapped dimer (Knaus, Morillas et al. 2001) might be a necessary process. However evidence suggests that this is not a necessary requirement *in vitro* (Welker, Raymond et al. 2002).

A more efficacious cell free conversion process protein misfolding cyclic amplification (PMCA) efficiently amplifies PrP-res in repeated cycles of sonication with the addition of the anionic detergent SDS (sodium dodecyl sulphate) (Saborio, Permanne et al. 2001). PrP^C conversion to PrP-res can be formed with an input PrP^{Sc} / PrP^C ratio of as little as 1:100 in molar terms compared to the 50:1 ratio of the original cell free system described above. A modified procedure has been suggested which does not involve SDS and sonication although it produces only a 6-fold and not 30-fold amplification (Lucassen, Nishina et al. 2003). Pancreatic RNase T1 and RNase A were shown to inhibit PrPres amplification using PCMA in a dose dependent manner and addition of total RNA isolated from hamster brain was shown to stimulate amplification in a species specific manner (Deleault, Lucassen et al. 2003). No single RNA has been suggested as a binding candidate and it is therefore not known whether amplification occurs as a general property of RNA in Prion conversion. Of particular concern is the issue of whether the enhancement of Prion conversion in these experiments is specific to the cyclic amplification process.

Since the initial writing of this introduction, a study has been published which makes use of the enhanced efficiency of the PCMA process to produce PrP^{Sc} *in vitro* from a 263 K Prion strain template (Castilla, Saa et al. 2005). Adequate quantities were formed to effectively dilute out the original template to a level where it had no activity, whilst the newly formed Prion successfully brought about infection in mouse models. This is the first successful demonstration of its kind and is a promising step in the field.

A further important paper has recently provided the first published evidence of the formation of synthetic mammalian Prions. Previously attempts to

demonstrate production of infectivity by refolding wild-type PrP^c into beta sheet rich isoforms have proved to be unsuccessful (Hill, Antoniou et al. 1999). A mutant recombinant PrP (MorPrP 89-230) was expressed in E-coli and fibrils were produced by either a seeded or non seeded technique (Baskakov, Legname et al. 2002). The resultant material was used as an inoculum in mice expressing MoPrP89-230 at 16 times the level of normal PrP. The results were a 382 day and 474 day incubation times for inoculums produced by the seeding and unseeded method respectively. Brain pathology was assessed and found to be similar to that of infection of wild type mice with the RML strain of Prion. The Prion showed the classical criteria of PK resistance. One caveat with the experiment is the use an animal over-expressing a transgene at 16 times the level of normal PrP. Particularly the concern might be that both the biochemical properties and the pathology might have been a result of PrP aggregation rather than Prion formation. Nevertheless, the crucial result of Prion propagation in normal FVB mice with inoculums from the first passage transgenic mice brains was also demonstrated. Whether this is a special case based on the peculiar mutant PrP form remains to be determined.

It remains unclear whether these *in vitro* models reflect the possibility that conversion of PrP^c to PrP^{sc} may well occur in the context of a membrane. This may occur within a non fibrillar assembly of GPI-anchored PrP^{sc} molecules in two dimensions (Wille, Michelitsch et al. 2002), or the membrane may thermodynamically permit the existence of monomeric PrP^{sc} which is not found *in vitro*. When PrP^c and PrP^{sc} were attached to separate membrane vesicles conversion was not efficient as long as GPI anchorage obtained or until these separate vesicles were fused (Baron, Wehrly et al. 2002). The conclusion of this study is that conversion occurs only if PrP^c and PrP^{sc} can interact within the same membrane.

In summary, work *in vitro* has previously faced the difficult task of demonstrating the infectivity of Prion like species that have been produced, and it has therefore been of uncertain relevance to actual Prion formation. However, recent advances in formation of synthetic Prion and Prion by *in vitro* amplification methodologies, may represent a major step forward in this field if these results are found to be robust. Studies of the differences between models

which have previously failed to produce infectivity *in vitro* and those which can produce infectivity may in the future reveal something critical about the molecular processes of Prion formation.

1.11. Cell Culture Models

There are a number of reasons why cell culture remains a key strategic resource for the study of a Prion disease. Firstly, cell culture offers a means of assessing the *in vivo* requirement for Prion replication. This includes investigation of the physiological dynamics of replication and also a search for other molecules that contribute to physiological infection. Secondly, cell culture offers a key method for both the screening of potential therapeutic drugs and for the discovery of Prion specific markers which are crucial for study of the disease agent and enhanced diagnosis.

The use of cell lines in the cell biology of Prion has been limited by the fact that only some cell lines appear to be susceptible to infection (see Table 1.3 for summary of many of these lines). The cell lines which are susceptible are not necessarily restricted to lineages associated with the lymphoreticular system or the nervous system (Vorberg, Raines et al. 2004). Cell lines which are susceptible to infection are not necessarily susceptible to multiple strains of Prion from within the same species (Milhavet, McMahon et al. 2000; Birkett, Hennion et al. 2001; Vorberg, Raines et al. 2004). It is also noteworthy that there has been little success in infecting primary neurons which would have been a key model for study of infectious process.

1.11.1. Cell culture models supporting Prion replication

Cell designation	Species of origin	Tissues of origin or cell type	TSE strain	Comments
Neural cell lines				
N2a	Mouse	Neuroblastoma	Chandler	
c-1300	Mouse	Neuroblastoma	Chandler	
N1E-115	Mouse	Neuroblastoma	Chandler	
N2a#58	Mouse	Neuroblastoma	22L/Chandler/139A	N2a overexpressing up to 6-fold higher level of PrP ^C
GT1	Mouse	Hypothalamic neural cell	22L/Chandler/139A	T-antigen immortalised cells
HaB	Hamster	Hamster brain cell line	Hamster strain	Spontaneously immortalised cells
MSC-80	Mouse	Schwann cell	Chandler	
Schwann cell	Mouse	Schwann cell	Scrapie	
DRG	Ovine PrP in transgenic mouse	Dorsal root ganglia	Natural sheep scrapie	
Non-neural cell lines				
SMB	Mouse	Brain cells from mesodermal origin	Chandler	
L fibroblast	Mouse	Fibroblast	Chandler	Cells present chromosome re-arrangement and change in chromosome morphology
L 23	Mouse	Unspecified	Compton or C-506	
NS1	Mouse	Fusing spleen cell from scrapie-infected mice with NS1 cell	Chandler	
PC12	Rat	Pheochromocytoma	139A/ME7	In presence of low concentrations of nerve growth factor
Glial cell	Rat	Glial cell monolayers from rat Gasserian ganglion	Chandler	
RK-13	Rabbit	Kidney epithelial	Natural sheep scrapie	RK13 cells express the ovine PrP

Table1.3 Summary of cell types utilised for the study of prion infection

Source of cell type, strain type with which they have been infected are also indicated.

Table adapted from (Solassol, Crozet et al. 2003)

Infected cell lines are created either by addition of infectious homogenates, by Scrapie associated fibrils (Race, Fadness et al. 1987), by cell culture derived homogenates (Bosque and Prusiner 2000) or cell co-cultures (Kanu, Imokawa et al. 2002). It has been argued that efficacy of infection in these model systems depends on the mode of infectious presentation either through cell contact, addition of cell homogenates, brain homogenates or conditioned medium from infected cultures (Bosque and Prusiner 2000; Kanu, Imokawa et al. 2002).

The *de novo* synthesis of PrP^{Sc} has been shown in cell culture systems though metabolic labelling (Caughey, Race et al. 1989) and also the use of tagged PrP molecules (Vorberg, Buschmann et al. 1999). The presence of PrP^{Sc} is established through the standard biochemical procedure of SDS-PAGE following Proteinase K treatment and ultracentrifugation of detergent lysates (see Fig 1.8. ScN2a +PK lane)

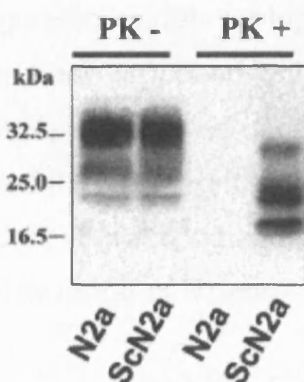


Figure 1.8. Assay for PrP^C and PrP^{Sc}

Western blot of infected or uninfected ScN2a cells post treatment with Proteinase K (PK+) or without Proteinase K (PK-). Adapted from (Solassol, Crozet et al. 2003)

Another technique has involved blotting following denaturation and this has demonstrated enhanced sensitivity over traditional western blotting techniques (Bosque and Prusiner 2000). There is no clearly established procedure for assessing whether a single cell, as opposed to a colony or dish, is infected. This is of particular importance given the consideration that when N2a cells are

subcloned, not all colonies recovered are infected (Race 1991; Bosque and Prusiner 2000; Nishida, Harris et al. 2000).

It is unclear whether infection has a direct effect on most cell lines. In the case of infected N2a cells which support expression of RML strain of Prion, there are no obvious changes in the cytosol (Butler, Scott et al. 1988). There have been reports of morphological differences following infection of N2a cell lines (Markovits, Dautheville et al. 1983) but equally these have been disputed (Borchelt, Scott et al. 1990). It is difficult to reconcile such claims given the expected differences in cell behaviours attributable to clonal variation.

Improvement in the initial infection of N2a's has been obtained by overexpressing mouse PrP and this has also facilitated infection with other mouse strains (Nishida, Harris et al. 2000). Differences of initial propensity to infection have also been improved by subcloning N2a cells to produce highly susceptible lines which can then be infected (Bosque and Prusiner 2000). Diagnostic models for highly sensitive determination of Prion infectivity have been proposed which make use of cell culture, and offer sensitivity by quantifying colonies of cells which have been infected following addition of the material to be diagnosed (Klohn, Stoltze et al. 2003). One limitation of these models in practice has been the limitation of the cell lines to infection by a narrow range of strains.

Other cell lines produced include GT1 cells which are a well differentiated neuronal cell line. Interestingly they have also been shown to demonstrate some cytopathological effects following infection (Schatzl, Laszlo et al. 1997) and Prion infection can impair their cellular response to oxidative stress (Milhavet, McMahon et al. 2000)

Schwann cell lines have been used as a model for Prion infection for the Chandler strain of Scrapie, which is of particular note given the potential role for Schwann cells in spread of infection (Follet, Lemaire-Vieille et al. 2002)

The Scrapie Mouse Brain cell line (SMB), represents an alternative approach to derivation of infected, uninfected cell line pairs. It is derived from a mouse initially infected with the Chandler isolate of Scrapie (Clarke and Haig 1970; Haig and Clarke 1971). An uninfected cell line was then derived from SMB by curing with pentosan sulphate on multiple passage (Birkett, Hennion et al. 2001). The resultant cells, PS cells, could be re-infected with multiple strains as demonstrated by pathology and incubation time when inoculated into mice. Unpublished observations, consistent with the original findings following derivation of the cell line, indicate that the SMB cell line is amongst the most stable in maintaining its infectivity on multiple passage.

1.11.2. Mutant PrP molecules in cell culture

Mutant PrP models, analogous to human disease in terms of sequence, have been constructed in cell culture. These models have delineated important steps in the cell biology of familial Prion disease but they may also bring insight to some issues that are more generally relevant to Prion infection. Mutant PrPs expressed in Chinese Hamster Ovary (CHO) cells and pulse labelled, have been shown to demonstrate a stage wise process in the acquisition of properties reminiscent of PrP^{Sc} as they are processed by the cell (Daude, Lehmann et al. 1997). The steps in this pathway which have been delineated are the acquisition of PIPLC resistance in the ER, the acquisition of detergent insolubility (maximal 1 hour post-chase), and the acquisition of partial protease resistance (maximal several hours post-chase) which is demonstrated after arrival of the protein at the cell surface. The model posits that misfolding occurs in the ER, followed by initial oligomerisation and then further aggregation at or beyond the plasma membrane. Further support for the role of the ER has come from immunocytochemistry and EM - disease associated mutations (e.g. P101L, D177N/M128) expressed in CHO cells are found to accumulate in the ER and are more weakly represented at the plasma membrane in comparison with wild type PrP molecules (Petersen, Parchi et al. 1996; Jin, Gu et al. 2000; Ivanova, Barmada et al. 2001).

Studies have also indicated a delayed maturation of mutant PrP molecules which leads to the delay in transiting the ER (Drisaldi, Stewart et al. 2003). One upshot of this body of work is the possibility that ER retention, as with some other human disorders, may be responsible for a component of toxicity in familial Prion disease (Aridor and Balch 1999).

1.11.3. Insights into Prion transfer from culture models

The mechanism/s for transfer of Prion between infected and non infected cells remain undetermined although cell culture models have been employed in the assessment of mechanisms for intercellular transfer. In the SMB/PS system described above one study (Kanu, Imokawa et al. 2002) has demonstrated that cell co-cultures can efficiently transfer infectivity and argues for the necessity of cell contact for Prion transfer. In support of this study, further elucidation of a possible transfer mechanisms has been indicated by work which demonstrates that PrP, like other GPI anchored proteins, may be transferred by a 'cell painting' mechanism (Liu, Li et al. 2002). The transfer elicited required cell contact but efficient transfer also required prior treatment of cell donor or acceptor cells with Phorbol Myristate Acetate. These two studies contrasts with other systems such as GT1 cells where cell culture medium has been found to contain infectivity (Schatzl, Laszlo et al. 1997) and studies in Scrapie infected rabbit epithelial cell lines (ROV) expressing ovine transgenes (Fevrier, Vilette et al. 2004). Infectivity derived from media of infected cultured ROV cells can be found to co-purify through differential centrifugation, with membrane material along with exosomal markers. The implication of this is that exosomal release of Prion may constitute one mechanism for infectious transfer and this work tallies with other recent studies on transfer of GPI anchored proteins which suggest vesicular release as a form of transport (Thery, Zitvogel et al. 2002). It is conceivable that multiple mechanisms for transfer exist both within one cell type and multiple but distinct mechanisms between cells types. Therefore the above studies may not be in contradiction with one another.

One potential means of transferring infectivity might be a templating that occurs across membranes between PrP^{Sc} molecules of an infected cell, and PrP^C

molecules of an uninfected cell. *In vitro* models utilising microsomal membranes which represent the opposition of the molecules at the cell surface demonstrate that templating does not occur and that fusion of membrane surfaces is needed in order for conversion to take place (Baron, Wehrly et al. 2002; Baron and Caughey 2003). These studies are however in artificial systems and it remains to be determined what relevance they have to the structure and dynamics of the membrane surfaces of cultured cells.

1.12. Progression of Prion disease and Pathogenesis

In animal models infection in the fastest possible time is achieved via intracerebral inoculation with an infectious source of Prion. Other routes include feeding, intravenous and intraperitoneal injection, intra ocular injection and grafts. There is a long latency between peripheral infection and the clinical symptoms of Prion disease and a large proportion of the incubation period is taken up by the agent gaining access to the central nervous system from the periphery (Aguzzi 1997).

1.12.1. Peripheral entry site for Prion

In the distal ileum there is an early rise in Prion infection following oral challenge in sheep and cows (Wells, Dawson et al. 1994; Terry, Marsh et al. 2003) and in particular Peyer's patches accumulate Prion protein. This is also true in the case of mouse models of Scrapie infection. The hypothesis suggested is that Peyer's patches are important sites in the transit of orally ingested Prion from the luminal side of the gastro-enteric tube to the CNS.

The identity of cells which might transport Prion from the intestinal mucosa to the Peyer's patches remains unclear. One candidate cell type has been the Membranous epithelial cell (M-cell) which has been shown to be a key sites of entry for enteric pathogens via trans-epithelial transport (Neutra, Frey et al. 1996) and M-cells were demonstrated to be sufficient for the passage of Prion across barriers in cell culture-models (Heppner, Christ et al. 2001).

1.12.2. Prions and Lymphocytes

Prion replication in lymphoid tissues may represent a necessary part of Prion pathogenesis and studies interfering with lymphoid Prion replication have led to delay or prevention of disease (Aucouturier, Geissmann et al. 2001; Huang, Farquhar et al. 2002). Peripheral pathogenesis of Prion disease is dependant on Lymphocytes in contrast to CNS progression which is not (Kitamoto, Muramoto et al. 1991; Lasmezas, Cesbron et al. 1996). Ablation of the T-cell compartment did not affect disease progression, whereas ablation of B-cells did affect progression (Klein, Frigg et al. 1997). However, Prion invasion occurs even when the B-cells have been transferred from PrP knockout mice to B-cell deficient mice (Klein, Frigg et al. 1998). The implication is that the presence of B-cells is a requirement for another cell-type to mediate infectious progression.

The leading candidate cell for mediation of the progression has been the follicular dendritic cell (FDC). Lymphocytes do not appear to carry a large amount of Prion infectivity themselves and the infectivity in the spleen resides in a stromal fraction (Aguzzi 2003). The contribution of FDCs to Prion pathogenesis is to some extent difficult to understand fully because specific markers have not been clearly defined for these cells. Elegant experiments have made use of the gene deletion results in mice which demonstrate that B-cell signalling via Lymphotoxins is required for FDC maturation and maintenance. (Koni, Sacca et al. 1997; Endres, Alimzhanov et al. 1999). Signalling thorough the Lymphotoxin- α/β complexes which bind to the LT- α/β receptor activates the pathway for development of FDCs and maintenance of FDCs in a differentiated state requires continuous interaction with B-lymphocytes expressing surface LT- $\alpha\beta$ (Gonzalez, Mackay et al. 1998). Treatment of mice with LT- β receptor immunoglobulin fusion protein leads to the death of mature FDCs within a day in both the spleen and the lymph nodes (Crowe, VanArsdale et al. 1994; Mackay, Majeau et al. 1997; Mackay and Browning 1998). This effect was used in ablation experiments to asses the contribution of FDCs to pathogenesis in Prion disease. FDCs were depleted by administration of LT- β -Ig fusion protein. Following inoculation with Scrapie, the mice were free of any PrP^{Sc} in the spleen up to 8 weeks later (Mabbott, Mackay

et al. 2000; Mabbott, Young et al. 2003). Usually following peripheral inoculation the spleen demonstrates infectivity within a few days and peaks in a few weeks (Bruce 1985). These experiments also demonstrate the potential for FDC depletion as a strategy in post-exposure prophylaxis of Prions for people working in fields with Prion material.

1.12.3. Prion entry into the nervous system

One key model for Prion neuro-invasion delineates two stages involving infection of Lymphatic systems followed by neuroinvasion (Aguzzi, Montrasio et al. 2001). The autonomic nervous system may be responsible for transport of Prion from lymphoid tissues to the CNS and the innervation of lymphoid organs is mainly sympathetic (Felten and Felten 1988; Felten, Felten et al. 1988). Sympathectomy itself delays the transport of Prion from lymphatic organs to the thoracic spinal chord (Glatzel, Heppner et al. 2001) and transgenic mice, with hyperinnervated spleens, develop Scrapie significantly faster than controls (Glatzel, Heppner et al. 2001). It is interesting that the variation in proximity of FDCs to the major splenic nerve alters the efficacy of Prion neuroinvasion although contact does not appear to be made between them (Prinz, Heikenwalder et al. 2003).

The velocity of Prion transport through peripheral nerves is slow (~1mm per day), and it is unclear how this transport occurs (Kimberlin, Hall et al. 1983). Spread may occur through axonal or non-axonal means of transport. It is however unlikely that fast-axonal transport is responsible for the spread given the kinetics and also the finding that in mice with a deficiency in fast axonal transport there is little perturbation in Prion infection (Kunzi, Glatzel et al. 2002).

One alternative model to axonal transport is a mechanism which involves conversion of PrP^C by adjacent PrP^{Sc} molecules in a domino fashion along axons. The propensity of Schwann cells for infection might be suggestive of a domino like route for such transport in the PNS (peripheral nervous system) without reference to axons. This could be tested by reference to a mouse in which PrP knockout is specifically targeted in Schwann cells.

1.12.4. Spread of Prion within the CNS

The spread of Prion has been investigated in the CNS by means of Ocular injection of Prion which leaves the blood brain barrier intact. It was initially assumed that the spread along the retinal pathway following intra-ocular injection of Prion occurred via axonal transport (Fraser 1982). This was further explored with respect to PrP^c dependence for transmission along this route. In one study PrP expressing neural grafts were used as indicators of Prion infectivity in the brain of a PrP knockout mice. Following intra ocular injection of PrP^{sc} in PrP^c deficient hosts no Scrapie was seen in neurons (Brandner, Isenmann et al. 1996). Therefore when the chain of PrP is interrupted it appears that intra-cerebral spread is not possible. It might be that PrP^c is required more specifically for propagation between synapses (Collinge, Whittington et al. 1994); alternatively a clear path from PrP^c molecule to PrP^c molecule may be necessary to create a domino effect (Aguzzi, Blattler et al. 1997).

1.13. Neuropathology

The cell types necessary for transmission and mediation of pathogenesis are unclear. In a mouse model in which PrP^c expression is restricted to Astrocytes (Raeber, Race et al. 1997), Prion disease progresses normally in the transgenic mice and this inveighs against the notion that neurons expressing PrP^c are necessary for pathogenesis. Whether this implicates Glial cells as a central means of transmission in Prion disease in general is unclear because in neurons where depletion of PrP^c is targeted following infection it is apparent that spongiform changes are reversible (Mallucci, Dickinson et al. 2003).

The necessity of PrP^c in Prion disease is most clearly evidenced with reference to the PrP knockout mice which do not show neurotoxicity or any development of Prion disease following inoculation with Prion. One obvious hypothesis would be that PrP^{sc} is the toxic species which requires PrP^c to replicate. PrP^{sc} toxicity has been assessed independently by introduction of neurografts which express prp, into knockout mice and then inoculating with Prion (Brandner, Isenmann et al. 1996). The grafts replicate and accumulate PrP^{sc} and substantial quantities

of PrP^{sc} are also delivered into the host brain. In these cases clinical disease is not elicited and neuropathology is not present, indicating that PrP^{sc} alone is unlikely to be the toxic species. Prion diseases where PrP^{sc} is not readily detectable also present a challenge to the hypothesis that PrP^{sc} is the key molecule in pathogenesis (Hegde, Mastrianni et al. 1998; Manson 1999)

The finding that PrP^{sc} is cytotoxic only in the presence of PrP^c has been supported in studies which demonstrate that a PrP peptide 106-126 which is toxic to cultured neurons from mouse brain is not toxic when the neurons do not express PrP^c (Forloni, Angeretti et al. 1993; Brown, Herms et al. 1994).

Hypotheses connected with mechanisms of cell death have focussed largely on issues concerning neuronal health. Apoptotic cell death has been described in various cell culture systems (Kretzschmar, Giese et al. 1997) and *in vivo* (Giese, Groschup et al. 1995; Gray, Adle-Biassette et al. 1999). Hypotheses which have been suggested for apoptosis have included oxidative stress (Milhavet and Lehmann 2002) and microglial mediated damage (Betmouni, Perry et al. 1996). One further hypothesis which has been discussed above, implicates a particular species, ctmPrP, in the process of disease. Although there is little evidence for ctmPrP as a significant species in normal disease, models of this sort are suggestive of the possibility of alternate PrP species which might be toxic and perhaps stimulated by PrP^{sc}.

1.14. Prion therapeutics

Prion has been cleared from cell culture models by polyionic compounds (Caughey and Raymond 1993) Congo red (Caughey and Raymond 1993), Amphotericin B (Mange, Nishida et al. 2000) Aporphyrins (Caughey, Raymond et al. 1998) and Quinacrine (Caughey, Raymond et al. 1998). Most of these compounds have proven to have little effect on incubation period *in vivo*.

One means of preventing infection is the use of PrP antibodies in order to perturb new conversion of PrP^c to PrP^{sc}. In cell culture models several studies

have demonstrated the ability of antibodies to clear infectivity. (Enari, Flechsig et al. 2001; Peretz, Williamson et al. 2001; Gilch, Wopfner et al. 2003).

Transgenic mice which express anti-PrP mu chains are also protected against peripheral Prion infection. In another study mice previously infected with Prion were immunised with anti-PrP monoclonal antibodies. PrP^{sc} levels in the spleens of the mice were reduced significantly and animals remained healthy for long extended periods after controls had died from the disease (White, Enever et al. 2003). Attempts to extend this technique to the CNS have proven unsuccessful and intra-cerebral injection of anti PrP antibodies causes considerable neuronal apoptosis (Solfrosi, Criado et al. 2004). Active immunisation as an approach is at present also limited by the self-tolerance to PrP although some studies have shown modest effects (Sigurdsson, Brown et al. 2002; Schwarz, Kratke et al. 2003).

Work has already been described which provides biochemical means of blocking peripheral Prion replication and subsequent neuroinvasion.

Administration of lymphotoxin receptor-IG fusion protein neutralises the lymphotoxin –B-receptor and thereby prevents FDC maturation. This process prevents Scrapie neuroinvasion following intraperitoneal Scrapie infection but is not helpful in the case of intracerebral infection (Mabbott, Mackay et al. 2000; Montrasio, Frigg et al. 2000; Mabbott, Young et al. 2003) .

One further possible intervention is the use of antibodies against PrP^{sc}, which might halt the spread of disease by inhibiting further replication of Prion and allowing cell clearance of existing disease agent. An antibody with specificity for PrP^{sc} was formed by immunisation with a Tyrosine-Tyrosine-Arginine containing PrP peptides in animals expressing endogenous PrP and clearance of PrP^{sc} using these antibodies was demonstrated in a cell culture model (Paramithiotis, Pinard et al. 2003).

1.15. Rationale for experiments of this thesis

The subject matter for the thesis below falls broadly into two categories. The first, and the smaller body of work, represents an attempt to consider the effect of glycosylation on infection. The identification of glycosylation with strain type has been a key argument in the identification and alignment of vCJD with BSE (Collinge, Sidle et al. 1996). Work has been undertaken to assess the preservation of glycoform properties in culture as a key means of understanding how this feature of Prion disease is propagated and how the glycoform profile is determined (Birkett, Hennion et al. 2001; Vorberg and Priola 2002).

The agent tunicamycin has been employed as a means of perturbing the glycosylation profile of PrP^c and consequently PrP^{sc} in cells. The purpose of these experiments is to ascertain to what extent glycosylation, particularly of PrP^{sc}, directs the infectious process. Two null hypotheses tested include a) that PrP^{sc} synthesis is disproportionately determined by the abundance of the unglycosylated PrP^c species and b) that PrP^{sc} glycosylation is necessary for transmission and recovery of glycosylation profile.

The second part of the thesis is centred on the use of GFP fusion proteins, as a means of tracking the dynamics of both PrP^c and, potentially, PrP^{sc}. The rational thrust of these experiments issues from two sources: firstly, there is at present no single cell assay, and no subcellular assay, for Prion and secondly, very little is understood about the dynamics of the PrP^c/ PrP^{sc} cellular system. The use of GFP fusion proteins over the time periods required for the studies described below is a risky and speculative process. It pushes the limits of current technology in microscopy, a time and resource intensive endeavour requiring the creation and refinement of a new microscopy system. It also speculates on the potential observability of the relevant events at the required resolution and whether the C-terminal portion of the fusion proteins (PrP^c) is converted to PrP^{sc}. Clarification is provided for the merits of this approach to address issues of Prion infection and how such approaches might be improved in the future. In particular hypotheses relating to Prion biophysics are addressed which relate to the transfer of infectivity and diffusion of Prion protein in the plasma membrane.

Chapter 2 Materials and Methods

2.1. Molecular Biology

2.1.1. Standard protocols employed for molecular biology

2.1.1.1. PCR (polymerase chain reaction)

0.5uM of each primer and 0.2mM dNTP mix were used unless otherwise stated. Magnesium was provided by the Taq PCR buffer and Taq enzyme was used following manufacturer's instructions (Invitrogen). Plasmid DNA was used as a template in a reaction following a standard PCR programme:

1) 95 °C	2 minutes
2) 95 °C	30 seconds
3) Annealing temperature	30 seconds
4) 72 °C	extension time
5) Go back to step 2, repeat 29 times	
6) 72 °C	10 minutes
7) 10 °C	HOLD

The annealing temperature used was 1 °C lower than the lowest melting temperature of the primers. Generally, 10ng of DNA template was used per PCR. PCR products were checked by gel electrophoresis, purified using Qiaquick gel extraction kit (Qiagen) and sequenced (MWG Biotech).

2.1.1.2. Restriction digestion and ligation of DNA

Unless otherwise stated, 1µg DNA was digested using 5 units of restriction enzyme (New England Biolabs) at 37°C for 2 hours. Digests were run on agarose gels and the DNA cleaned using Qiaquick gel extraction kit (Qiagen). Ligations were carried out using T4 DNA ligase (Invitrogen) according to manufacturer's instructions.

2.1.1.3. Preparation of DNA

Epicurian Coli, XL2 Blue Ultra competent cells (Stratagene) were used for transformation following manufacturer's instructions). Approximately 50ng of DNA was used for each transformation The PIAH vector was ampicillin

resistant. All other vectors described in this thesis have a backbone including a kanamycin resistance gene. The concentration of ampicillin used for agar plates was 50µg/ml and for kanamycin plates was 30µg/ml.

Maxi preps and mini preps were carried out according to manufacturer's instructions (Qiagen). Briefly, alkali lysis of bacteria was followed by DNA separation using the column provided in the kit. Plasmid DNA was then eluted in salt buffer and precipitated using isopropanol.

DNA concentration and purity was determined by taking the A260/A280 ratio (a value of 1.8 was taken as ideal for the ratio).

2.1.2. Generation of constructs: GFP in fusion with PrP, DsRedII in fusion with PrP and 3F4 mutant fusion

The fusion constructs were generated as two separate parts which were independently cloned into the vector providing the fluorescent tag.

The signal peptide of the mouse protein was indicated by the previous, successful design on which the construct is based (Lee, Magalhaes et al. 2001) and cross checked with reference to Signal IP, a bioinformatics online tool (<http://www.cbs.dtu.dk/services/SignalP>).

The signal peptide of mouse PrP (amino acids 1-22 inclusive) was generated by PCR from the pIAH vector (a kind gift from Dr Chris Birkett, IAH) using forward (TCCACCGGTTCTGCCGCCACCATGGCGAACCT) and reverse (CAGACCGGTGCGCAGAGGCCGACATCAGTCC) primers. The primers introduced an AgeI site which was used to clone the signal peptide upstream of GFP in the pEGFPC3 vector (Clontech). The C-terminus of PrP was also generated by PCR from the pIAH vector using forward (GCCCTCGAGAAAAAGCGGCCAAAGCCT) and reverse (GCCCTCGAGTCATCCCACGATCAGGAA) primers which introduced an XhoI site at each end. The fragment was cloned in-frame into pEGFPC3-Prp signal peptide using the XhoI site downstream of the GFP.

The signal peptide for the DSRed fusion was similarly generated by PCR and cloned into the AgeI site upstream of the DSRedII vector (Clontech). DsRedII is a mutant of the original DsRed protein designed to decrease oligomerisation. The C-terminus of PrP was generated by PCR from the PIAH vector using forward (CGTGAATTCGAAAAAGCGGCCAAAGCCT) and reverse (CGTGGATCCTCATCCCACGATCAGGAA) primers which introduced an EcoRI and BamHI site respectively. These sites were used to clone the C-terminus into the DSred2-signal peptide vector downstream and in-frame with the DSRed.

2.1.3. Site-directed mutagenesis to generate the 3F4 epitope

Leu¹⁰⁸ and Val¹¹¹ of mouse PrP were each mutated in the context of the GFP-PrP construct, to Methionine residues to generate the 3F4 epitope. The Quick-Change Site-Directed Mutagenesis kit from Stratagene was used and manufacturer's instructions were followed. Briefly, forward (CCAAAAACCAACAT**GA**AGCATATGGCAGGGGCTGCGGCA) and reverse (TGCCGCAGCCCCTGCCATATGCTT**CA**TGTTGGTTTTTGG) primers each containing three point mutations (indicated in bold) were used in a circular PCR to generate a mutated plasmid with nicked staggered ends. 17 PCR cycles were performed, as recommended by the manufacturer. Parental DNA was digested using DpnI and the mutated, nicked plasmid transformed into XL-1 blue super competent cells (Stratagene) which repair the nicks.

2.1.4. Other vectors employed

GFP-GPI was kindly donated by Kai Simons. It contains an EGFP (Enhanced Green Fluorescent Protein) fused at the C-terminus to a GPI anchor sequence (of lymphocyte function associated antigen 3 (LFA-3)) and at the N-terminus to a signal sequence of lactase phlorizin hydrolase (Keller, Toomre et al. 2001).

CFP (cyan fluorescent protein) PrP was kindly donated by Nnenna Kanu. This vector shares the same basic design with the GFP-PrP fusions, i.e. the signal

peptide of PrP is placed N-terminally to CFP and the remainder of PrP is placed c-terminal to CFP.

It was employed to ensure that the specific linker added between the fluorescent protein and the PrP C-terminus was not responsible for cleavage. The difference in linker is illustrated in bold (KKRPK marks the start of the PrP c-terminal portion of the fusion proteins).

PrP-GFP junction (linker in bold):

K **Y S D L E K** K R P K

PrP-CFP junction (no linker):

K -----K K R P K

Zsgreen (Proteasome sensor vector: Clontech) is a vector which encodes a destabilized green fluorescent protein (ZSGREEN) in fusion with a degradation motif for removal by the 26S proteasome.

2.2. Cell culture

2.2.1. Cell transfection

Cells were plated onto 35mm dishes, 24 hours prior to transfection, at approximately 50% confluence. Cells were transfected with cDNAs using Gene Juice (Novagen) following manufacturers specifications for all procedures. For each 35mm dish 1µg cDNA was used with 3µl of gene juice mixture. Media was changed 1 day post transfection.

2.2.2. Cell lines and cell media

SMB cells were produced by culture of brains from mice infected with the Chandler scrapie isolate (Clarke and Haig 1970; Clarke and Haig 1971). Scrapie mouse brain cells (SMB) cells and Pentosan sulphate (PS) cells were

obtained from Dr C. Birkett, I.A.H. Compton. PS cells were produced by curing of SMB cells with pentosan sulphate (Birkett, Hennion et al. 2001). Cells were grown on plastic culture flasks for all passaging and experiments unless otherwise specified. Media employed were M199 (M199 Gibco, BRL), with 5% new Foetal calf serum (Firstlink Foetal calf serum) and 10% New born calf serum (GibcoBRL (Invitrogen post takeover), New born calf serum), penicillin 50i.u./ml (Sigma), streptomycin 50µg/ml (Sigma). Cells were grown in a humidified incubator at 37°C and 7.5% CO₂. Cells, for the purpose of ordinary passage, were split with a ratio of 1:3 approximately every 7 days.

These media were employed for all experiments described in chapter 1.

However, it was advised, (pers comm. Telling group, Kentucky) that problems in these cell lines with transfection efficiency and selection could be ameliorated by growth in DMEM (Dulbecco's modified Eagle's medium) rather than M199. Therefore cells described after chapter 1 are grown in the recommended medium: DMEM (DMEM Gibco BRL), with 10% new Foetal calf serum (Firstlink Foetal calf serum).

2.2.3. Cell lines expressing fusion protein

Initial attempts at cloning cells met with failure. Even attempts to grow cells at low density, e.g. 1:50 split (not clonal dilutions) died. Higher ratios of split (e.g. 1:10) produced groups of cells in relatively isolated clumps which could be taken with cloning rings, but it was clear that these cells did not themselves represent clones. As described in chapter 4, attempts in the laboratory to overcome these difficulties including the use of conditioned media, transfection with large T antigen, and feeder layers have previously not been successful.

Therefore a recommended bulk selection procedure was employed.

To produce cell lines expressing fusion proteins, cDNA was transfected using the gene juice reagent as described (see below). Media were changed the day after transfection and cells permitted to grow to confluence. Cells were then split at 50% confluence and 0.5mg/ml of neomycin was added to begin selection.

Cells were kept in the selection media and split at 1:4 for the next passage.

Cells were split as normal thereafter but kept in selection medium for at least 3

weeks (from initial addition). Cells froze and thawed with the same kind of efficiency as regular PS cells and therefore in general cells were frozen at low passage and not grown beyond p20 before revival of the lower passage cells.

2.2.4. Preparation of culture materials by lysis

Cell were lysed in cell lysis buffer (see below) following removal of media and washing 2x in Hank's balanced salt solution (HBSS : Invitrogen, Gibco BRL) or Phosphate buffered saline without calcium (Invitrogen, Gibco BRL) depending on whether the samples were cultured in M199 or DMEM respectively. In general a 162 cm² black cap flask was lysed in 1.5 ml of buffer. Samples were then frozen at -20°C prior to analysis.

2.2.5. Preparation and infection with dead cell freeze-thaw lysates

A confluent flask, 162 cm², of the desired cells was washed in PBS (Gibco BRL) twice and subsequently, all liquid was carefully removed to ensure volume was minimised. Cells were then lysed in a further 1ml of PBS by scraping the bottom of the flask. The resulting cell mixture was then mixed thoroughly by vortexing and pipetting. The material was passed 3 x through a 19 gauge syringe needle and was then put through 4 cycles of freezing in liquid nitrogen and thawing at 37°C.

Infection was carried out in 25 cm² flasks, in which cells were grown to 50% confluence. A third of the total homogenate produced from the SMB/PS culture was used for an infection to create the paired cell lines. (This was slightly different in the Tunicamycin treated cases as described below). It was added to new media and pipetted thoroughly. The media containing the dispersed homogenate was then placed onto the cells and the cells left for 3 days. Media were then changed and the cells were left for a further 1 day prior to splitting, and expansion, as normal.

2.2.6. Treatment with Tunicamycin

Tunicamycin (Sigma) was prepared in 75% methanol and added to culture flasks after a change of media as the experiment required. Tunicamycin was always added to confluent cells at 1 or 10µg / ml as specified. In general, after treatment for a period of 48 hours or greater, cells appeared refractory and some death occurred. Therefore careful handling of cultures for lysis was necessary to keep cells adherent to the flasks prior to lysis.

For the experiments which required production of freeze-thaw lysates from Tunicamycin treated cells, 2 x 162 cm² flasks were used. Samples were normalized for total protein using the BCA assay (Bicinchoninic acid protein assay; see below) and then were adjusted appropriately for comparison with the control samples prior to infection.

2.2.7. Biotinylation protocol (Walmsley, Zeng et al. 2001)

Cells were incubated at confluence, with 0.5mg/ml of Sulpho-NHS biotin, for 30 minutes at 0 degrees C. Cells were then washed 3x in 50mM glycine to absorb unreacted biotin. Cells were then lysed in cell lysis buffer and incubated with streptavidin coated beads (DynaL Biotech – dyna bead M280 streptavidin) according to the manufacturers specifications. Briefly: Two black caps (162cm²) were used for each condition. 50 µl of bead suspension at (6.7 x10⁸ beads /ml) was used per ml of lysate. Following resuspension of beads that had been incubated overnight with the samples, 10 % was removed for PrP^c analysis (re-suspended in sample buffer, boiled, supernatant taken for western blotting) and 90% was re-suspended in lysis buffer and digested with Proteinase K, supernatant taken, and processed for PrP^{Sc} thereafter as normal.

2.2.8. PIPLC treatment to cleave GPI anchored fusion protein

Cells were cultured on cover slips coated with laminin (sigma) at 20µg/ml until confluence was reached. They were washed in PBS and placed in L-15 medium without serum but containing PIPLC (ICN) at 2units /ml, for 1 hour at 4° C. Control cells had no PIPLC added over this period.

2.2.9. Preparation of cells for Microscopy

2.2.9.1. Time-lapse

Glass bottom dishes (35mm dishes with 14mm glass insert Matek U.S.) were coated with laminin 20µg/ml (Sigma) for 1 hour. They were washed in PBS and finally in medium prior to addition of cells.

Depending on the configuration desired cells were split in different ways. For example the configuration of cells depicted in results Chapter 5 Figures 5.3, cells were split so that the majority cell line would be at 50 % confluence. The minority indicator cell line was split at 1:100. Prior to plating, the cells were mixed by pipetting. For time-lapse on mobile cell populations cells were split at 1:10 or 1:8 and mixed with their co-culture partner to a final confluency of 1:5 or 1:4. The cells were cultured in normal medium until the desired density and then removed to the time-lapse apparatus after changing into a non carbonate buffered medium Leibowitz L-15 (Gibco), with the same constituents as the normal DMEM complete medium.

Initially cells were counted for the purposes of controlling for differences in density that might arise between experiments. However, it proved more accurate to split the cells from confluence to an appropriate density in order to arrive at the desired configuration for microscopy.

2.2.9.2. Preparation of cells for Immunocytochemistry

Cells were split onto cover slips that were sterilised and pre-treated with laminin (20µg/ml; Sigma) in the same manner as the glass bottom dishes. They were then placed in 4 well dishes and cultured in the usual manner until required for further analysis.

2.2.9.3. Preparation of cells for Confocal microscopy

For use of an upright confocal, cells were grown on glass slides in wells defined by silicone gaskets (Multi-well system: Molecular Probes), which were coated

with laminin 20µg/ml. The cells were washed and placed in L-15 media prior to microscopy and kept at 37°C.

For the confocal on the Zeiss LSM microscope, an inverted microscope, well glass bottom chambers (Nunclon) were coated with laminin and the cells cultured as normal until required. They were then transferred to L-15 media.

2.3. Microscopy

2.3.1. Time-lapse microscopy

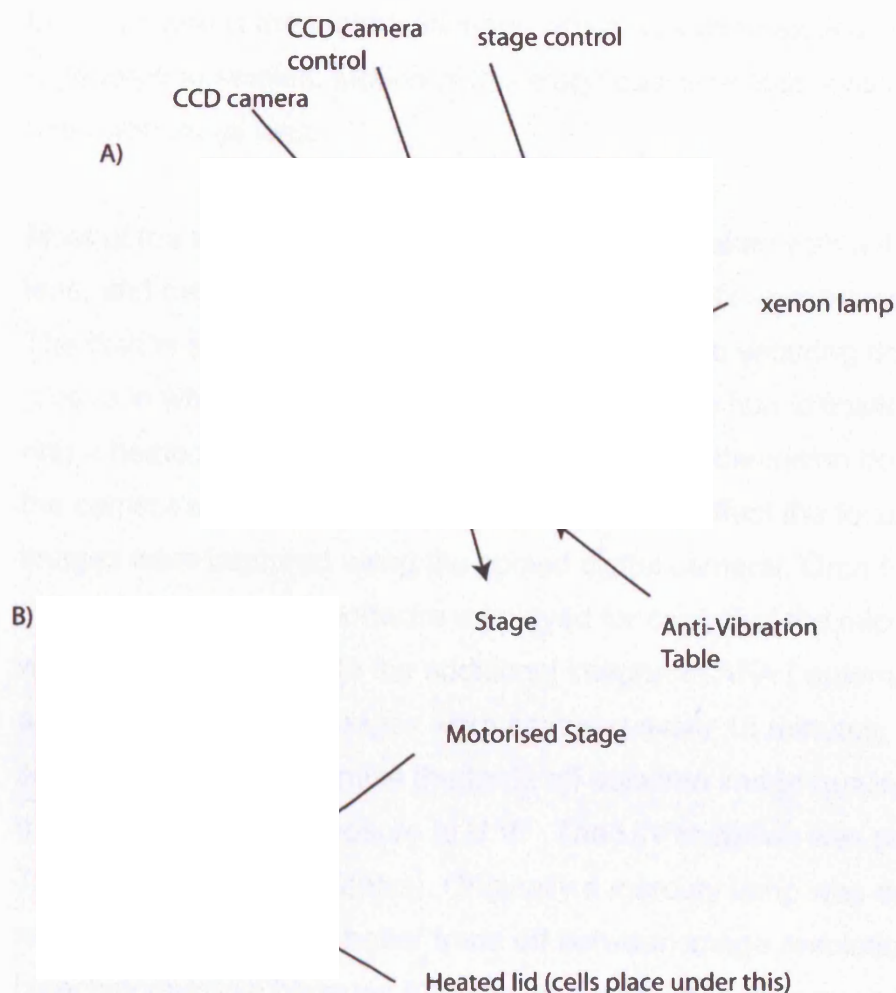


Figure 2.1. Time-lapse apparatus.

A) The time lapse set up is indicated in broad overview, with the full temperature controlled chamber in place over the inverted microscope. An anti-vibration table was added in order to help maintain focus.

B) The motorised stage is visible from this angle more clearly. This was used primarily by the newt research group but could potentially be useful for studies of infected cell behaviour at lower resolution. Note the circular heated lid (red wire is connected to it). Condensation does not form and obstruct the camera path above the dish. Cells are fixed into a metal ring with lens in place, and left to equilibrate for at least an hour to test whether focus is maintained before continuing with time-lapse observations.

(Digital Images kindly given by Amy Duckmanton)

Over a 4 year period, a time-lapse system has been developed to permit the maintenance, in a controlled environment, of mammalian cells. Fig 2.1 shows the Zeiss Axiovert S100 inverted microscope, with Orca ER, camera for acquisition and the surrounding temperature control environment. Also included in this picture is the motorised stage which was used extensively for regeneration studies. Motion of this stage caused a total loss of focus when used with an oil lens.

Most of the images described in chapter 5 were taken with a 40x neofluor oil lens, and cytoplasmic cells were imaged with a 20x apochromat lens. The dish is secured at the centre of the stage. The securing ring contains a groove in which water is placed in order to ensure humidification. On top of this ring a heated lid is placed which ensures that condensation does not obscure the camera's path and that drips of liquid do not affect the focus. Fluorescent images were captured using the cooled digital camera, Orca ER, (Hamamatsu). The software employed for control of the microscope set up was Image Pro plus with the additional integrated AFA (automatic fluorescence acquisition) module. Images were captured every 15 minutes, using 2x binning setting in order to maximise the trade off between image quality and cell damage caused by exposure to U.V. The U.V radiation was produced by a 75W xenon lamp (Carl Zeiss). Originally a mercury lamp was employed but the xenon lamp provided a better trade off between image resolution and cell bleaching/survival because it produces a level intensity across the spectra rather than the higher peaks of intensity of the mercury emission spectrum. Filters were designed so that the emission signal was filtered to separate DsRed (Discosoma red) and GFP emissions: GFP filter (525/40nm Chroma technologies) and a DsRed filter 620/40nm (Chroma technologies) A single exciter was used on the excitation filter wheel, and Images were acquired using different emission wheel positions (for the two filters) in 12 bit grey scale mode and then pseudo colour added during image processing to highlight the different channels.

Preparation for time-lapse included a process of equilibration; first, equilibration of the equipment at 37°C, and then the sample on the glass bottom dish which

is ideally equilibrated overnight or for a minimum of 1 hour in order to ascertain whether focus drift is likely to occur.

2.3.2. Microscopy for immunocytochemical studies

Imaging of cells following immunocytochemistry were taken on a Zeiss axioplan 2 upright microscope using a CCD camera (Axiocam HRC Zeiss), co-ordinated with the Zeiss Axiovision software. For visualisation of the GFP signal the FITC (fluorescein isothiocyanate) filter set was used and for visualisation of the TRITC (tetramethyl rhodamine isothiocyanate) secondary antibody a Texas red filter set was employed. Images were taken using a 63x oil objective.

2.3.3. Use of confocal for FRAP (fluorescence recovery after photobleaching) measurements

2.3.3.1. Experimental set 1

A Biorad radiance 2100, an upright confocal, was used at the Laboratory for Molecular Cell Biology, UCL. Cells were prepared on multi-well chamber glass cover slides (for use with an oil lens) as described, or on glass bottom dishes (Matek) for use with a 40x water immersion lens. They were kept at 37°C by placing them on a heated tray with a glass base. The system suffered a lot of drift and the torsion was placed at maximum on the z-stage in order to minimise this effect. Using the Laser sharp 2000 software package, cells were initially imaged at low intensity (4% of the maximum laser intensity) and a bleach box of 3 microns and a control box surrounding the cell were defined. The pin hole aperture was opened fully for FRAP measurement on this set up in order to minimise the effects of focus drift. Images were taken as 512x512 resolution. 3 prescan images were taken at 4% laser intensity, 5s apart and then 15 bleach scans at 100% intensity, the pinhole was then opened fully and intensity changes measured at 4% laser intensity, scanning every 5 seconds. Experiments were ended when there appeared to be no more change in either the bleach box or the control box intensity values, or when focus was lost.

2.3.3.2. Experimental set 2

Imaging was carried out using an inverted confocal microscope (LSM 510; Carl Zeiss Inc) at the London School for Hygiene and Tropical Medicine. Fluorescence excitation was achieved for GFP using the 488 nm laser line. Cells prepared on 6 well glass slide chambers (Nunc) and were placed in a temperature controlled environment surrounding the microscope set up at 37°C. Images were taken using a 40x plan neofluar objective (1.3NA). The confocal pinhole was set at 1 Airy unit. Bleach and control boxes were defined as described above but the width set to 1 μ M for the bleach region. 3 prescans were taken, at low laser intensity. Photobleaching was achieved with 10 scans at full power. Recovery was measured every 0.4s.

2.3.3.3. Data analysis of FRAP experiments

Data was transferred to excel spreadsheet format. A programme was written in Matlab in order to a) normalise the data and b) find the diffusion coefficient. The steps in the programme (see appendix) to process the data from the bleach strip in which recovery occurred were as follows:

Input the data from each spread sheet into the programme vector representations → normalise all bleach recovery (post bleach measurement) values by dividing by their corresponding control box time point value → renormalize to zero by subtracting the initial value post bleach from all recovery values → calculate the diffusion coefficient by fitting this data to the equation for 1 dimensional diffusion: gives the parameter D
→ Finally the programme compared all the recovery values to a prebleach mean value and plotted the data. From this the immobile fraction was also calculated as the difference between the asymptotic value of the recovery and the prebleach value. NB: the crucial piece of data was the shape of the recovery curve – from this the diffusion coefficient in $\mu\text{m}^2/\text{s}$ could be calculated.

2.4. Biochemistry

2.4.1. Processing for analysis of PrP^{sc} and PrP^c

Following lysis of a 162 cm² flask in lysis buffer (see buffers below) nuclei are removed by centrifugation at 1000g, 4°C, for 5 minutes. Samples are then divided for PrP^{sc} and PrP^c analysis. 90 % of the post nuclear spin supernatant is taken for PrP^{sc} analysis and 10% is taken for PrP^c analysis. 100 µl approximately is available for PrP^c which is methanol precipitated by addition of 900µl (9x by volume) of methanol, -20 °C methanol, and the samples are themselves kept at -20°C for a minimum of 1 hour. Precipitates are then pelleted by centrifugation at 1000g , 4°C, for 15 minutes and resuspended in 100 µl of 1x sample buffer.

The other 90% of the post nuclear supernatant, for PrP^{sc} analysis, is incubated for an hour at 37 °C with 30µg/ml of Proteinase K. The protease activity is then blocked by addition of PMSF (phenyl methyl sulfonyl fluoride) to 1mM on ice for 20 minutes. Samples are then centrifuged at 365, 000g for 15 minutes at 4 degrees C in a Beckman ultracentrifuge using a TLA, 120.1 rotor. Supernatant is removed and pellets are solubilised in 30µl of 1x sample buffer and stored at -20°C.

2.4.2. BCA assay for total protein quantification

In order to determine total protein concentration for normalisation prior to loading of western blots the Bicinchoninic acid protein assay (BCA assay; Pierce) was employed. Dilutions of a standard were made in the range of 0 to 250µg/ml from a 2mg/ml BSA (bovine serum albumin) stock. All samples for analysis were diluted in 40x sample buffer, the same diluent used for the BSA standard dilutions. The advantage of this assay was that it was fully compatible with the detergents in the samples. The assay was completed according to manufacturer's instructions. Reading from the 96 well plate were taken using the MRX micro plate reader, absorbance set at 562nm. The programme estimated the sample concentrations from the dilution series of standards.

2.4.3. Preparation of samples with N-glycanase

N-glycanase (N-glycanase : Glyko) was used according to manufacturer's specifications. Briefly, pellets from PrP^c and PrP^{sc} analysis as described above (either methanol precipitated for PrP^c or ultracentrifuged for PrP^{sc}), were resuspended in the N-glycanase 1x buffer, boiled for 2 minutes and cooled. The SDS (0.5%) was diluted out by addition of NP-40 to a final concentration of 2% NP-40, and 5µl of N-glycanase added to a sample which had been resuspended in 100µl of buffer for the PrP^c pellets and 2.5 µl added to a sample which had been resuspended in 30 µl of buffer for the PrP^{sc} pellets. Samples were incubated overnight at 37degrees. Control samples were taken through the same procedure but no N-glycanase was added. 4x sample buffer was made up and added to produce a final concentration of 1.5x sample buffer in each sample.

2.4.4. Western blotting

Western blotting was undertaken, according to standard procedure (Sambrook et al , 1989). Samples were electrophoresed at 200V for 50 minutes using Novex pre-cast tris-glycine 12% polyacrylamide gels (Invitrogen), prior to blotting onto nitrocellulose membranes (Schleicher and Schuel). Following transfer for 1.5 hours at 150mA , membranes were rinsed western washing buffer (see below) of Tris buffered saline with 0.1% Tween, and blocked for 14 minutes in 3% non-fat powdered milk (Nestle). Membranes were then incubated with antibody overnight. Antibodies were diluted (see below) to the required concentrations in block. Blots were rinsed once and then washed 4 times for 5 minutes in TBST (Tris-buffered saline Tween). They were then incubated at room temperature for 1h with horseradish peroxidase conjugated rabbit anti mouse antibody (DAKO rabbit anti mouse HRP antibody) at a 1:5000 dilution. Proteins were prepared for chemi-luminescent visualisation using an Enhance Chemiluminescence kit (Amersham, ECL kit). Images were then either developed using Kodak film (Kodak xls film) or the Fujifilm Luminescent Image Analyser (LAS 2000).

The standard processing of a 162 cm² flask of SMB cells for PrP^{Sc} analysis affords 3 western blot results. In contrast 10% of that same material, taken for PrP^C analysis, will afford enough sample to run 10 blots of equal intensity to that from the prion western signal described. (An example is shown in results Chapter 3 , Fig3.2 of the standard blot and the control samples from the Fig3.6 as a more formal example). The approximate ratio from the above observations, is 1:30. i.e. roughly 3.3 % of PrP species are prion in an SMB sample.

2.4.4.1. Quantification of western blots

Following blot preparation with ECL, blots were immediately taken with the Fujifilm Luminescent Image Analyser (LAS 2000). Images were then analysed in Image Gauge v3.1. Average, background corrected, intensities of dilutions were compared to give a rough indication that measurement was being taken in the linear range. The final intensity value was calculated as the weighted average intensity of the dilutions for each sample condition.

2.4.5. Immunoprecipitation

Samples were lysed as normal. For the key experiments 2 black caps were taken for each condition. Lysates were incubated with a 1:100 dilution of rabbit anti-GFP (Clontech) or a control rabbit anti-Rb (Retinoblastoma) (Brookes lab antibody) for 1.5 hours at room temperature.

60µl of Magnetic beads conjugated to secondary antibody (DynaL biotech M-280 sheep anti rabbit conjugated magnetic beads), were then added (stock dilution at $6-7 \times 10^8$ beads/ml) to 1ml of lysate and rotated in an Eppendorf tube overnight. NB: Beads to be used for Immunoprecipitation were washed in TBS and resuspended in lysis buffer before use Following overnight incubation, beads were washed using TNT 4x and resuspended, using the magnetic particle separator (DynaL biotech) to remove supernatants. A final wash in TBS was then undertaken. For PrP^C analysis, 10 % of the TBS resuspension beads were taken and removed to 1x sample buffer and boiled for 3 minutes. Supernatants were run on western blots.

For PrP^{sc} analysis, the remaining portion of the TBS beads was taken. Samples were resuspended thoroughly in lysis buffer (back to the 1ml volume post lysis per 162 cm² flask) and Proteinase K added. The samples were mixed thoroughly every 10 minutes during this period. Beads were removed and the supernatants processed for PrP^{sc} as described above. Pellets were resuspended and samples pooled: the processed sample from 2 x 162 cm² flasks were run on each western blot lane.

Background controls were also taken by resuspension of antibody in 1ml lysis buffer at normal concentration, and then taking it through the same processes as described above for cell lysates.

2.4.6. Immunofluorescence studies

2.4.6.1. Fixation protocols

Cells were washed 2x in PBS and fixed using 3% PFA (paraformaldehyde), for 5 minutes

Cells were then washed in PBS 2x, washed once in block (10% goats serum in PBS), and then blocked for 15 minutes. Antibodies diluted in block were added for 1 hour, cells were washed in PBS (4 x 5 minutes) and incubated with secondary antibody (diluted in block at 1:100) for 1 hour and subsequently, rinsed once and washed 4x5 minutes in PBS.

For permeabilisation protocols, post fixation, 0.1% Triton was added to block and PBS for washing.

Antibodies used in this thesis for immunofluorescence, and their respective concentrations/dilutions of use are enumerated below.

2.5. Reagents

2.5.1. Antibodies

2.5.1.1. For western blotting

The following antibodies were used for western blotting

6H4 (0.5µg/ml) (Prionics AG) , 3F4 (kindly provided by Chris Birkett, I.A.H. Compton, and anti GFP monoclonal antibody(mixture of two monoclonal antibodies) (Roche: mouse anti GFP), 0.2 µg/ml.

2.5.1.2. For immunocytochemistry

Primary antibodies:

6H4 (Prionics Ch)) was employed at 1:100 dilution (from 5mg/ml stock)

BrdU (Brockes laboratory) employed at 1:60 (from 3.4mg/ml stock)

GFP polyclonal was used (Clontech) at 1:100

Secondary antibodies:

FITC or TRITC conjugated goat anti mouse (DAKO), antibodies were used at a dilution of 1:100 (10µg/ml final concentration). TRITC conjugated swine anti rabbit (DAKO) was used at 1:100 dilution.

2.5.2. Solutions and Buffers

2.5.2.1. General purpose

Tris-EDTA

10mM Tris-HCl, pH 8.0

1mM EDTA

LB broth

10g bacto-tryptone

5g bacto yeast extract

10g NaCl

1 litre ddH₂O (deionised)

2.5.2.2. Cell culture

Lysis buffer (regular use)

10mM Tris-HCl , pH8.0

100mM NaCl

10mM EDTA

0.5% NP40 (Nonidet P40)

0.5% sodium deoxycholate

For experiments where protease inhibition is required

Addition of 1 tablet of complete protease inhibitor cocktail mini (Roche), including Pancrease extract, Pronase, Thermolysin, Chymotrypsin and Papain was added to 7ml buffer and dissolved prior to use.

2.5.2.3. Preparation for and generation of Western blot

N-glycanase buffer 1x complete

50mM 2-beta mercapto ethanol

0.5 % SDS

5x supplied N-glycanase kit buffer solution

in ddH₂O

Phenyl methyl sulphonyl fluoride (PMSF)

200mM PMSF diluted in methanol

Proteinase K

1mg/ml diluted in water

2x sample buffer

100mM Tris-HCl, pH 6.8

4% SDS (ordinary SDS)

0.2% bromophenol blue

20 % glycerol

Transfer buffer, pH8.3

50mM Tris

40mM glycine

0.08% SDS (electrophoresis grade)

20% methanol

2.5.2.4. Western blotting procedure

Western blot washing buffer (TBS-Tween (TBST)):

50mM Tris-HCl

100mM NaCl

0.1% Tween 20

2.5.2.5. Immunoprecipitation

Washing buffer TNT:

50mM Tris 8.0

200mM NaCl

2% NP40

2% Tween

TBS

50mM Tris-HCl , pH8.0

200mMNaCl

Chapter 3 The Role of Glycoform in Infection

3.1. Introduction

Cell lines capable of maintaining infection provide a means for the study of the nexus between the molecular mechanisms underlying prion disease and the cellular context in which they operate. This chapter briefly explicates the SMB/PS system and explores one strategy for asking clear questions about the importance of glycosylation for the process of infection.

The critical cell line employed in this thesis, Scrapie Mouse Brain Cell (SMB), was derived from the cultured mouse brain of an animal which was infected with the Chandler strain of Scrapie (Clarke and Haig 1970; Haig and Clarke 1971). The outstanding property of these cells is their ability to stably maintain infectivity, roughly one LD₅₀ per 100 cells, over multiple passage; cells stably maintain the production of PrP^{Sc} from endogenous PrP^C expression. In order to produce an infected/uninfected cell line pair, SMB cells were cured with the sulphated glycan, Pentosan Sulphate, yielding a cell line, nominated 'PS'. PS cells contain no PrP^{Sc}, as assayed by western blotting, and no infectious titre, as assayed by inoculation of mice (Birkett, Hennion et al. 2001). The mechanism of Pentosan Sulphate action remains unclear, but suggestions have included binding to PrP^{Sc}, binding to PrP^C to prohibit substrate conversion (Gabizon, Meiner et al. 1993) and stimulation of PrP^C endocytosis (Shyng, Lehmann et al. 1995).

One central question that has not been addressed in Prion disease is the relevance to infection of the glycan residues of PrP^{Sc} and PrP^C. PrP^C can be glycosylated at two potential sites, and in the SMB system the glycoform species of PrP^C which are represented include un-, mono- and diglycosylated forms of the protein. The overall pattern of glycosylation is termed the glycoform profile. In an organism there may be some variation of PrP^C glycoform profile between cell types and brain areas (DeArmond, Sanchez et al. 1997).

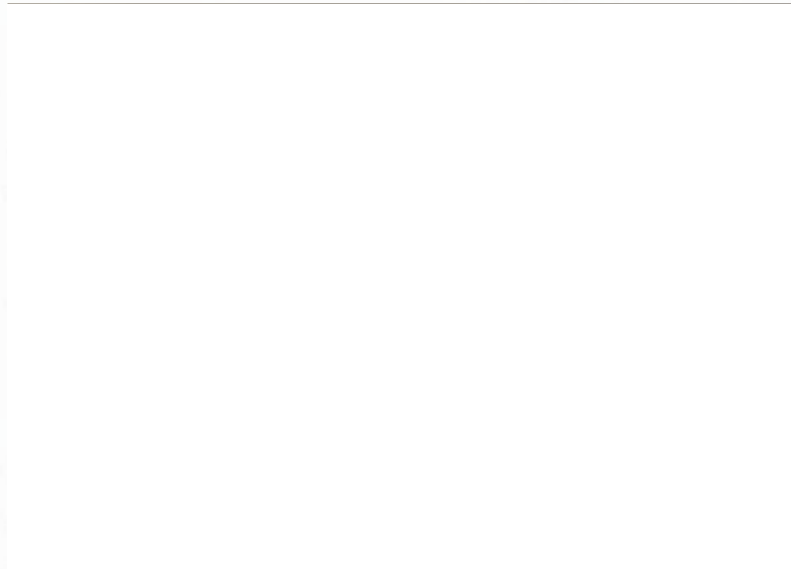


Figure 3.1. Analysis of TSE strain glycoform profiles passed in mice

The profiles are defined by the ratio between high, H, (diglycosylated) and low, L, (mono and unglycosylated) glycoforms of PrP^{Sc}. 79A is closest to the glycoform profile of SMB cells which display little diglycosylated PrP^{Sc}

(From a slide of Robert Sommerville : pers comm. to Jeremy Brockes)

Different strains of Scrapie demonstrates a wide variety of glycoform profiles (see Fig 3.1) and in most cases these profiles are maintained on passage to a new host of the same species. It has been suggested that the glycoform profile of the Prion associated with a particular strain is indicative of the strain type and in particular this has been used as evidence for the existence of a causal relationship between BSE and vCJD (Collinge, Sidle et al. 1996; Hill, Desbruslais et al. 1997). An open question remains in the Prion field as to how glycoform profiles of PrP^{Sc} are stably maintained on passage to a new organism. A sub question which this chapter focuses on is whether glycoform profiles of PrP^{Sc} are causally relevant to the process of infection or just epiphenomena in this regard.

Cell culture models have been employed in the study of strain and glycoform profile and PS cells have been shown to support infection by 22F, 139A, and 79A strains of Scrapie (Birkett, Hennion et al. 2001). Culture models have also been used to address the relevance of PrP^c glycosylation by creating constructs

which lack the glycosylation sites. It has been argued that deletion of one of the glycosylation sites leads to aberrant trafficking and conversion (DeArmond, Sanchez et al. 1997) although later studies employing different mutations of the glycosylation sites (N180Q and N196Q) did not lead to aberrant trafficking and the mutant PrP supported conversion (Korth, Kaneko et al. 2000). These data support the conclusion that an unglycosylated PrP^c can act as a substrate for effective conversion in culture, and that multiple strains can be supported in culture.

In this chapter, the PS/SMB system is assessed as a means for investigating some of the issues associated with glycoforms. The main tool used has been tunicamycin, a reagent for blocking N-linked glycosylation *in vivo*, and its suitability as a reagent for studies of Prion glycosylation has been assessed in the context of this system. In particular, this chapter makes use of tunicamycin to ask whether the glycoform profile of an infectious source is causally related to the glycoform profile of newly formed Prion, which is established following infection.

3.2. SMB and PS: Assay for infectivity

Biochemical assay for infectivity relies upon the differential properties of PrP^{sc} and PrP^c: the abnormal isoform, in contrast to its normal counterpart, is both resistant to limited proteolysis and insoluble in non-denaturing detergents. Following lysis in detergent buffer, samples to be processed for PrP^c are methanol precipitated whilst those for PrP^{sc} analysis are treated with Proteinase K and ultracentrifuged. Samples taken through this procedure for PrP^{sc} analysis are indicated in figure 3.2 and elsewhere in this thesis by the '+PK' marked lanes. An example below (see fig3.2) illustrates the detection of the PrP isoforms following the standard biochemical procedure and assay on a western blot using the 6H4 antibody which is able to recognise PrP^{sc} following partial denaturation. Proteinase K completely digests PrP^c (PS, + PK lane). In contrast, PrP^{sc} undergoes only partial proteolysis and is cleaved in its N-terminus, leaving a 149 amino acid protease resistant species nominated PrP²⁷⁻³⁰ because it runs at a lower molecular weight than PrP^c (SMB, +PK

lane). PrP^{Sc} species of PrP represent less than 4% of the total PrP population in an SMB sample (see Materials and Methods 2.4.4).

The glycoform profile of PrP^{Sc} can be seen to differ from PrP^C. In particular PrP^{Sc} displays virtually no diglycosylated species and an abundance of mono and unglycosylated forms. In contrast, the majority species of PrP^C appears to be the diglycosylated form and the unglycosylated species is a minority form. This relationship between glycoforms is not a general feature of all systems but varies, dependent on strain property and cell type (see Fig. 3.1).

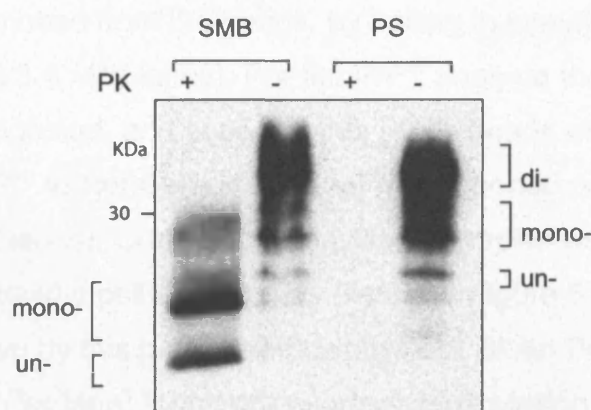


Figure 3.2. Processing of SMB and PS cells for detection of Prion and normal isoforms

Cells are lysed in a buffered detergent and processed for PrP^{Sc} or PrP^C as described in Materials and Methods. PrP^{Sc} assay, which is usually undertaken on 90% of the sample compared to 10% taken for PrP^C analysis, involves treatment with Proteinase K which completely digests PrP^C. In PS cells, where only PrP^C is present, treatment with Proteinase K completely digests all PrP (PS, +PK). In contrast, SMB cells contain both normal and prion isoforms and protease digests PrP^C completely and digests PrP^{Sc} to leave a protease resistant core (SMB, +PK). N-linked Glycosylation of PrP^C varies in extent, and a mixture of di, mono and un glycosylated forms are found within the cell. In the SMB/PS cell system PrP^C is most abundantly di glycosylated, with the unglycosylated species representing the minority form. PrP^{Sc}, by contrast, shows little of the diglycosylated form and a mixture of mono-glycosylated and unglycosylated species. PrP^{Sc} represents less than 4% of the PrP species in SMB cells (see Materials and Methods 2.4.4). The relatively low abundance may be a particular feature of this cell line.

3.3. PrP localisation

Immunocytochemistry with 6H4 demonstrate that the majority of PrP^c is found on the cell surface (Fig 3.3). There are few clear differences between PS and SMB cells except for a slightly more pronounced peri-nuclear PrP population in SMB.

In order to ascertain whether PrP^{sc} was present on the plasma membrane, SMB cells were surface biotinylated (see Materials and Methods). Lysates were incubated with streptavidin beads overnight to pull down biotinylated species, washed and resuspended. 10% of the sample was taken for PrP^c analysis, pull down material removed from the beads, by boiling in sample buffer, and run on western blots (Fig 3.4 –PK lanes). For the PrP^{sc} analysis the remainder of the sample was PK digested, and supernatants (once beads were removed) were processed for PrP^{sc} as normal and the final resuspended pellets run on western blots (Fig3.4 +PK lanes). Control unbiotinylated samples were also taken through the streptavidin pull downs. The results in Figure 3.4 indicate that PrP^c can be pulled down by this process efficiently (-PK Biotin PrPc lane). The lack of PrP^{sc} (Biotin PrPsc lane) found after surface biotinylation indicates that there is little PrP^{sc} on the surface.

(An estimate places it at less than 10 % although this is a very rough estimate based on the relative efficiency of PrP^c pull down and the expected signal of the PrP^{sc} input without pull down).

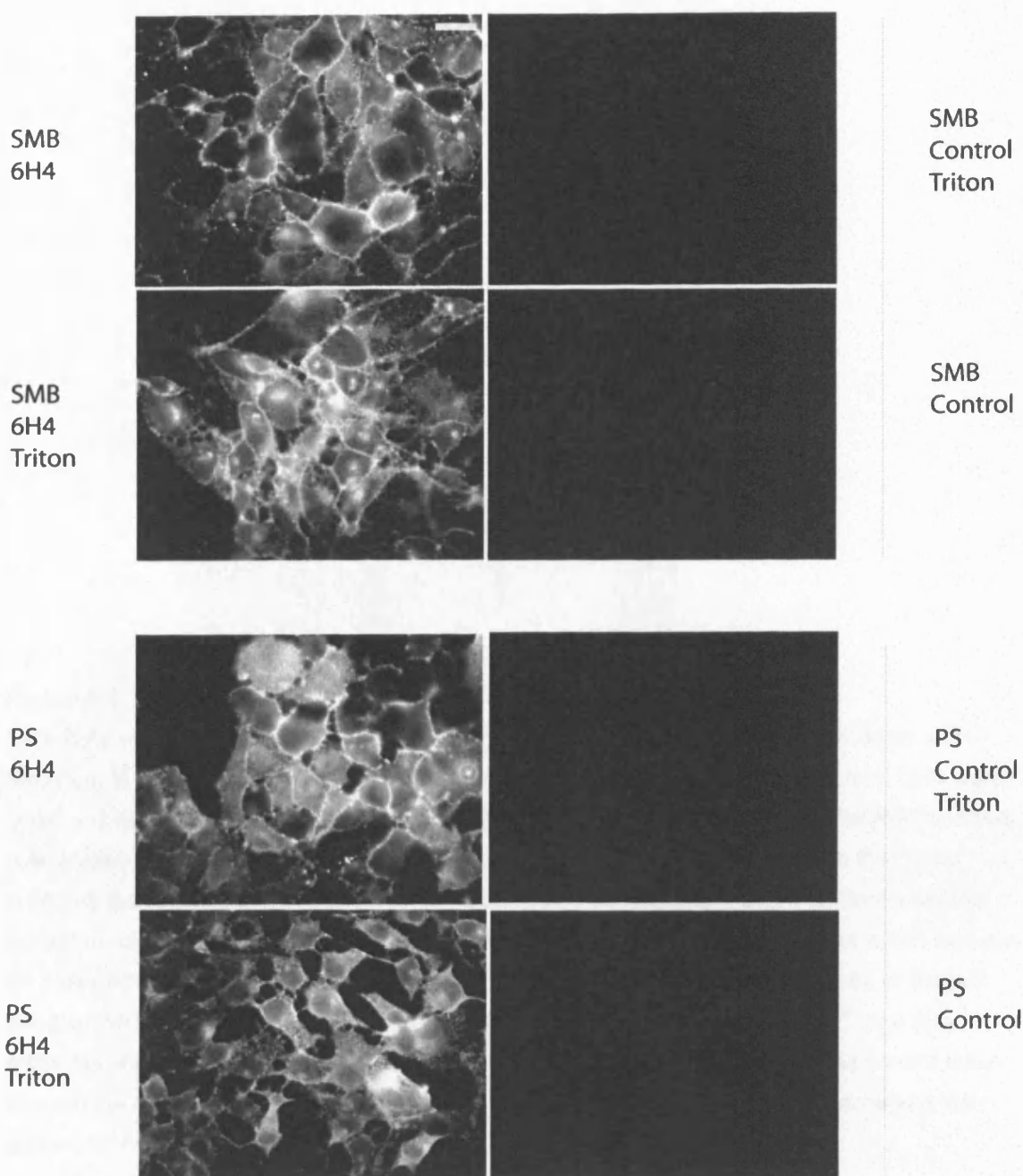


Figure 3.3. Immunocytochemistry of PS and SMB cells

Cells were fixed with 3% PFA and stained with monoclonal antibody 6H4 at 1:100 dilutions with or without Triton permeabilisation (see Materials and Methods). Alternatively cells were stained with a control primary antibody (Brdu) at the same concentration prior to addition of secondary. In the top two sets of panels staining of SMB cells is indicated. (scale bar = 20 microns). Note that Triton permeabilisation of SMB cells reveals an increased perinuclear accumulation of PrP species. (Greater than 5 fields for each condition was observed and the experiment was reproduced).

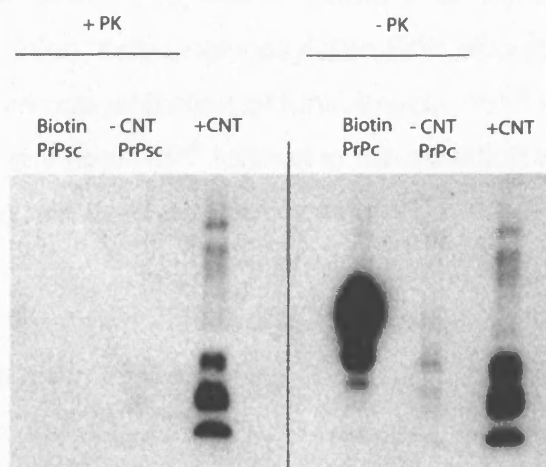


Figure 3.4. Surface biotinylation of SMB cells

SMB cells were biotinylated (Biotin lanes) following the protocol described in Materials and Methods, in parallel with controls (-CNT lanes). Following quenching of the reaction, cells were lysed and incubated with streptavidin beads. Material removed from the beads for PrP^c analysis (see Materials and Methods) was run on the right half of the western blot. 'Biotin PrP^c' lane indicates the result of this pull down for the biotinylated sample and '-CNT PrP^c' indicates the control un-biotinylated sample. +CNT is a 6H4 positive brain homogenate control which was run as a western blotting reference only. The left half of this figure indicates the results of the pull down of the biotinylated material processed for PrP^{sc} analysis in the 'Biotin PrP^{sc}' lane (see Materials and Methods) and the '-CNT PrP^{sc}' lane represents a non-biotinylated control taken through the same process (-CNT PrP^{sc}). Note that efficient pull down of PrP^c is achieved via surface biotinylation but not PrP^{sc}. This result was reproducible.

3.4. Glycosylation of PrP^c and PrP^{sc}

In vivo manipulation of glycoform profile in PrP^c and consequently PrP^{sc}, can be achieved by blocking N-linked glycosylation using Tunicamycin an inhibitor of N-acetyl glucosamine transferases. PrP^c turnover is in the order of 3-6 hours (Borchelt, Scott et al. 1990) and therefore after a short period of blocking N-linked glycosylation, only unglycosylated PrP^c should be present in cells treated with an effective concentration of tunicamycin. PrP^c is the substrate for PrP^{sc} and therefore any new PrP^{sc} formed in the situation where all the cellular PrP^c is unglycosylated, will itself be unglycosylated.

The effects of 1 µg/ml of tunicamycin treatment on SMB cells for 48 hours were compared with an *in vitro* stripping of oligosaccharides using N-glycanase (fig 3.5). The lanes indicated as '-PK' represent samples processed for PrP^c which were either treated with tunicamycin in culture (T and T-ctl the control) or treated with N-glycanase post lysis (N and N-ctl the respective control). Use of tunicamycin in culture or use of N-glycanase *in vitro*, have the same effect on PrP^c glycoform profile which is to collapse it to an unglycosylated species. The treatment also collapses the PrP^{sc} to a largely unglycosylated form (see Fig 3.5 '+PK' lanes). It is noteworthy that other lower molecular weight bands are apparent for PrP^c (-PK, T or N lanes) indicating the existence of proteolytic fragments. These are not apparent, as discussed below, for PrP^{sc}.

This experiment indicates that tunicamycin is a valid means of manipulating glycoform profile of PrP^{sc} without the need for denaturation of the proteins which is required by the *in vitro* procedure using N-glycanase. This means that proteins can be used for further experiment following deglycosylation, in their native conformations.

One suggestion of interest might be that the PrP^{sc} glycoform profile does not truly represent a mixture of the mono and unglycosylated species. This could be of significance if it turned out for example, that one species in particular was more active in the conversion process. The hypothesis might be considered therefore that the apparent lower molecular weight band of PrP^{sc} which is

described normally as unglycosylated is actually a cleaved product of a mono-glycosylated species. However, the experiment of Fig 3.5 indicates that treatment to remove oligosaccharides does not collapse the glycoform profile of PrP^{Sc} to a molecular weight below that of the putative unglycosylated PrP^{Sc}. By contrast PrP^C following treatment reveals bands that run below the putative unglycosylated weight, which are likely to have been shorter glycosylated fragments of protein, prior to deglycosylation.

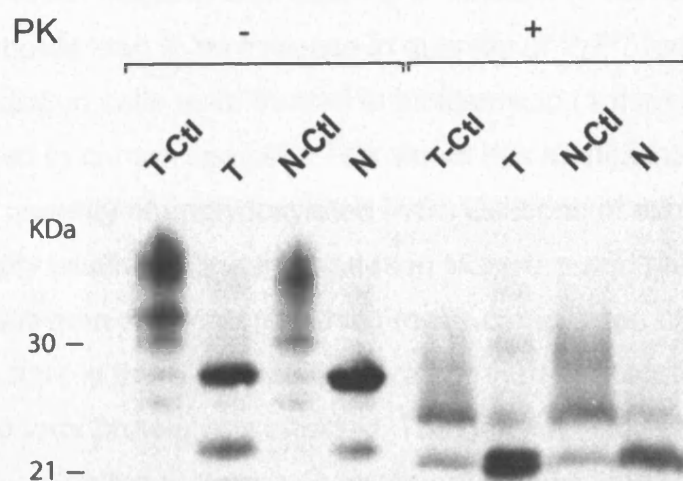


Figure 3.5. Manipulation of PrP^{Sc} and PrP^C glycoform species in SMB cells

In order to assess the glycoform profile, oligosaccharides were removed in two ways: either by inhibition of biosynthesis or by enzymatic digestion. SMB cells were treated for 48 hours in tunicamycin (1 µg/ml) prior to assay for PrP^{Sc} and PrP^C, (lanes marked T for treated and T-ctl for control untreated samples). Alternatively, N-glycanase was employed following lysis (lanes marked N or N-ctl for control untreated) as described in Materials and Methods. The left half of the gel represents the effects of these treatments on PrP^C (-PK lanes) whilst the right half represents the effects on PrP^{Sc} (+PK lanes). Note that the effect of pre incubation with tunicamycin or post treatment with N-glycanase has the main outcome of collapsing the glycoform profile to the unglycosylated form, although there are further bands which result below the expected weight indicating that shorter fragments of PrP^C exist. By contrast, multiple fragments of PrP^{Sc} are not revealed following removal of oligosaccharides.

3.5. Relative contribution of glycoform species to *in vivo* conversion

The unglycosylated form of PrP^c represents less than 5% of total PrP^c (Fig 3.7 C), and yet the unglycosylated form of PrP^{sc} represents 35% of the total PrP^{sc} (Fig 3.7 D). The non equivalence in glycoform stoichiometries suggests the hypothesis that unglycosylated PrP^c might be a preferential substrate for conversion to the prion form. One prediction that might be inferred from this hypothesis is that increasing the abundance of the unglycosylated form of PrP^c protein, whilst keeping total quantity a constant (relative to a normal sample of PrP^c), should lead to an increase in quantity of PrP^{sc} formed. Therefore, to test this prediction cells were treated in tunicamycin (1 µg/ml) for 48 hours and compared to control samples. The aim of this manipulation was to increase the relative quantity of unglycosylated PrP^c. Dilutions of samples were run in order to quantify within the linear range (see Materials and Methods). Cell viability varied between experiments which made comparison of experiments difficult and the data is therefore indicative rather than quantitatively conclusive because total protein was affected. The general trend of a reduction in total PrP^{sc} following the tunicamycin treatment was however reproducible. In the experiment indicated in Fig 3.6, total PrP^c in Tunicamycin treated samples decreased in abundance by 40% compared to controls (Fig3.6 –PK and quantified in Fig7A) and PrP^{sc} in the treated samples decreased by 66% compared to controls (Fig6 +PK and Fig 7B). The decrease in total PrP^c was not anticipated and makes it difficult to assess the validity of the hypothesis that was stated above i.e. that increasing the relative abundance of the unglycosylated species of PrP^c, keeping total PrP^c constant compared to normal samples, would lead to an increase in total PrP^{sc}.

Another reason for undertaking this experiment was to assess the use of tunicamycin as a means of increasing the levels of PrP^{sc} (a prediction that was described above) which would be a potentially useful tool for infection studies. Overall a reduction in PrP^{sc} is found with use of tunicamycin and therefore it does not represent a useful tool for increasing total levels of infectious material.

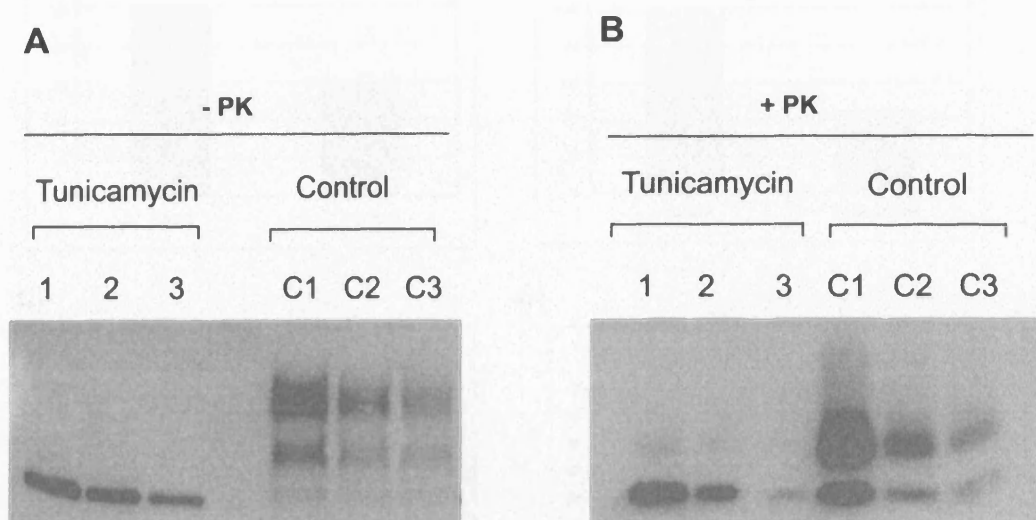


Figure 3.6. SMB cells treated with tunicamycin

SMB cells were treated with tunicamycin (1 $\mu\text{g/ml}$) for 48 hours prior to cell lysis. Treated and control samples were normalized for total protein content using the BCA assay, prior to analysis by western blot and total signal in a lane was quantified using image gauge and the average values for total protein calculated – see Fig 3.7A and B. (For measurement of ratios of glycoform species in Fig 3.7 C and D, the glycoform bands visible in the control samples were individually quantified). Dilutions of treated and control samples were run in order to assess the efficacy of quantification by reference to a linear range. Panel A indicates the results for PrP^{C} treated with tunicamycin (dilutions 1,2,3) or controls (C1, C2, C3). Panel B represents the results for PrP^{Sc} processed from the same sample. The effect of prolonged inhibition of N-linked glycosylation is to reduce PrP^{C} to an entirely unglycosylated form and as a result PrP^{Sc} is also reduced to an unglycosylated form.

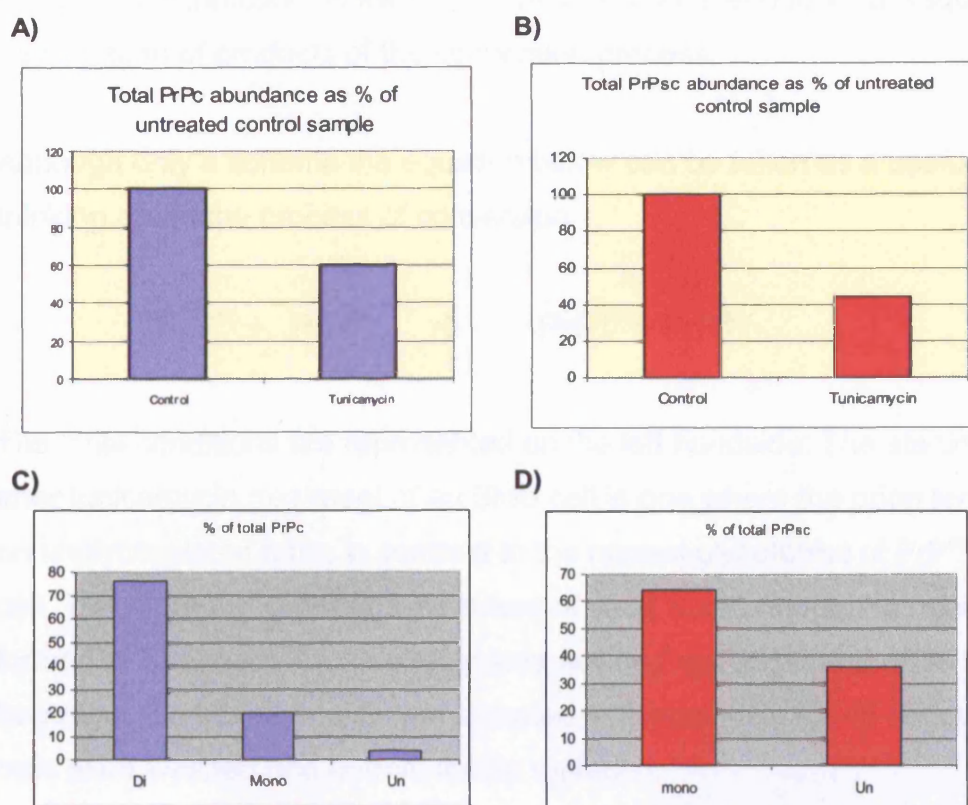


Figure 3.7. Quantification of total PrP^c (A) and total PrP^{sc} (B) following tunicamycin treatment and quantification of normal glycoform profile of PrP^c (C) and PrP^{sc} (D) in SMB cells.

A and B Total protein in the lanes of the gel represented in Fig3.6 were quantified using image gauge (see Materials and Methods). Total abundances are expressed as a percentage of control, untreated, samples. Note that PrP^{sc} Abundance is decreased to 40 % of the level of the control following 48 hours of tunicamycin treatment, in contrast to PrP^c which is 60 % of the level of the control.

C and D The control samples from Fig3.6 were utilized as a means of assessing the ratios between glycoforms species of PrP^{sc} and PrP^c in SMB cells. Individual glycoform species of the control sample were quantified using image gauge. Results are indicated as a percentage of the total of PrP^{sc} or PrP^c in the sample. Note that Un-glycosylated PrP^c represents 4% of the total PrP^c in comparison to unglycosylated PrP^{sc} which represents 36% of total PrP^{sc}.

3.5.1. Glycosylation as a determinant of Prion infection

It remains to be determined how glycosylation contributes to the process of prion conversion. One hypothesis might be that perturbation of the initial conditions of infection, in the PrP^{sc} template, might lead to a subsequent perturbation of products of the conversion process.

Although only a schema the equation below can be taken as a useful way for thinking about the process of conversion.



The initial conditions are represented on the left handside. The starting condition after tunicamycin treatment of an SMB cell is one where the prion template is in an unglycosylated form, in contrast to the normal glycoforms of PrP^{sc} in an SMB cell. Therefore the question was asked of what would happen to new PrP^{sc} formed in SMB cells if tunicamycin was washed out at the end of 48 hours of treatment. To this end, cells were treated in tunicamycin for 48 hours and then cells were washed and normal media replaced.

Figure 3.8 B demonstrates that it takes 96 hours for the full PrP^{c} glycoform profile to return following removal of tunicamycin and 96 hours for PrP^{sc} to recapture its full profile (Fig3.8A). This experiment is indicative of the result that from an unglycosylated PrP^{sc} template (the condition at the time when tunicamycin is washed out) one is able to regain the full glycosylated PrP^{sc} profile after 96 hours. One hypothesis stated earlier was that a perturbation in the PrP^{sc} glycoform profile of a cell will leads to perturbation of the profile of newly formed Prion by the cell. The experiment above, following the effects on PrP^{sc} after tunicmaycin treamtment and wash out, indicates that this hypothesis is not valid.

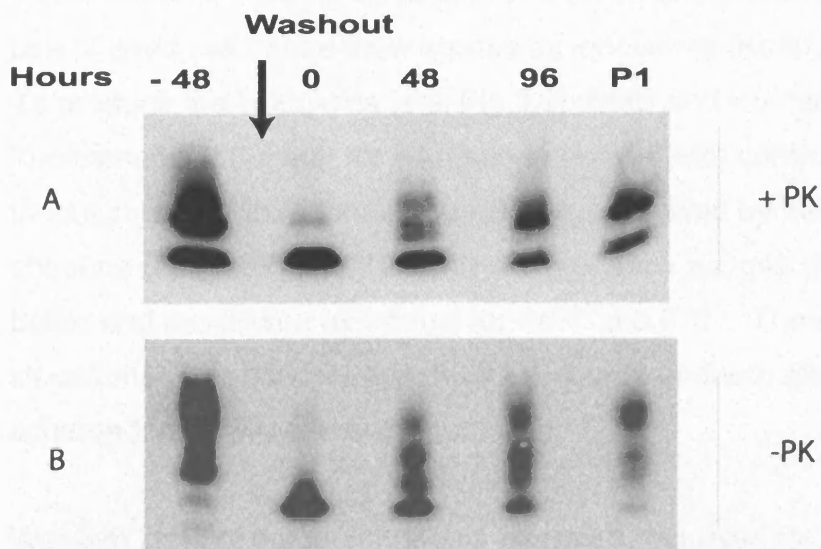


Figure 3.8. Washout of tunicamycin from SMB cells

SMB cell cultures were treated in tunicamycin for 48 hours (Tunicamycin was added at -48 hours), and tunicamycin then removed by replacing the medium (Wash out begins at 0 hours).

Cells were lysed at, 0, 48, 96 hours after removal of tunicamycin or after 1 passage (P1).

Cells lysed at -48 hours are untreated SMB cells which represent controls. Samples in gel A

(+PK) represent PrP^{Sc} and in gel B represent PrP^C (-PK). Note that PrP^{Sc} returns to its full

glycoform profile after 96 hours despite the presence of a converting template at 0 hours which is largely unglycosylated.

In order to further clarify the finding that unglycosylated PrP^{sc} can act as a template for the conversion of all PrP^c glycoform species, an experiment was carried out which added two elements to the experiment described in Fig3.8. Firstly, a fully unglycosylated PrP^{sc} template was produced to rule out contribution from other PrP^{sc} glycoforms and secondly, the starting PrP^c glycoform profile was a full profile. The process of cell infection was achieved by use of dead cell freeze-thaw lysates as inoculums (Korth, Kaneko et al. 2000). To produce the inoculums (see Fig 3.9), SMB and PS cells were treated with Tunicamycin (10µg/ml) for 64 hours in parallel with controls (see fig 3.9). Inoculums were then formed by PBS lysis followed by freeze thawing and shearing (see methods). Roughly a 1/3 of each sample was diluted in lysis buffer and processed as normal for PrP^{sc} and PrP^c. The remnant of the two inoculums were used as an infectious source on fresh plates of PS cells (see schema for the experiment Figure 3.9).

Western blots of the four inocula prepared and used for the infections can be seen in Figure 3.10; The four inoculums were SMB cells treated or untreated with tunicamycin and PS cells treated or untreated with tunicamycin which were all taken through the freeze thaw lysis process. The effect of prolonged tunicamycin treatment is to produce an unglycosylated PrP^{sc} (Fig 3.10 +PK : SMB-TM lane) in contrast to a control sample. PS cells treated for this period (Figure3.10 +PK : PS-TM lane) do not produce a protease resistant band.

As illustrated in the schema of fig3.9 these inoculums were then used as sources of infection on separate PS cell cultures which were expanded over the following weeks. It was noted that the addition of the tunicamycin treated inoculums, whether PS or SMB in origin, caused a marked decrease in cell viability compared to cultures to which the non-tunicamycin inoculums were added. After assay for PrP^{sc} (Fig 3.11 +PK lanes) it was apparent that a full glycoform profile for PrP^{sc} was produced from the unglycosylated template as illustrated in the SMB-Tm lane although the abundance of the PrP^{sc} was greatly reduced. Addition of inoculums PS and PS-Tm (Fig3.10) did not lead to formation of PrP^{sc}.

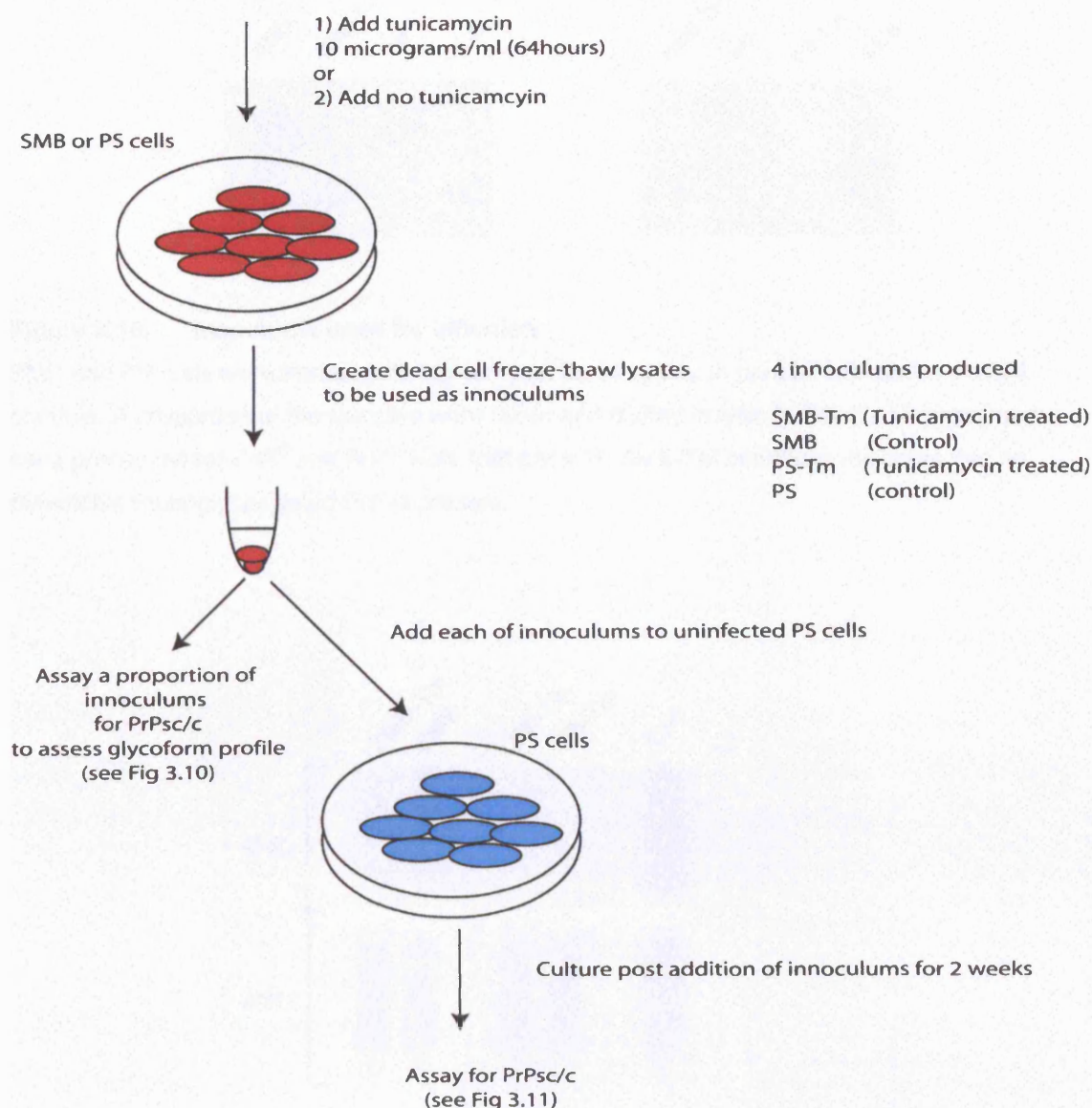


Figure 3.9. Schema of process of infection with manipulated Prion glycoforms

SMB and PS cells were cultured in the presence of 10 µg/ml Tunicamycin for 64 hours. No tunicamycin was added to control SMB and PS cells during this period. Dead cell freeze-thaw lysates were then produced by PBS lysis, followed by 4 freeze thaw cycles in liquid nitrogen and shearing with a syringe (Bosque and Prusiner 2000). A proportion of the material from each inoculum produced was analyzed for PrP^{sc}/ PrP^c. The remnant was normalized for total protein and added to PS cells, and left for 3 days before media were changed. Cells were then cultured for a further two weeks and assayed for PrP^{sc}/ PrP^c.

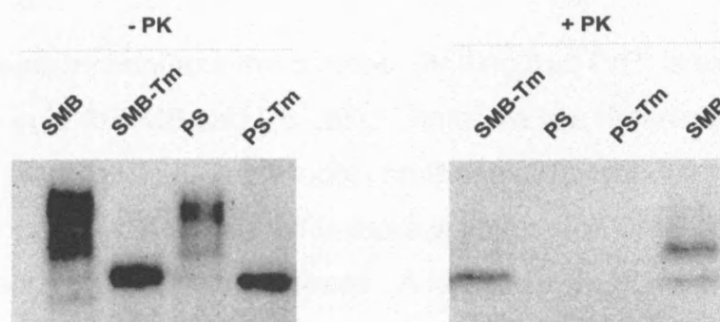


Figure 3.10. Inoculums used for infection

SMB and PS cells were treated with tunicamycin for 64 hours, in parallel with sham treated controls. A proportion of the samples were taken and diluted in lysis buffer (2x strength) and were processed for PrP^{sc} and PrP^c. Note that panel B, SMB-TM condition, indicates that no detectable monoglycosylated PrP is present.

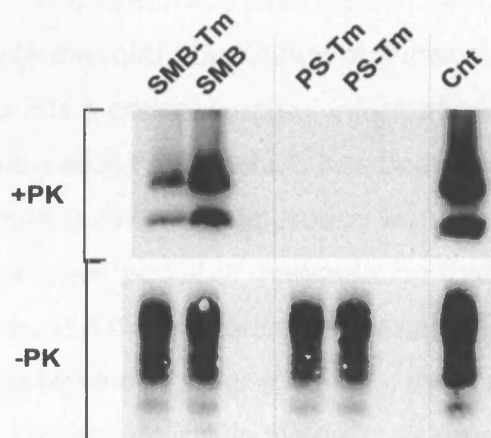


Figure 3.11. Analysis of PS cells after infection with cell derived inoculums

After 2 weeks of culture, the 4 samples of PS cells that had been infected with different cell preparations (inoculums) were normalized for total protein and assayed for PrP^{sc} and PrP^c in parallel with an SMB cell culture (Cnt). SMB-Tm and SMB represent the PS cultures infected with the tunicamycin and sham treated SMB derived inoculums. PS-Tm and PS represent the PS cultures infected with the tunicamycin and sham treated PS derived inoculums. Note that although less abundant, a full glycoform profile is regained after infection with an entirely unglycosylated template as illustrated in the +PK : SMB-Tm lane.

3.6. Discussion

Immunocytochemistry confirms the common finding that PrP^C is expressed on the cell surface in both SMB and PS cells. There are few differences observed with or without permeabilisation protocols on these cells, although it is noteworthy that peri-nuclear material is more visible in the SMB cells than PS which may be a function of cellular stress. A key problem in the Prion field has been the lack of a robust Prion specific antibody, and the 6H4 used for this immunocytochemistry is thought to have very low affinity for PrP^{Sc} and perhaps it is not surprising that post membrane compartments like endosomes or lysosomes, which have been indicated as one possible sink for PrP^{Sc}, do not show up differentially between the infected and non-infected cell types. In order to confirm the presence of PrP^{Sc} on the surface, which has been demonstrated for other cellular systems (Shyng, Moulder et al. 1995; Vey, Pilkuhn et al. 1996), biotinylation was carried out. The result indicates that PrP^C is found to be abundantly accessible to surface biotinylation and in contrast PrP^{Sc} is not. It is difficult to calculate the total abundance of surface and non surface forms from other studies, but it is a critical piece of information because the surface is one of the putative sub-cellular sites which has been suggested for prion conversion. A more quantitative approach would be useful for future experiments. One other possible manipulation that would enable triangulation of previous studies and the present study would be separation of plasma membrane compartments in order to assess the quantity of PrP^{Sc} present by another means. The result, in this thesis, may also be a feature of the SMB cell line for other reasons. It may be that PrP^{Sc} is not accessible to surface biotinylation because the cell compartments at the surface are invaginated to a greater extent than in other cell systems and structural differences of this kind might limit access of reagents such as biotin. It would therefore also be worth using other cell lines as further controls.

PrP^{Sc} in SMB cells is comprised of unglycosylated and mono-glycosylated species and lacks diglycosylated forms in contrast to its substrate PrP^C, which displays abundant diglycosylated species and a minority unglycosylated

species. In order to rule out the hypothesis that putative unglycosylated species of PrP^{sc} are actually mono glycosylated fragments of the full molecule, N-glycanase was used to collapse the glycoform profile to a completely unglycosylated form. Removal of the carbohydrate residues did not lead to an overall shift of the PrP^{sc} profile as the hypothesis would have predicted.

The relative abundance of unglycosylated PrP^{sc} and PrP^c might suggest the hypothesis that unglycosylated PrP^c is a more efficacious substrate for conversion. One means of testing this hypothesis was to ask whether a bias towards the unglycosylated form would therefore produce more PrP^{sc}. The effect of treating cells with tunicamycin for 48 hours was to reduce total PrP^c which makes it difficult to assess this hypothesis. Irrespective of this point, a clear effect of treatment with tunicamycin in general was to reduce total cellular PrP^{sc} and therefore this manipulation does not represent a useful tool for increasing Prion abundance in the SMB cultures.

After treatment of SMB cells with tunicamycin for a period of 48 hours PrP^c (Fig3.8B) was reduced to an entirely unglycosylated form and PrP^{sc} only demonstrated a small amount of the mono-glycosylated species (Fig3.8A). When tunicamycin was removed, PrP^c came back to its full glycoform profile very slowly, in 96 hours, despite its relatively fast turn over. One reason for this might be that the cells have suffered considerable stress as a result of a treatment which disrupts glycosylation in general and activates documented cell stress pathways such as the unfolded protein response (Niwa, Sidrauski et al. 1999). Nevertheless, at the point where tunicamycin is removed and PrP^c glycosylation begins to return to normal, PrP^{sc} is largely unglycosylated. The fact that PrP^{sc} returns to its full profile after the 96 hours, in line with PrP^c, indicates that the largely unglycosylated form is able to convert other glycoform species of PrP^c in order to re-establish the profile.

Two caveats with this experiment are that the cells are in a poor state by the end of the process and, more importantly that there is some visible mono-glycosylated PrP^{sc}.

The final experiment of this chapter addressed the question of the informational requirements in an inoculum for propagation of glycoform profile. In order to address concerns about cell viability and presence of unwanted glycoform species the experiment was undertaken with samples prepared from freeze-thaw lysates of cells which had been previously manipulated with tunicamycin. Using a source of Prion which is entirely unglycosylated as an inoculum returns a glycoform profile which is the same as infection with a full glycoform Prion template.

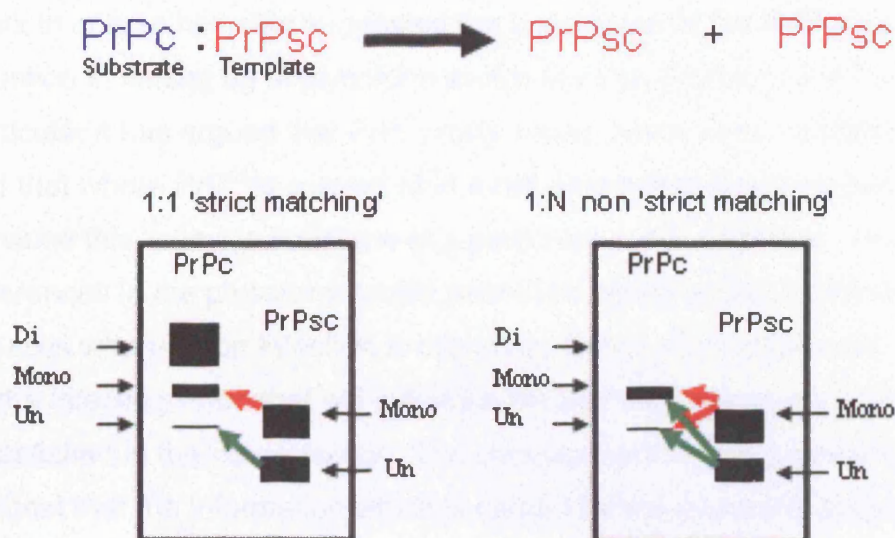


Figure 3.12. Schema of two hypotheses for glycoform maintenance

This experiment indicates that informational requirements for the transfer and maintenance of glycoform profile do not reside in the glycoform species themselves. In its most limited form the hypothesis can be stated with reference to a strict matching hypothesis and a non-strict matching hypothesis (Fig 3.12). On the strict matching hypothesis unglycosylated template PrP^{sc} converts PrP^{c} only in its unglycosylated form and mono-glycosylated PrP^{sc} only converts PrP^{c} of monoglycosylated form and so on.... The explanation for why there is no diglycosylated form when a new infection is initiated, would then be that there is not an accompanying diglycosylated species in the inoculum. Glycoform profiles would partly be explained, on this hypothesis, by the

presence or absence of particular glycoform species from an initial inoculum. A full explanation of the transfer and maintenance of glycoform profile would also require some explanation of the relative abundance of species present. The strict matching hypothesis may seem trivial as a hypothesis which has been disproved by this experiment, but it is useful in dissecting questions and models that address how glycoform profiles might be maintained following Prion infection. A key question that is highlighted by this work is whether or not the other glycotypes of PrP^{Sc} can be seen to have any converting activity and whether the glycotypes differ in their efficiency of converting activity.

Work in culture has also suggested the importance of the PrP^C side of the equation in setting up of glycoform profile of Prion (Vorberg and Priola 2002). In particular it has argued that PrP^C profile varies between compartments in a cell and that where PrP^{Sc} is converted in a cell determines the glycoform profile because this is where substrate of a particular sort is available. However, differences in the glycoform profile cannot be solely explained on the basis of the cells where Prion infection is occurring. Some information must be carried by the infecting Prion that will influence the eventual glycoform profile which is established in the new infection. The compartmentalisation model would suggest that the information which is carried by the infectious source will determine the site of conversion for Prion.

When the glycoform profile of a strain is referred to it refers to the resulting western blot of a brain homogenate, and not individual cell populations – in this sense it represents an aggregate of what might be different profiles of distinct cell populations in that brain. This is one possible weakness of using cell culture models for study of glycoform profile. Nevertheless, it must be the case that some information that will lead to glycoform profile in a newly infected host, must be stored in the PrP^{Sc} molecule of an inoculum, as discussed, and this work investigates one hypothesis regarding that information. The work suggests that the glycotypes of the prion template (e.g. of the inoculum) are not themselves the key source of the information required for re-establishment and maintenance of the glycoform profile in the newly infected host.

Chapter 4 Cell lines expressing PrP fluorescent fusion proteins

4.1. Introduction

One major obstacle to progress in the prion field has been the absence of an antibody that is specific for PrP^{Sc} and therefore an absence of clear means for the elucidation of the sub cellular behaviour of Prion.

This chapter focuses on the characterisation of fusion proteins between PrP and a fluorescent reporter, Green Fluorescent Protein (GFP). It explores whether fusion constructs could be used to report appropriately to reveal differences in localisation between infected and uninfected contexts. There are two potential ways in which the fusion protein when expressed in infected and uninfected contexts might report on differences in localisation. In the first mode the fusion protein is hypothesised to report directly on differences in localisation because the c-terminal portion is converted to and therefore trafficked as PrP^{Sc} (i.e. GFP-PrP^C becomes GFP-PrP^{Sc} in the infected context). In a second, indirect mode, differences in localisation are hypothesised to occur in virtue of differences in trafficking of PrP^C between infected and uninfected contexts. Expression of fusion proteins in different contexts was investigated by microscopy for this purpose. The second issue explored is whether or not, in the context of an intact fluorescent fusion protein, PrP^C is converted to PrP^{Sc} - a prerequisite for the fusion to act as a direct marker for Prion.

Previously GFP has been produced in fusion with PrP to assess the dynamics of PrP endocytosis and trafficking (Lee, Magalhaes et al. 2001; Magalhaes, Silva et al. 2002; Hachiya, Watanabe et al. 2004) to assess the effects of mutation on accumulation and trafficking (Gu, Verghese et al. 2003). and recently, a transgenic mouse expressing GFP in fusion with PrP has been reported (Barmada, Piccardo et al. 2004). However, there are no published reports to date which assess the behaviour of PrP fluorescent fusion constructs in an infectious context. It has been reported that attempts to elicit conversion of PrP^C to PrP^{Sc} in a fusion protein in which the GFP is inserted near to the GPI anchor have been unsuccessful (pers comm. at D. Harris group poster at Keystone Conference 2002). This thesis therefore follows an alternative approach of inserting the GFP molecule close to the N-terminus, in between

the signal peptide and the rest of PrP (Lee, Magalhaes et al. 2001). The N-terminus has been shown to be an unstructured domain from NMR studies (Zahn, Liu et al. 2000) which is distinct from the part of PrP (broadly: residues 90-230) ordinarily implicated in the PrP^{Sc} transition. It is therefore hoped that it is a reasonable place to insert a protein like GFP, with the expectation that the GFP will both fold appropriately and not interfere with any PrP folding necessary for Prion formation.

In summary, this chapter addresses the critical question of whether PrP^C conversion to PrP^{Sc} occurs in the context of the fusion with GFP. It also acts as a description of cell types expressing PrP-GFP fusion constructs which can be used to study general trafficking and dynamic issues relating to PrP^C. These observations of fusion behaviour are critical for further work that will explore the dynamics of PrP in the context of the plasma membrane and intercellular exchange.

4.2. Construction of fluorescent fusion proteins

Fluorescent constructs were designed which placed PrP in fusion with Green Fluorescent protein (GFP). In order to ensure appropriate trafficking along the secretory pathway, the cDNA coding for the signal peptide of PrP, residues 1-22, was placed N-terminal to the EGFP construct in the Clontech EGFP-C3 vector backbone by PCR (see Chapter 2: Materials and Methods). The remaining C-terminal portion of PrP, the cDNA coding for residues 23 onwards, was placed in the cloning site of EGFP-C3 and in frame with the EGFP sequence. The construct formed by this method is denoted gfp-prp for the cDNA and GFP-PrP for the fusion protein itself (see fig4.1B). The fusion protein derived from mutagenesis of GFP-PrP was expected to react with the 6H4 antibody and to be distinguished by weight – previously, fusion proteins with similar design have been attributed the weight of around 57Kda on expression (Lee, Magalhaes et al. 2001). In order to assay for conversion of PrP^C in the context of an intact fusion protein to PrP^{Sc} by the usual biochemical procedures (i.e. to assay for whether a proportion of GFP-PrP^C has become GFP-PrP^{Sc}) it is necessary to introduce a digestion step using Proteinase K.

This would therefore cleave the GFP from the putative PrP^{Sc} portion of the fusion, and when run on a western blot the putative PrP^{Sc} portion of the fusion would run in the same weight range, and be obfuscated by, the endogenous PrP^{Sc}. (Note that this was not expected for western blotting where Proteinase K is not introduced because the full fusion weight is higher than endogenous PrP as described above). Therefore a modification was made to GFP-PrP to introduce an epitope which would be specific for the antibody 3F4 (Telling, Tremblay et al. 1997).

The residues 108 and 111 of mouse PrP correspond to 109 and 112 of hamster PrP, and mutation of the Leucine and Valine residues to a Methionine at these positions produces a 3F4 epitope. Therefore these mutations were introduced by site directed mutagenesis to generate a fusion protein denoted F4-GFP-PrP which could be recognised by the antibody 3F4 (see Fig 4.1C).

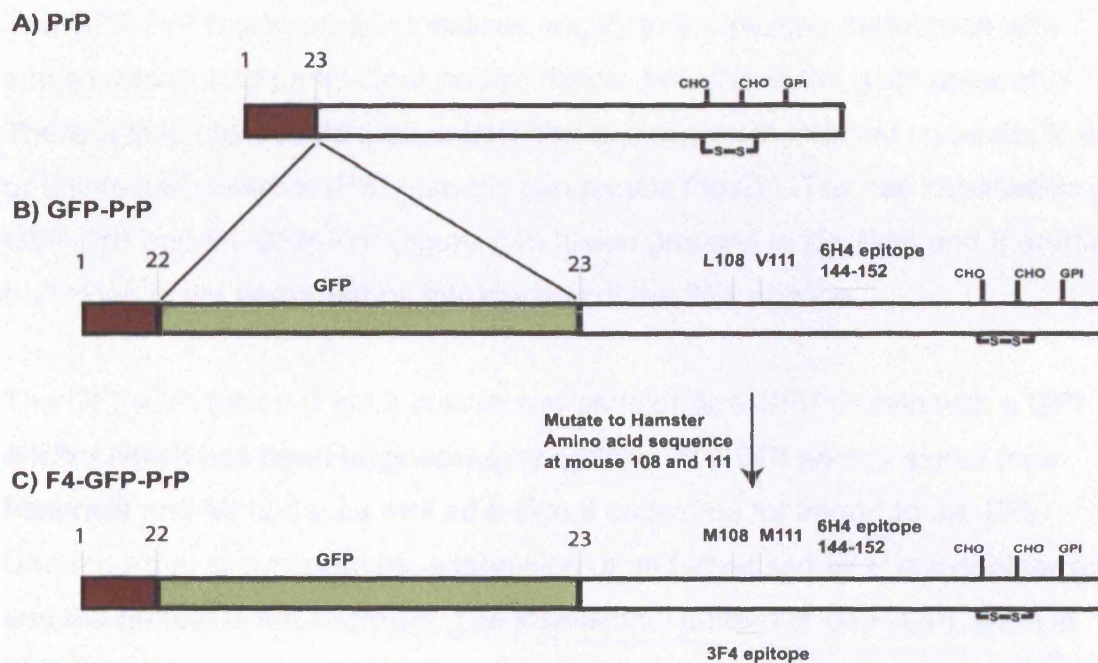


Figure 4.1. Construction of GFP-PrP fluorescent fusion proteins

CHO represents the carbohydrate residues, S S the disulphide bond and GPI, the position of the GPI addition sequence. **A)** Schema for the nascent PrP polypeptide. The sequence indicated in red from amino acid 1-22 comprises the signal peptide and cleavage before residue 23 occurs on transit into the ER. **B)** EGFP was effectively inserted between the signal peptide and the rest of the PrP molecule (see Materials and Methods). **C)** The construct described in B) had a specific hamster epitope added by site directed mutagenesis at sites 108 and 111 effecting the changes in amino acid sequence of L108M and V111M.

4.3. Transient expression of constructs

To ensure that the constructs were transcribed and translated appropriately they were expressed transiently in the PS/SMB cell system (see Materials and Methods) and the localisation of the fusion proteins was assessed. The ideal aim of using the two constructs at this stage was to establish that the F4-GFP-PrP functioned appropriately so that it could replace the GFP-PrP construct from which it was derived in later studies. The hypothesis was described earlier that there might be some difference between trafficking of PrP in infected and uninfected contexts, and for this reason constructs were expressed in both PS and SMB cells. As a further control of interest, a vector coding for the same EGFP protein with a GPI anchor addition sequence was obtained and expressed in the SMB and PS cells (see Materials and Methods).

The GFP-PrP fusion protein localises largely to the plasma membrane with some indication of perinuclear accumulation, possibly in the golgi apparatus. There is little obvious difference between expression in infected contexts (SMB) or uninfected contexts (PS) (see top two panels Fig4.2). The cell localisation of GFP-PrP and F4-GFP-PrP (figure 4.2) fusion proteins is identical and therefore trafficking is not perturbed by introduction of the 3F4 epitope.

The GFP-GPI fusion (Fig4.2 bottom two panels), is a GFP protein with a GPI anchor which has been engineered by addition of a GPI anchor signal (see Materials and Methods) as well as a signal sequence for import to the ER. Under normal circumstances, expression of underivatised GFP is cytoplasmic, and the protein is not secreted. The localisation pattern of GFP-GPI seen in Fig4.2 is the same as that of the other PrP fusions: plasma membrane and perinuclear localisation, indicating the sufficiency of the GPI anchor and a signal sequence for this localisation pattern.

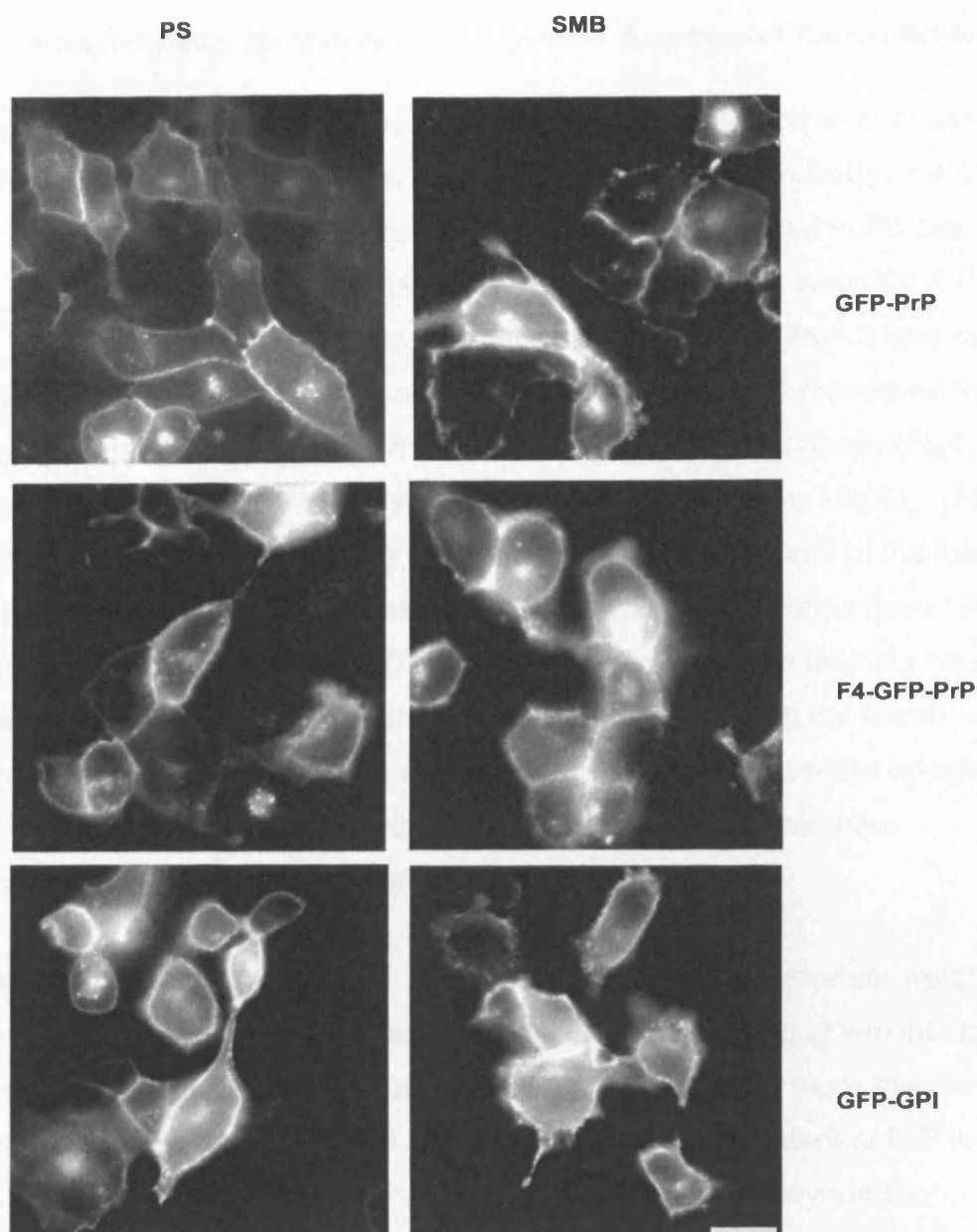


Figure 4.2. Transient expression of constructs in PS and SMB cells

GFP-PrP, F4-GFP-PrP and GFP-GPI were expressed in the SMB/PS cell system (see Materials and Methods). Panels on the left represent expression of constructs in PS cells and those on the right in SMB cells. The scale bar indicates 20 microns. Note that the basic localisation of all the fusion proteins is plasma membrane with some evidence of perinuclear staining. There is no clear difference found between localisation of a particular fusion protein in SMB or PS cells. There is no difference in localisation of GFP-PrP fusion protein or F4-GFP-PrP fusion protein in the cells, indicating that the mutations introduced to form the latter protein do not alter trafficking. The GPI anchored GFP protein (GFP-GPI) also appears to have the same localisation. These experiments were reproduced independently. In each case multiple fields ($n \geq 6$) were observed for each condition. No signal was observed in untransfected cells.

4.4. Biochemistry of transiently expressed fluorescent fusion proteins

Fusion proteins were transiently expressed in PS cells which were subsequently processed for PrP^c and western blotted with an anti GFP antibody or 6H4 (see Fig 4.3 and Materials and Methods). Gfp-prp was expressed in PS cells which were processed for PrP^c and run in 3 fold dilutions (Fig 4.3 lanes GFP-PrP 1,2,3) . In parallel a cytoplasmic GFP was also expressed (Fig4.3 lane cyt-GFP). As a further comparator untransfected PS cells were processed for PrP^c (Fig 4.3 lane PrP). The blot with an anti GFP monoclonal antibody (Fig4.3 left panel) indicates the fusion protein running at a weight above 45Kda. There appear to be two distinct bands, as seen in the lower dilutions) of the fusion construct, which may correspond to different glycosylated forms (lane GFP-PrP1 and 2). Cytoplasmic GFP is found at two weights, the majority band just above 30 kda. Also of note is the presence of some GFP in the fusion constructs, at the same weight as the lower weight band from the cytoplasmic GFP sample. It is unclear why this signal was not seen in the more concentrated sample (Fig4.3 GFP-PrP 3 anti GFP blot).

The 6H4 blot indicates both the GFP-PrP fusion at the appropriate weight of between 50 and 60 Kda, and also endogenous PrP running at weights below 45 Kda. It is noteworthy that the fusion is highly expressed, at more than two times the level of endogenous PrP. It is also apparent that the extent of PrP in the fusion lanes (Fig4.3 lanes GFP-PrP 1,2,3 6H4 blot) runs beyond the endogenous weights, possibly indicating degradation products of the fusion.

The f4-gfp-prp construct was transiently transfected into SMB cells and processed for PrP^c (Fig4.4 GFP-PrP lanes). A positive control for the efficacy of the 3F4 antibody was included (lanes marked +Cnt) in the form of a recombinant hamster PrP protein. A negative control, cytoplasmic GFP expressed in SMB cells, was also run to assess the specificity of the 3F4 antibody for the engineered hamster epitope. The fusion protein F4-GFP-PrP appears to run at the same weight as the unmutated fusion from which it is derived above 45Kda and probably between 50 and 60 Kda (antiGFP blot lane

F4-GFP-PrP), and two species are distinguishable. Some GFP appears to be found at a lower weight, indicating proteolysis of the fusion. The 3F4 blot indicates that the mutant fusion is picked up efficiently by the antibody and that the negative control is not (Fig 4.4 3F4 blot: F4-GFP-PrP and PrP lanes respectively) . A note of caution applies to the result which reveals that the endogenous PrP is expressed at a lower level than the fusion (compare Fig 4.4 6H4 blot: F4-GFP-PrP and PrP lanes), and may not blot with 3F4 to some extent as a result of quantitative difference in loading. Therefore this is not a stringent test of 3F4 specificity but highly indicative. It is noteworthy, nevertheless, that the 3F4 blot reveals such a clear signal in the F4-GFP-PrP lane at weights below the fusion protein. This indicates that much of the material is not endogenous, and is derived from the fusion protein itself. This issue is discussed in detail below.

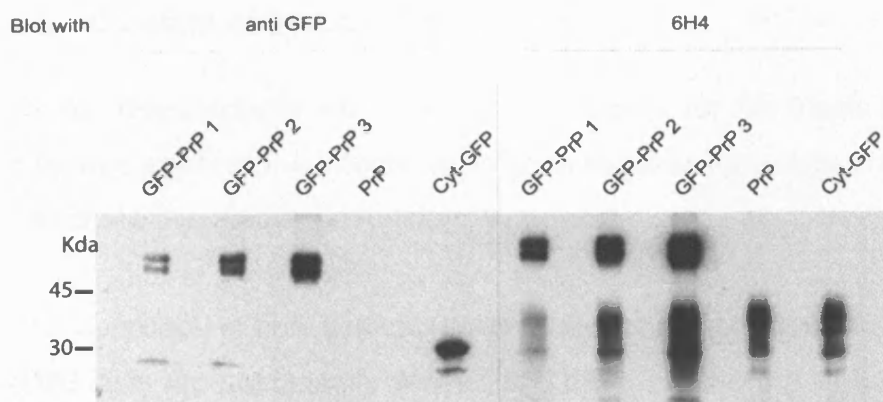


Figure 4.3. Transient expression of GFP-PrP fusion protein

Constructs were transiently transfected into PS cells (see Materials and Methods) and processed for PrP^C. GFP-PrP 1, 2 and 3 represent three dilutions of the same sample from cell transfected with the gfp-prp construct. The lane marked PrP represents an untransfected sample and cyt-GFP indicates PS cells transfected with a cytoplasmic GFP.

The left half of the gel is blotted for GFP and the right half for PrP with 6H4. Blotting with 6H4 reveals endogenous PrP at the normal weights but clearly picks up the higher weight PrP which is part of the fusion protein. Note that at the weight of the fusion protein, between 50 and 60 Kda, a doublet can be seen on the GFP blot possibly indicating different extents of glycosylation.

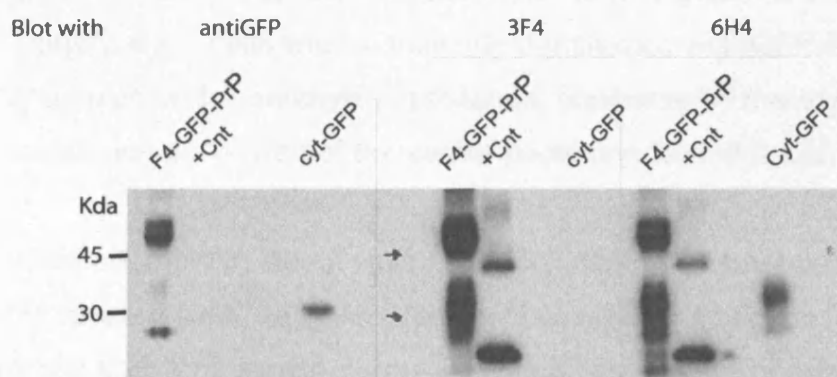


Figure 4.4. Transient expression of F4-GFP-PrP fusion protein

The lanes marked F4-GFP-PrP indicate SMB cells which were transiently transfected with the 3F4 epitope tagged fusion protein and processed for PrP^C.

+Cnt denotes a recombinant hamster PrP control, containing both 3F4 and 6H4 epitopes, and cyt-GFP represents an SMB sample which was transfected with a cytoplasmic GFP. The cyt-GFP sample also acts as a control for endogenous PrP^C. Gels were blotted with an anti-GFP polyclonal antibody, 3F4 or 6H4. Note that in all cases the fusion construct can be seen to run at the appropriate weight, above the 45Kda marker. The 3F4 antibody blot reveals no signal in the 'cyt-GFP' lane because endogenous PrP does not contain a 3F4 epitope. However, material at the endogenous PrP^C weight is found in the gel blotted with 3F4, indicating that this material is not endogenous PrP^C but is derived from the fusion construct.

4.5. Creation of Stable Transfectants

Stable Transfectants are a necessary endpoint for this thesis because the intended study of the infectious process requires long term analysis in culture and therefore stable expression.

The approach of bulk selection was taken for two principle reasons. Firstly, SMB cells are not clonally derived and therefore there may be a range of important phenomena to be observed in a mixed cell population. Secondly, repeated attempts to clone SMB and PS cells in the laboratory have proven unsuccessful in the past (Brockes, Kanu and Landy data unpublished). Cells will not grow at clonal density and do not survive at very low, densities. Attempts to affect a more transformed phenotypes have previously been undertaken in the laboratory: large T antigen was transfected into SMB cells resulting in a more transformed phenotype but a loss of infectivity (Brockes and Kanu data unpublished). Survival and consequent cell growth is not ameliorated significantly by the usual manipulation of conditioning media (data not shown) or growth on feeder layers (Brockes and Kanu unpublished data). Therefore PS cells were transiently transfected with GFP-PrP and F4-GFP-PrP and selected for neomycin resistance, conferred by the expression of neomycin resistance gene, part of the vector backbone for the fusion constructs.

Initial attempts to select cells led to cell death and poor percentages of fluorescent cells, however a protocol using bulk selection (pers comm. Telling group keystone symposium – see Materials and Methods) led to the production of cell lines which were 95-100 % fluorescent.

Fig 4.5 represents micrographs of cell lines produced by transfection of PS cells followed by bulk selection (left panels). The fusions expressed in each case are indicated on the right. These cell lines were then used to create infected counterparts by the procedure employed in chapter 3 of culturing with infectious freeze-thawed cell lysates (see Materials and Methods). The uninfected stable cell line expressing the GFP-PrP fusion is denoted GFP-PrPst, the cell lines expressing F4-GFP-PrP is denoted F4-GFP-PrPst. The suffix 'Inf' is added to indicate the infectious partner e.g. F4-GFP-PrPstInf represent the infected cell

line expressing F4-GFP-PrP protein. Cells in both cell lines expressed the constructs at detectable levels and showed the same localisation of fusion protein to the plasma membrane with some perinuclear fluorescent accumulation. Again, as with the transient transfectants, the F4-GFP-PrP is localised in all cases in the same way as its non mutated counterpart GFP-PrP. There are no clear differences between the expression in the infected cell lines and their uninfected partners for either of the fusion constructs.

In order to ascertain whether the fusion construct was appropriately tethered by the GPI anchor to the plasma membrane, phosphatidylinositol-specific phospholipase C (PIPLC) was employed. F4-GFP-PrPst and F4-GFP-PrPstInf cells were grown on glass cover slips coated with laminin and treated for 1h with PIPLC in parallel with controls (see Materials and Methods). Micrographs were then taken of the cells at 63 x magnification, which revealed that the results of PIPLC treatment was to remove the majority of the plasma membrane fusion protein (Fig4.6). The remnant of perinuclear material is more pronounced after treatment and this may be because some internalisation of material has occurred or because material obscuring the interior fluorescence has been removed.

It may be that some fusion protein in the cells is denatured in the process of trafficking or conversion, and fluorescence may be extinguished by the low pH of certain cellular compartments like the lysosome. For this reason antibody staining was undertaken on fixed cells in the hope that any alternative pattern to GFP signal alone might be revealed. Surface staining did not reveal anything unusual (data not shown) and therefore a permeabilisation protocol was employed (see Materials and Methods). Infected and uninfected stable cell lines (and stInf cells) were stained with 6H4, anti GFP polyclonal antibody, and a Brdu control antibody (fig 4.7 A F4-GFP-PrPst and 4.7 B F4-GFP-PrPstInf cells). The primary antibody used is indicated on the right of the relevant panel and in each case the GFP signal is illustrated on the left in green. In summary, there are no differences in localisation revealed by ordinary GFP and antibody staining.

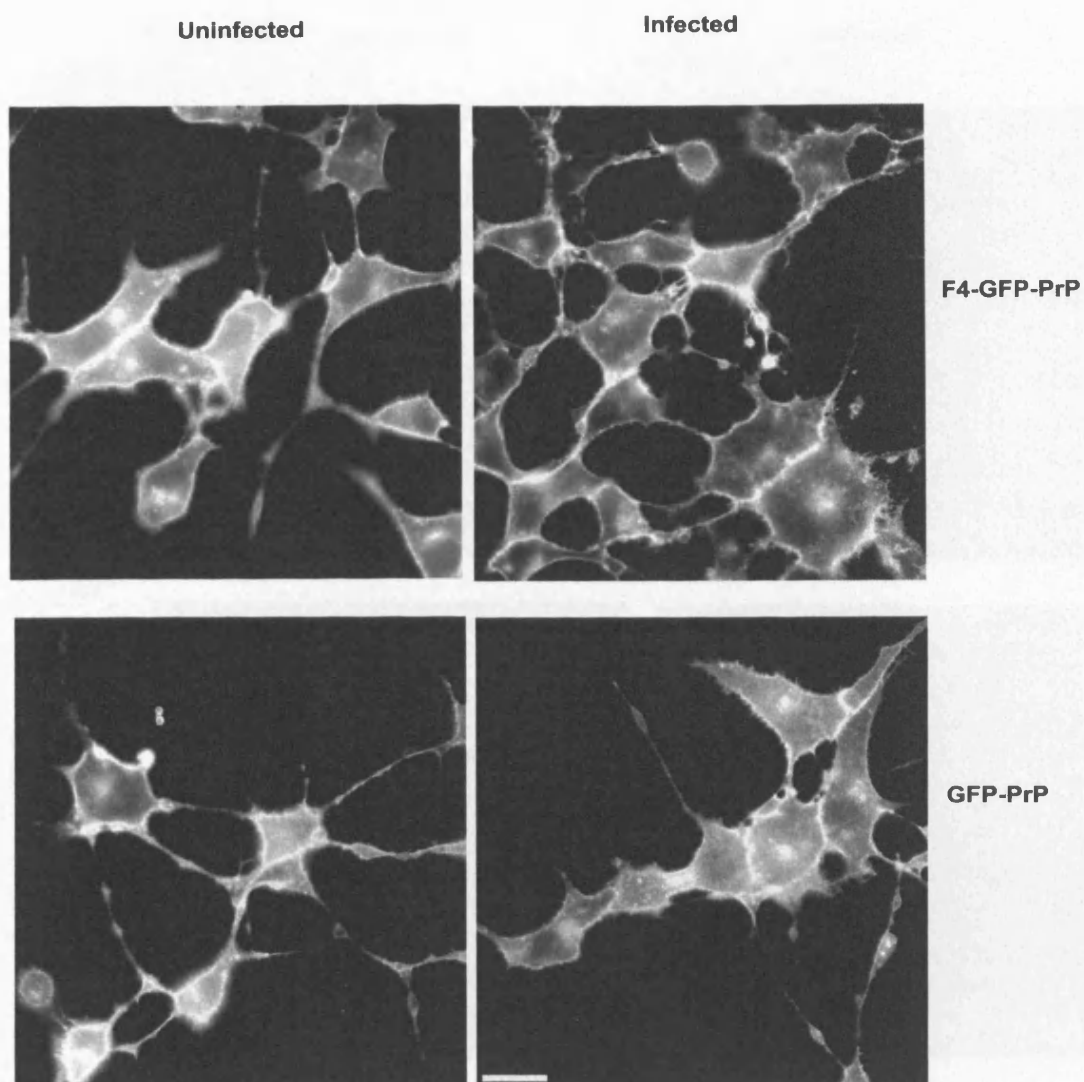


Figure 4.5. Micrographs of stable transfectants

Cells were transfected with either the gfp-prp or the f4-gfp-prp constructs (indicated on the right of the panels above) and bulk selected for neomycin resistance (see Materials and Methods). The resulting populations were almost entirely fluorescent cells (see below). The cells were then infected with freeze-thaw lysates of SMB cells, with the result of two pairs of infected/uninfected cell lines expressing the fusion constructs (see Materials and Methods). Micrographs of live cells were taken at 63x magnification in order to avoid fixation artefacts. The distribution of constructs reflects that of PrP in general: most of the material is found on the plasma membrane, with some perinuclear PrP accumulation. No clear differences were visible between infected and non-infected cells. Observations were made in $n \geq 5$ fields for each condition, and the experiment was reproduced. The F4-GFP-PrP cells (uninfected and infected) have also been used for multiple further experiments in time-lapse and no differences observed between them).

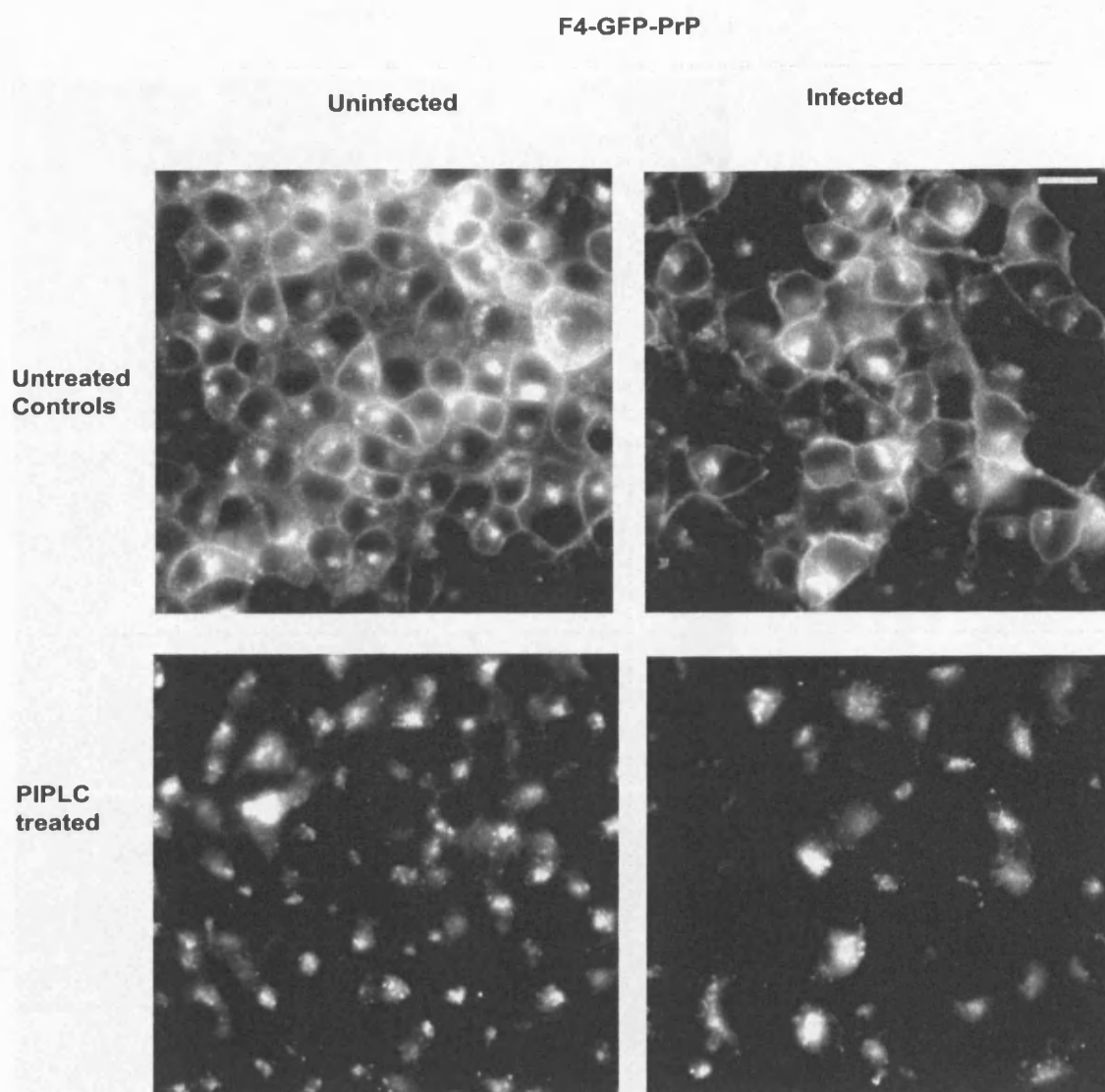


Figure 4.6. PIPLC treatment of cell pairs expressing F4-GFP-PrP

The stable infected and uninfected cell lines expressing F4-GFP-PrP (F4-GFP-PrPst and F4-GFP-PrPstInf) were grown to confluence on the glass cover slips coated in laminin, in order to maximise their adhesion to the dish following treatments. Cells were either kept on ice at 4 degrees for 1 hour in L-15 medium or kept on ice for 1 hour in L-15 medium supplemental with 2 units/ml of PIPLC (see Materials and Methods). The results of treatment of both infected and uninfected cells is shown in the micrographs above (fig4.6) at 63x magnification. Note that the majority of PrP is removed by PIPLC treatment for 1 hour indicating the GPI anchorage of the fusion at the plasma membrane. This result was reproducible.

**F4-GFP-PrP
Uninfected**

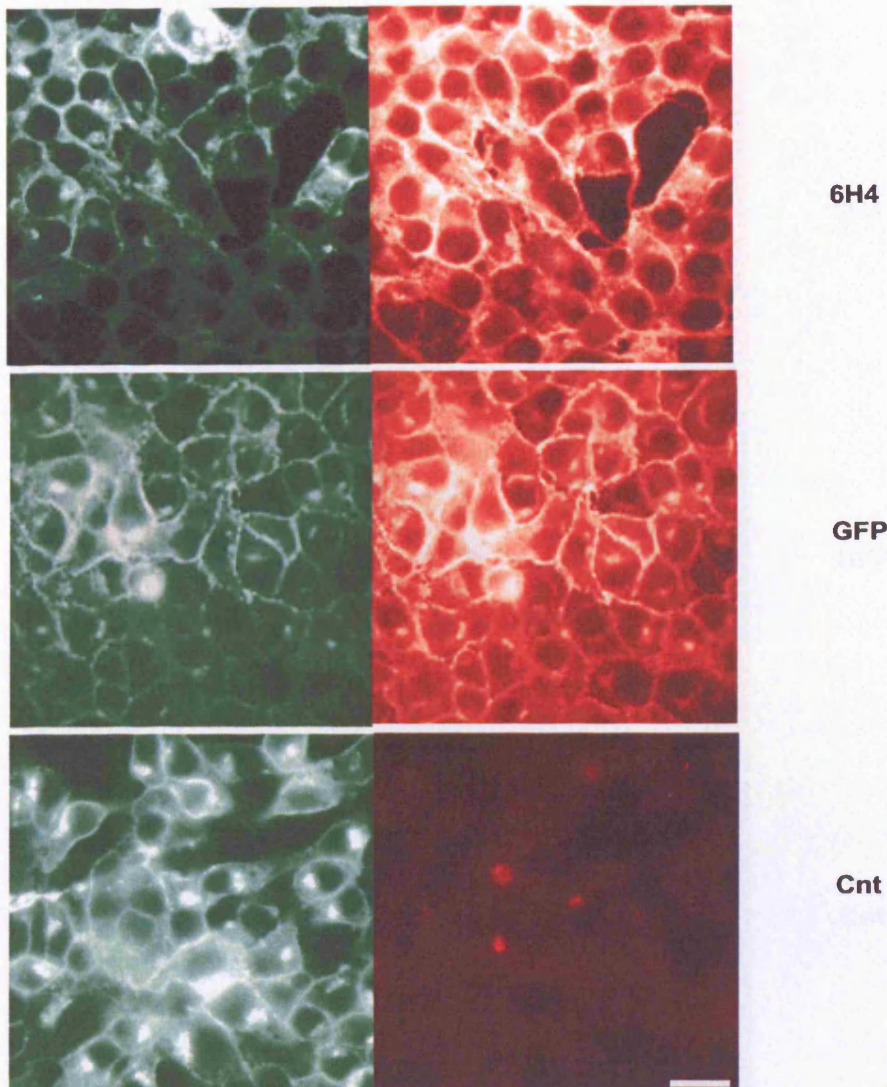


Figure 4.7. Micrographs of fixed F4-GFP-PrPst uninfected cells stained with antibodies to PrP or GFP

Cells were fixed in PFA and permeabilised with 0.1% Triton (see Materials and Methods). They were then stained with antibodies 6H4 (1/100 dilution), anti GFP (1/200 dilution) or a control monoclonal antibody to Brdu, diluted to the same final concentration. A TRITC conjugated secondary to mouse or rabbit was added depending on the use of a monoclonal or polyclonal primary antibody. Micrographs at 63x magnification were taken in FITC Channels, to view GFP, indicated in green, and TRITC channels to view the secondary antibody, indicated in red. Note that the antibodies did not reveal a clear difference in staining pattern to live cells as might have been expected. Also, antibody staining does not appear to reveal any clear differences over GFP fusion localisation seen in the FITC channel.

**F4-GFP-PrP
Infected**

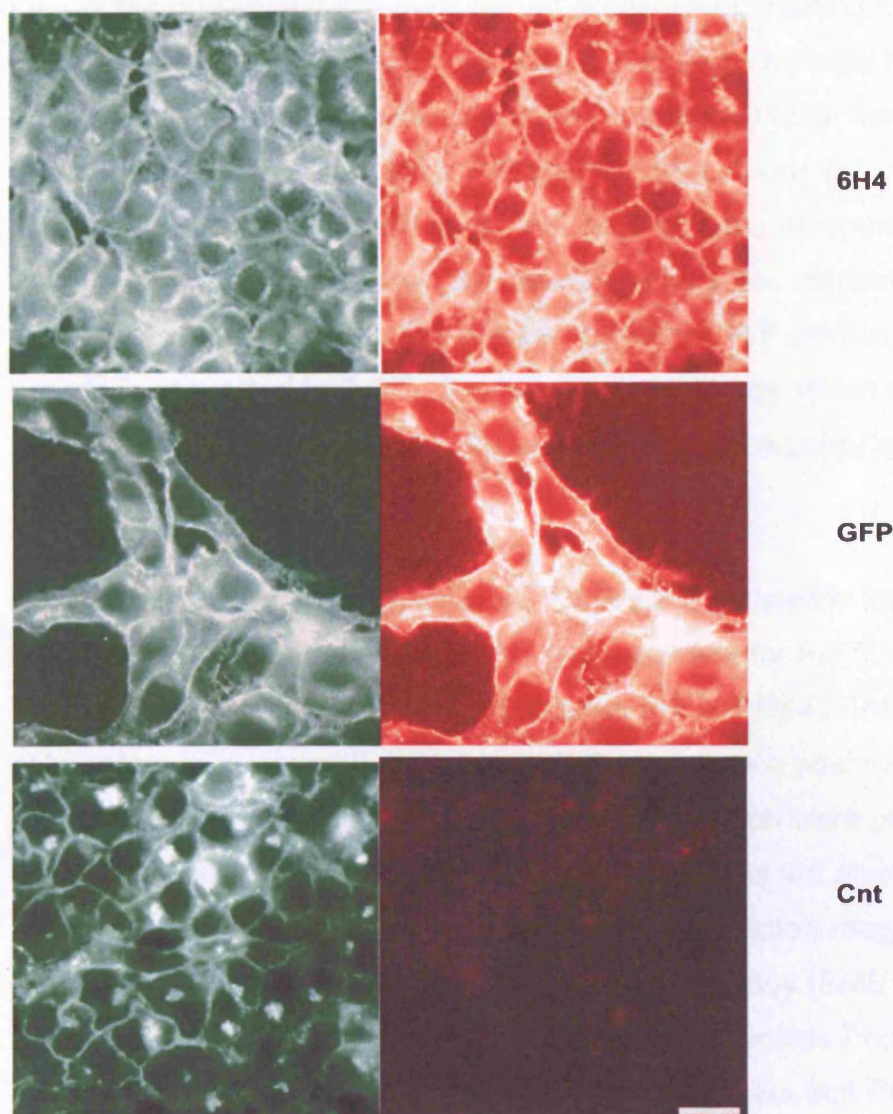


Figure 4.8. Micrographs of fixed F4-GFP-PrPstInf, infected cells stained with antibodies to PrP or GFP

Cells were fixed in PFA and permeabilised with 0.1% Triton (see Materials and Methods). They were then stained with antibodies 6H4 (1/100 dilution), anti GFP (1/200 dilution) or a control monoclonal antibody to Brdu, diluted to the same final concentration. A TRITC conjugated secondary to mouse or rabbit was added depending on the use of a monoclonal or polyclonal primary antibody. Micrographs at 63x magnification were taken in FITC Channels, to view GFP, indicated in green, and TRITC channels to view the secondary antibody, indicated in red. Note that the antibodies did not reveal a clear difference in staining pattern to live cells (see Fig 4.5) or to GFP signal in the FITC channel.

4.6. Conversion of PrP^c in fusion to PrP^{sc}

One of the original aims in pursuing an approach of creating fusion proteins between PrP and GFP is the possibility of creating a reporter for PrP^{sc}: a difference in localisation in an infectious context may have been indicative of/attribution to the prion form. Although evidence from the immunofluorescence studies so far indicates no clear difference in localisation of the fusion proteins between infected and uninfected contexts, a key question that remains to be answered is whether or not the PrP portion of the fusion protein is converted to PrP^{sc}. It is also important to ascertain whether a converted PrP species is still in fusion with the GFP reporter molecule following its conversion.

F4-GFP-PrP fusion was expressed in SMB cells transiently for 3 days (see Materials and Methods) and cultures were assayed for PrP^{sc}. Fig 4.9 illustrates the sample blotted with 3F4 or 6H4 in lanes marked F4-GFP-PrP.

+Cnt refers to a recombinant hamster PrP loaded as a positive control for the efficacy of 3F4 and SMB refers to SMB cultures which were processed in parallel as controls for endogenous Prion (these cells are also transfected with a cytoplasmic GFP as a control for effects of transfection reagent on Prion). The endogenous Prion is not picked up by the 3F4 antibody (SMB lane: 3F4 blot) and therefore the signal in the F4-GFP-PrP lane indicates Prion that is from the fusion because it contains the 3F4 epitope. It appears that PrP from the fusion construct is therefore converted after transient expression.

The same process was repeated for the infected stable cell line F4-GFP-PrPstInf which was analysed for PrP^{sc} and PrP^c and western blotted using 3F4 and 6H4 antibodies (Fig 4.10 lanes Infected F4-GFP-PrP). Uninfected cells (F4-GFP-PrPst) were also processed in order to ensure that GFP in fusion, did not confer protease resistance to normal PrP (Uninfected F4-GFP-PrP lane). As a further control, HMH8 cells were infected and assayed in parallel (infected HMH8 lanes). These cells are stable expressors of a chimerical Hamster, Mouse Hamster construct which also includes the 3F4 epitope and has

previously been shown not to undergo conversion (see Materials and Methods). The gels marked +PK are westerns of samples which have been processed for PrP^{sc}, and those marked -PK are samples processed for PrP^c. The HMH chimera is not converted in these conditions (+PK, 3F4 blot : infected HMH8 lane). Of note is the key result that, as with the transient expression, the PrP portion of the fusion protein is converted in stable transfectants (+PK, 3F4 blot: infected F4-GFP-PrP lane).

This result initially seems to suggest the successful conversion to prion of the F4-GFP-PrP fusion, but the PrP^c biochemistry of the fusion proteins discussed (Fig 4.10 – PK blot) begs the question of whether this conversion occurs before or after a cleavage event occurring in the cells. Specifically, signal should not be present below the weight of the full fusion (Fig 4.10 –pk panel, 3f4 blot, infected and uninfected F4-GFP-PrP lanes). The presence of this signal indicates that both in the infected and uninfected cell lines, PrP is being cleaved from the GFP in the fusion. It is also clear that this is occurring prior to residue 108 of PrP because the 3F4 epitope remains intact. Furthermore, comparison of the similarity in weight of this cleaved product and HMH8 PrP^c (-PK blot , 3f4, infected HMH8 lane) also indicates the proximity of the cleavage to the junction between the GFP and C-terminal portion of the fusion.

A key question is why cleavage of the fusion protein is occurring and three basic hypotheses were tested (Fig 4.11). In order to assess the hypothesis that the cleavage is a specific property of the F4-GFP-PrP fusion or more general, a comparative analysis of F4-GFP-PrP and the non mutated GFP-PrP fusion was undertaken. The constructs were expressed transiently in PS cell prior to analysis for PrP^c and blotted with 3F4, 6H4, or an antiGFP antibody (see Materials and Methods). Comparing the fusion constructs it can be seen that the mutant (3F4 blot, lane: – F4-GFP-PRP) is being cleaved as discussed previously. The material below the weight of the fusion is not attributable to endogenous signal in this gel. This approach cannot be used for fusion protein without the 3F4 epitope to answer the same question. However, when blotting with an anti GFP antibody (see GFP blot: lanes F4-GFP-PrP) GFP is being seen at around the weight of cytoplasmic GFP and therefore this is a further

indication of cleavage from the fusion because GFP has been liberated. The normal fusion protein also demonstrates liberated GFP material (GFP blot lane: GFP-PrP). Therefore it appears that cleavage is not a direct result of the introduction of the 3F4 epitope.

In order to further assess whether there was a specific issue with the linker in the design of the fusion proteins a CFP-PrP fusion (produced by Nenna Kanu) was included by way of comparison. This represents a direct fusion between the end of the GFP molecule and the c-terminus of PrP, in contrast to the fusions described above which include a short linker sequence. The anti-GFP polyclonal antibody employed for western blots also recognised CFP. A comparison of CFP-PrP lanes in the GFP blot with the other fusions (see GFP blot: CFP-PrP lane vs GFP-PrP or F4-GFP-PrP lanes) also indicates cleavage given the liberation of CFP from the full fusion.

The possibility that the cleavage is an artefact introduced by protease release and action following cell lysis was tested. The normal lysis buffer employed in studies assaying for PrP^{Sc} does not include protease inhibitor cocktails in order to avoid interference with protease digestion involved in the PrP^{Sc} biochemical assay. Therefore conditions of lysis including protease inhibitor (see Materials and Methods) were compared with those omitting it and this is indicated by the + or – signs above each lane. The experiment demonstrates no clear difference between lysis conditions which included protease inhibition and those which did not (see Fig 4.11: compare + and – lanes for fusion expressing cells). In general approximately 50 percent of the material appears to be in the full fusion form and the remnant is cleaved. The proteolysis appears not to be particular to the mutant form of the fusion protein and more generally is not dependent on the specific linker of this design of fusion. Proteolysis is also unlikely to be an artefact introduced during the lysis of the cells.

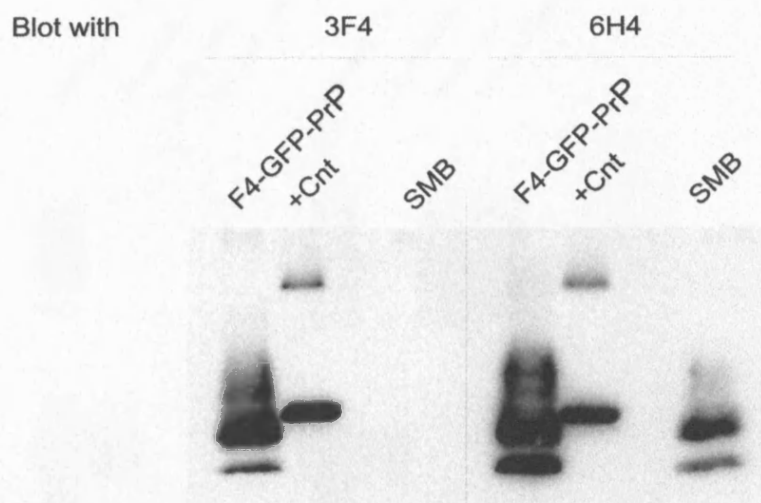


Figure 4.9. Transient expression of F4-GFP-PrP in SMB cells

In order to assay for conversion of the fusion protein to Prion recourse was made to the specific 3F4 epitope in order to distinguish Prion from the fusion against endogenous prion background. F4-GFP-PrP lane represents material transiently transfected into SMB cells and then processed for PrP^{Sc} (see Materials and Methods). Lanes marked + Cnt represent hamster recombinant PrP^{C} loaded as a positive control for 3F4 antibody efficacy. SMB, represents an SMB sample (transfected with cytoplasmic GFP) processed for PrP^{Sc} . Gels were blotted with 3F4 or 6H4 as indicated above. Note that endogenous PrP^{Sc} is not picked up by the 3F4 antibody as seen in the SMB lane on the 3F4 blotted gel. This implies that material in the F4-GFP-PrP lane in the 3F4 blot, is Prion from the fusion construct.

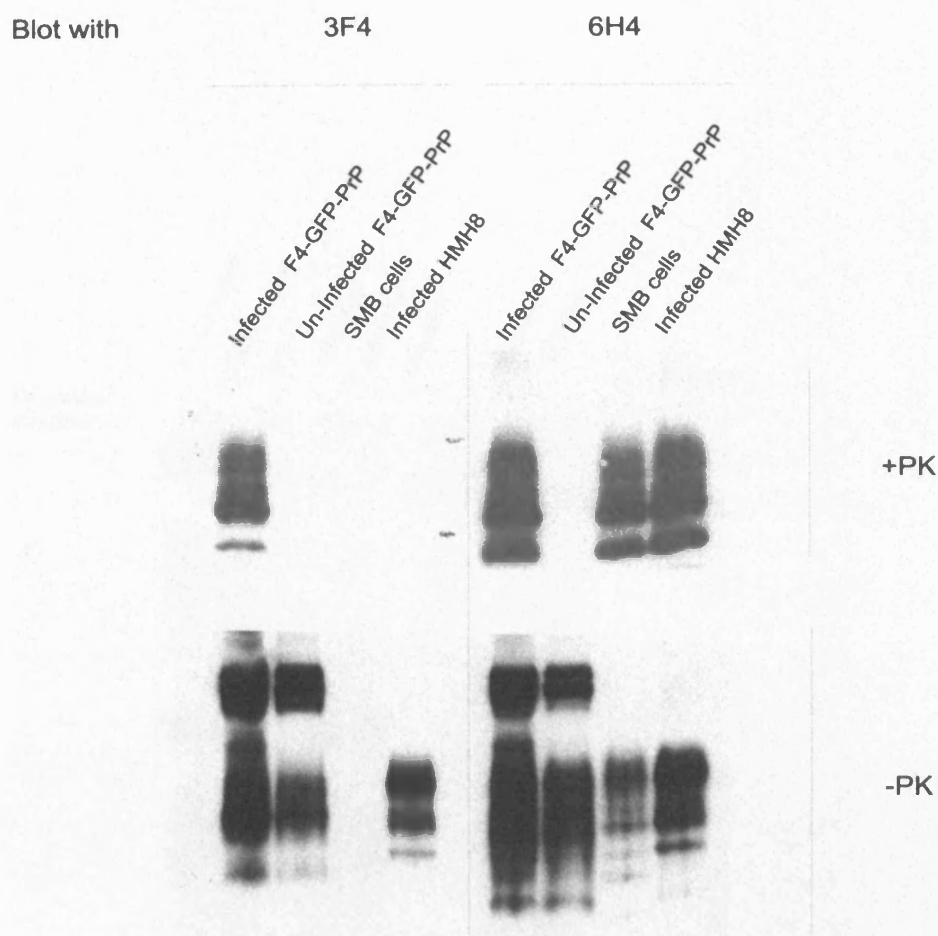


Figure 4.10. Conversion to Prion isoform of PrP^c in fusion protein expressed in stable transfectants

Infected and uninfected F4-GFP-PrPst cells were processed for PrP^{Sc} and PrP^c.

Infected HMH8 cells, which express a chimeric hamster, mouse PrP, and a control SMB sample, were taken through the same procedure. The +PK gel and -PK gels represent blots for PrP^{Sc} and PrP^c respectively. Note that the infected cells expressing the fusion F4-GFP-PrP fusion, yield prion with the 3F4 epitope (+PK, 3F4 blot :infected F4-GFP-PrP lane). The -PK blot for PrP^c indicates that the fusion undergoes some cleavage because 3F4 positive material is seen at the endogenous weight below the full fusion weight (-PK, 3F4 blot: lane F4-GFP-PrP). This result was reproducible.

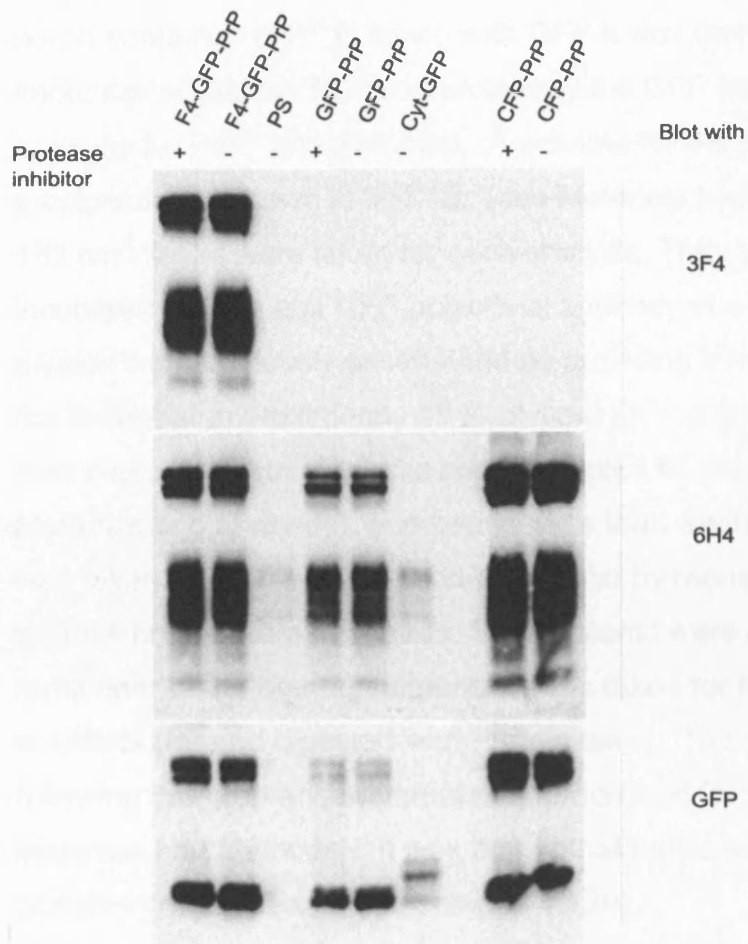


Figure 4.11. Cleavage of the fusion protein

PS cells were transiently transfected with either the f4-gfp-prp, with gfp-prp or with a cfp-gfp (see Materials and Methods). Cells were processed for PrP^c either in the presence of protease inhibitors or without (indicated by +/- protease inhibitors). Control samples included PS cells (PS lanes) or PS cells transfected with a cytoplasmic GFP (cyt-GFP lanes). Samples were loaded and blotted with 3F4, 6H4 or anti GFP antibodies. The GFP blot is critical because it indicates that GFP is liberated from the fusion in all the transfected samples. Also note that the CFP-PrP fusion, designed with a different linker undergoes this proteolysis. The inclusion of protease inhibitors (+lanes) does not abrogate proteolysis.

4.6.1. Immunoprecipitation experiments

It has been established that cleavage of fusion protein occurs and for this reason, although it has been shown above that the PrP portion of the fusion is converted to PrP^{sc}, it cannot be confirmed whether there is any PrP^{sc} in fusion with GFP. In order to assess the question of whether material existed in the cell which contained PrP^{sc} in fusion with GFP it was therefore necessary to carry out immunoprecipitation of fusion protein by the GFP part of the molecule and then to assay for PrP^{sc} after this step. A schema for the process of immunoprecipitation is shown in fig4.12. (see Materials and Methods also). Briefly two 162 cm² flasks were taken for each analysis. They were lysed and were incubated with an anti GFP polyclonal antibody at a dilution of 1:100. This dilution was previously ascertained as providing a maximum efficiency for IP of the fusion, at approximately 25 % of input GFP (data not shown). Lysates were then incubated with magnetic beads coupled to secondary antibody (see Materials and Methods), and beads were then washed and resuspended. 10% was taken for PrP^c analysis and processed by resuspension in sample buffer to remove protein from the beads. Supernatants were run on western blots. The remainder of the bead resuspension was taken for PrP^{sc} analysis, resuspended in lysis buffer and digested with Proteinase K. The beads were removed following this step and supernatants processed for PrP^{sc} as usual (see Materials and Methods). It was hoped that protease digestion would cleave protein from the beads (see schema 4.12B).

The entire process was repeated with the polyclonal antibody to mouse Rb protein as a control for non specific immunoprecipitation.

An illustration of samples taken through this process is seen in fig4.13.

Samples SC1,2 3, refer to 10 fold dilutions of PrP^{sc} from F4-GFP-PrPstInf cells, which were the source for the IP. The highest concentration represents a sixth of the input to the IP. Material Processed for PrP^{sc} following the IP is indicated in lane 1a. The control condition where IP is undertaken with an Rb antibody is indicated in lane 1b. Note that no PrP^{sc} is seen at the expected weight, although

antibody is seen to be removed from the bead following digestion, which runs just below the weight of the fusion protein. Lanes 3 and 4 indicate controls for this antibody background and are dilutions of antibody in lysis buffer which have been taken through PrP^{Sc} analysis in parallel with the other samples. IP of the fusion protein through its GFP component is successful as seen in lane 2a and is specific when compared with IP using the control antibody (lane 2b).

The lowest dilution of control sample (lane Sc3) represents approximately 1/600 of the input total PrP^{Sc} available in the sample processed for PrP^{Sc} in this IP. The experiment was repeated with the non mutant fusion, using GFP-PrP^{StInf} cells, and the same result obtained (data not shown). When the beads that had been taken through the PrP^{Sc} analysis were boiled in sample buffer, large amounts of antibody were found and a mess of species at around 100 kda but no material was seen at weights below 45kda (the rough weight at which this antibody background is in evidence). This experiment therefore illustrates that GFP is not present in fusion with PrP^{Sc} in these cell lines.

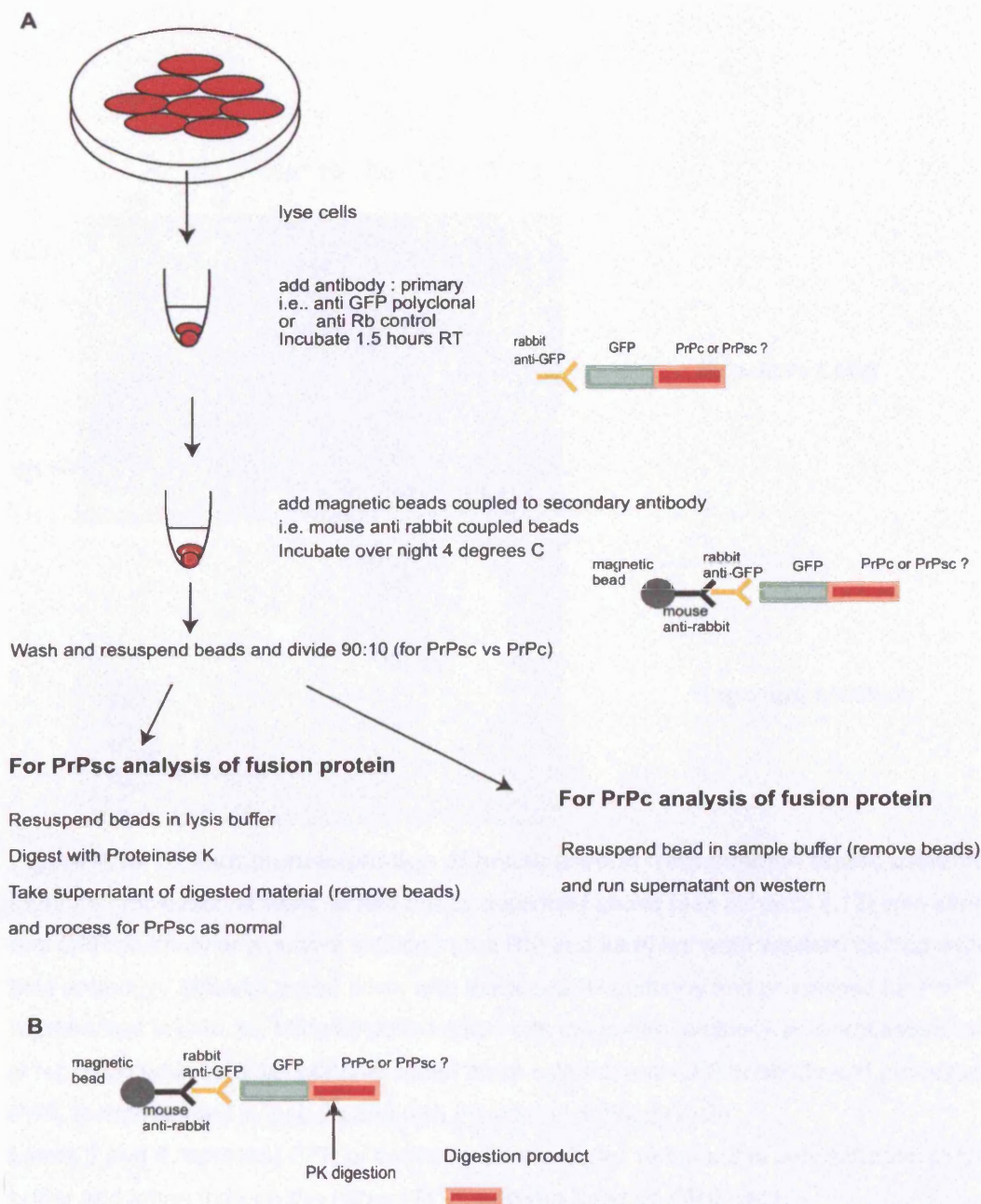


Figure 4.12. Schema for Immuno precipitation of fusion protein from infected cells

A: Infected cell, F4-GFP-PrPstInf, were lysed and samples are incubated with an anti GFP polyclonal antibody (or a control antibody to Rb protein) for 1.5 hours and then, following addition of magnetic beads conjugated to secondary antibody, were incubated overnight at 4°C. Samples for PrP^c analysis were then washed and PrP^c removed by boiling in sample buffer. Samples for PrP^{sc} analysis were digested with Proteinase K and supernatants taken through the standard PrP^{sc} analysis. Samples were blotted with 6H4 antibody. **B:** Diagram indicating the proposed cleavage of putative PrP^{sc} from the fusion after pull down by the GFP part of the fusion protein.

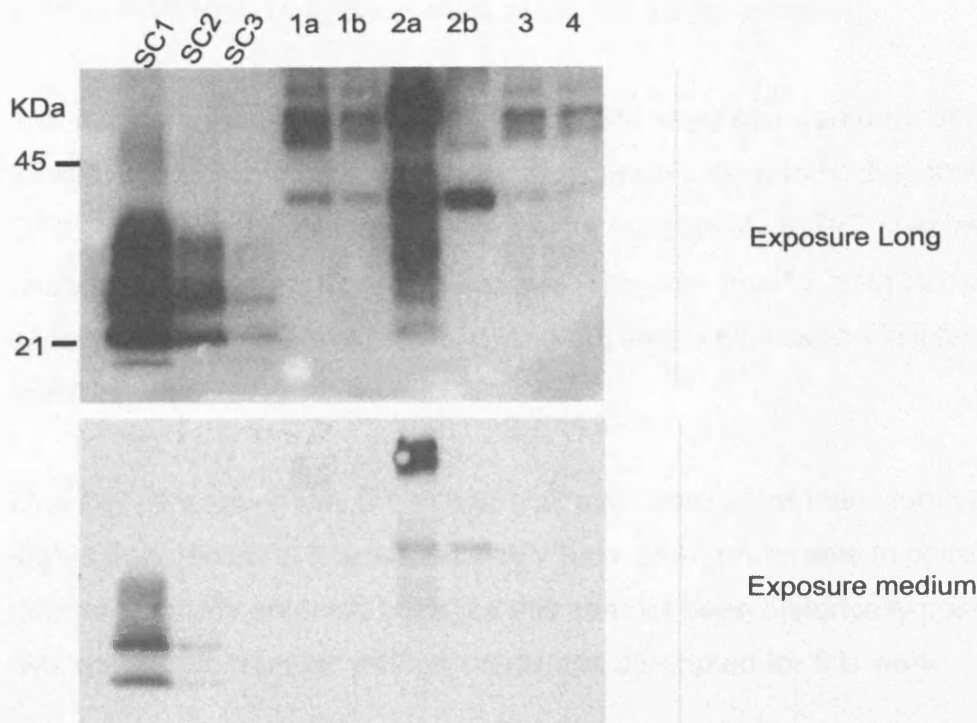


Figure 4.13. Immunoprecipitation of fusion protein from infected stable transfectants

Immuno precipitations were carried out as described above (see schema 4.12) with either an anti GFP antibody or a control antibody (anti Rb) and samples were western blotted with the 6H4 antibody. Material pulled down with the anti GFP antibody and processed for PrP^{sc}, is represented in lane 1a. Material pulled down with the control antibody and processed for PrP^{sc}, is represented in lane 1b. Material pulled down with the anti GFP antibody and processed for PrP^c, is represented in lane 2a and with the control antibody in 2b.

Lanes 3 and 4 represent GFP or control antibody diluted to the same concentration in lysis buffer and taken through the normal PrP^{sc} analysis used on SMB cells.

SC1,2 and 3 represent 10 fold dilutions of the F4-GFP-PrP infected cells processed for PrP^{sc}.

Two exposures of the gels are indicated. Note that PrP^c in fusion is efficiently immunoprecipitated (lane 2a) but not PrP^{sc} (lane 1a). This result was reproducible.

4.7. Discussion

In this chapter the basic properties of fusions between GFP and PrP were assessed. In particular the question was addressed of whether conversion of PrP^C to PrP^{Sc} occurs in the context of the full fusion protein.

The normal fusion and mutant derived fusion were compared for differences in localisation or other behaviours and none were found, indicating that the F4-GFP-PrP fusion protein is a useful tool for distinguishing PrP species from the fusion rather than endogenous sources. This was true for both transient expression and stable expression and applied to expression in infected and in uninfected contexts.

One key procedure was the use of bulk selection rather than cloning to produce stable transfectants. It would probably have been preferable to compare many different clonally selected lines but this has not been historically possible and it was not possible under various conditions attempted for this work.

One feature of this work was to establish the pattern of localisation of fusion proteins between PrP and GFP and these fusion proteins have much the same pattern as endogenous PrP (see chapter 3). The use of PIPLC treatment to clear fluorescent fusion protein from the cell surface indicated that it was appropriately attached by a GPI anchor to the plasma membrane. One experiment that has not been attempted might involve the use of PIPLC to clear material from the surface and then, as mentioned above, watch the evolution of fluorescent protein. Along these lines, it should be emphasised that the conditions assayed here are conditions of stable equilibrium and that differences in dynamics of trafficking are not assessed.

There seemed to be no obvious differences in localisation of fusion protein between infected and uninfected contexts. The most obvious possibility to be considered given the evidence presented in this chapter, is that these fusions do not report on the localisation of PrP^{Sc}, because the PrP^{Sc} is not found in fusion with GFP. Either a cleavage event occurred prior to conversion or post

conversion. Alternatively, it may be that PrP^{sc} is found in fusion with GFP, but that there are no clear differences in trafficking between PrP^{sc} and PrP^c. The lack of an antibody to PrP^{sc} makes it difficult to clearly assess the evidence for or against positions taken on the localisation of PrP^{sc} as distinct from PrP^c. Another possibility remains which is that the relative abundances of PrP^{sc} and PrP^c make it hard to practically distinguish any fine differences. Ordinarily PrP^{sc} represents much less than 10% (and in the range of 3-5 percent) of the total PrP population in these cells. It may be then that differences in localisation would be hard to see against this majority background. Hypotheses were tested which assessed whether differences in localisation might be obscured by problems with the reporter protein, GFP. It is conceivable that denaturation occurs or that fluorescence is quenched in some cellular compartments for example. In order to try and rule this hypothesis out, antibody staining was employed with a permeabilisation protocol, and did not reveal any obvious differences in pattern of localisation from that indicated by the fusion proteins in live cells.

One of the vexing issues of this thesis has been the exploration of the finding that significant proteolysis of the fusion protein appears to take place.

Experiments were described which assessed whether this proteolysis might be either an artefact or specific to the linker in the fusion construct. However this does not appear to be the case. An alternative design of fusion, placing of GFP closer to the PrP c-terminus, is not desirable because it is likely to cause disruption of folding.

The immunoprecipitation was designed to assess whether, although cleavage occurs, there might still be a proportion of PrP^{sc} in fusion with GFP. However, although GFP in fusion with PrP^c could be immunoprecipitated, GFP in fusion with PrP^{sc} could not. Given the large amounts of PrP^{sc} that appear to be derived directly from the fusion, as assayed by the 3F4 epitope, and given the lack of any immunoprecipitated GFP-PrP^{sc}, it is a reasonable indication that conversion occurs after a cleavage event. It is also possible, although less likely, that the conversion does occur in the context of the intact fusion and that the cleavage event occurs immediately following this.

The hypothesis that I would suggest is that proteolysis is separating PrP prior to or shortly after conversion. A key experiment would be to try and inhibit the proteolysis and then assay for conversion again by immunoprecipitation.

It may be that the proteolysis is specific at a given sequence in which case the fusion could be re-engineered to remove it (Yao, Ren et al. 2003). It may be that a more general shredding (Parkin, Watt et al. 2004) is occurring and that specific inhibitors might act to prohibit those molecules responsible for this. It would remain to be seen whether these interventions would themselves prohibit proper trafficking of PrP and its conversion to PrP^{sc}.

One final consideration would be that the GFP protein in fusion is simply an obstacle to conversion wherever it is placed and irrespective of whether it is cleaved. It may interfere with the necessary seeding or folding needed for conversion of the Prion portion of the molecule. This hypothesis could be tested through the *in vitro* conversion assay on recombinant fusion protein.

In summary, GFP-PrP fusion proteins were expressed in cells and found to localise much as endogenous PrP. Although conversion of material from the fusion protein occurs, as assayed through an engineered specific 3F4 epitope, there is no PrP^{sc} in fusion with GFP, as assayed by Immunoprecipitation. The indication is that at some point, prior to or post conversion, the GFP and PrP c-terminal to it, are separated by proteolysis.

Chapter 5 Applications of fluorescent fusion proteins in the study of system dynamics

5.1. Introduction

The last chapter argued that the GFP-PrP fusion constructs might not be adequate in their present form to report on PrP^{Sc} localisation. It is important to emphasise that this does not obviate their use, even in present form. Although they might not be direct reporters of differences between infected and uninfected cells which are attributable to Prion, there may be other critical differences between these cell conditions which are reflected in PrP^C behaviour. For example it might be that trafficking of PrP^C differs between infected and uninfected contexts. It is also possible that a mode of transfer of infectivity between cells, for example a putative vesicular release, might transfer PrP^C along with PrP^{Sc} and therefore make the GFP-PrP fusion protein a useful reporter for such a process.

One further issue relating to the proteolysis of the fusion proteins that will be raised at this point in the thesis, is that questions can be asked about the object of visualisation in any observations of fluorescent signal. It would seem possible that signal could be attributed either to the intact fusion or to GFP that has been released from the fusion following proteolysis. One point in response to this difficulty is particularly relevant for those studies below which include visualisation or measurement of the fusion in the context of the membrane. The design of the fusion entails the fact that anchorage to the membrane is through the PrP portion of the fusion by GPI anchorage (see Chapter 4). Therefore, fluorescent signal which is membrane localised is likely to be attributable to intact GFP in fusion with PrP.

The molecular explanation for Prion conversion will need to be validated and elaborated upon in a cellular context. A number of central questions remain in that context for which only tentative answers have been posed. The first of these, considered in this thesis, is how a cell becomes infected. Two distinct questions which can be asked along this theme are how an infected cell propagates its infectivity to cause infection in a neighbouring uninfected cell and how sporadic or genetic Prion disease are initiated in a cell?

The question of inter-cellular infection is addressed in this chapter through the development of a time-lapse approach. The work described below attempts to employ time-lapse microscopy to investigate events that may be relevant to the process of inter-cellular infection. In particular, the central remit of the project given at the beginning of the Ph.d., was to create a system which might permit observation of these events over a time period of 48 hours, encompassing the period over which a cell becomes infected in co-culture (Kanu, Imokawa et al. 2002). Microscopy of this time frame, at this resolution, has not been undertaken before and therefore the technical aspects, as much as any result, are crucial to an understanding of whether it can be a useful technique for future use.

The second question, about initiation of conversion in a cell without intervention of an external Prion source, was discussed in a number of sections in the Introduction, and of particular note was the recent debate on the relevance of ERAD to the potential formation of protease resistant and self propagating species (Ma and Lindquist 2002; Drisaldi, Stewart et al. 2003). This chapter investigates the extension of general claims in this area to the SMB/PS cell system.

Finally, a question that remains is the role of membrane dynamics in Prion conversion. This work was undertaken relatively late in the project and represents a starting point for consideration of the questions it poses. It has been suggested that the membrane is a potential locus for conversion of Prion in a cell and that PrP may reside in distinct domains i.e. inside or outside of rafts, inside or outside of caveolae like domains and inside or outside of clathrin coated pits (see Introduction). If PrP is localised to a differential extent in an infected context to a domain which behaves like caveolae, perhaps this could be tested via investigation of populations with different diffusion coefficients. For example the protein caveolin-1 one has been found to be relatively immobile in studies of diffusion (Kenworthy, Nichols et al. 2004). Alternatively, distinct populations may also exist in an uninfected context and this might indicate something interesting about PrP dynamics that becomes highly relevant after infection.

There are also general reasons why an understanding of the diffusion of PrP species in the context of the plasma membrane could be crucial. Prion conversion is a dynamic process which is poorly understood, and changes in diffusion, even if fairly small, could potentially have a significant impact on this process. It may be possible to answer a number of basic questions about PrP dynamics through the technique of Fluorescence Recovery After Photobleaching (FRAP) which bleaches a selected area in a cell and observes recovery by diffusion of fluorescent protein back into the bleached area (Lippincott-Schwartz, Snapp et al. 2001). One of the most basic questions that can be addressed as a first step is to ask whether the diffusion of PrP is comparable with diffusion of other reported GPI anchored proteins (Kenworthy, Nichols et al. 2004). A second step is to ask whether differences can be observed in this diffusion of PrP between infected and uninfected contexts and an approach is formulated below to answer this question.

5.2. The time-lapse approach and Proteasomal inhibition

The role of proteasomal degradation in Prion disease remains contentious as discussed in the Introduction. It is an important issue to clarify because potentially it could explain the *de novo* cellular formation of Prion and provide a potential explanation for the link between Prion and cell toxicity. It would be interesting to extend these observations and the debate to the SMB/PS system and particularly to do so in light of the observations on fusion protein in the cell lines that have been created and described in Chapter 4.

This is the first demonstration of the use of time-lapse in this thesis and therefore some description of its role would be appropriate at this point. Time-lapse microscopy was an important remit of this project and it has proved to be difficult. The time-lapse system was developed over a 3-4 year period (rather than importing one from a company) and is therefore a bespoke system which addresses particular technical needs. This system was developed in parallel and shared with newt regeneration researchers who needed to assay

multiple position time-lapses, at lower resolution, over an extended period of 48 hours. Although it was possible to undertake the time-lapse for the latter purpose, there were a number of obstacles that have still not been surmounted at the higher resolution necessary for a GPI anchored membrane protein.

A number of issues in the use of the time-lapse system which have been addressed, entirely or in part, as they have arisen during the thesis include:

- 1) bleaching
- 2) cell survival
- 3) resolution / quality
- 4) focus drift

In order to ameliorate survival a heated chamber was produced which includes the possible use of CO₂ media. It took considerable time to enable this chamber to maintain temperature at the desired level, and this has now been achieved. Resolution and quality of image have been a major obstacle for viewing PrP fusion protein. One issue that plagued the time-lapse was that of condensation forming on the apparatus. This was removed by a bespoke designed heated lid. In general a 40x oil lens has been necessary to get an image that could potentially report on any movements of fusion protein, but many other lenses including a high resolution 20x lens, and 40 dry lens have been tried and tested. The main issue which has prohibited the remit from being completed has been focus drift. Focus drift is particularly bad for membrane localised proteins and has proven not to be such an issue for cytosolic proteins or bright field time-lapse, for two reasons: focus drift is much worse with an oil immersion lens, and has a more deleterious effect on image quality in the case of membrane observation than for general cell distribution, such as cytoplasmic expression. Many variations were attempted to ameliorate these problems and the complete list of elements employed is described in Materials and Methods. An example of typical focus drift and refocus was found with the experiment described below which assayed for proteasomal changes. Although not discussed in this chapter, a new time-lapse was purchased by the Department at the end of the period of completion of experimental work and, given the development in

microscopy over the period of 5 years, it offers a considerable improvement in resolution of image. However, it is still being adapted for the use of time-lapse of living cells, and the time-lapses obtained do not add anything at this point to the data discussed below.

The study of the proteasome serves as a good starting point to introduce actual investigation using time-lapse into this thesis.

To assay for efficacy of the proteasome inhibitor used - MG132 (Ma and Lindquist 2002), a control indicator cell line was created which made use of the proteasome sensor vector from Clontech (see Materials and Methods). This vector encodes for a destabilised green fluorescent protein (Zs green) which has a c-terminal fusion with a degradation motif for removal by the 26S proteasome. There is therefore no need for ubiquitination in order to target it to the proteasome. The ZSGREEN protein, when expressed in a normal cell, is degraded and not visible, under conditions of normal proteasomal activity. However, effective inhibition of the proteasome should lead to an abrogation of protein degradation and consequently green fluorescence should accumulate. Cells were transfected with zsgreen plasmid and bulk selected for 10 days. MG132 (to 50 μ M) was added to cells and time-lapse is taken over 15 hours. Cells have already been in inhibitor for 1 hour in the first frame (Fig5.1C). Although the majority of cells effectively degrade all the ZSGREEN, a small percentage of cells do not seem to degrade ZSGREEN entirely. This is useful for the purposes of time-lapse in order to set up the focus of an otherwise blank field. Therefore a field was chosen where two cells which did not degrade ZSGREEN could be visualised from the start of the time-lapse process. By 7.5 hours fluorescence is beginning to appear in other cells and therefore the proteasome inhibitor has probably taken effect by this time. After 15 hours a substantial increase in fluorescence is seen. It would therefore be tentatively concluded that proteasomal inhibition has been relatively effective prior to 7.5 hours post addition of MG132.

F4-GFP-PrPst cells (the control sample) were plated onto glass bottom dishes and time lapse analysis was performed over a 15 hour period, at 40x magnification with an oil lens. Fig. 5.1 A described 3 frames taken at 1 hour, 7.5

hours and 15 hours into the time-lapse. Areas of interest from these panels are repeated at full scale in Fig5.2 A. They were compared to a time-lapse of the same cells with 50 μ M of MG132, a proteasome inhibitor (Fig5.1B). Again, an area of interest is taken and compared to the controls in Fig5.2 B. It can be seen that after 15 hours, accumulation of fluorescent material has occurred in the cell to which MG132 has been added and that this process has started by 7.5 hours to some extent. This is more clearly seen in Fig5.2B after 15 hours when fluorescence appears to be largely confined to the peri-nuclear region. This finding parallels accumulation of PrP observed previously following proteasomal inhibition (Ma and Lindquist 2001).

It was therefore interesting to assess whether or not claims surrounding the nature of PrP species formed after inhibition could be substantiated in the PS system. In order to assess the effects of proteasomal inhibition on formation of PrP^{Sc} like species (see Materials and Methods), PS cells were treated with Proteasome inhibitor, 50 μ M MG132, for either 3 hours or 24 hours and processed for PrP^C and PrP^{Sc}. The biochemical analysis (Fig 5.3) indicates that there are no obvious changes to PrP^C as a result of inhibition (Fig 5.3 -PK : lanes PS 3h MG132 and PS 24 h MG132 compared to SMB and PS control lanes). Although Prion is seen to be present in the control sample (Fig 5.3 +PK :SMB lane) there are no Prion like species observed in PS cell samples treated with proteasomal inhibitor for either 3h (+PK : PS 3h MG132) or for 24 hours (+PK : PS 24h MG132).

The tentative conclusion is that species which are similar to the Prion observed in SMB cells as assayed by the normal procedures in this laboratory, are not produced by inhibition of the proteasome, even though some apparent differences in localisation may be observed following treatment.

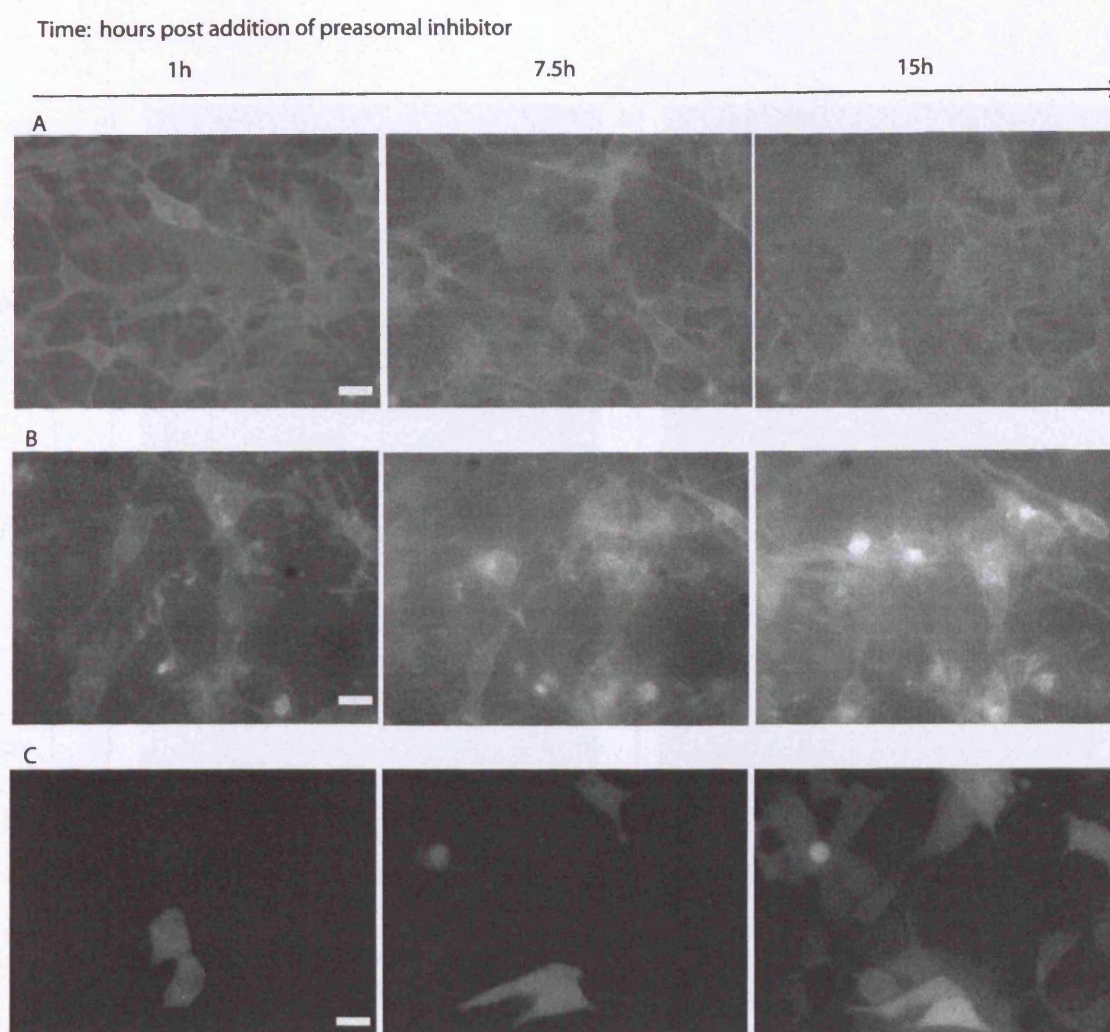


Figure 5.1. Effects of proteasomal inhibition on F4-GFP-PrPst cells

A) F4-GFP-PrPst cells were plated onto glass bottom dishes and time-lapse taken over a 15 hour period. Panel A represent 3 frames taken from this time-lapse at 1hour, 7.5hours and 15hours. The scale bar represents 30microns. **B)** Panel B is a time-lapse over the same period of F4-GFP-PrPst cells but MG132, to 50µM, was added at t=0 hours. **C)** Panel C represents cells expressing the ZSGreen proteasome sensor vector from clontech (see Materials and Methods). Proteasome inhibitor MG132 was added at t=0 hours to 50µM.

Time-lapse first frame is indicated at t= 1hour as a result of difficulty in maintenance of initial focus following addition of inhibitor in 5.1B. The proteasome inhibitor seems to be effective in inhibiting the proteasome and this has started by 7.5 hours (panel C, 7.5h). The effects of proteasomal inhibition on localization of the fusion protein seems to be an accumulation at a perinuclear location (panel B 15h). Also see corresponding movies 5.1 A, B and C for further illustration.

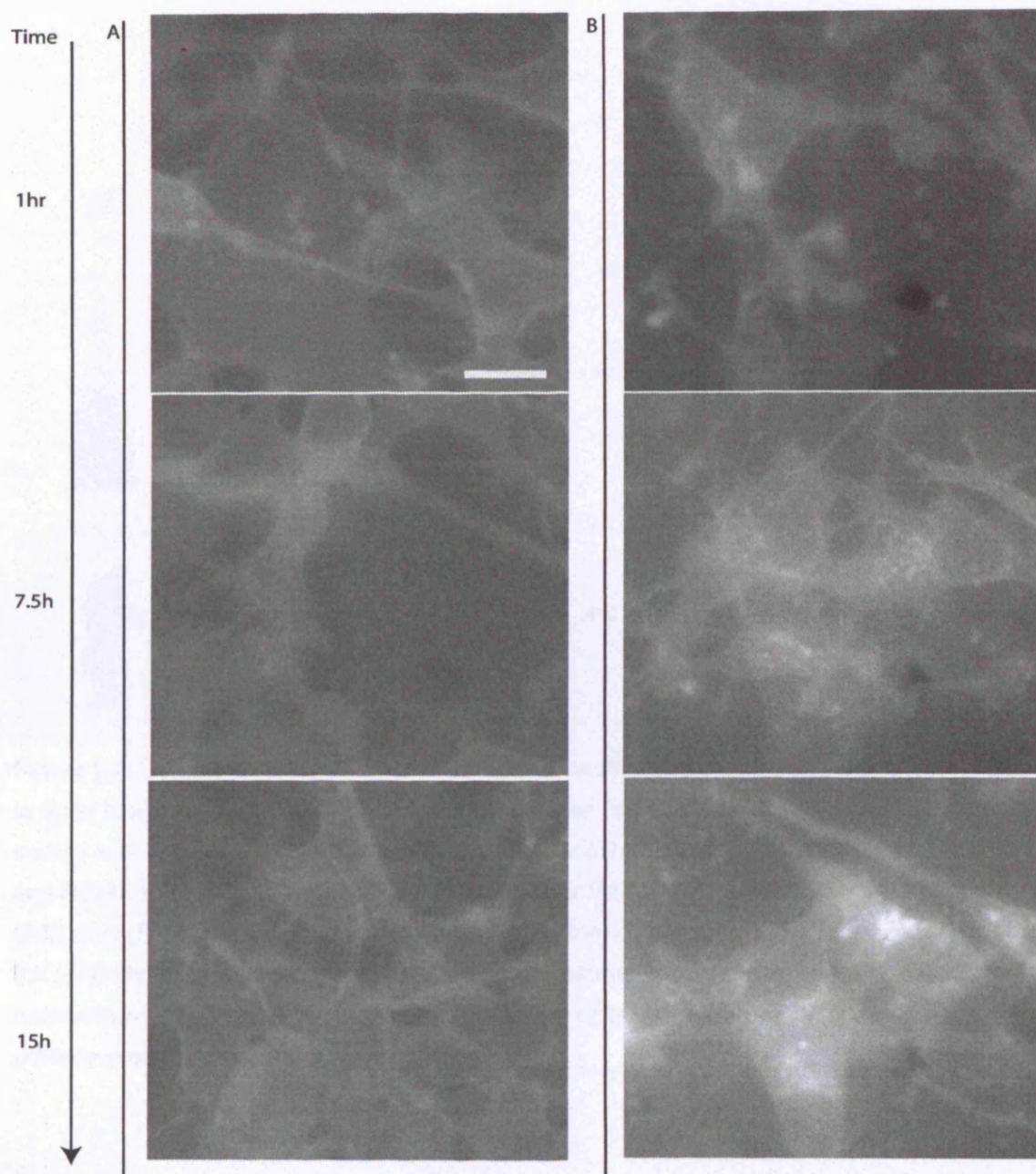


Figure 5.2. Effects of proteasomal inhibition on F4-GFP-PrPst cells in detail

The panels A and B represent enlarged areas of interest from panels A (control F4-GFP-PrPst cells) and B (cells treated with inhibitor) from figure 5.1. The scale bar again represents 30 microns. The key panel is seen at 15 hours after addition of inhibitor (5.2 B: 15hours). A marked accumulation of fluorescent protein is visible around the nucleus and to some extent spread throughout the cytoplasm (see movies 5.1A and 5.1B for further illustration).

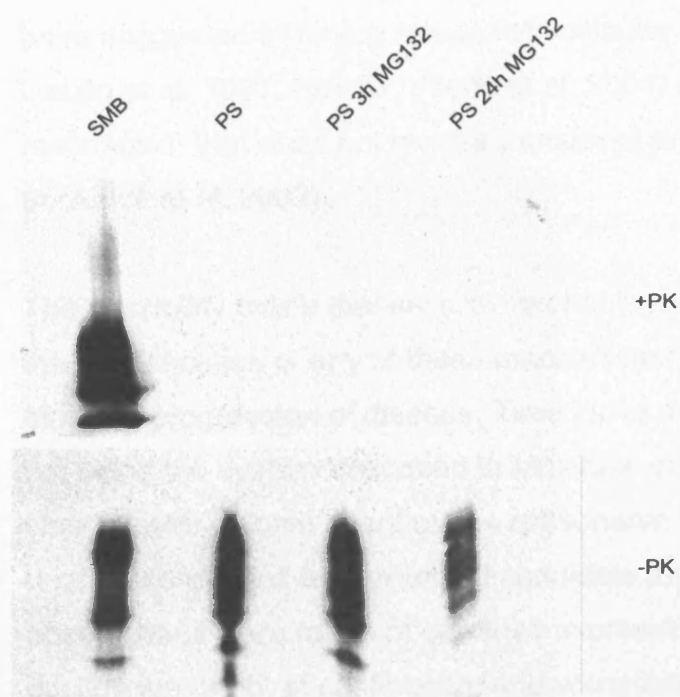


Figure 5.3. Effect of Proteasomal inhibition on PS cells

In order to assess the effects of proteasomal inhibition (see Materials and Methods), cells were treated with Proteasome inhibitor, 50 μ M MG132, for either 3hours or 24 hours (PS 3h MG 132 and PS24h MG132 lanes). Cells were processed for PrP^{sc} (+PK blot) and PrP^c (-PK blot) with SMB cells (SMB lane) and untreated PS cells (PS lane) as controls. Blots were undertaken with the antibody 6H4. There were no clear effects of treatment with inhibitor on PrP^c. Note that treatment with inhibitor for 3h (+PK :PS 3h MG 132) or 24hours (+PK: PS 24h MG 132) did not produce protease resistant species.

5.3. Investigations of Prion protein transfer between cells by time-lapse microscopy

One of the questions that underlined the remit of the project is how an infected cell manages to transfer infectivity to its neighbour. A number of hypotheses for this were discussed in the introduction to this thesis but there is no clear understanding of a mechanism for transfer and many different alternatives have been suggested including release of vesicular material from cells (Schatzl, Laszlo et al. 1997; Fevrier, Vilette et al. 2004) and a cell contact based mechanism that does not require transfer of any material per se (Kanu, Imokawa et al. 2002).

The possibility exists that several mechanisms operate to transfer infectivity and that identification of any of these mechanisms would offer potential routes for blocking progression of disease. Time lapse microscopy studies were carried out using the system described in Materials and Methods with a speculative view to seeing some event over a reasonable time period that could be pursued later in more detail as a potential candidate for transfer. In general the observations were made of cell lines expressing the fusion proteins at confluence or not at confluence, and sometimes alone or juxtaposed to alternatively coloured cells to try and increase the ability to visualise any transfer against the background fluorescence. A frame from an sample time lapse is shown in Fig 5.4 of the F4-GFP-PrP^{Sc} cell line in co-culture with a cell line which was created by transfecting PS cells with DsRedII, a fluorescent red coral protein (see Materials and Methods). This time-lapse was taken over a period of 5 hours and although no transfer of green fluorescent fusion protein is evident it can be seen that material has issued from the cytoplasmically marked cells. In some way, this offers a positive control for the ability at least to visualise material released from cells.

A further example of a time-lapse in the same configuration is provided in Fig 5.5, in which the infectivity status of the two cell types has been swapped. Here the green fluorescent cells are uninfected (F4-GFP-PrP cells) and the DsRed expressing cells are the infected PS counter part of the cell line described

above. Again it can be seen that material is released from the DsRed expressing cells, as illustrated in Fig 5.5A. The material can be seen to move away from the source cell and out of the frame of interest as illustrated in panel B of the same figure over a 6 hour period. Co-localisation with vesicles containing green fluorescent material is possible given the yellow colour of vesicles seen (a superposition of the red and green colours) although it cannot be ruled out that this co localisation is actually only the red colour of the released material set against a background of green. The general conclusion of these movies, and other movies considering the infected, uninfected pairing, and status of the cells as confluent or mobile, has illustrated the same lack of any obvious result i.e. no release of fusion protein is clearly evident. In general it has been my conclusion that the time lapses are of too poor a resolution to enable this kind of study. Attempts to time-lapse membrane proteins at 40x resolution using oil lenses, over periods of 24 hours or more have not been reported in the literature. It may be that the next generation of microscopes will enable such studies to continue apace given the background in technical expertise that the laboratory has acquired in this area.

One possibility that remained was to try and view co-localisation by contrasting different colours of fusion protein. To this end a red fluorescent fusion protein was formed by analogy with the previous design, placing DsRed in fusion with PrP. However, this fusion, in contrast to the GFP-PrP fusion, was poorly expressed, and produced an intracellular localisation pattern (figure 5.6). Although this may be interesting for further study in itself, it does not aid in the time-lapse process.

One clear result of the work undertaken, apart from the technical improvements to the time-lapse set up, was the conclusion that cytoplasmically localised fluorescent protein does seem to be released from cells. Although not in the original remit of the project, this was pursued by making cell line pairs of cytoplasmic green fluorescent infected and uninfected cells to complement the DsRed infected/uninfected pair (see Materials and Methods).

The first question that was addressed was whether the release was specific to the DsRed protein. Fig5.7A shows a frame 9 hours into a time-lapse taken over a period of 24 hours. Images were acquired every 15 minutes. It is easier to undertake time-lapse over this period with these cells because a non-oil, 20 x lens, could be used and a slight change in focus does not lead to a complete loss of image as with membrane protein observation. It can be seen, even in this one frame, that there is abundant material of red and green colour that has been released by these cells and therefore the phenomenon of release does not appear to be restricted to the Dsred protein. In general the release of this material did not depend on whether one or other of the cell lines are infected. It is not clear how this material is being released and time-lapses with shorter interval would be helpful in this respect and worthwhile future experiments. However, one area of interest is taken and depicted in fig5.7B. This is the same movie as in figure A but 13 hours in. In the first set of panels, a green fluorescent cell can be seen to contact and extend a process into a cell expressing Dsred (both cell lines are uninfected in this particular case) and then to retract after 30 minutes. The result is the release of what appears to be a red vesicle from the contacted cell and this is highlighted in an identical set of panels below for clarity. It is very difficult to spot events like these and it would be very helpful to run these movies in multiple positions at short time intervals between exposures.

This work on cytoplasmically marked cells was undertaken relatively close to the end of the experimental period of the PhD, and had the focus of observing transfer. However, this system does offer the possibility of observing more general cellular behaviour that could be relevant to infection. Cell tracking was attempted using the tracking facility in the programme Volocity (Improvisations) but at this resolution these cells are too frenetic and in contact too often to enable the software to separate them. Considerable effort was made to identify alternative software that could enable this analysis but the present algorithms employed by most commercially available applications are not suited to these data sets and are not capable of individuating the cells. It would have been interesting to ask questions about the speed and directionality of cells which are infected and uninfected. Such differences could affect the way in which infection

progresses in an organism for example. Attempts were made to make manual measurements of cell behaviour along these lines but proved too time-intensive (It would take weeks of manual analysis for relatively small sample numbers).

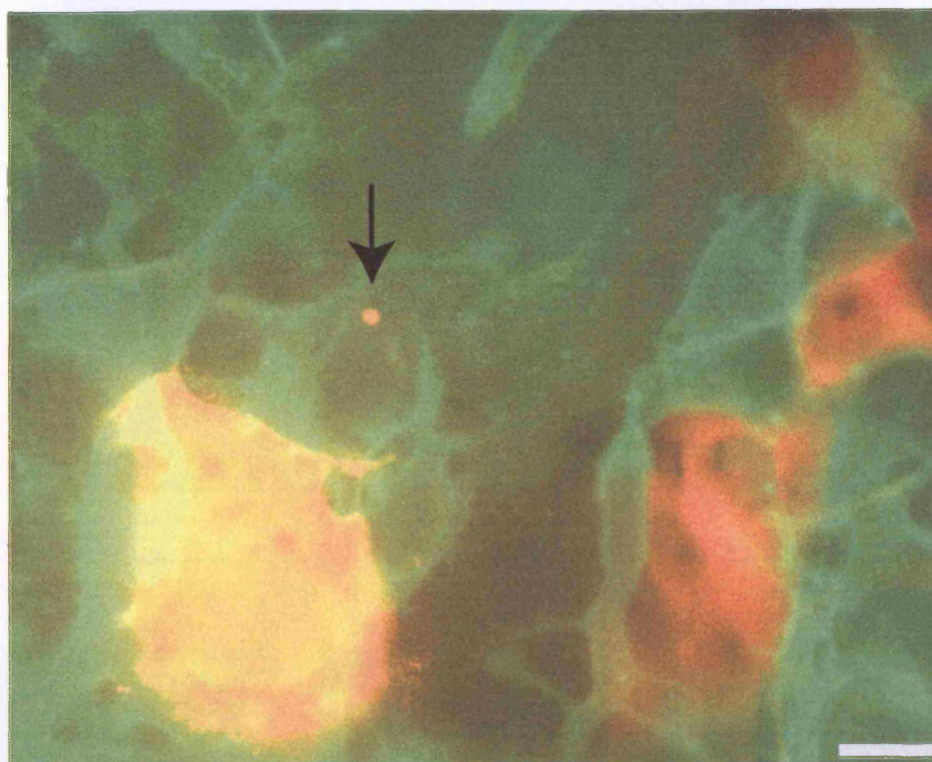


Figure 5.4. Release of cytoplasmic material from uninfected cells expressing DsRed

The panel above (Fig 5.4) is a frame taken from a time-lapse over 5 hours of Infected cells (F4-GFP-PrPstIn) expressing the fusion construct, in co-culture with PS cells expressing a cytoplasmic DsRed. The scale bar indicates 30 microns. The quality of these time-lapse images often makes it difficult to assess the exchange of membrane species, however, clear release of Dsred containing material can be seen as indicated by the arrow. Each time-lapse was repeated in this configuration within 4 permutations available, confluent fusion protein expressing cells (infected or uninfected) with cytoplasmic marker cells (infected or uninfected). Repeats of movies were also made of non-confluent cells expressing fusion protein (infected or uninfected) in juxtaposition to marker cells (uninfected only). Release of cytoplasmic material from the DsRed expressing cells was common in all cases but no clear transfer of fusion protein could be identified. (see movie 5.4 for further illustration).

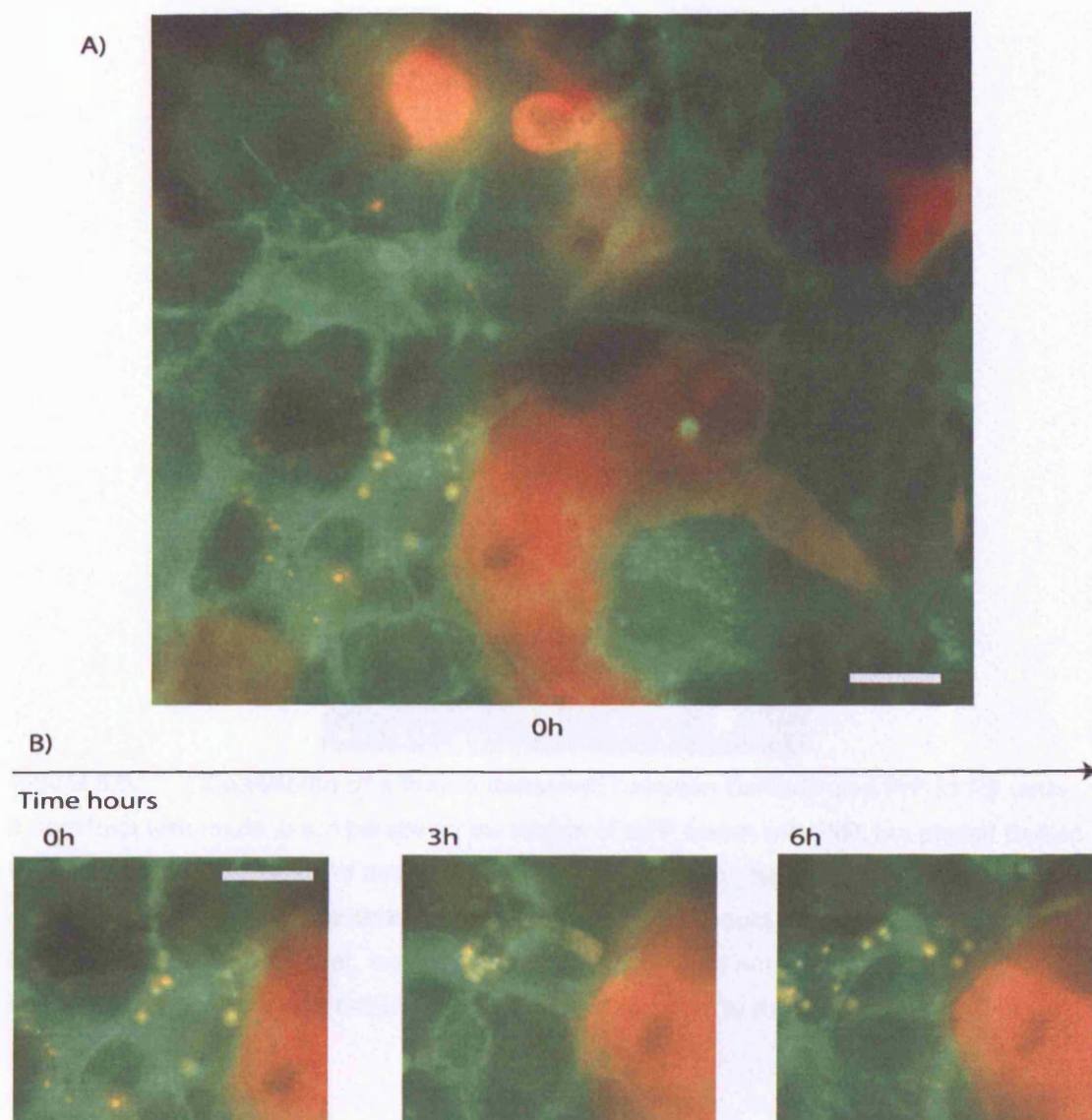


Figure 5.5. Release of cytoplasmic DsRed from Infected PS cells expressing DsRed

A) The panel above (Fig 5.5A) is the first frame of a time-lapse over 6 hours of uninfected cells (F4-GFP-PrPst cells) expressing the fusion protein F4-GFP-PrP, in co-culture with infected cells expressing a cytoplasmic DsRed protein. The scale bar indicates 30 microns. The frame from the time-lapse shown indicates that there is release of material from the DsRed expressing cells (Fig 5.5 A).

B) The main area of interest where exchange is occurring was followed over 6 hours (Fig 5.5 B). Note that material can be seen moving away from the Dsred expressing cell in the frame (see movie 5.5 for further illustration).

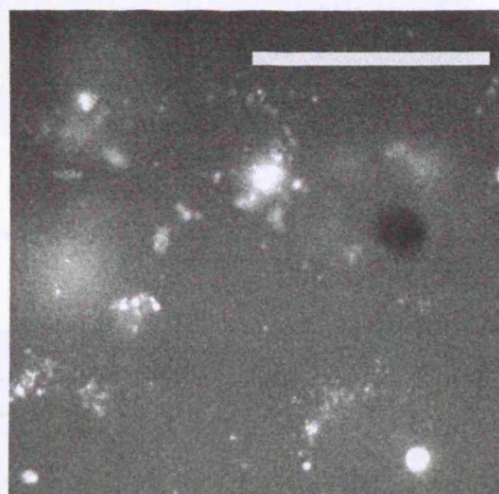


Figure 5.6. Expression of a fusion construct between DsRedII and PrP in PS cells

A construct was made which paralleled the design of GFP fusion with PrP, but placed DsRed in fusion with PrP. Expression of this construct was intended to highlight exchange of any fusion protein by visualising co localisation – it was hoped that this would enhance the poor quality of the time-lapse data. However, expression of this construct did not yield a normal localisation for PrP and generally either did not express well or was localised to the cytoplasmic spots or perinuclear regions of cells.

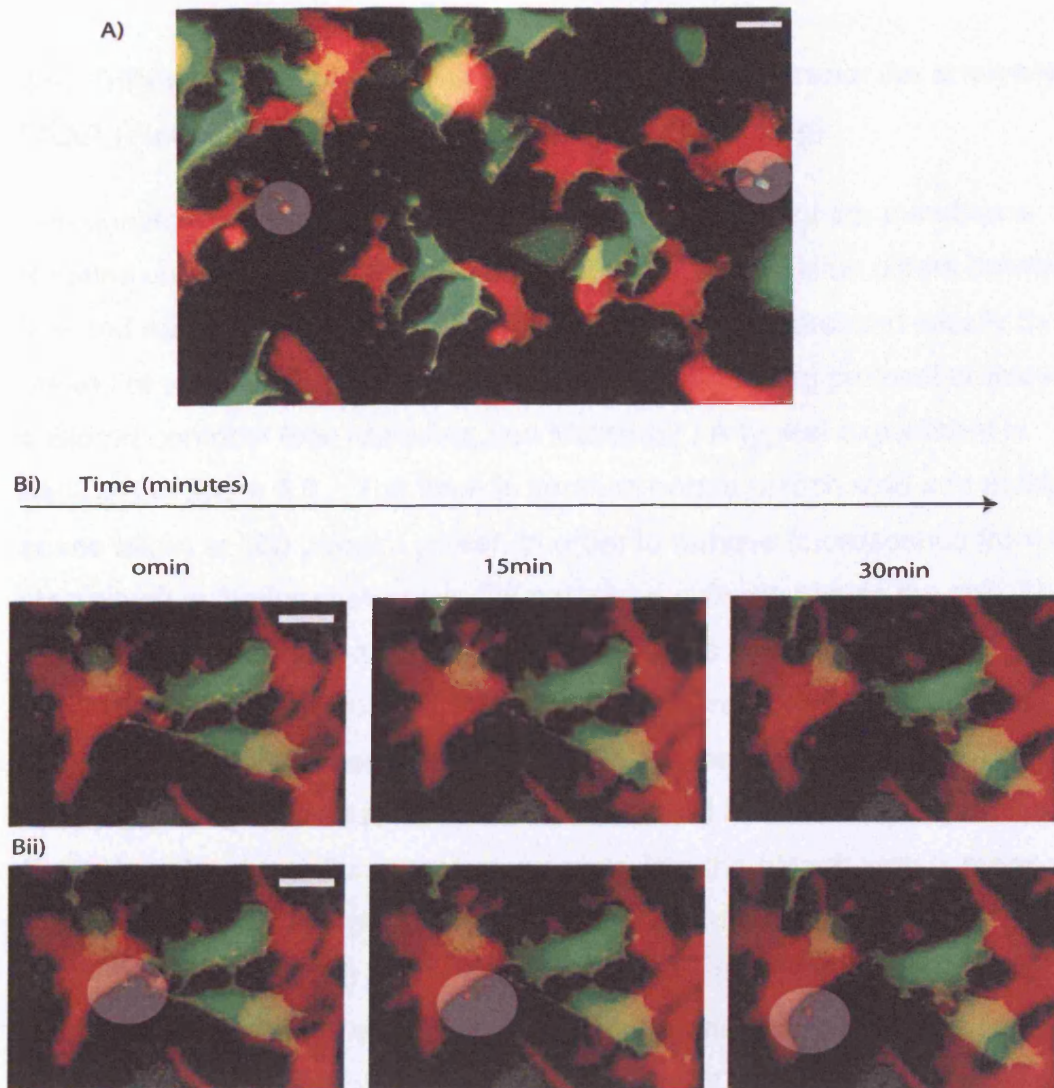


Figure 5.7. Time-lapse of cells expressing cytoplasmic fluorescent proteins.

In order to further investigate the exchange of cytoplasmic material between cells, stable transfectants were produced which expressed DsRed and GFP. From these, uninfected and infected counterparts were produced (see Materials and Methods). Figure 5.7. illustrates uninfected cells expressing DsRed or GFP. Each of the possible configurations explored was repeated (i.e. green uninfected vs red uninfected, green infected vs red uninfected, green uninfected vs red infected) except for the case of infected green vs infected red.

Panel A represents a frame 9 hours into a 24 hour time-lapse. It is clear from this panel that cytoplasmic material has been released by some means from both GFP and DsRed expressing cells. Two areas where material can be seen are highlighted (see movie 5.7 A for further illustration). **Panel B** represents an area of interest from the time-lapse, at three time points ($t=0$ represents a point 13 hours into the same time-lapse). A GFP expressing cell makes contact with, and appears to extend a process into, a DsRed expressing neighbour, subsequent to which a DsRed containing vesicle appears to be released from the cell. Bii) represent the same panels but highlight the area in question for ease of reference (see movie 5.7B for further illustration).

5.4. Diffusion of Prion protein in the plasma membrane: An analysis by FRAP (Fluorescence Recovery After Photobleaching)

The question of how Prion species diffuse in the plane of the membrane remains uninvestigated, and it is unknown whether diffusion differs between infected and uninfected contexts. The question was addressed initially by means of a Fluorescence recovery after photo bleaching protocol employed on a Biorad confocal (see Materials and Methods). A typical experiment is depicted in figure 5.8. The laser is zoomed onto a bleach strip and multiple scans taken at 100 percent power, in order to remove fluorescence from that strip which is 3 micrometers in diameter and extends across the cell. The laser intensity is then reduced to a minimum to capture images (at 4% power) and measurements taken from an area of interest encompassing the bleach strip. A further area of interest encompasses the whole cell and is used as a control for the purposes of normalisation (see Materials and Methods and figure 5.8 A). Following bleaching, fluorescence recovery into the bleach strip is measured over an extended time period, and can be seen to have largely returned after 160 seconds (figure 5.8 B). In order to calculate the diffusion coefficients an approach was taken of effectively solving, numerically, an equation for diffusion by curve fitting to the data (Ellenberg, Siggia et al. 1997) . The approximate diffusion equation is

$$I(t) = I(\infty)(1 - (w^2 / (w^2 + 4 \cdot \pi \cdot D \cdot t))^{1/2})$$

Where $I(t)$ describes intensity in the bleach strip at time t post bleach, $I(\infty)$ represents the asymptotic value of fluorescence intensity, w represents the width of the bleach strip and D represents the parameter of greatest interest for the purposes of this chapter that is the diffusion coefficient. A nonlinear regression fit of simulated curves to the data are made estimating the parameter D . A programme was written in Matlab to enable both the normalisation and the non linear regression of the data as described (see Materials and Methods and Appendix).

A typical graph of the results using the Biorad system is shown in figure 5.8C. The data itself represents intensity data for recovery into the bleach strip. This data has been normalised to the control AOI (accounting for any general bleaching or mild focus drift) and then further normalized for presentation purposes (see Materials and Methods). The circles represent this actual data and the line through it represents the best fit curve.

Typical values for a GPI anchored protein (Kenworthy, Nichols et al. 2004) have been described at around $0.5 \mu\text{m}^2/\text{s}$ but it is generally accepted that some variation occurs between setups, and therefore diffusion coefficients should be treated with caution when quoted as absolute values without reference to an experimental setup. The setup in this case (the biorad confocal) which was used initially was not suitable to FRAP. In particular there was no temperature controlled environment for living cells, and the temperature fluctuation led to focus drift that invalidated much of the experimental data. It was also found that the diffusion coefficient (for $n=12$) was $0.072 \mu\text{m}^2/\text{s}$ for the F4-PrP-GFP fusion construct expressed transiently in PS cells. This figure, even given the cautionary note on differences between systems seems too low and given the technical difficulty with the system another set up was sought.

Permission to use a Zeiss LSM 510, ideally suited to FRAP, with a temperature control unit was given close to the end of the project. Therefore the n values are small. However, a similar protocol was carried out to that described above (see Materials and Methods). The quality of the data appeared to be significantly better. Figure 5.9 illustrates a typical data set taken from one experiment. 0 seconds is the time post bleaching. The data has been normalised as described above, but further normalised by comparing to the prebleach intensity (see Materials and Methods). In effect these normalisations correct for change in overall intensity of fluorescence in the cell (change which does occur because some bleaching takes place from normal confocal scanning at low intensities). From this a typical calculation of the immobile fraction can be made. Recovery is often not complete (i.e. not to the level of the prebleach value), and this is because a percentage of the molecules bleached are immobile. Therefore when diffusion occurs to equilibrium there is an overall decrease in intensity to the extent of this fraction. 4 FRAP experiments were carried out on uninfected cells

expressing the fusion construct ,F4-GFP-PrPst cells, (see figure 5.10 A) and 5 infected cells, F4-GfP-PrPstInf cells, (see figure 5.10B). The data were analysed as described above and the diffusion coefficients for each are displayed in the corresponding table below (table 5.1). The mean value (n=4) for the diffusion coefficient of the fusion protein in the uninfected cells was $0.31 \mu\text{m}^2/\text{s}$ and was $0.39 \mu\text{m}^2/\text{s}$ in the infected cell context (n=5). The mean mobile fraction was 90.6% for uninfected cells and 89.9 % for the infected cell samples. These figures are in line with previously reported figures for diffusion in the context of the plasma membrane for GPI anchored proteins(Kenworthy, Nichols et al. 2004). It is unclear whether there is a significant difference between diffusion in the infected and uninfected contexts. A sample closer to n=20, would permit a simple t test to determine this. It would be unclear why diffusion was faster, as this data would indicate, in the case of the infected cells but it could be important and clarification of this result would be worthwhile. Given the small sample it is also somewhat speculative to infer anything from the high standard deviation of the infected cell diffusion coefficients (see table 5.1 infected cell (I) experiments). However, there are quite large differences (50% roughly) between diffusion coefficients for different experiments on infected cultures and perhaps this reflects the possibility of two populations of cells, with two corresponding diffusion coefficients. Either way, this experiment has validated the technical aspects of the FRAP necessary to test the simple hypothesis that there are significant differences between diffusion coefficients in infected and uninfected contexts. More experiments would clearly be required and use of the fusion proteins and cell lines established in Chapter 4 would be appropriate for this experimental approach.

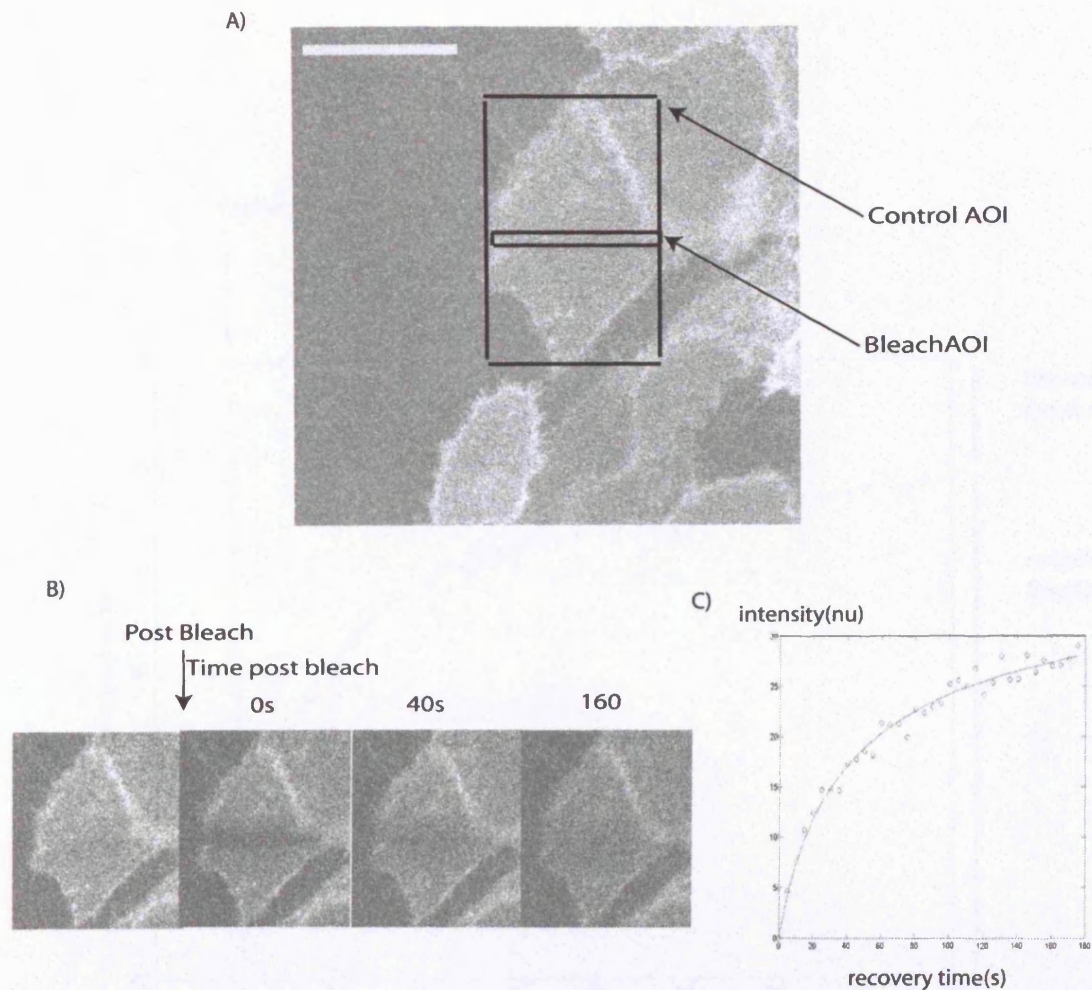


Figure 5.8. Illustrative diagramme of technique for fluorescence recovery after photo bleaching

A typical experiment is illustrated from a FRAP. A) illustrates the control area of interest and the bleach box (3microns). Bleaching is obtained by zoom of the laser and repeat scanning of the bleach box, subsequently measurements are taken after bleach from both boxes to enable later normalisation of bleach box data (see Materials and Methods). B illustrates a time course for the example experiment. Note that by 160 seconds most of the recovery towards an asymptote has taken place. The first frame is a prebleach frame. Following this 15 bleach zooms were undertaken to create the bleach strip on the biorad confocal at full laser intensity. Note that there is some general bleaching caused by low level scanning during the experiment but normalisation using the control box should account for this in the calculation of the diffusion coefficient. C) Illustration of bleach strip data which has been normalised. The shape of the curve is critical in determining the diffusion co-efficient. The co-efficient is calculated by non-linear regression fit to the approximate equation for diffusion (In this case it is $0.038\mu\text{m}^2/\text{s}$).

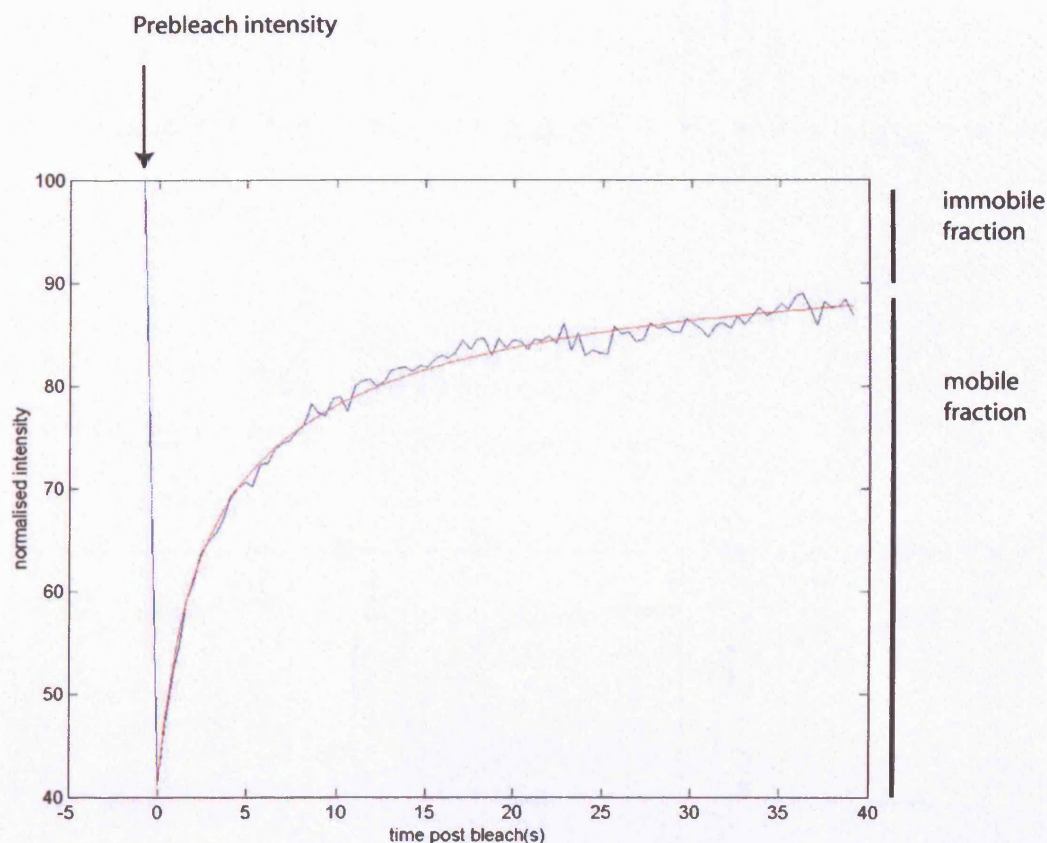


Figure 5.9. Experimental result from FRAP using a Zeiss LSM 510

The set up used for the first set of FRAP experiments did not produce expected results, and particularly was not adapted to live cell work. Therefore, a set up was found with environmental control which was specifically used for qualitative FRAP but could be used for the simulations carried out here. The figure above illustrates the data collected from one experiment. The blue line represents actual data taken and the red line the predicted curve from parameters calculated to the data. The data point at -5 s represent the prebleach value intensity value. All values displayed are expressed as a percentage of this value (and have also been corrected using the control region). The mobile fraction is indicated on this graph, assuming the end point represent a point on the asymptote.

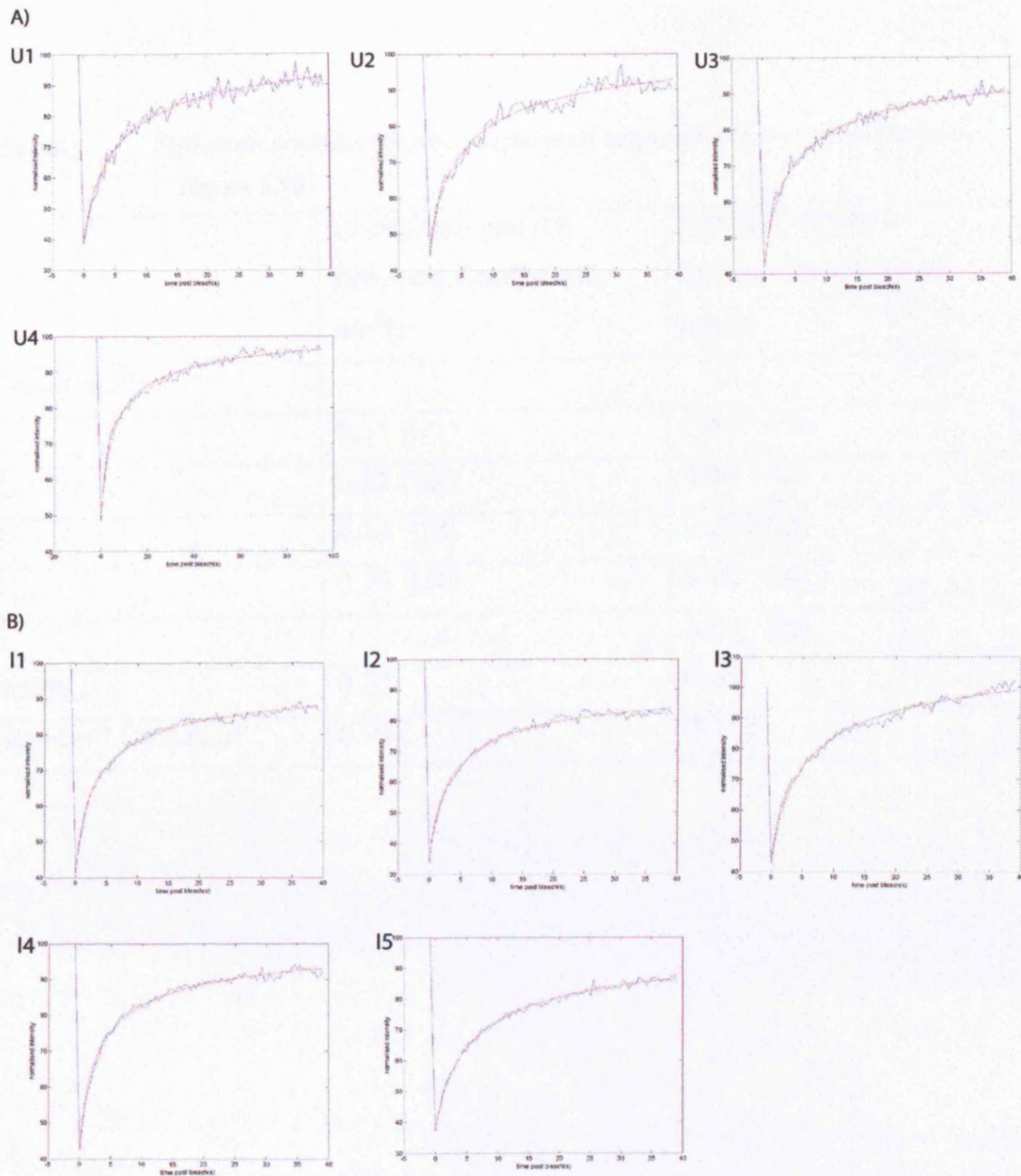


Figure 5.10. Results of FRAP experiments on uninfected (panels in A) and infected F4-GFP-PrP cells (panels in B).

The blue line represents actual data points and the red line the exponential predicted from parameters calculated from the data. The mean diffusion coefficients for uninfected cell are $0.310 \mu\text{m}^2/\text{s}$ (std 0.022) and for infected cells is $0.391 \mu\text{m}^2/\text{s}$ (std 0.113). Note that the sample sizes are too small to test significance for the difference in these samples. It is of particular note that the variance within the infected sample appears to be greater – this may be indicative of two populations of cells but will require greater N numbers to test for significance.

Table5.1. Diffusion coefficients associated with experimental results depicted in Figure 5.10

	Uninfected cell (U) Diffusion Coefficients $\mu\text{m}^2/\text{s}$	Infected Cell (I) Diffusion Coefficients $\mu\text{m}^2/\text{s}$
Experiments		
1	0.31 (U1)	0.48 (I1)
2	0.32 (U2)	0.45 (I2)
3	0.33 (U3)	0.279 (I3)
4	0.28 (U4)	0.50 (I4)
5		0.26 (I5)
Mean	0.31	0.39
Standard Deviation	0.022	0.113

5.5. Discussion

The main focus of this chapter has been on issues that might relate to the dynamics of PrP. These have fallen broadly into two groups, firstly those relating to transfer of material between cells, and secondly, those relating to diffusion of PrP within the membrane. The approach which has underlined the study of intercellular transfer has been based on the development of a time-lapse system in parallel to regeneration researchers who are also pursuing a time-lapse approach, although at lower resolution. The approach has proven difficult and in particular the problem of focus drift has been difficult to address. There a number of questions that need to be asked in the field which will require a temporal richness/continuity of information that cannot be easily provided without reference to a dynamic picture. Particularly it is worth noting that time-lapse is not supposed to be a surrogate for cytochemical staining under different conditions. Its final aim is quite straightforwardly to individuate distinct objects through time and to follow those objects moment to moment in their behaviour. It will then be possible to capture information that would otherwise be missing – for example the brief contact event over 45 minutes depicted in Figure 5.7 B, that leads to release of a vesicle. One question that could be asked was what the rationale was for attempting such long time periods – why not make short movies of trafficking events? The answer is that the question of Prion transfer, or transfer of infectivity, seems to occur over an extended period between cells in culture, and indeed also when material is added to cells (Kanu, Imokawa et al. 2002). One interpretation of this fact is that the events necessary for effective transfer are occurring sporadically, and therefore a long time period will be necessary to visualise them. This is an assumption which has not been validated and therefore it would be worth repeating experiments for shorter time periods, although probably if this is the case it would be better done on a confocal microscope which would permit a much higher resolution of image in general.

The first experiment of this chapter looked at the effects of proteasomal inhibition in the PS/SMB system. The inhibitor chosen was taken because it was one of the inhibitors used by two laboratories which have made differing claims

about results following proteasomal inhibition. One laboratory (Ma and Lindquist 2002) has claimed that ERAD occurs normally in cells and that proteasomal inhibition leads to improper ERAD and a resultant cytoplasmic accumulation of PrP following retro translocation from the ER, and subsequently the formation of a protease resistant, self propagating, species. The other laboratory (Drisaldi, Stewart et al. 2003) claims essentially that ERAD is not occurring in this case, that the species observed were never transported across the ER, and that the results regarding the self-perpetuating nature of the species are artefactual for other reasons. It would be interesting to investigate the nature of the accumulated species. The particular experiment which this author had in mind was to produce the claimed protease resistant species by proteasomal inhibition and to follow on with the question of whether these species produced were infectious by using the freeze-thaw cell lysate preparation method described above to produce inoculums of proteasomal inhibitor treated cells. However, the biochemical results (Figure 5.3) demonstrated that as assayed by our normal procedure for Prion detection, there was no protease resistant material to be found, either after 3 hours or 24 hours of treatment. This is surprising in some ways since the microscopy (Figure: 5.1 and 5.2) indicated that an accumulation of PrP was expected after 15 hours to a significant level, given that this behaviour was seen in the fusion protein. This accumulation was also seen in the previous studies using inhibitors (Ma and Lindquist 2001). It was seen that the inhibitor was efficacious in inhibiting proteasome function prior to 7.5 hours after addition and given that it would take time for accumulation of fluorescence to be visualized at this point, inhibition had probably been effective considerably earlier. Although it was not possible to time-lapse over a further extended period, it would be interesting to try and keep cells alive beyond the 24 hour treatment point, because it may be that this is not enough time for the accumulating species to start a conversion process. Aggregation seemed to occur around a perinuclear region and it seems possible that this is the Golgi apparatus and not the cytoplasm. This accumulation may also reflect a build up of material through blocking of normal trafficking as a stress response of the cell. Nevertheless, in this system no protease resistant material was found and therefore given the unlikely relevance to Prion infection it was not pursued further.

The question of transfer of infectivity was difficult to answer for the reasons described. No clear evidence was seen of any transfer of fusion protein between cells, in any movies. Even at low confluency where the green background did not make it hard to pick out any potential exchange release of fusion protein material was not in evidence. However, some evidence was seen of release and possible transfer of cytoplasmic material. The studies undertaken here showed that this phenomenon is not particular to DsRed expressing cells, and that it appear to be a process that occurs independently of whether cells are infected or uninfected. These observations are somewhat speculative because it is possible that the putatively released material is part of a cellular structure, like a filopodium. It is unclear how general these observations are with respect to other cell lines, and also what their relevance might be to Prion infection.

It would have been useful to compare two membrane fusions of different colour in juxtaposition, in order to assess any direct exchange between neighbouring cells. This work would best be done by reference to a Cyan and Yellow fluorescent protein system which is a more standard set used for two colour microscopy. It would also be better pursued with reference to a confocal set up which would enable higher resolution study of any co-localisation. There are no clear results from the work done here, but technical advances have been made. The result of being able to time-lapse over a roughly 24 hour period at a resolution required to visualise membrane localised protein has taken considerable effort and may be useful for future investigations in the future when the knowledge can be applied to development of the new higher resolution time-lapse system.

The issue of the dynamics of PrP^c in the membrane, as assayed by reference to quantitative investigation of diffusion, has not been addressed in previous studies in the literature. Factors relevant to the process of infection of a cell, or even maintenance of infection, may only differ in their quantitative aspects when comparing infected and uninfected cells, and it is conceivable that a quantitative approach to define the relevant differences could be helpful. The work

described here outlines the beginning of a project which could address how PrP diffuses in the plane of the plasma membrane. The initial results suggest that the protein is diffusing in much the same way as other GPI anchored proteins but as mentioned above, it would be important to include further comparators within the experimental system in future. The key hypothesis here to test was whether there was a difference in diffusion coefficients between infected and uninfected contexts. It was found, with a very small sample number, that there is a difference, and that diffusion is faster in the case of the infected context. It is unclear whether or not this difference is significant from a statistical point of view and these experiments might be repeated in future with greater n numbers. It is also of note that in the infected sample there seemed roughly half the cells with a 1x diffusion coefficient and the other with a 2x coefficient. This may be a feature of this specific set of data which is removed with higher n numbers but it may indicate that there are different populations of cells within an infected sample, and that the key variable defining the populations might be that some cells are infected and some are not. One issue is how this would be relevant to Prion conversion if the difference was to prove significant between infected and uninfected contexts. Let us suppose that there was a significant difference, or the hypothesis that there are two populations in the infected sample was proved significant with greater n numbers. There would then be a second question as to what is responsible for the difference. Is it a difference in general plasma membrane fluidity or a difference in compartmentalisation (e.g. to particular membrane domains) of the PrP fusion protein? This could be addressed by observing bleaching of dyes which specifically bind to the lipids in the plasma membrane, and comparing infected and uninfected cells in this regard. A related question to be addressed, and perhaps the question which underlies all of these studies, would be whether or not this difference was an epiphenomenon, not particularly relevant to infection but issuing from it, or whether it was causative or necessary in some aspect of infection. To make this less abstract I would suggest an entirely speculative hypothesis that encompasses these latter two questions: that infection is preceded by a change in plasma membrane fluidity which is necessary for effective infection. The question would then be to address how to model this effect and create perturbation in experimental systems to test the models.

Chapter 6 Summary, discussion, and future directions

This discussion summarises the key results of the thesis and motivates future experiments, either straightforward follow ups or broader research directions.

Chapter 3 raised a key question about the use of antibody to identify Prion in an immunocytochemical context. There is no antibody currently available in the field which can act as a marker for Prion in this context and this was one part of the motivation for the work undertaken with fluorescent fusion proteins. It is discussed further below.

PrP^{Sc} was not found on the surface of SMB cells following surface biotinylation protocols. Surface PrP^{Sc} has been identified on the surface of cells in other studies (Shyng, Moulder et al. 1995; Vey, Pilkuhn et al. 1996). However, there was very little quantitative data available from these studies to indicate how much Prion, as a proportion of total cellular Prion, was found on the surface. There is also an issue of differences between this study and the mode of assay for Prion used in other studies. In particular the process for detection of PrP^{Sc} used in this thesis is different in some respects than that employed in the other studies. In particular, protease digestion is 10 fold higher than in one study (Shyng, Moulder et al. 1995) and detergent insolubility is also included as a criterion for PrP^{Sc}. This experiment could be repeated with another infected cell line as a control and with less stringent requirements for PrP^{Sc} analysis.

A central theme of Chapter 3 was the investigation of glycosylation in the context of infection. A key question that motivated this work, a question which remains unanswered in the Prion field, is what the mechanism is for maintenance of the same glycoform profile in Prion of a newly infected host as in Prion of the infectious source. The key result of the chapter is that a completely unglycosylated template of PrP^{Sc} is able to act as a template for conversion of cellular PrP^C to new PrP^{Sc}. Fig 3.12 depicted a non-matching hypothesis and a matching hypothesis. The matching hypothesis argued that the PrP^{Sc} template would have to be of the same glycoform condition as the PrP^C it was converting. The explanation for why there is little or no

diglycosylated PrP^{Sc} found in the SMB system would be, on the strict matching hypothesis, that there is no diglycosylated PrP^{Sc} available in the inoculum to convert the diglycosylated PrP^{C} of the cells. This hypothesis was disproven because it was shown that unglycosylated PrP^{Sc} can act as a converting template for at least in the case of monoglycosylated PrP^{C} , converting it to monoglycosylated PrP^{Sc} .

A further hypothesis, perhaps unlikely, but which has never been tested, is whether only unglycosylated PrP^{Sc} has converting activity. It has never been proven that glycosylated PrP^{Sc} species have any converting activity. Further experiments that might be attempted in SMB cells could involve separation of glycosylated PrP^{Sc} species from unglycosylated species. It is not clear that this is possible (they may be structurally interconnected for example) but a potential procedure could be to make use of Lectins to separate glycosylated protein.

At steady state two main factors contribute to the quantity of Prion in the cell. Firstly, the rate of synthesis (rate of production per unit time) of Prion and secondly, the rate of degradation (rate of destruction per unit time) of Prion. There may be other contributions to the amount of Prion in a cell (e.g. transfer from another cell) and in reality cell division complicates the issue, but consider these two processes for simplicity. The balance of synthesis and degradation will contribute ultimately to the quantity of Prion in a cell. This balance is also applicable to consideration of the relative abundance not just of the total amount of Prion but also of the particular glycoform species of Prion and it may be that different net effects of synthesis and degradation obtain for each glycoform species of PrP^{Sc} . This basic framework would argue that a consideration of the relative rates of synthesis and degradation could explain the particular glycoform profile of a particular cell. For example, if there is a relatively fast degradation of diglycosylated PrP^{Sc} , perhaps because it is less stable as a species, it may be that there is no 'net' production of diglycosylated PrP^{Sc} .

One prediction of this model would be that there are different rates of synthesis or degradation for each species and to test these hypotheses pulse chase protocols could be employed. If there were a means of completely blocking

degradation of protein in cells (not just the proteasome) for a period this would also be a useful test but I am not aware of an experimental intervention that would permit this.

One final consideration is that de-glycosylation occurs in cells. There is no evidence for this in the context of the Prion field but this has not been independently tested.

In summary, the results in Chapter 3 indicated that carbohydrate additions to PrP do not carry the information required to transfer and maintain a glycoform profile, because using an infectious source as an inoculum which lacks these residues still leads to the maintenance of the original, full glycoform profile following infection. It has been argued that synthesis and degradation of Prion may need to be considered more carefully to understand the heart of the glycoform maintenance problem. However, synthesis and degradation may not be steady state, for example when cells divide, and synthesis may be coupled to degradation by a cellular mechanism. Therefore this research direction may prove to be highly complex even if essential to a thorough understanding of the phenomenon of the maintenance of glycoform profile.

There were two distinct ways in which a fusion protein between GFP and PrP, described in Chapter 4, could be a useful indicator of localisation. It could be used as a direct indicator of PrP^{Sc} localisation i.e. if the PrP portion of the fusion is converted, or it could be used as an indirect indicator of infected contexts, if PrP^C trafficking differs between infected and uninfected contexts. The fusion protein, although appropriately trafficked along the secretory pathway and tethered by a GPI anchor to the plasma membrane, did not show any differences in localisation when expressed in infected or uninfected contexts. A key question with respect to the process of direct reporting on PrP^{Sc} localisation, was whether or not the PrP fusion protein was converted to PrP^{Sc} and remained in fusion with GFP. A 3F4 epitope was engineered into the fusion protein and it was used to biochemically identify PrP^{Sc} issuing from the fusion protein against the endogenous background. Initial biochemical studies indicated that successful conversion was occurring.

However, the observation that fusion protein also underwent substantial proteolysis raised the question of whether the conversion, assayed biochemically, represented an event happening after separation of the PrP from the GFP protein. Studies were undertaken which demonstrated that neither the specific linker between the PrP and GFP in the fusion described here, nor the introduction of the mutant epitope, were responsible for this proteolysis. The hypothesis that protease action following lysis was responsible for the observed cleavage was also tested but not supported.

Despite proteolysis, biochemistry and microscopy indicated that there was still an abundance of intact fusion protein. It therefore remained a possibility that intact fusion protein, which has not undergone the proteolysis, could include GFP in fusion with PrP^{Sc}. This was tested ultimately by immunoprecipitation experiments that isolated intact fusion protein, and these experiments demonstrated that in this fusion protein PrP^{Sc} is not found in fusion with GFP. The most likely explanation for the series of observation is that a cleavage event is separating the PrP portion of the fusion prior to or just following conversion to PrP^{Sc}.

The first follow up experiment which might be attempted would be to carefully assess whether a C-terminal insertion of GFP in a 3F4 epitope mutated mouse PrP, undergoes the same proteolysis and whether the 3F4 portion undergoes conversion. Two suggestions that were made in chapter 4 were that the proteolysis was either directed and specific, or general. In the former case, a motif at which proteolysis occurs might be identified by creating a series of deletion constructs. Alternatively, if general protease action is responsible in the cell, then an array of inhibitors could be tested to attempt to find whether a specific class of proteases (e.g. zinc metalloproteinases) is responsible for the action. One possibility that remains, which was not discussed, is that PrP itself has some protease action. However, there is no suggestion of this in the literature, and there is no bioinformatics to support such a claim.

If the problems with conversion and cleavage cannot be overcome there still remains a use for the fusion proteins described in this thesis. Before

considering the use to which they were put in the final results chapter, I would like to return to the issue of localisation. Two localisation effects were described above, direct and indirect. It might be that although conversion to Prion does not occur in the context of the fusion protein, indirect reporting on differences in PrP^c trafficking could be interesting and informative. However, differences were not seen between expression in infected or uninfected contexts. There are two possible reasons for this which could be explored. Firstly, there may be differences, but these are not seen in the equilibrium condition where trafficking of PrP has settled to a steady state. Secondly, there may just be too much background to see this happening given the resolution of the present system. The first question could be addressed by reference to an inducible PrP-GFP fusion construct. This has been attempted in the laboratory and has proven technically very difficult but an approach with this intention may reveal differences in trafficking that cannot be observed ordinarily under conditions of equilibrium.

The final results Chapter considered uses for the fusion protein. Firstly, the debate over the effects of proteasomal inhibition were considered in the context of the PS system. Aggregation of F4-PrP-GFP was found over 15 hours, and initiated prior to 7.5 hours, post addition of proteasomal inhibitor. However, biochemical assay revealed no formation of protease resistant, PrP^{sc} like species. This was observed for 24 hours of treatment, a period much longer than that of the original study which reported formation of Prion like species, using MG132, after 3 hours (Ma and Lindquist 2002). Again, following the discussion of the biotinylation result, there are noted differences in the assay procedure for Prion. In particular the study above did not employ the criterion of detergent insolubility and only employed the criterion of partial protease resistance. Both of the studies undertaken attempted to address the question of whether ERAD could be observed by this manipulation of the proteasome. It would be interesting to test this hypothesis by making use of an antibody to the signal peptide for PrP in the context of the experiments described in the PS cell system.

Time-lapse microscopy was undertaken to assess whether there was any visible exchange of fusion protein between cells in culture, and specifically whether there were any differences in this respect between infected and uninfected cells. No exchange of fusion protein was found in either infected or uninfected cell lines expressing the fusion constructs although cytoplasmic exchange was indicated. This exchange did not depend on the infectious status of cells as assayed by time-lapse of cytoplasmically marked infected and uninfected cell line pairs. It may be that vesicular or other release mechanisms are not a feature of the PS/SMB system. This has been indicated by studies taking conditioned media from SMB cells and using them to attempt to infect PS cells (Kanu, Imokawa et al. 2002). Alternatively it may be that a higher resolution approach is required in order to clearly assess whether this exchange is occurring. It was described how time-lapse of a fusion protein over long periods is pushing the boundaries of what is technically feasible. However, if money were no object a multiphoton confocal set up, using lower bleach intensities, could be used with sophisticated software to provide a very high resolution, and overcome some of the focus issues. The costs of such a dedicated system would be prohibitive however. Alternatively, shorter time-lapse at high resolution might indicate transfer events which are frequent and short lived, although events occurring more sporadically would be missed.

One further experiment that has not been undertaken in this thesis, would be to observe the effects of juxtaposing cells which express different coloured membrane fusion proteins. It is possible that exchange is occurring via cell contact directly between membranes, and not by vesicular release. This would be more clearly observed with a PrP-CFP, PrP-YFP fusion pair if it were occurring. This would be a priority as an experiment to complete the time-lapse analysis.

Further use of the fusion constructs was made by FRAP analysis in a series of experiments which sought to set up a system to assess the diffusion of PrP species in the plasma membrane. At present the diffusion of PrP has not been assessed in the literature. Experiments carried out on a second confocal (Zeiss LSM 510) demonstrated a robust system for this analysis and curves were fitted

to the data collected in order to obtain the relevant parameter describing the diffusion coefficient. The samples are very small and perhaps not too much should be read into the results at this stage. However, it was found that in an infected context the diffusion coefficient was higher than that of PrP in an uninfected context. It is unclear whether this result is significant and the first experiments that should be undertaken is to increase the n numbers to test this hypothesis conclusively. It was also found that the variance was high in the infected sample. This may again reflect the small n number, or alternatively it may reflect the existence of distinct populations of cells within an infected sample. At present, it is not known how many infected cells there are in an SMB culture. Until there is an antibody available to test for Prion immunocytochemically, it would be very difficult to assess the hypothesis that the two populations of cells, defined by different diffusion coefficients, correspond to an infected and an uninfected population of cells.

Extensions to research in the area of diffusion could involve attempts to identify distinct population of PrP in the same cell by diffusional criteria. For example, if a substantial population of PrP were in contact with transmembrane protein, two populations might be distinguishable with two distinct diffusion coefficients. Simulations could be carried out to test the limits in sensitivity of the modelling process employed here to assess what that proportion of bound populations would need to be, under a set of reasonable assumptions about the diffusion of such putative complexes.

If it does turn out that there is a significant difference between the infected and uninfected samples, it would be interesting to know why. Is it a direct effect of infection? Is it an effect which is particular to PrP between infected and uninfected contexts? These questions could be addressed with reference to other fusion constructs (e.g. the GFP-GPI construct employed in chapter 4). One final point that has not been considered is the contribution of dynamics, movement and collision, to conversion. The picture that is often conjured up is a process of slow seeding or templated conversion – often mirrored by long phases seen during *in vitro* analysis of Prion formation. However, little is known about conversion in the context of membranes. The critical initial events may

occur while the proteins are in motion and the chances of Prion meeting and converting PrP^c might be determined by dynamics in the plane of the membrane. This kind of dynamic effect has never been studied. It is only relatively recently that the tools to consider some of these questions with any robustness or accuracy have become available. Further research would also permit manipulation of cell membrane fluidity and assessment of the effects this has on diffusion (i.e. whether it is causative of changes). Although speculative, it may be that general cell fluidity is responsible for differences in diffusion and that a cell falling within boundary conditions for this fluidity is necessary for some aspects of conversion.

This thesis has been a study in a specific cell culture system of a specific set of issues. One crucial question, stepping back from the work undertaken in this system, would be whether primary cultures of neurons might be a better model for Prion infection. There are no recorded instances of successful infection of primary neurons in culture. Also of note, as described in the introduction, is the fact that only a limited number of cell lines demonstrate a propensity for infection, and an even smaller number, of which SMB is one, maintain stable infection. For these reasons, primary cultures would be very difficult models to work with. However, infected neurons from transgenic mice expressing fusion constructs might be co-cultured with uninfected neurons, or co-cultures of other cell infected cells and primary neurons could be considered.

The lack of a Prion specific antibody, a reagent which can identify Prion clearly in an immunocytochemical context, represents a barrier to faster progress in the field of Prion cell biology. It is not clear why it has been so difficult to produce such a reagent and it may be prove to be in principle very difficult, although the lack of structural information on PrP^{sc} makes it hard to assess this suggestion. One point that has not been emphasised, is that even if this reagent was discovered, the questions of Prion dynamics would still be pertinent for all the reasons described. The specific reagent would not address these dynamic issues although it would be an invaluable tool in addition to these studies because the variable under consideration here, of greatest interest, has been

that of infectivity. It is a variable that at present cannot be independently determined on a cell by cell basis.

An attempt to identify mechanisms for transfer of infectivity was undertaken in this thesis i.e. how an infected cell is able to infect an uninfected cell.

These have been addressed in cell culture in the work described, but there are a number of issues which remain that have not been addressed in animal models and might be relevant to directed clinical interventions. Although it has been demonstrated that PrP expression in peripheral nerves is sufficient for transfer of Prion infection in mouse models (Race, Oldstone et al. 2000) the question of whether other cell types are also sufficient has also not been clearly addressed. These issues could be modelled by reference to infection of PrP knockout in populations of cells with specific promoters. One potential candidate for such a study would be the Schwann cell population. If the fusion proteins can be designed in future which can act as surrogate markers for PrP^{sc} (i.e. they can be used to create intact fusions between GFP and PrP^{sc} and these fusions display differences in localisation) then transgenic mice expressing these proteins would be of great value in study of Prion disease progression.

In summary, some of the issues investigated in this thesis have included, the question of how Prion glycoform profile is maintained, the creation and potential conversion of PrP in the context of fusion with GFP, and the potential use of such fusion proteins for observation of PrP behaviour. The investigation of these issues has required a technically demanding approach through time-lapse microscopy and has pushed the boundaries of technical know-how forward. It is hoped that this work will make some contribution to the future state of knowledge in Prion cell biology and potentially clinical outcomes, through defining and attempting to answer the questions posed and through advancing the required technical approaches which will be needed to address these questions.

7. References

- Aguzzi, A. (1997). "Neuro-immune connection in spread of prions in the body?" Lancet **349**(9054): 742-3.
- Aguzzi, A. (2003). "Prions and the immune system: a journey through gut, spleen, and nerves." Adv Immunol **81**: 123-71.
- Aguzzi, A., T. Blattler, et al. (1997). "Tracking prions: the neurografting approach." Cell Mol Life Sci **53**(6): 485-95.
- Aguzzi, A. and M. Glatzel (2004). "vCJD tissue distribution and transmission by transfusion--a worst-case scenario coming true?" Lancet **363**(9407): 411-2.
- Aguzzi, A., F. Montrasio, et al. (2001). "Prions: health scare and biological challenge." Nat Rev Mol Cell Biol **2**(2): 118-26.
- Aguzzi, A. and C. J. Sigurdson (2004). "Antiprion immunotherapy: to suppress or to stimulate?" Nat Rev Immunol **4**(9): 725-36.
- Allen, K. D., R. D. Wegrzyn, et al. (2004). "Hsp70 chaperones as modulators of prion life cycle: novel effects of Ssa and Ssb on the *Saccharomyces cerevisiae* prion [PSI+]." Genetics.
- Alper, T., W. A. Cramp, et al. (1967). "Does the agent of scrapie replicate without nucleic acid?" Nature **214**(90): 764-6.
- Alper, T., D. A. Haig, et al. (1966). "The exceptionally small size of the scrapie agent." Biochem Biophys Res Commun **22**(3): 278-84.
- Alper, T., D. A. Haig, et al. (1966). "The exceptionally small size of the scrapie agent." Biochem Biophys Res Commun **22**(3): 278-84.
- Alpers, M. P. (1987). Epidemiology and clinical aspects of kuru. Prions-novel infectious pathogens causing scrapie and Creutzfeldt-Jakob disease. S. B. Prusiner and M. P. McKinley. Orlando, Academic Press: 451-465.
- Anderson, R. G. (1998). "The caveolae membrane system." Annu Rev Biochem **67**: 199-225.
- Anderson, R. M., C. A. Donnelly, et al. (1996). "Transmission dynamics and epidemiology of BSE in British cattle." Nature **382**(6594): 779-88.
- Aridor, M. and W. E. Balch (1999). "Integration of endoplasmic reticulum signaling in health and disease." Nat Med **5**(7): 745-51.
- Arnold, J. E., C. Tipler, et al. (1995). "The abnormal isoform of the prion protein accumulates in late-endosome-like organelles in scrapie-infected mouse brain." J Pathol **176**(4): 403-11.
- Aucouturier, P., F. Geissmann, et al. (2001). "Infected splenic dendritic cells are sufficient for prion transmission to the CNS in mouse scrapie." J Clin Invest **108**(5): 703-8.
- Barmada, S., P. Piccardo, et al. (2004). "GFP-tagged prion protein is correctly localized and functionally active in the brains of transgenic mice." Neurobiol Dis **16**(3): 527-37.
- Baron, G. S. and B. Caughey (2003). "Effect of glycosylphosphatidylinositol anchor-dependent and -independent prion protein association with model raft membranes on conversion to the protease-resistant isoform." J Biol Chem **278**(17): 14883-92.
- Baron, G. S., K. Wehrly, et al. (2002). "Conversion of raft associated prion protein to the protease-resistant state requires insertion of PrP-res (PrP(Sc)) into contiguous membranes." Embo J **21**(5): 1031-40.
- Baskakov, I. V., G. Legname, et al. (2002). "Pathway complexity of prion protein assembly into amyloid." J Biol Chem **277**(24): 21140-8.

- Basler, K., B. Oesch, et al. (1986). "Scrapie and cellular PrP isoforms are encoded by the same chromosomal gene." Cell **46**(3): 417-28.
- Baylis, M. and W. Goldmann (2004). "The genetics of scrapie in sheep and goats." Curr Mol Med **4**(4): 385-96.
- Behrens, A., N. Genoud, et al. (2002). "Absence of the prion protein homologue Doppel causes male sterility." Embo J **21**(14): 3652-8.
- Bellinger-Kawahara, C. G., E. Kempner, et al. (1988). "Scrapie prion liposomes and rods exhibit target sizes of 55,000 Da." Virology **164**(2): 537-41.
- Bendheim, P. E., H. R. Brown, et al. (1992). "Nearly ubiquitous tissue distribution of the scrapie agent precursor protein." Neurology **42**(1): 149-56.
- Bessen, R. A., D. A. Kocisko, et al. (1995). "Non-genetic propagation of strain-specific properties of scrapie prion protein." Nature **375**(6533): 698-700.
- Bessen, R. A. and R. F. Marsh (1992). "Biochemical and physical properties of the prion protein from two strains of the transmissible mink encephalopathy agent." J Virol **66**(4): 2096-101.
- Bessen, R. A. and R. F. Marsh (1992). "Identification of two biologically distinct strains of transmissible mink encephalopathy in hamsters." J Gen Virol **73**(Pt 2): 329-34.
- Bessen, R. A. and R. F. Marsh (1994). "Distinct PrP properties suggest the molecular basis of strain variation in transmissible mink encephalopathy." J Virol **68**(12): 7859-68.
- Bessen, R. A., G. J. Raymond, et al. (1997). "In situ formation of protease-resistant prion protein in transmissible spongiform encephalopathy-infected brain slices." J Biol Chem **272**(24): 15227-31.
- Betmouni, S., V. H. Perry, et al. (1996). "Evidence for an early inflammatory response in the central nervous system of mice with scrapie." Neuroscience **74**(1): 1-5.
- Birkett, C. R., R. M. Hennion, et al. (2001). "Scrapie strains maintain biological phenotypes on propagation in a cell line in culture." Embo J **20**(13): 3351-8.
- Bockman, J. M., S. B. Prusiner, et al. (1987). "Immunoblotting of Creutzfeldt-Jakob disease prion proteins: host species-specific epitopes." Ann Neurol **21**(6): 589-95.
- Bolton, D. C., M. P. McKinley, et al. (1982). "Identification of a protein that purifies with the scrapie prion." Science **218**(4579): 1309-11.
- Bolton, D. C., M. P. McKinley, et al. (1984). "Molecular characteristics of the major scrapie prion protein." Biochemistry **23**(25): 5898-906.
- Bolton, D. C., R. D. Rudelli, et al. (1991). "Copurification of Sp33-37 and scrapie agent from hamster brain prior to detectable histopathology and clinical disease." J Gen Virol **72**(Pt 12): 2905-13.
- Borchelt, D. R., M. Scott, et al. (1990). "Scrapie and cellular prion proteins differ in their kinetics of synthesis and topology in cultured cells." J Cell Biol **110**(3): 743-52.
- Borchelt, D. R., A. Taraboulos, et al. (1992). "Evidence for synthesis of scrapie prion proteins in the endocytic pathway." J Biol Chem **267**(23): 16188-99.
- Bosque, P. J. and S. B. Prusiner (2000). "Cultured cell sublines highly susceptible to prion infection." J Virol **74**(9): 4377-86.
- Bounhar, Y., Y. Zhang, et al. (2001). "Prion protein protects human neurons against Bax-mediated apoptosis." J Biol Chem **276**(42): 39145-9.

- Brandner, S., S. Isenmann, et al. (1996). "Normal host prion protein necessary for scrapie-induced neurotoxicity." *Nature* **379**(6563): 339-43.
- Brimacombe, D. B., A. D. Bennett, et al. (1999). "Characterization and polyanion-binding properties of purified recombinant prion protein." *Biochem J* **342 Pt 3**: 605-13.
- Brown, D. R. and A. Besinger (1998). "Prion protein expression and superoxide dismutase activity." *Biochem J* **334 (Pt 2)**: 423-9.
- Brown, D. R., J. Herms, et al. (1994). "Mouse cortical cells lacking cellular PrP survive in culture with a neurotoxic PrP fragment." *Neuroreport* **5**(16): 2057-60.
- Brown, D. R., K. Qin, et al. (1997). "The cellular prion protein binds copper in vivo." *Nature* **390**(6661): 684-7.
- Brown, D. R., W. J. Schulz-Schaeffer, et al. (1997). "Prion protein-deficient cells show altered response to oxidative stress due to decreased SOD-1 activity." *Exp Neurol* **146**(1): 104-12.
- Brown, D. R., B. S. Wong, et al. (1999). "Normal prion protein has an activity like that of superoxide dismutase." *Biochem J* **344 Pt 1**: 1-5.
- Brown, D. R., B. S. Wong, et al. (1999). "Normal prion protein has an activity like that of superoxide dismutase." *Biochem J* **344 Pt 1**: 1-5.
- Brown, P., F. Cathala, et al. (1987). "The epidemiology of Creutzfeldt-Jakob disease: conclusion of a 15-year investigation in France and review of the world literature." *Neurology* **37**(6): 895-904.
- Brown, P., M. A. Preece, et al. (1992). "'Friendly fire' in medicine: hormones, homografts, and Creutzfeldt-Jakob disease." *Lancet* **340**(8810): 24-7.
- Bruce, M., A. Chree, et al. (1994). "Transmission of bovine spongiform encephalopathy and scrapie to mice: strain variation and the species barrier." *Philos Trans R Soc Lond B Biol Sci* **343**(1306): 405-11.
- Bruce, M. E. (1985). "Agent replication dynamics in a long incubation period model of mouse scrapie." *J Gen Virol* **66**(Pt 12): 2517-22.
- Bruce, M. E., I. McConnell, et al. (1991). "The disease characteristics of different strains of scrapie in Sinc congenic mouse lines: implications for the nature of the agent and host control of pathogenesis." *J Gen Virol* **72**(Pt 3): 595-603.
- Bruce, M. E., R. G. Will, et al. (1997). "Transmissions to mice indicate that 'new variant' CJD is caused by the BSE agent." *Nature* **389**(6650): 498-501.
- Bueler, H., M. Fischer, et al. (1992). "Normal development and behaviour of mice lacking the neuronal cell-surface PrP protein." *Nature* **356**(6370): 577-82.
- Butler, D. A., M. R. Scott, et al. (1988). "Scrapie-infected murine neuroblastoma cells produce protease-resistant prion proteins." *J Virol* **62**(5): 1558-64.
- Capellari, S., S. I. Zaidi, et al. (1999). "Prion protein glycosylation is sensitive to redox change." *J Biol Chem* **274**(49): 34846-50.
- Carleton, A., P. Tremblay, et al. (2001). "Dose-dependent, prion protein (PrP)-mediated facilitation of excitatory synaptic transmission in the mouse hippocampus." *Pflügers Arch* **442**(2): 223-9.
- Casaccia, P., A. Ladogana, et al. (1989). "Levels of infectivity in the blood throughout the incubation period of hamsters peripherally injected with scrapie." *Arch Virol* **108**(1-2): 145-9.
- Castilla, J., P. Saa, et al. (2005). "In vitro generation of infectious scrapie prions." *Cell* **121**(2): 195-206.

- Caughey, B., K. Brown, et al. (1994). "Binding of the protease-sensitive form of PrP (prion protein) to sulfated glycosaminoglycan and congo red [corrected]." J Virol **68**(4): 2135-41.
- Caughey, B., D. A. Kocisko, et al. (1995). "Aggregates of scrapie-associated prion protein induce the cell-free conversion of protease-sensitive prion protein to the protease-resistant state." Chem Biol **2**(12): 807-17.
- Caughey, B., R. E. Race, et al. (1989). "Prion protein biosynthesis in scrapie-infected and uninfected neuroblastoma cells." J Virol **63**(1): 175-81.
- Caughey, B. and G. J. Raymond (1991). "The scrapie-associated form of PrP is made from a cell surface precursor that is both protease- and phospholipase-sensitive." J Biol Chem **266**(27): 18217-23.
- Caughey, B. and G. J. Raymond (1991). "The scrapie-associated form of PrP is made from a cell surface precursor that is both protease- and phospholipase-sensitive." J Biol Chem **266**(27): 18217-23.
- Caughey, B. and G. J. Raymond (1993). "Sulfated polyanion inhibition of scrapie-associated PrP accumulation in cultured cells." J Virol **67**(2): 643-50.
- Caughey, B., G. J. Raymond, et al. (1997). "Scrapie infectivity correlates with converting activity, protease resistance, and aggregation of scrapie-associated prion protein in guanidine denaturation studies." J Virol **71**(5): 4107-10.
- Caughey, B. W., A. Dong, et al. (1991). "Secondary structure analysis of the scrapie-associated protein PrP 27-30 in water by infrared spectroscopy." Biochemistry **30**(31): 7672-80.
- Caughey, W. S., L. D. Raymond, et al. (1998). "Inhibition of protease-resistant prion protein formation by porphyrins and phthalocyanines." Proc Natl Acad Sci U S A **95**(21): 12117-22.
- Chernoff, Y. O., S. L. Lindquist, et al. (1995). "Role of the chaperone protein Hsp104 in propagation of the yeast prion-like factor [psi⁺]." Science **268**(5212): 880-4.
- Chernoff, Y. O., S. M. Uptain, et al. (2002). "Analysis of prion factors in yeast." Methods Enzymol **351**: 499-538.
- Chesebro, B., R. Race, et al. (1985). "Identification of scrapie prion protein-specific mRNA in scrapie-infected and uninfected brain." Nature **315**(6017): 331-3.
- Chiarini, L. B., A. R. Freitas, et al. (2002). "Cellular prion protein transduces neuroprotective signals." Embo J **21**(13): 3317-26.
- Chiesa, R., A. Pestronk, et al. (2001). "Primary myopathy and accumulation of PrP^{Sc}-like molecules in peripheral tissues of transgenic mice expressing a prion protein insertional mutation." Neurobiol Dis **8**(2): 279-88.
- Chiesa, R., P. Piccardo, et al. (1998). "Neurological illness in transgenic mice expressing a prion protein with an insertional mutation." Neuron **21**(6): 1339-51.
- Clarke, M. C. and D. A. Haig (1970). "Evidence for the multiplication of scrapie agent in cell culture." Nature **225**(227): 100-1.
- Clarke, M. C. and D. A. Haig (1971). "Multiplication of scrapie agent in mouse spleen." Res Vet Sci **12**(2): 195-7.
- Cohen, A. S. (1994). "Clinical aspects of amyloidosis, including related proteins and central nervous system amyloid." Curr Opin Rheumatol **6**(1): 68-77.

- Collinge, J. (2001). "Prion diseases of humans and animals: their causes and molecular basis." *Annu Rev Neurosci* **24**: 519-50.
- Collinge, J., K. C. Sidle, et al. (1996). "Molecular analysis of prion strain variation and the aetiology of 'new variant' CJD." *Nature* **383**(6602): 685-90.
- Collinge, J., M. A. Whittington, et al. (1994). "Prion protein is necessary for normal synaptic function." *Nature* **370**(6487): 295-7.
- Collinge, J., M. A. Whittington, et al. (1994). "Prion protein is necessary for normal synaptic function." *Nature* **370**(6487): 295-7.
- Cousens, S. N., E. Vynnycky, et al. (1997). "Predicting the CJD epidemic in humans." *Nature* **385**(6613): 197-8.
- Crowe, P. D., T. L. VanArsdale, et al. (1994). "A lymphotoxin-beta-specific receptor." *Science* **264**(5159): 707-10.
- Czekay, R. P., T. A. Kuemmel, et al. (2001). "Direct binding of occupied urokinase receptor (uPAR) to LDL receptor-related protein is required for endocytosis of uPAR and regulation of cell surface urokinase activity." *Mol Biol Cell* **12**(5): 1467-79.
- d'Aignaux, J. N., S. N. Cousens, et al. (2001). "Predictability of the UK variant Creutzfeldt-Jakob disease epidemic." *Science* **294**(5547): 1729-31.
- Daude, N., S. Lehmann, et al. (1997). "Identification of intermediate steps in the conversion of a mutant prion protein to a scrapie-like form in cultured cells." *J Biol Chem* **272**(17): 11604-12.
- DeArmond, S. J. (2004). "Discovering the mechanisms of neurodegeneration in prion diseases." *Neurochem Res* **29**(11): 1979-98.
- DeArmond, S. J., H. Sanchez, et al. (1997). "Selective neuronal targeting in prion disease." *Neuron* **19**(6): 1337-48.
- DeBurman, S. K., G. J. Raymond, et al. (1997). "Chaperone-supervised conversion of prion protein to its protease-resistant form." *Proc Natl Acad Sci U S A* **94**(25): 13938-43.
- Deleault, N. R., R. W. Lucassen, et al. (2003). "RNA molecules stimulate prion protein conversion." *Nature* **425**(6959): 717-20.
- Diringer, H. (1984). "Sustained viremia in experimental hamster scrapie. Brief report." *Arch Virol* **82**(1-2): 105-9.
- Donne, D. G., J. H. Viles, et al. (1997). "Structure of the recombinant full-length hamster prion protein PrP(29-231): the N terminus is highly flexible." *Proc Natl Acad Sci U S A* **94**(25): 13452-7.
- Drisaldi, B., R. S. Stewart, et al. (2003). "Mutant PrP is delayed in its exit from the endoplasmic reticulum, but neither wild-type nor mutant PrP undergoes retrotranslocation prior to proteasomal degradation." *J Biol Chem* **278**(24): 21732-43.
- Duffy, P., J. Wolf, et al. (1974). "Letter: Possible person-to-person transmission of Creutzfeldt-Jakob disease." *N Engl J Med* **290**(12): 692-3.
- Edenhofer, F., R. Rieger, et al. (1996). "Prion protein PrP^C interacts with molecular chaperones of the Hsp60 family." *J Virol* **70**(7): 4724-8.
- Ellenberg, J., E. D. Siggia, et al. (1997). "Nuclear membrane dynamics and reassembly in living cells: targeting of an inner nuclear membrane protein in interphase and mitosis." *J Cell Biol* **138**(6): 1193-206.
- Ellgaard, L., M. Molinari, et al. (1999). "Setting the standards: quality control in the secretory pathway." *Science* **286**(5446): 1882-8.

- Elsen, J. M., Y. Amigues, et al. (1999). "Genetic susceptibility and transmission factors in scrapie: detailed analysis of an epidemic in a closed flock of Romanov." *Arch Virol* **144**(3): 431-45.
- Enari, M., E. Flechsig, et al. (2001). "Scrapie prion protein accumulation by scrapie-infected neuroblastoma cells abrogated by exposure to a prion protein antibody." *Proc Natl Acad Sci U S A* **98**(16): 9295-9.
- Endo, T., D. Groth, et al. (1989). "Diversity of oligosaccharide structures linked to asparagines of the scrapie prion protein." *Biochemistry* **28**(21): 8380-8.
- Endres, R., M. B. Alimzhanov, et al. (1999). "Mature follicular dendritic cell networks depend on expression of lymphotoxin beta receptor by radioresistant stromal cells and of lymphotoxin beta and tumor necrosis factor by B cells." *J Exp Med* **189**(1): 159-68.
- Felten, D. L. and S. Y. Felten (1988). "Sympathetic noradrenergic innervation of immune organs." *Brain Behav Immun* **2**(4): 293-300.
- Felten, S. Y., D. L. Felten, et al. (1988). "Noradrenergic sympathetic innervation of lymphoid organs." *Prog Allergy* **43**: 14-36.
- Fevrier, B., D. Vilette, et al. (2004). "Cells release prions in association with exosomes." *Proc Natl Acad Sci U S A* **101**(26): 9683-8.
- Follet, J., C. Lemaire-Vieille, et al. (2002). "PrP expression and replication by Schwann cells: implications in prion spreading." *J Virol* **76**(5): 2434-9.
- Ford, M. J., L. J. Burton, et al. (2002). "A marked disparity between the expression of prion protein and its message by neurones of the CNS." *Neuroscience* **111**(3): 533-51.
- Forloni, G., N. Angeretti, et al. (1993). "Neurotoxicity of a prion protein fragment." *Nature* **362**(6420): 543-6.
- Fraser, H. (1982). "Neuronal spread of scrapie agent and targeting of lesions within the retino-tectal pathway." *Nature* **295**(5845): 149-50.
- Gabizon, R., Z. Meiner, et al. (1993). "Heparin-like molecules bind differentially to prion-proteins and change their intracellular metabolic fate." *J Cell Physiol* **157**(2): 319-25.
- Gabriel, J. M., B. Oesch, et al. (1992). "Molecular cloning of a candidate chicken prion protein." *Proc Natl Acad Sci U S A* **89**(19): 9097-101.
- Gajdusek, D. C., C. J. Gibbs, et al. (1966). "Experimental transmission of a Kuru-like syndrome to chimpanzees." *Nature* **209**(25): 794-6.
- Gambetti, P., Q. Kong, et al. (2003). "Sporadic and familial CJD: classification and characterisation." *Br Med Bull* **66**: 213-39.
- Gauczynski, S., J. M. Peyrin, et al. (2001). "The 37-kDa/67-kDa laminin receptor acts as the cell-surface receptor for the cellular prion protein." *Embo J* **20**(21): 5863-75.
- Ghani, A. C. (2002). "The epidemiology of variant Creutzfeldt-Jakob disease in Europe." *Microbes Infect* **4**(3): 385-93.
- Ghani, A. C., N. M. Ferguson, et al. (2000). "Predicted vCJD mortality in Great Britain." *Nature* **406**(6796): 583-4.
- Ghani, A. C., N. M. Ferguson, et al. (2003). "Short-term projections for variant Creutzfeldt-Jakob disease onsets." *Stat Methods Med Res* **12**(3): 191-201.
- Ghetti, B., S. R. Dlouhy, et al. (1995). "Gerstmann-Straussler-Scheinker disease and the Indiana kindred." *Brain Pathol* **5**(1): 61-75.

- Gibbs, C. J., Jr., D. C. Gajdusek, et al. (1968). "Creutzfeldt-Jakob disease (spongiform encephalopathy): transmission to the chimpanzee." Science **161**(839): 388-9.
- Giese, A., M. H. Groschup, et al. (1995). "Neuronal cell death in scrapie-infected mice is due to apoptosis." Brain Pathol **5**(3): 213-21.
- Gilch, S., F. Wopfner, et al. (2003). "Polyclonal anti-PrP auto-antibodies induced with dimeric PrP interfere efficiently with PrPSc propagation in prion-infected cells." J Biol Chem **278**(20): 18524-31.
- Glatzel, M., F. L. Heppner, et al. (2001). "Sympathetic innervation of lymphoreticular organs is rate limiting for prion neuroinvasion." Neuron **31**(1): 25-34.
- Glover, J. R. and S. Lindquist (1998). "Hsp104, Hsp70, and Hsp40: a novel chaperone system that rescues previously aggregated proteins." Cell **94**(1): 73-82.
- Goldmann, W., N. Hunter, et al. (1991). "Different forms of the bovine PrP gene have five or six copies of a short, G-C-rich element within the protein-coding exon." J Gen Virol **72**(Pt 1): 201-4.
- Gonzalez, M., F. Mackay, et al. (1998). "The sequential role of lymphotoxin and B cells in the development of splenic follicles." J Exp Med **187**(7): 997-1007.
- Gorodinsky, A. and D. A. Harris (1995). "Glycolipid-anchored proteins in neuroblastoma cells form detergent-resistant complexes without caveolin." J Cell Biol **129**(3): 619-27.
- Gray, F., H. Adle-Biassette, et al. (1999). "[Neuronal apoptosis in human prion diseases]." Bull Acad Natl Med **183**(2): 305-20; discussion 320-1.
- Gu, Y., S. Verghese, et al. (2003). "Mutant prion protein-mediated aggregation of normal prion protein in the endoplasmic reticulum: implications for prion propagation and neurotoxicity." J Neurochem **84**(1): 10-22.
- Hachiya, N. S., K. Watanabe, et al. (2004). "Anterograde and retrograde intracellular trafficking of fluorescent cellular prion protein." Biochem Biophys Res Commun **315**(4): 802-7.
- Haig, D. A. and M. C. Clarke (1971). "Multiplication of the scrapie agent." Nature **234**(5324): 106-7.
- Haire, L. F., S. M. Whyte, et al. (2004). "The crystal structure of the globular domain of sheep prion protein." J Mol Biol **336**(5): 1175-83.
- Harris, D. A. (2003). "Trafficking, turnover and membrane topology of PrP." Br Med Bull **66**: 71-85.
- Harris, D. A., A. Gorodinsky, et al. (1996). "Cell biology of the prion protein." Curr Top Microbiol Immunol **207**: 77-93.
- Harris, D. A., M. T. Huber, et al. (1993). "Processing of a cellular prion protein: identification of N- and C- terminal cleavage sites." Biochemistry **32**(4): 1009-16.
- Harrison, P. M., H. S. Chan, et al. (1999). "Thermodynamics of model prions and its implications for the problem of prion protein folding." J Mol Biol **286**(2): 593-606.
- Hegde, R. S., J. A. Mastrianni, et al. (1998). "A transmembrane form of the prion protein in neurodegenerative disease." Science **279**(5352): 827-34.
- Hegde, R. S., S. Voigt, et al. (1998). "Regulation of protein topology by trans-acting factors at the endoplasmic reticulum." Mol Cell **2**(1): 85-91.

- Heppner, F. L., A. D. Christ, et al. (2001). "Transepithelial prion transport by M cells." Nat Med **7**(9): 976-7.
- Herms, J. W., H. A. Kretzschmar, et al. (1995). "Patch-clamp analysis of synaptic transmission to cerebellar purkinje cells of prion protein knockout mice." Eur J Neurosci **7**(12): 2508-12.
- Hill, A. F., M. Antoniou, et al. (1999). "Protease-resistant prion protein produced in vitro lacks detectable infectivity." J Gen Virol **80**(Pt 1): 11-4.
- Hill, A. F., M. Desbruslais, et al. (1997). "The same prion strain causes vCJD and BSE." Nature **389**(6650): 448-50, 526.
- Horiuchi, M. and B. Caughey (1999). "Prion protein interconversions and the transmissible spongiform encephalopathies." Structure Fold Des **7**(10): R231-40.
- Horiuchi, M. and B. Caughey (1999). "Specific binding of normal prion protein to the scrapie form via a localized domain initiates its conversion to the protease-resistant state." Embo J **18**(12): 3193-203.
- Horiuchi, M., S. A. Priola, et al. (2000). "Interactions between heterologous forms of prion protein: binding, inhibition of conversion, and species barriers." Proc Natl Acad Sci U S A **97**(11): 5836-41.
- Houston, F., J. D. Foster, et al. (2000). "Transmission of BSE by blood transfusion in sheep." Lancet **356**(9234): 999-1000.
- Hsiao, K., H. F. Baker, et al. (1989). "Linkage of a prion protein missense variant to Gerstmann-Straussler syndrome." Nature **338**(6213): 342-5.
- Hsiao, K. K., C. Cass, et al. (1991). "A prion protein variant in a family with the telencephalic form of Gerstmann-Straussler-Scheinker syndrome." Neurology **41**(5): 681-4.
- Hsiao, K. K., D. Groth, et al. (1994). "Serial transmission in rodents of neurodegeneration from transgenic mice expressing mutant prion protein." Proc Natl Acad Sci U S A **91**(19): 9126-30.
- Huang, F. P., C. F. Farquhar, et al. (2002). "Migrating intestinal dendritic cells transport PrP(Sc) from the gut." J Gen Virol **83**(Pt 1): 267-71.
- Huang, Y. S., J. H. Carson, et al. (2003). "Facilitation of dendritic mRNA transport by CPEB." Genes Dev **17**(5): 638-53.
- Hunter, N., J. Foster, et al. (2002). "Transmission of prion diseases by blood transfusion." J Gen Virol **83**(Pt 11): 2897-905.
- Ironside, J. W. (1996). "Human prion diseases." J Neural Transm Suppl **47**: 231-46.
- Ironside, J. W. (1998). "Prion diseases in man." J Pathol **186**(3): 227-34.
- Ivanova, L., S. Barmada, et al. (2001). "Mutant prion proteins are partially retained in the endoplasmic reticulum." J Biol Chem **276**(45): 42409-21.
- Jackson, G. S., I. Murray, et al. (2001). "Location and properties of metal-binding sites on the human prion protein." Proc Natl Acad Sci U S A **98**(15): 8531-5.
- Jansen, K., O. Schafer, et al. (2001). "Structural intermediates in the putative pathway from the cellular prion protein to the pathogenic form." Biol Chem **382**(4): 683-91.
- Jarrett, J. T. and P. T. Lansbury, Jr. (1993). "Seeding "one-dimensional crystallization" of amyloid: a pathogenic mechanism in Alzheimer's disease and scrapie?" Cell **73**(6): 1055-8.

- Jeffrey, M., C. M. Goodsir, et al. (1992). "Infection specific prion protein (PrP) accumulates on neuronal plasmalemma in scrapie infected mice." Neurosci Lett **147**(1): 106-9.
- Jin, T., Y. Gu, et al. (2000). "The chaperone protein BiP binds to a mutant prion protein and mediates its degradation by the proteasome." J Biol Chem **275**(49): 38699-704.
- Kaneko, K., H. L. Ball, et al. (2000). "A synthetic peptide initiates Gerstmann-Straussler-Scheinker (GSS) disease in transgenic mice." J Mol Biol **295**(4): 997-1007.
- Kaneko, K., M. Vey, et al. (1997). "COOH-terminal sequence of the cellular prion protein directs subcellular trafficking and controls conversion into the scrapie isoform." Proc Natl Acad Sci U S A **94**(6): 2333-8.
- Kaneko, K., L. Zulianello, et al. (1997). "Evidence for protein X binding to a discontinuous epitope on the cellular prion protein during scrapie prion propagation." Proc Natl Acad Sci U S A **94**(19): 10069-74.
- Kanu, N., Y. Imokawa, et al. (2002). "Transfer of scrapie prion infectivity by cell contact in culture." Curr Biol **12**(7): 523-30.
- Kao, R. R., M. B. Gravenor, et al. (2002). "The potential size and duration of an epidemic of bovine spongiform encephalopathy in British sheep." Science **295**(5553): 332-5.
- Kao, R. R., F. Houston, et al. (2003). "Epidemiological implications of the susceptibility to BSE of putatively resistant sheep." J Gen Virol **84**(Pt 12): 3503-12.
- Keller, P., D. Toomre, et al. (2001). "Multicolour imaging of post-Golgi sorting and trafficking in live cells." Nat Cell Biol **3**(2): 140-9.
- Kenworthy, A. K., B. J. Nichols, et al. (2004). "Dynamics of putative raft-associated proteins at the cell surface." J Cell Biol **165**(5): 735-46.
- Kim, S. J., R. Rahbar, et al. (2001). "Combinatorial control of prion protein biogenesis by the signal sequence and transmembrane domain." J Biol Chem **276**(28): 26132-40.
- Kimberlin, R. H., S. M. Hall, et al. (1983). "Pathogenesis of mouse scrapie. Evidence for direct neural spread of infection to the CNS after injection of sciatic nerve." J Neurol Sci **61**(3): 315-25.
- Kitamoto, T., T. Muramoto, et al. (1991). "Abnormal isoform of prion protein accumulates in follicular dendritic cells in mice with Creutzfeldt-Jakob disease." J Virol **65**(11): 6292-5.
- Klein, M. A., R. Frigg, et al. (1997). "A crucial role for B cells in neuroinvasive scrapie." Nature **390**(6661): 687-90.
- Klein, M. A., R. Frigg, et al. (1998). "PrP expression in B lymphocytes is not required for prion neuroinvasion." Nat Med **4**(12): 1429-33.
- Klein, R. and L. J. Dumble (1993). "Transmission of Creutzfeldt-Jakob disease by blood transfusion." Lancet **341**(8847): 768.
- Klohn, P. C., L. Stoltze, et al. (2003). "A quantitative, highly sensitive cell-based infectivity assay for mouse scrapie prions." Proc Natl Acad Sci U S A **100**(20): 11666-71.
- Knaus, K. J., M. Morillas, et al. (2001). "Crystal structure of the human prion protein reveals a mechanism for oligomerization." Nat Struct Biol **8**(9): 770-4.
- Koch, T. K., B. O. Berg, et al. (1985). "Creutzfeldt-Jakob disease in a young adult with idiopathic hypopituitarism. Possible relation to the

- administration of cadaveric human growth hormone." N Engl J Med **313**(12): 731-3.
- Kocisko, D. A., J. H. Come, et al. (1994). "Cell-free formation of protease-resistant prion protein." Nature **370**(6489): 471-4.
- Kocisko, D. A., P. T. Lansbury, Jr., et al. (1996). "Partial unfolding and refolding of scrapie-associated prion protein: evidence for a critical 16-kDa C-terminal domain." Biochemistry **35**(41): 13434-42.
- Kocisko, D. A., S. A. Priola, et al. (1995). "Species specificity in the cell-free conversion of prion protein to protease-resistant forms: a model for the scrapie species barrier." Proc Natl Acad Sci U S A **92**(9): 3923-7.
- Kong et al (2004). "Inherited Prion Diseases" from *Prion Biology and Diseases*, 2nd edition, ed. Prusiner, S pp673-775.
- Koni, P. A., R. Sacca, et al. (1997). "Distinct roles in lymphoid organogenesis for lymphotoxins alpha and beta revealed in lymphotoxin beta-deficient mice." Immunity **6**(4): 491-500.
- Korth, C., K. Kaneko, et al. (2000). "Expression of unglycosylated mutated prion protein facilitates PrP(Sc) formation in neuroblastoma cells infected with different prion strains." J Gen Virol **81**(Pt 10): 2555-63.
- Kretzschmar, H. A., A. Giese, et al. (1997). "Cell death in prion disease." J Neural Transm Suppl **50**: 191-210.
- Kretzschmar, H. A., T. Tings, et al. (2000). "Function of PrP(C) as a copper-binding protein at the synapse." Arch Virol Suppl(16): 239-49.
- Kunzi, V., M. Glatzel, et al. (2002). "Unhampered prion neuroinvasion despite impaired fast axonal transport in transgenic mice overexpressing four-repeat tau." J Neurosci **22**(17): 7471-7.
- Kurschner, C. and J. I. Morgan (1995). "The cellular prion protein (PrP) selectively binds to Bcl-2 in the yeast two-hybrid system." Brain Res Mol Brain Res **30**(1): 165-8.
- Kurschner, C. and J. I. Morgan (1995). "The cellular prion protein (PrP) selectively binds to Bcl-2 in the yeast two-hybrid system." Brain Res Mol Brain Res **30**(1): 165-8.
- Kurschner, C. and J. I. Morgan (1996). "Analysis of interaction sites in homo- and heteromeric complexes containing Bcl-2 family members and the cellular prion protein." Brain Res Mol Brain Res **37**(1-2): 249-58.
- Kuwahara, C., A. M. Takeuchi, et al. (1999). "Prions prevent neuronal cell-line death." Nature **400**(6741): 225-6.
- Lansbury, P. T., Jr. and B. Caughey (1995). "The chemistry of scrapie infection: implications of the 'ice 9' metaphor." Chem Biol **2**(1): 1-5.
- Lasmézas, C. I., J. Y. Cesbron, et al. (1996). "Immune system-dependent and -independent replication of the scrapie agent." J Virol **70**(2): 1292-5.
- Lasmézas, C. I., J. P. Deslys, et al. (1996). "BSE transmission to macaques." Nature **381**(6585): 743-4.
- Latarjet, R., B. Muel, et al. (1970). "Inactivation of the scrapie agent by near monochromatic ultraviolet light." Nature **227**(265): 1341-3.
- Lee, K. S., A. C. Magalhaes, et al. (2001). "Internalization of mammalian fluorescent cellular prion protein and N-terminal deletion mutants in living cells." J Neurochem **79**(1): 79-87.
- Leucht, C., S. Simoneau, et al. (2003). "The 37 kDa/67 kDa laminin receptor is required for PrP(Sc) propagation in scrapie-infected neuronal cells." EMBO Rep **4**(3): 290-5.

- Lippincott-Schwartz, J., E. Snapp, et al. (2001). "Studying protein dynamics in living cells." *Nat Rev Mol Cell Biol* **2**(6): 444-56.
- Liu, T., R. Li, et al. (2002). "Intercellular transfer of the cellular prion protein." *J Biol Chem* **277**(49): 47671-8.
- Lledo, P. M., P. Tremblay, et al. (1996). "Mice deficient for prion protein exhibit normal neuronal excitability and synaptic transmission in the hippocampus." *Proc Natl Acad Sci U S A* **93**(6): 2403-7.
- Lopez Garcia, F., R. Zahn, et al. (2000). "NMR structure of the bovine prion protein." *Proc Natl Acad Sci U S A* **97**(15): 8334-9.
- Lucassen, R., K. Nishina, et al. (2003). "In vitro amplification of protease-resistant prion protein requires free sulfhydryl groups." *Biochemistry* **42**(14): 4127-35.
- Ma, J. and S. Lindquist (2001). "Wild-type PrP and a mutant associated with prion disease are subject to retrograde transport and proteasome degradation." *Proc Natl Acad Sci U S A* **98**(26): 14955-60.
- Ma, J. and S. Lindquist (2002). "Conversion of PrP to a self-perpetuating PrP^{Sc}-like conformation in the cytosol." *Science* **298**(5599): 1785-8.
- Ma, J., R. Wollmann, et al. (2002). "Neurotoxicity and neurodegeneration when PrP accumulates in the cytosol." *Science* **298**(5599): 1781-5.
- Mabbott, N. A., F. Mackay, et al. (2000). "Temporary inactivation of follicular dendritic cells delays neuroinvasion of scrapie." *Nat Med* **6**(7): 719-20.
[taf/DynaPage.taf?file=/nm/journal/v6/n7/full/nm0700_719.html](http://www.nature.com/nature/taf/DynaPage.taf?file=/nm/journal/v6/n7/full/nm0700_719.html)
[taf/DynaPage.taf?file=/nm/journal/v6/n7/abs/nm0700_719.html](http://www.nature.com/nature/taf/DynaPage.taf?file=/nm/journal/v6/n7/abs/nm0700_719.html).
- Mabbott, N. A., J. Young, et al. (2003). "Follicular dendritic cell dedifferentiation by treatment with an inhibitor of the lymphotoxin pathway dramatically reduces scrapie susceptibility." *J Virol* **77**(12): 6845-54.
- Mackay, F. and J. L. Browning (1998). "Turning off follicular dendritic cells." *Nature* **395**(6697): 26-7.
- Mackay, F., G. R. Majeau, et al. (1997). "Lymphotoxin but not tumor necrosis factor functions to maintain splenic architecture and humoral responsiveness in adult mice." *Eur J Immunol* **27**(8): 2033-42.
- Madore, N., K. L. Smith, et al. (1999). "Functionally different GPI proteins are organized in different domains on the neuronal surface." *Embo J* **18**(24): 6917-26.
- Magalhaes, A. C., J. A. Silva, et al. (2002). "Endocytic intermediates involved with the intracellular trafficking of a fluorescent cellular prion protein." *J Biol Chem* **277**(36): 33311-8.
- Mallucci, G. and J. Collinge (2004). "Update on Creutzfeldt-Jakob disease." *Curr Opin Neurol* **17**(6): 641-7.
- Mallucci, G., A. Dickinson, et al. (2003). "Depleting neuronal PrP in prion infection prevents disease and reverses spongiosis." *Science* **302**(5646): 871-4.
- Mallucci, G. R., S. Ratte, et al. (2002). "Post-natal knockout of prion protein alters hippocampal CA1 properties, but does not result in neurodegeneration." *Embo J* **21**(3): 202-10.
- Mange, A., N. Nishida, et al. (2000). "Amphotericin B inhibits the generation of the scrapie isoform of the prion protein in infected cultures." *J Virol* **74**(7): 3135-40.
- Manson, J. C. (1999). "Understanding transmission of the prion diseases." *Trends Microbiol* **7**(12): 465-7. _00001619 _00001619.

- Manson, J. C., A. R. Clarke, et al. (1994). "129/Ola mice carrying a null mutation in PrP that abolishes mRNA production are developmentally normal." Mol Neurobiol **8**(2-3): 121-7.
- Manson, J. C., E. Jamieson, et al. (1999). "A single amino acid alteration (101L) introduced into murine PrP dramatically alters incubation time of transmissible spongiform encephalopathy." Embo J **18**(23): 6855-64.
- Marella, M., S. Lehmann, et al. (2002). "Filipin prevents pathological prion protein accumulation by reducing endocytosis and inducing cellular PrP release." J Biol Chem **277**(28): 25457-64.
- Markovits, P., C. Dautheville, et al. (1983). "In vitro propagation of the scrapie agent. I. Transformation of mouse glia and neuroblastoma cells after infection with the mouse-adapted scrapie strain c-506." Acta Neuropathol (Berl) **60**(1-2): 75-80.
- Marsh, R. F. and W. J. Hadlow (1992). "Transmissible mink encephalopathy." Rev Sci Tech **11**(2): 539-50.
- Marsh, R. F. and R. H. Kimberlin (1975). "Comparison of scrapie and transmissible mink encephalopathy in hamsters. II. Clinical signs, pathology, and pathogenesis." J Infect Dis **131**(2): 104-10.
- McBride, P. A., M. I. Wilson, et al. (1998). "Heparan sulfate proteoglycan is associated with amyloid plaques and neuroanatomically targeted PrP pathology throughout the incubation period of scrapie-infected mice." Exp Neurol **149**(2): 447-54.
- McKinley, M. P., A. Taraboulos, et al. (1991). "Ultrastructural localization of scrapie prion proteins in cytoplasmic vesicles of infected cultured cells." Lab Invest **65**(6): 622-30.
- Mead, S., M. P. Stumpf, et al. (2003). "Balancing selection at the prion protein gene consistent with prehistoric kurulike epidemics." Science **300**(5619): 640-3.
- Medori, R., P. Montagna, et al. (1992). "Fatal familial insomnia: a second kindred with mutation of prion protein gene at codon 178." Neurology **42**(3 Pt 1): 669-70.
- Meyer, R. K., A. Lustig, et al. (2000). "A monomer-dimer equilibrium of a cellular prion protein (PrPC) not observed with recombinant PrP." J Biol Chem **275**(48): 38081-7.
- Milhavet, O. and S. Lehmann (2002). "Oxidative stress and the prion protein in transmissible spongiform encephalopathies." Brain Res Brain Res Rev **38**(3): 328-39.
- Milhavet, O., H. E. McMahon, et al. (2000). "Prion infection impairs the cellular response to oxidative stress." Proc Natl Acad Sci U S A **97**(25): 13937-42.
- Miller, M. W. and E. S. Williams (2004). "Chronic wasting disease of cervids." Curr Top Microbiol Immunol **284**: 193-214.
- Mobley, W. C., R. L. Neve, et al. (1988). "Nerve growth factor increases mRNA levels for the prion protein and the beta-amyloid protein precursor in developing hamster brain." Proc Natl Acad Sci U S A **85**(24): 9811-5.
- Monari, L., S. G. Chen, et al. (1994). "Fatal familial insomnia and familial Creutzfeldt-Jakob disease: different prion proteins determined by a DNA polymorphism." Proc Natl Acad Sci U S A **91**(7): 2839-42.

- Montrasio, F., R. Frigg, et al. (2000). "Impaired prion replication in spleens of mice lacking functional follicular dendritic cells." Science **288**(5469): 1257-9.
- Moore, R. C., I. Y. Lee, et al. (1999). "Ataxia in prion protein (PrP)-deficient mice is associated with upregulation of the novel PrP-like protein doppel." J Mol Biol **292**(4): 797-817.
- Moore, R. C., N. J. Redhead, et al. (1995). "Double replacement gene targeting for the production of a series of mouse strains with different prion protein gene alterations." Biotechnology (N Y) **13**(9): 999-1004.
- Mouillet-Richard, S., M. Ermonval, et al. (2000). "Signal transduction through prion protein." Science **289**(5486): 1925-8.
- Naslavsky, N., R. Stein, et al. (1997). "Characterization of detergent-insoluble complexes containing the cellular prion protein and its scrapie isoform." J Biol Chem **272**(10): 6324-31.
- Neutra, M. R., A. Frey, et al. (1996). "Epithelial M cells: gateways for mucosal infection and immunization." Cell **86**(3): 345-8.
- Nishida, N., D. A. Harris, et al. (2000). "Successful transmission of three mouse-adapted scrapie strains to murine neuroblastoma cell lines overexpressing wild-type mouse prion protein." J Virol **74**(1): 320-5.
- Niwa, M., C. Sidrauski, et al. (1999). "A role for presenilin-1 in nuclear accumulation of Ire1 fragments and induction of the mammalian unfolded protein response." Cell **99**(7): 691-702.
- Oesch, B., D. Westaway, et al. (1985). "A cellular gene encodes scrapie PrP 27-30 protein." Cell **40**(4): 735-46.
- Osherovich, L. Z. and J. S. Weissman (2002). "The utility of prions." Dev Cell **2**(2): 143-51.
- Paitel, E., C. Alves da Costa, et al. (2002). "Overexpression of PrP^C triggers caspase 3 activation: potentiation by proteasome inhibitors and blockade by anti-PrP antibodies." J Neurochem **83**(5): 1208-14.
- Palmer, M. S., A. J. Dryden, et al. (1991). "Homozygous prion protein genotype predisposes to sporadic Creutzfeldt- Jakob disease." Nature **352**(6333): 340-2.
- Pan, K. M., N. Stahl, et al. (1992). "Purification and properties of the cellular prion protein from Syrian hamster brain." Protein Sci **1**(10): 1343-52.
- Paramithiotis, E., M. Pinard, et al. (2003). "A prion protein epitope selective for the pathologically misfolded conformation." Nat Med **9**(7): 893-9.
- Parkin, E. T., N. T. Watt, et al. (2004). "Dual mechanisms for shedding of the cellular prion protein." J Biol Chem **279**(12): 11170-8.
- Patino, M. M., J. J. Liu, et al. (1996). "Support for the prion hypothesis for inheritance of a phenotypic trait in yeast." Science **273**(5275): 622-6.
- Pattison, I. H. (1965). Experiments with scrapie with special reference to the nature of the agent and the pathology of the disease. Slow, latent and temperate virus infections. D. C. Gajdusek, C. J. Gibbs and M. P. Alpers. Washington DC, NINDB Monogr. **2**: 249-257.
- Pattison, I. H., M. N. Hoare, et al. (1972). "Spread of scrapie to sheep and goats by oral dosing with foetal membranes from scrapie-affected sheep." Vet Rec **90**(17): 465-8.
- Pauly, P. C. and D. A. Harris (1998). "Copper stimulates endocytosis of the prion protein." J Biol Chem **273**(50): 33107-10.

- Peretz, D., R. A. Williamson, et al. (2001). "Antibodies inhibit prion propagation and clear cell cultures of prion infectivity." Nature **412**(6848): 739-43.
- Petersen, R. B., P. Parchi, et al. (1996). "Effect of the D178N mutation and the codon 129 polymorphism on the metabolism of the prion protein." J Biol Chem **271**(21): 12661-8.
- Prinz, M., M. Heikenwalder, et al. (2003). "Positioning of follicular dendritic cells within the spleen controls prion neuroinvasion." Nature **425**(6961): 957-62.
- Prusiner, S. B. (1982). "Novel proteinaceous infectious particles cause scrapie." Science **216**(4542): 136-44.
- Prusiner, S. B. (1998). "Prions." Proc Natl Acad Sci U S A **95**(23): 13363-83.
- Prusiner, S. B., D. C. Bolton, et al. (1982). "Further purification and characterization of scrapie prions." Biochemistry **21**(26): 6942-50.
- Prusiner, S. B., M. Fuzi, et al. (1993). "Immunologic and molecular biologic studies of prion proteins in bovine spongiform encephalopathy." J Infect Dis **167**(3): 602-13.
- Prusiner, S. B., W. J. Hadlow, et al. (1977). "Sedimentation properties of the scrapie agent." Proc Natl Acad Sci U S A **74**(10): 4656-60.
- Prusiner, S. B., W. J. Hadlow, et al. (1978). "Sedimentation characteristics of the scrapie agent from murine spleen and brain." Biochemistry **17**(23): 4987-92.
- Prusiner, S. B., M. P. McKinley, et al. (1983). "Scrapie prions aggregate to form amyloid-like birefringent rods." Cell **35**(2 Pt 1): 349-58.
- Prusiner, S. B., M. Scott, et al. (1990). "Transgenic studies implicate interactions between homologous PrP isoforms in scrapie prion replication." Cell **63**(4): 673-86.
- Prusiner, S. B. and M. R. Scott (1997). "Genetics of prions." Annu Rev Genet **31**: 139-75.
- Race, R. (1991). "The scrapie agent in vitro." Curr Top Microbiol Immunol **172**: 181-93.
- Race, R., M. Oldstone, et al. (2000). "Entry versus blockade of brain infection following oral or intraperitoneal scrapie administration: role of prion protein expression in peripheral nerves and spleen." J Virol **74**(2): 828-33.
- Race, R. E., L. H. Fadness, et al. (1987). "Characterization of scrapie infection in mouse neuroblastoma cells." J Gen Virol **68**(Pt 5): 1391-9.
- Raeber, A. J., R. E. Race, et al. (1997). "Astrocyte-specific expression of hamster prion protein (PrP) renders PrP knockout mice susceptible to hamster scrapie." Embo J **16**(20): 6057-65.
- Raymond, G. J., J. Hope, et al. (1997). "Molecular assessment of the potential transmissibilities of BSE and scrapie to humans." Nature **388**(6639): 285-8.
- Richter, J. D. (2001). "Think globally, translate locally: what mitotic spindles and neuronal synapses have in common." Proc Natl Acad Sci U S A **98**(13): 7069-71.
- Rieger, R., F. Edenhofer, et al. (1997). "The human 37-kDa laminin receptor precursor interacts with the prion protein in eukaryotic cells." Nat Med **3**(12): 1383-8.

- Rieger, R., F. Edenhofer, et al. (1997). "The human 37-kDa laminin receptor precursor interacts with the prion protein in eukaryotic cells." Nat Med **3**(12): 1383-8.
- Riek, R., S. Hornemann, et al. (1996). "NMR structure of the mouse prion protein domain PrP(121-321)." Nature **382**(6587): 180-2.
- Riek, R., S. Hornemann, et al. (1997). "NMR characterization of the full-length recombinant murine prion protein, mPrP(23-231)." FEBS Lett **413**(2): 282-8.
- Roesler, R., R. Walz, et al. (1999). "Normal inhibitory avoidance learning and anxiety, but increased locomotor activity in mice devoid of PrP(C)." Brain Res Mol Brain Res **71**(2): 349-53.
- Rossi, D., A. Cozzio, et al. (2001). "Onset of ataxia and Purkinje cell loss in PrP null mice inversely correlated with Dpl level in brain." Embo J **20**(4): 694-702.
- Rossi, G., G. Giaccone, et al. (2000). "Creutzfeldt-Jakob disease with a novel four extra-repeat insertional mutation in the PrP gene." Neurology **55**(3): 405-10.
- Saborio, G. P., B. Permanne, et al. (2001). "Sensitive detection of pathological prion protein by cyclic amplification of protein misfolding." Nature **411**(6839): 810-3.
- Safar, J., P. P. Roller, et al. (1993). "Conformational transitions, dissociation, and unfolding of scrapie amyloid (prion) protein." J Biol Chem **268**(27): 20276-84.
- Safar, J., H. Wille, et al. (1998). "Eight prion strains have PrP(Sc) molecules with different conformations." Nat Med **4**(10): 1157-65.
- Sakaguchi, S., S. Katamine, et al. (1996). "Loss of cerebellar Purkinje cells in aged mice homozygous for a disrupted PrP gene." Nature **380**(6574): 528-31.
- Sanchez, Y., J. Taulien, et al. (1992). "Hsp104 is required for tolerance to many forms of stress." Embo J **11**(6): 2357-64.
- Schatzl, H. M., M. Da Costa, et al. (1995). "Prion protein gene variation among primates." J Mol Biol **245**(4): 362-74.
- Schatzl, H. M., L. Laszlo, et al. (1997). "A hypothalamic neuronal cell line persistently infected with scrapie prions exhibits apoptosis." J Virol **71**(11): 8821-31.
- Schwarz, A., O. Kratke, et al. (2003). "Immunisation with a synthetic prion protein-derived peptide prolongs survival times of mice orally exposed to the scrapie agent." Neurosci Lett **350**(3): 187-9.
- Scott, M., D. Foster, et al. (1989). "Transgenic mice expressing hamster prion protein produce species- specific scrapie infectivity and amyloid plaques." Cell **59**(5): 847-57.
- Shyng, S. L., J. E. Heuser, et al. (1994). "A glycolipid-anchored prion protein is endocytosed via clathrin-coated pits." J Cell Biol **125**(6): 1239-50.
- Shyng, S. L., M. T. Huber, et al. (1993). "A prion protein cycles between the cell surface and an endocytic compartment in cultured neuroblastoma cells." J Biol Chem **268**(21): 15922-8.
- Shyng, S. L., S. Lehmann, et al. (1995). "Sulfated glycans stimulate endocytosis of the cellular isoform of the prion protein, PrPC, in cultured cells." J Biol Chem **270**(50): 30221-9.

- Shyng, S. L., S. Lehmann, et al. (1995). "Sulfated glycans stimulate endocytosis of the cellular isoform of the prion protein, PrPC, in cultured cells." J Biol Chem **270**(50): 30221-9.
- Shyng, S. L., K. L. Moulder, et al. (1995). "The N-terminal domain of a glycolipid-anchored prion protein is essential for its endocytosis via clathrin-coated pits." J Biol Chem **270**(24): 14793-800.
- Si, K., M. Giustetto, et al. (2003). "A neuronal isoform of CPEB regulates local protein synthesis and stabilizes synapse-specific long-term facilitation in aplysia." Cell **115**(7): 893-904.
- Si, K., S. Lindquist, et al. (2003). "A neuronal isoform of the aplysia CPEB has prion-like properties." Cell **115**(7): 879-91.
- Sigurdsson, E. M., D. R. Brown, et al. (2002). "Immunization delays the onset of prion disease in mice." Am J Pathol **161**(1): 13-7.
- Silverman, G. L., K. Qin, et al. (2000). "Doppel is an N-glycosylated, glycosylphosphatidylinositol-anchored protein. Expression in testis and ectopic production in the brains of Prnp(0/0) mice predisposed to Purkinje cell loss." J Biol Chem **275**(35): 26834-41.
- Simoneau, S., S. Haik, et al. (2003). "Different isoforms of the non-integrin laminin receptor are present in mouse brain and bind PrP." Biol Chem **384**(2): 243-6.
- Simons, K. and E. Ikonen (1997). "Functional rafts in cell membranes." Nature **387**(6633): 569-72.
- Snow, A. D., T. N. Wight, et al. (1990). "Immunolocalization of heparan sulfate proteoglycans to the prion protein amyloid plaques of Gerstmann-Straussler syndrome, Creutzfeldt- Jakob disease and scrapie." Lab Invest **63**(5): 601-11.
- Solassol, J., C. Crozet, et al. (2003). "Prion propagation in cultured cells." Br Med Bull **66**: 87-97.
- Solfrosi, L., J. R. Criado, et al. (2004). "Cross-linking cellular prion protein triggers neuronal apoptosis in vivo." Science **303**(5663): 1514-6.
- Somerville, R. A., A. Chong, et al. (1997). "Biochemical typing of scrapie strains." Nature **386**(6625): 564.
- Sparrer, H. E., A. Santoso, et al. (2000). "Evidence for the prion hypothesis: induction of the yeast [PSI⁺] factor by in vitro- converted Sup35 protein." Science **289**(5479): 595-9.
- Spielhauer, C. and H. M. Schatzl (2001). "PrPC directly interacts with proteins involved in signaling pathways." J Biol Chem **276**(48): 44604-12.
- Spraker, T. R., M. W. Miller, et al. (1997). "Spongiform encephalopathy in free-ranging mule deer (*Odocoileus hemionus*), white-tailed deer (*Odocoileus virginianus*) and Rocky Mountain elk (*Cervus elaphus nelsoni*) in northcentral Colorado." J Wildl Dis **33**(1): 1-6.
- Stahl, N., D. R. Borchelt, et al. (1987). "Scrapie prion protein contains a phosphatidylinositol glycolipid." Cell **51**(2): 229-40.
- Stewart, R. S., B. Drisaldi, et al. (2001). "A transmembrane form of the prion protein contains an uncleaved signal peptide and is retained in the endoplasmic Reticulum." Mol Biol Cell **12**(4): 881-9.
- Stewart, R. S. and D. A. Harris (2001). "Most pathogenic mutations do not alter the membrane topology of the prion protein." J Biol Chem **276**(3): 2212-20.

- Sunyach, C., A. Jen, et al. (2003). "The mechanism of internalization of glycosylphosphatidylinositol-anchored prion protein." Embo J **22**(14): 3591-601.
- Supattapone, S. (2004). "Prion protein conversion in vitro." J Mol Med **82**(6): 348-56.
- Tanaka, M., P. Chien, et al. (2004). "Conformational variations in an infectious protein determine prion strain differences." Nature **428**(6980): 323-8.
- Taraboulos, A., A. J. Raeber, et al. (1992). "Synthesis and trafficking of prion proteins in cultured cells." Mol Biol Cell **3**(8): 851-63.
- Taraboulos, A., M. Scott, et al. (1995). "Cholesterol depletion and modification of COOH-terminal targeting sequence of the prion protein inhibit formation of the scrapie isoform." J Cell Biol **129**(1): 121-32.
- Taraboulos, A., D. Serban, et al. (1990). "Scrapie prion proteins accumulate in the cytoplasm of persistently infected cultured cells." J Cell Biol **110**(6): 2117-32.
- Telling, G. C., T. Haga, et al. (1996). "Interactions between wild-type and mutant prion proteins modulate neurodegeneration in transgenic mice." Genes Dev **10**(14): 1736-50.
- Telling, G. C., P. Parchi, et al. (1996). "Evidence for the conformation of the pathologic isoform of the prion protein enciphering and propagating prion diversity." Science **274**(5295): 2079-82.
- Telling, G. C., M. Scott, et al. (1995). "Prion propagation in mice expressing human and chimeric PrP transgenes implicates the interaction of cellular PrP with another protein." Cell **83**(1): 79-90.
- Telling, G. C., P. Tremblay, et al. (1997). "N-terminally tagged prion protein supports prion propagation in transgenic mice." Protein Sci **6**(4): 825-33.
- Terry, L. A., S. Marsh, et al. (2003). "Detection of disease-specific PrP in the distal ileum of cattle exposed orally to the agent of bovine spongiform encephalopathy." Vet Rec **152**(13): 387-92.
- Thadani, V., P. L. Penar, et al. (1988). "Creutzfeldt-Jakob disease probably acquired from a cadaveric dura mater graft. Case report." J Neurosurg **69**(5): 766-9.
- Thery, C., L. Zitvogel, et al. (2002). "Exosomes: composition, biogenesis and function." Nat Rev Immunol **2**(8): 569-79.
- Tobler, I., S. E. Gaus, et al. (1996). "Altered circadian activity rhythms and sleep in mice devoid of prion protein." Nature **380**(6575): 639-42.
- Turk, E., D. B. Teplow, et al. (1988). "Purification and properties of the cellular and scrapie hamster prion proteins." Eur J Biochem **176**(1): 21-30.
- Uptain, S. M. and S. Lindquist (2002). "Prions as protein-based genetic elements." Annu Rev Microbiol **56**: 703-41.
- Vey, M., S. Pilkuhn, et al. (1996). "Subcellular colocalization of the cellular and scrapie prion proteins in caveolae-like membranous domains." Proc Natl Acad Sci U S A **93**(25): 14945-9.
- Vorberg, I., A. Buschmann, et al. (1999). "A novel epitope for the specific detection of exogenous prion proteins in transgenic mice and transfected murine cell lines." Virology **255**(1): 26-31.
- Vorberg, I. and S. A. Priola (2002). "Molecular basis of scrapie strain glycoform variation." J Biol Chem **277**(39): 36775-81.

- Vorberg, I., A. Raines, et al. (2004). "Susceptibility of common fibroblast cell lines to transmissible spongiform encephalopathy agents." J Infect Dis **189**(3): 431-9.
- Waggoner, D. J., B. Drisaldi, et al. (2000). "Brain copper content and cuproenzyme activity do not vary with prion protein expression level." J Biol Chem **275**(11): 7455-8.
- Walmsley, A. R., F. Zeng, et al. (2001). "Membrane topology influences N-glycosylation of the prion protein." Embo J **20**(4): 703-12.
- Warner, R. G., C. Hundt, et al. (2002). "Identification of the heparan sulfate binding sites in the cellular prion protein." J Biol Chem **277**(21): 18421-30.
- Wegrzyn, R. D., K. Bapat, et al. (2001). "Mechanism of prion loss after Hsp104 inactivation in yeast." Mol Cell Biol **21**(14): 4656-69.
- Weissmann, C. (1991). "A 'unified theory' of prion propagation." Nature **352**(6337): 679-83.
- Weissmann, C. (1996). "The Ninth Datta Lecture. Molecular biology of transmissible spongiform encephalopathies." FEBS Lett **389**(1): 3-11.
- Welker, E., L. D. Raymond, et al. (2002). "Intramolecular versus intermolecular disulfide bonds in prion proteins." J Biol Chem **277**(36): 33477-81.
- Welker, E., W. J. Wedemeyer, et al. (2001). "A role for intermolecular disulfide bonds in prion diseases?" Proc Natl Acad Sci U S A **98**(8): 4334-6.
- Wells, G. A., M. Dawson, et al. (1994). "Infectivity in the ileum of cattle challenged orally with bovine spongiform encephalopathy." Vet Rec **135**(2): 40-1.
- White, A. R., P. Enever, et al. (2003). "Monoclonal antibodies inhibit prion replication and delay the development of prion disease." Nature **422**(6927): 80-3.
- Wickner, R. B. (1994). "[URE3] as an altered URE2 protein: evidence for a prion analog in *Saccharomyces cerevisiae*." Science **264**(5158): 566-9.
- Wickner, R. B., D. C. Masison, et al. (1995). "[PSI] and [URE3] as yeast prions." Yeast **11**(16): 1671-85.
- Wientjens, D. P., Z. Davanipour, et al. (1996). "Risk factors for Creutzfeldt-Jakob disease: a reanalysis of case-control studies." Neurology **46**(5): 1287-91.
- Wilesmith, J. W., J. B. Ryan, et al. (1991). "Bovine spongiform encephalopathy: epidemiological studies on the origin." Vet Rec **128**(9): 199-203.
- Will, R. G. (1998). "New variant Creutzfeldt-Jakob disease." Dev Biol Stand **93**: 79-84.
- Will, R. G., J. W. Ironside, et al. (1996). "A new variant of Creutzfeldt-Jakob disease in the UK." Lancet **347**(9006): 921-5.
- Will, R. G. and R. H. Kimberlin (1998). "Creutzfeldt-Jakob disease and the risk from blood or blood products." Vox Sang **75**(3): 178-80.
- Will, R. G., W. B. Matthews, et al. (1986). "A retrospective study of Creutzfeldt-Jakob disease in England and Wales 1970-1979. II: Epidemiology." J Neurol Neurosurg Psychiatry **49**(7): 749-55.
- Wille, H., M. D. Michelitsch, et al. (2002). "Structural studies of the scrapie prion protein by electron crystallography." Proc Natl Acad Sci U S A **12**: 12.
- Wong, C., L. W. Xiong, et al. (2001). "Sulfated glycans and elevated temperature stimulate PrP(Sc)-dependent cell-free formation of protease-resistant prion protein." Embo J **20**(3): 377-86.

- Yao, Y., J. Ren, et al. (2003). "Amino terminal interaction in the prion protein identified using fusion to green fluorescent protein." J Neurochem **87**(5): 1057-65.
- Yedidia, Y., L. Horonchik, et al. (2001). "Proteasomes and ubiquitin are involved in the turnover of the wild-type prion protein." Embo J **20**(19): 5383-91.
- Zahn, R., A. Liu, et al. (2000). "NMR solution structure of the human prion protein." Proc Natl Acad Sci U S A **97**(1): 145-50.
- Zanata, S. M., M. H. Lopes, et al. (2002). "Stress-inducible protein 1 is a cell surface ligand for cellular prion that triggers neuroprotection." Embo J **21**(13): 3307-16.
- Zeidler, M. and J. W. Ironside (2000). "The new variant of Creutzfeldt-Jakob disease." Rev Sci Tech **19**(1): 98-120.

8. Appendix Matlab script

```

%find_diff coefficient
%normalise data, fit curve by estimating paramers, plot data and fitted curve
%find mobile fraction
function [D] = tim_script(name);
[s,sh] = xlsinfo(name) ;
sheets = strvcat(sh)
end
for ii=1:length(sh)
    data_in = xlsread(name, sheets(ii,:))
    t=data_in(:,1).';
    tedit = t(1:2:length(t))
    bl= data_in(:,2).';
    bl_edit = bl(1:2:length(t))
    control= data_in(:,3).';
    control_edit = control(1:2:length(t))
    p = [tedit', bl_edit',control_edit']
    L_final = length (tedit)
end
t_recovery = tedit(4:L_final)
bleach_recovery = bl_edit (4:L_final)
control_recovery = control_edit(4:L_final)
L_new = length(t_recovery)
check = [t_recovery',bleach_recovery',control_recovery']
end
bleach_recovery_norma1 = 100*(bleach_recovery./control_recovery)
%bleach_recovery_normaled = bleach_recovery_norm1 * 100
bleach_recovery_normal_zero = bleach_recovery_norma1 -
    bleach_recovery_norma1(1)
t_recovery_zero = t_recovery - t_recovery(1)
check2 = [t_recovery_zero']
check3 = [bleach_recovery_normal_zero']

```

```

end
plot (t_recovery_zero, bleach_recovery_normal_zero)
end
    xdata=t_recovery_zero
    ydata=bleach_recovery_normal_zero
x0 = [100,0.002]
x = lsqcurvefit(@my_stages, x0, xdata, ydata)
%my_stages : is function file with break down as below of the diffusion equation
% w=3 for biorad set up and 1 for lsm setup
w=1;
xsim = xdata ;
F1=(w^2 + x(2).^4*pi*xsim);
F2= F1.^(-1);
F3= F2*w^2;
F4= F3.^(1/2);
F5= 1- F4;
F6= F5.*x(1);
F = F6;
ysim = F;
%mobile fraction calculation
end
mpb = mean(bl_edit (1:3))
mpc = mean(control_edit(1:3))
start = mpc/mpb
assym = mean (ydata(L_new-4 : L_new))
final_assym = bleach_recovery_norma1(1) + assym
correction = start * final_assym

interval = t_recovery(2) - t_recovery(1)
interval2= 2*interval
t_new = [-interval2, xdata]
ydata_new = bleach_recovery_norma1 * start
ydata_final = [100, ydata_new]

```

```
%put the simulated data back to the same level  
xsim_final = [xsim]  
ysim_finala = ysim + bleach_recovery_norma1(1)  
ysim_final = ysim_finala * start
```

```
%plot normalised versions of data and simulated  
plot (t_new,ydata_final,'b')  
hold on  
plot (xsim_final, ysim_final,'r')  
xlabel('time post bleach(s)')  
ylabel('normalised intensity')
```

```
diffusion= x(2)  
mobile = correction
```